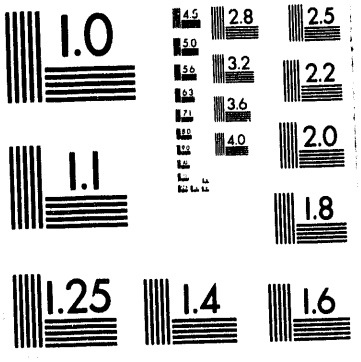
1.0
1.1
1.25
1.4
1.6
1.8
2.0
2.2
2.5
2.8
3.2
3.6
4.0
4.5
5.0
5.6
6.3
7.1
8.0
9.0

1 of 3

LBL-34897
UC-408

The Application of Psoralens to the Study of DNA Structure, Function and Dynamics

Peter Hans Spielmann
Ph.D. Thesis

Department of Chemistry
University of California

and

Division of Structural Biology
Lawrence Berkeley Laboratory
University of California
Berkeley, California

April 1991

This work was supported by the Director, Office of Energy Research, Office of Health Effects Research, of the U.S. Department of Energy under Contract No. DE-AC03-76SF00098 and National Institutes of Health grant FD 8R1 GM41911A-03-NF-03/92

The Application of Psoralens

to the Study of DNA Structure, Function and Dynamics

by

Peter Hans Spielmann

The Application of Psoralens

to the Study of DNA Structure, Function and Dynamics

by

Peter Hans Spielmann

Abstract

A series of six nitroxide spin-labeled psoralens were designed, synthesized and tested as probes for DNA dynamics. The synthesis of these spin-labeled psoralen derivatives and their photoreactivity with double-stranded DNA fragments is described. The spin labels (nitroxides) were demonstrated to survive the UV irradiation required to bind the probe to the target DNA. EPR spectra of the photobound spin-labels indicate that they do not wobble with respect to the DNA on the time-scales investigated.

We have used psoralen modified DNA as a model for the study of DNA repair enzyme systems in human cell free extracts. We have shown that damage-induced DNA synthesis is associated with removal of psoralen adducts and therefore is "repair synthesis" and not an aberrant DNA synthesis reaction potentiated by deformation of the DNA by adducts. We have found that all DNA synthesis induced by psoralen monoadducts is the consequence of removal of these adducts. By the same approach we have obtained evidence that this *in vitro* system is capable of removing psoralen cross-links as well.

Reported here are synthetic methods that make use of high intensity lasers coupled with HPLC purification to make homogeneous and very pure micromole quantities of furan-side monoadducted, cross-linked, and pyrone-side monoadducted DNA oligonucleotides. These molecules are currently being studied by NMR and X-ray crystallography. The application of the site-specifically psoralen modified oligonucleotides synthesized by these methods to the construction of substrates for the investigation of DNA repair is also discussed.

John E. Hearst

April 25, 1991

Mann macht es nicht so genau daß kein Haar dazwischen geht.

Table of Contents

Acknowledgements

Firstly, I acknowledge the friendship, and continuous and consistent support by my research director Professor John E. Hearst. I feel compelled to thank him for supplying a bewildering and almost infinite array of tools that allowed me to dig myself into a number of deep holes.

I would have been incapable of making use of the opportunities presented to me at Berkeley without the support, training, and encouragement of the Late Professor Robert V. Stevens of the University of California at Los Angeles.

My work would not have been possible without the contributions of my co-workers and labmates. The people that I collaborated with in the course of the work presented here are listed in each section. I extend heartfelt thanks to the members of the Hearst, Tinoco and Schultz groups who made my stay at Berkeley both very interesting and memorable. There is no way to list all of the people to whom I owe thanks.

HRI Research and Development, Inc., especially "Mr. President" Steve Isaacs, George Cimino, John Tessman, and Ken Metchette, generously donated a variety of tritiated and unlabeled psoralens and advice. Without this support my job would have been much more difficult. I thank them for putting me up in their less than spacious laboratory for the six months when the Hildebrand elevator was on the fritz. They were a valuable source of advice on psoralen chemistry and photochemistry. Their trials and tribulations have been an informative window into the industrial world

I thank my parents Hans and Rose for their love and the multitude of things that they have done for me in my life.

Finally, and above all, I thank Susie Chun with all my heart. Without her love, respect and understanding, all things would have been different.

This work was supported by the Director, Office of Energy Research, Office of Basic Energy Sciences, Energy Biosciences Division, of the U. S. Department of Energy under Contract No. DE-AC03-76SF00098.

Chapter 1

Synthesis and Application of Spin Labeled Psoralens to the Study of DNA Dynamics

Our goal was to develop a series of probes that could be introduced into native DNA, that would allow the study of DNA dynamics in the time domain of milli- to nano-seconds. Molecular dynamics calculations can give useful information for processes that occur on the pico-second time scale; and fluorescence techniques can give information on processes occur up to the micro-second time scale. However, many biological processes occur on time scales that are many orders of magnitude longer. For example, DNA polymerases synthesize DNA during replication at approximately 1000 nucleotides per second. The normal B-form DNA helix is 10 base pairs per turn and if one could observe the postulated polymerase driven rotation of the DNA about the helix axis, it would have a frequency of about 100 Hz. Other biological processes that occur in this time domain are transcription and translation. DNA dynamics, both sequence dependent and global, have biological importance. The recognition of DNA by various proteins has been postulated to be dependent on the structural reorganization of the target DNA sequence. Repair of DNA damage sites by ABC excinuclease may be targeted through a process in which lesions alter the DNA helix dynamics and thus influence binding of the repair complex rather than through recognition of a particular static structural distortion of the helix (Lin and Sancar, 1989; Pu *et al.*, 1989). It has been observed that the affinity of the phage 434 repressor protein dimer for its operator sequence can be reduced 50-fold by changes in the DNA sequence at the center of the operator (Koudelka *et al.*, 1987). This happens despite the

failure of the protein to make direct contacts with the DNA in this region (Anderson *et al.*, 1987). Many other techniques have been used to measure DNA dynamics. NMR studies of short DNA oligomer dynamics have been interpreted in terms of motions over a range of 10 orders of magnitude (Opella *et al.*, 1981). The motion of the bases in the helix has been studied mainly by fluoresence polarization anisotropy (Ashikawa *et al.*, 1984). EPR is a technique that has been used to study dynamic processes in the milli- to nano-second time regime. Electron spin resonance (ESR) spectroscopy has been proven to be a very powerful technique for studying DNA and RNA dynamics and their affinities toward proteins. Early EPR studies of nucleic acids involved the use of spin-labeled tRNA to investigate tRNA dynamics (for a review, see (Dugas, 1977)). Since then, different methods and techniques have been developed to prepare spin-labeled nucleic acids and to use spin labeling to study the physical and biochemical properties of nucleic acids (Bobst, 1979; Kamzolova and Postnikova, 1981). A family of nitroxide spin-labeled reagents that bind to nucleic acids by non-covalent interactions have been developed. These include modified ethidium bromide, aminoacridines, aminoazaacridine, aminofluorene, aminoanthracene, and aminochrysene. These spin probes have dynamic motion independent of the nucleic acid that they are bound to on the nano-second time scale. EPR has been used to measure motions of spin-labeled intercalators bound to DNA. Motions on a 40 nsec time scale were detected by this method and interpreted as torsional base motion (Robinson *et al.*, 1980). Because of this relatively short correlation time, probes of this kind are not suitable for studies of longer time domain processes.

Three kinds of probes have been used for the spin labeling of nucleic acids: (1) paramagnetic metal ions, especially manganese(II) ions (Rauben and Gabbay, 1975); (2) stable nitroxide radicals; (3) moderately stable positive ion radicals, such as the chlorpromazine cation (Ohnishi and McConnell, 1965; Piette and Hearst, 1983). The stable nitroxide have been the most widely used in biological systems. Site-specific spin-labeling methods for nucleic acids have been carried out in some selected tRNAs containing

minor bases in positions known from sequencing (Bobst, 1979). However, it is difficult to introduce a covalently bound site-specific EPR label into nucleic acids by chemical or enzymatic means. Direct attachment of a spin-labeled probe to DNA has been accomplished using both enzymatic and chemical syntheses (Bobst *et al.*, 1984; Kao and Bobst, 1985; Kirchner *et al.*, 1990; Spaltenstein *et al.*, 1989). It is clear from these studies that the length and structure of the tether which connects the nitroxide reporter group to the DNA has a profound influence on the EPR spectra obtained. Long tethers that permitted free rotation of the probe relative to the DNA were unable to give spectra with correlation times greater than a few nanoseconds. A nitroxide spin-label analog of thymidine in which the methyl group is replaced by an acetylene tether spin-label site-specifically incorporated by chemical synthesis into DNA oligomers has given isotropic rotational correlation times of up to 100 nanoseconds (Spaltenstein *et al.*, 1989). Steric inhibition of rotation of the nitroxide by the surrounding DNA has been implicated as the factor that allows such long correlation times to be observed (Kirchner *et al.*, 1990).

We have been involved in the study of many fundamental aspects of psoralen chemistry. A variety of specifically functionalized and radiolabeled psoralens have been developed in our laboratory (Hearst, 1981; Hearst *et al.*, 1984), and (Cimino *et al.*, 1985). One of our current interests is the construction of a series of probes that will allow us to study the dynamics of nucleic acids and their interaction with proteins. Toward this end, we have developed a series of spin-labeled psoralens that will allow us to place spin labels at specific sites in DNA and/or RNA molecules. Utilizing the well characterized properties of psoralens, we set out to design, synthesize, and test a family of nitroxide substituted psoralens that would allow us to observe DNA dynamic motions. What makes nitroxides so appealing as spin labels is that they are chemically stable under normal laboratory conditions, and they are also commercially available with many different reactive functional groups that can be modified or condensed with other molecules of interest. The

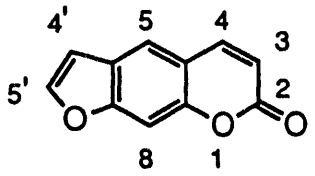

psoralen

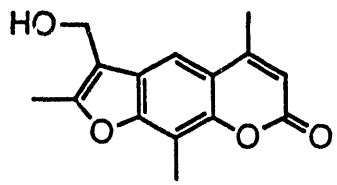

4'-hydroxymethyl-4,5',8-trimethylpsoralen (HMT)

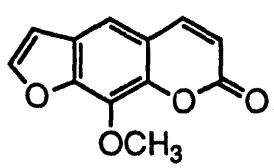

8-methoxypsoralen

Figure 1.1 Structures of Psoralen, HMT, and 8-MOP with the ring numbering system

work described below was done in collaboration with Dr. Dae-Yoon Chi and Mr. Nathan Hunt. Parts of this work have been previously published (Shi *et al.*, 1990).

An introduction to the chemistry of Psoralens

Psoralens are linear bifunctional furocoumarins that photochemically alkylate pyrimidine bases in nucleic acids (Figure 1.1). Reactions take place at the 3,4 or 4',5' double bonds of the psoralen with the 5,6 double bond in pyrimidines. The primary base that reacts with psoralens in DNA is thymidine. Figure 1.2 shows the kinetic scheme for the reactions of psoralens with DNA. The first step is the intercalation of the psoralen between base pairs of a double stranded nucleic acid. The intercalated psoralen then reacts with the pyrimidine bases to form either furan-side or pyrone-side monoadduct when irradiated with long wave-length UV light (320-410 nm). Furan-side monoadducts can photoreact with adjacent pyrimidine bases on the opposite strand to give an interstrand cross-link by absorbing a second photon. Pyrone-side monoadducts do not absorb light at wavelengths above 320 nm, so they can not be driven on to interstrand cross-links with long wave-length UV light. Rather than forming an interstrand cross-link, the primary photoreaction of the pyrone-side adduct upon absorption of a photon is photoreversal. Upon absorption of a photon, the cross-link can be photoreversed to yield either a furan-side or pyrone-side monoadduct and the unmodified DNA (Shi and Hearst, 1987b). In addition to the formation of interstrand cross-links, furan-side monoadduct can be photoreversed and can photochemically isomerize in the helix to give pyrone-side monoadduct (Tessman *et al.*, 1985). The reversal of the furan-side monoadduct can be accomplished either photochemically or by base catalyzed reversal (Shi *et al.*, 1988; Yeung *et al.*, 1988). The cross-link can also be reversed to give pyrone-side adduct by the base catalyzed reversal reaction. Figure 1.3 shows the structure of the three main adducts between thymidine and HMT. The detailed structure of both monoadducts and diadducts

Figure 1.2 Psoralen-DNA Kinetic Scheme

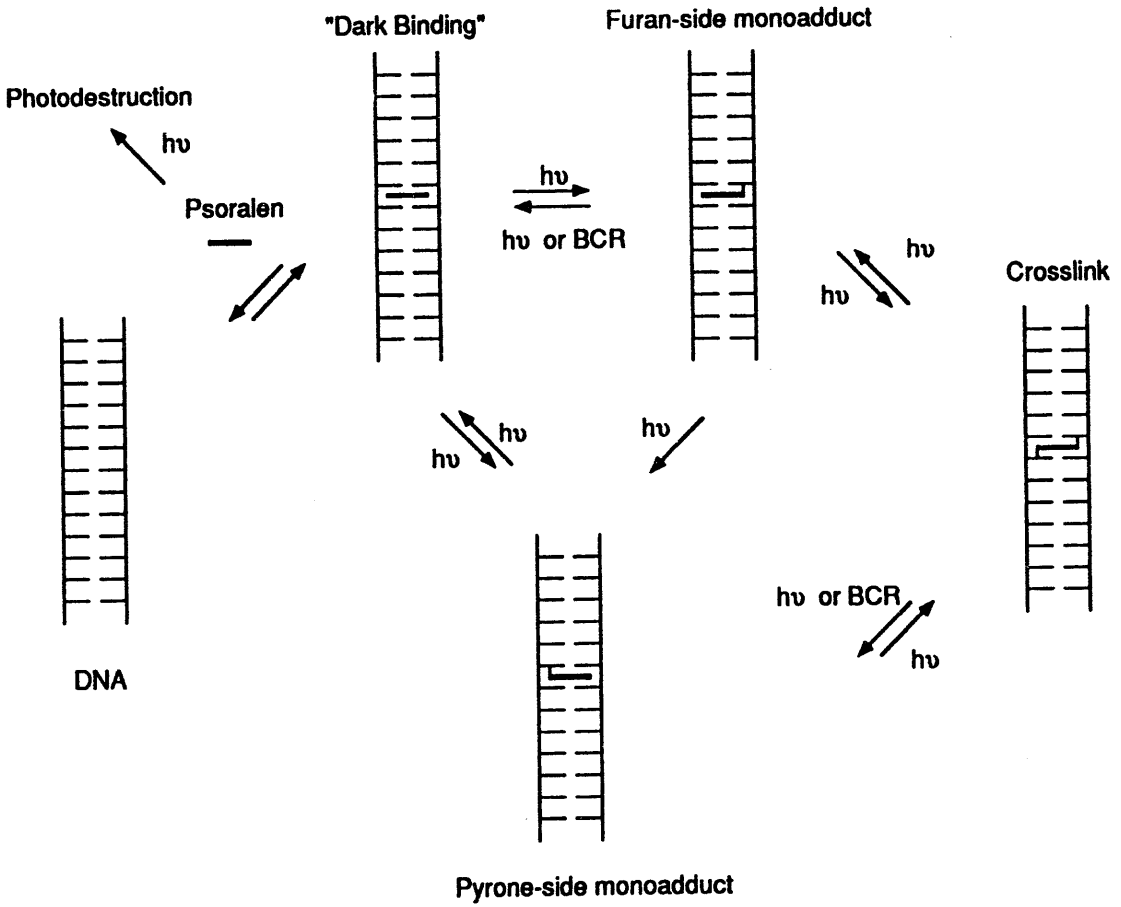

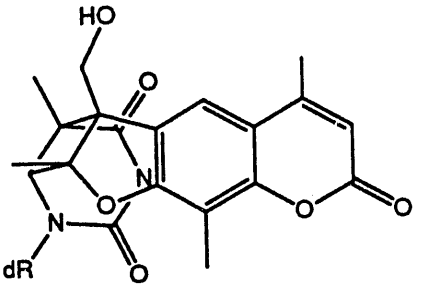

dT-HMT furan-side monoadduct, *cis-syn* conformation

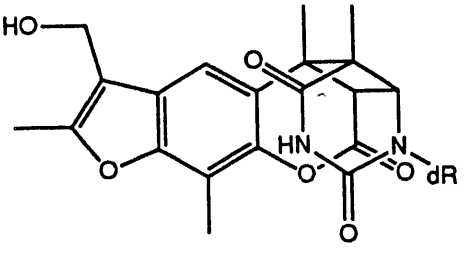

dT-HMT pyrone-side monoadduct, *cis-syn* conformation

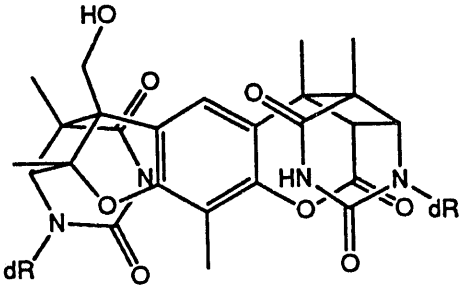

dT-HMT-dT diadduct, cis-syn conformation

Figure 1.3 Structures of the three main types of HMT-Thymidine adducts formed during the photo reaction of HMT with DNA. [Cimino et. al., 1985]

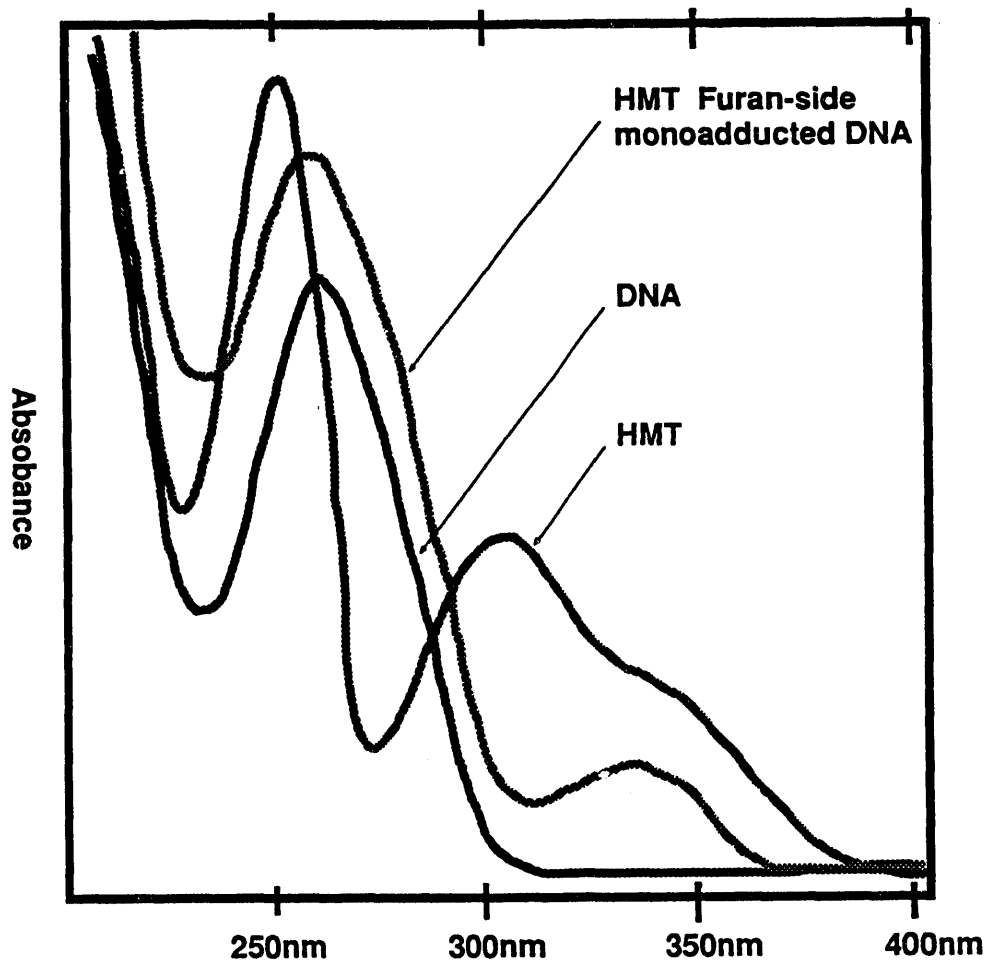

Figure 1.4 Comparison of the uncorrected UV absorption spectra of DNA, HMT, and a furanside monoadducted DNA 13 mer oligonucleotide (not normalized)

formed between DNA and several different psoralen derivatives have been reported including the crystal structure of the furan-side 8-MOP thymine monoadduct. The absorption spectra of these three adducts have been determined and their action spectra for the photochemistry described above have been determined (Shi and Hearst, 1987a). Figure 1.4 shows a comparison of the spectrum of HMT, a furan-side monoadducted oligonucleotide and DNA.

Synthesis of Spin-Labeled Psoralens:

In this study we make use of the well-characterized photochemistry of psoralen with nucleic acids to covalently attach spin labels at specific sites in nucleic acids. The spin labels attached in this way to their targets faithfully report the dynamics of nucleic acids. To synthesize a spin-labeled psoralen derivative with the properties of a rigid reporter group, the following points must be considered in the design of these photochemically attached EPR probes.

The first design consideration is maintaining the photoreactivity of a spin-labeled psoralen derivative with nucleic acids. Factors that affect the photoreactivity of a psoralen include steric interactions between the bulky spin-label on the psoralen and nucleic acids during the noncovalent binding or intercalation step, lowered solubility of the psoralen derivative in aqueous solution due to the large nonpolar spin label, and electronic interaction between the spin label and the psoralen nucleus which may reduce the photoreaction efficiency. Therefore, the functionality that is placed on the psoralen nucleus must be carefully chosen so that the photoreactivity of the psoralen is not adversely affected and at the same time the psoralen retains the ability to form cross-links and monadduct with oligonucleotides which can be enzymatically ligated to other pieces of DNA and/or RNA for the purpose of generating site specifically labeled large DNA and/or RNA.

Second, one must address the photochemical stability of the spin label. Since the spin-label reporter group on the psoralens are covalently attached to nucleic acids through a photo addition reaction, the spin label on the psoralen derivative must be photochemically stable under the conditions where psoralen photochemistry takes place. Nitroxides have a weak absorption at 410 nm. They can undergo photoreduction to the hydroxylamine, photoaddition insertion reactions, and in the case of 1-Oxyl-2,2,5,5-tetramethyl-3-pyrroline, the photo-extrusion of nitrous oxide. One of our first experiments was to irradiate a sample of TEMPONE in water with 300 mW/cm^2 320-380 nm light to determine its stability. After 5 min of irradiation under these conditions, there was no loss of EPR signal.

Third, mobility of the spin label in a nucleic acid helix after photochemical attachment must be held to a minimum. The steric bulk of the DNA surrounding the nitroxide was used to inhibit the independent motion of the reporter group. For the probe to faithfully report the motion of the nucleic acid to which it is attached, any independent motion of the spin label must be minimized. A 2-D ^1H NMR study of the oligonucleotide $d(GGGTACCC)_2$ cross-linked at the central 5'-TpA-3' site with AMT indicated that there was a 53° bend in the helix axis into the major groove and a 56° unwinding of the helix (Tomic *et al.*, 1987). Our first approach at modeling the DNA-spin label steric interactions involved using Dreiding models. A model of the AMT cross-linked oligomer was constructed using coordinates obtained from the solution NMR structure and the amino group of the AMT was replaced with the appropriate spin label moiety to give models of compounds **4**, **5**, and **6**. The 8-methyl group was replaced with the appropriate linker arm and spin label to model compounds **6**, **7**, and **8**. Using this method, we felt that placement of spin labels into the major or minor groove was possible. We then used the program Chem 3D to computer model these same compounds using these same NMR coordinates. No minimization of the resulting structures was done. The results obtained from this analysis were used qualitatively to help convince us that the molecules we intended to

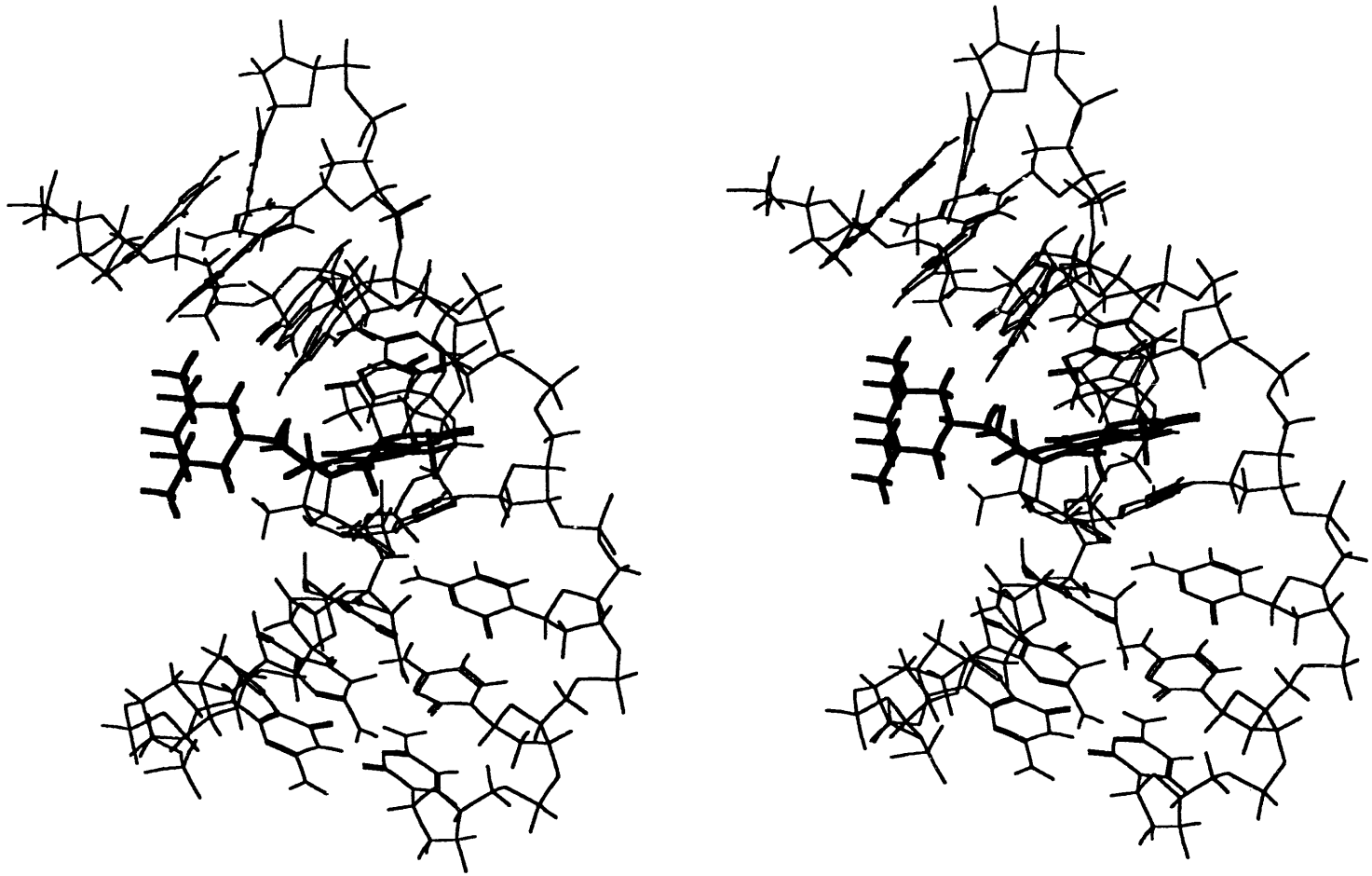

Figure 1.5 Stereo view of the 8 mer d(GGGTACCC) crosslinked at the central 5'-TpA-3' with AMT that has been substituted at the 4' position with TEMPAMINE. The psoralen is in bold lines.

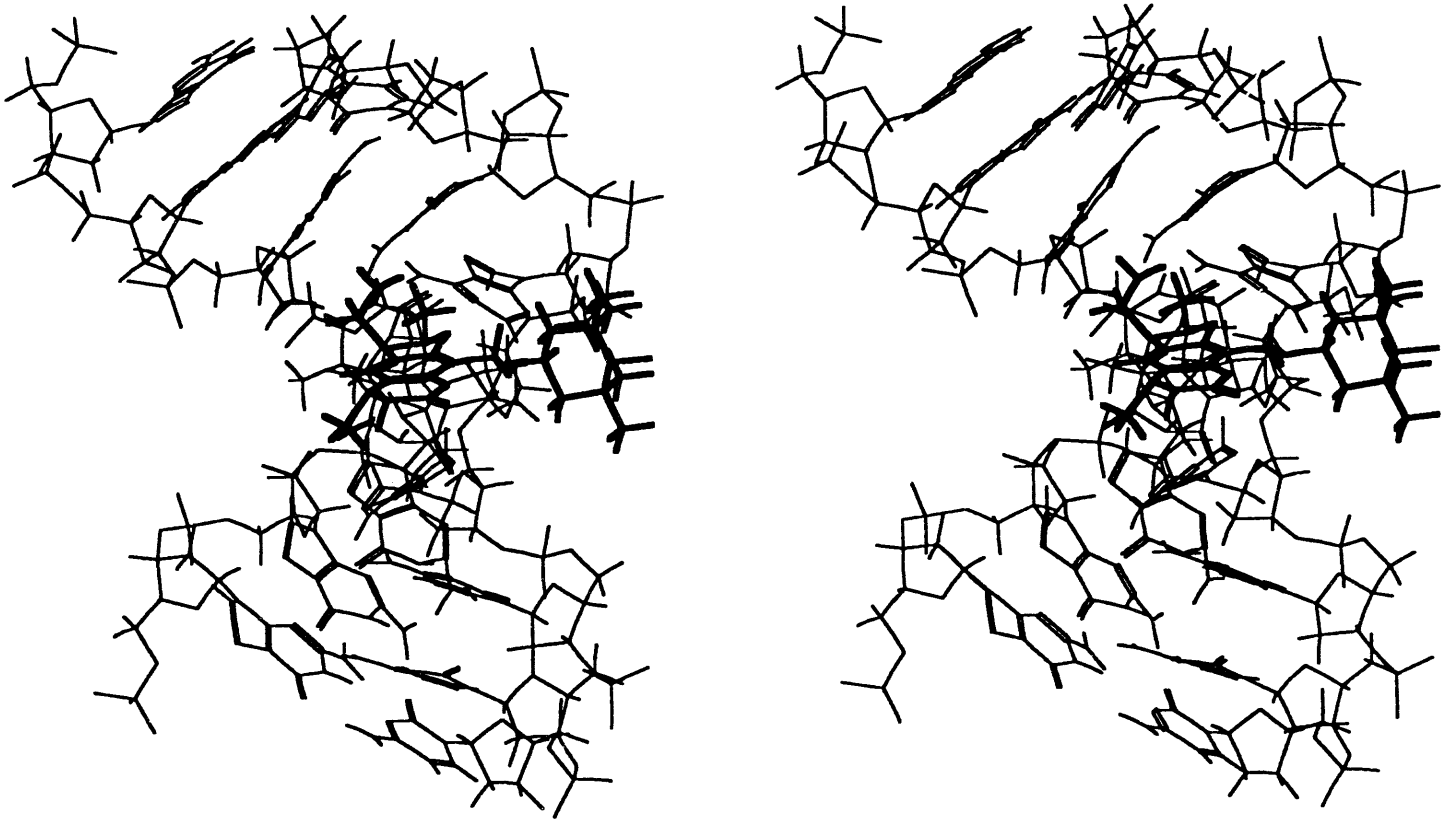

Figure 1.6 Stereo view of the 8 mer d(GGGTACCC) crosslinked at the central 5'-TpA-3' with AMT that has been substituted at the 8 position with TEMPAMINE. The psoralen is in bold lines.

synthesize stood a chance of working. We determined that substituting the amino group of the AMT cross-linked into the DNA with a bulky spin-label reporter group would maximize the steric interactions between the DNA and the nitroxide spin-label. Inspection of the structures of the T-HMT-T cross-link reveals that the substituents on the 4, 5, 4', and 5' positions of the psoralen are in the major groove of a DNA double helix. Substituents on the 8-position of the psoralen are in the minor groove. Figure 1.5 is a stereo view of the DNA 8-mer d(GGGTACCC)$_2$ cross-linked at the central 5'-TpA-3' site with AMT in which the 4'-amino group has been substituted by TEMPAMINE. It shows that there are significant steric interactions with the surrounding DNA that would inhibit free rotation of the spin label reporter group. Figure 1.6 is a stereo view of the same 8-mer where the TEMPAMINE has been attached to the 8-position of the AMT. Free motion of the spin label moiety appears to be hindered by many steric interactions between the spin label moiety and the surrounding DNA, most notably with the deoxyribose residues that make up the walls of the minor groove. It has been predicted that the DNA duplex can be kinked as much as 70° off the main axis into the major groove when psoralen cross-link is formed (Kim *et al.*, 1983) and it has been demonstrated that the preferred site of psoralen reactivity is the 5'-TpA-3' site in duplex DNA (Gamper *et al.*, 1984). The psoralen molecule is most easily functionalized at the 4' and 8 positions. The substituent groups on the psoralen effect each step of its interaction with nucleic acids. The position, steric, and electronic characteristics of the substituent groups on the psoralen ring system determine the psoralen's ability to intercalate and photoreact with the DNA. The intercalation complex is a very important factor in the cross-linking of psoralens to DNA because if a psoralen can not get to the furan-side monoadduct then it certainly cannot continue on to form cross-link. Some of the general trends for how substituent groups on the psoralen affect the intercalation and subsequent photoreactivity are as follows: Methylation of a psoralen increases the dark binding affinity, the quantum yield of photoaddition and the quantum yield of photobreakdown of the compound. A methoxy group at the 8-position slows both

the photochemistry with DNA and the photodestruction of the drug. Strong electron withdrawing or donating substituents such as hydroxy, amino or nitro groups drastically reduce or eliminate the ability of the psoralen to undergo photocylcoaddition with nucleic acids. Substitution at the 3-position of the psoralen nucleus with electronically active substituents is particularly unfavorable for high reactivity with nucleic acids. Relatively bulky groups which are positively charged and placed at the 4' and 5-positions of the psoralen ring system form compounds which have both high dark binding constants and high photoreactivity with DNA. This is important in the design of a spin labeled psoralen because of the bulky nature of the nitroxide group. The presence or absence of a methyl group at the 4-position of the psoralen has been shown to have a major role in controlling the amount of pyrone-side monoadduct formed with DNA. As mentioned above, pyrone-side adduct is a photochemical dead end on the path to cross-link. Since our model for steric constraint of the motion of the nitroxide was based on data for the interstrand cross-link, we wanted to synthesize molecules that would be good cross-linkers. Psoralens that contain a 4-methyl group such as TMP, HMT, and 4,5'-dimethyl-8-methoxypsoralen form less than 2% pyrone-side monoadduct when irradiated at 365 nm. This has been attributed to steric interference between the 4-methyl group of the psoralen and the 5-methyl group of thymidine in the intercalation complex with which the psoralen predominantly reacts. The reaction is a 2 + 2 photocylcoadditon forming a cyclobutane ring. The structure of the adducts formed between psoralens and nucleic acids are determined by the intercalation geometry of the psoralen and the nucleic acid. Psoralens react first primarily at the 4'5' double bond giving a furan-side monoadduct that still has a coumarin chromaphore. Molecular orbital calculations indicate that the psoralen is most reactive in its excited state at its 3,4 double bond. The minimum-energy geometry of the complex between 8-MOP and the oligonucleotide d(CGCGATATCGCG)$_2$, has been calculated with the psoralen derivative intercalated in between the central A,T base pairs (Demaret *et al.*, 1989). After the intercalation of 8-MOP within the oligonucleotide and energy minimization by

molecular mechanics, the geometry of the intercalation which was found predicts that photoreaction would result at the 4',5' double bond of the psoralen with the 5,6 double bond of the thymidine. The 3,4 double bond of the psoralen is too far removed from the pyrimidine 5,6 double bond to photoreact in this calculated geometry. Psoralens that do not contain a 4-methyl group such as 8-MOP and psoralen form up to 20% pyrone-side monoadduct with DNA. The size of the spin label as well as the length and position of attachment of the linker arm to the psoralen is important because the further away from the DNA the nitroxide is in the intercalation complex, the smaller the influence it's presence will be felt by the initial photochemical event of monoaddition.

With these restrictions in mind, we synthesized two sets of compounds that have spin label (nitroxides) reporter groups attached to the psoralen via single bonds that act as electronic insulators of the spin-label from the psoralen nucleus (Figure 1.7). One set is AMT (4'-aminomethyl-4,5',8-trimethylpsoralen. **1**) derivatives, **3**, **4**, and **5**, and the other set is 8-MOP (8-hydroxymethylpsoralen, *2*) derivatives, **6**, **7**, and **8**. Ideally, the nitroxide spin-label would be attached to the psoralen in such a fashion that it was incapable of any motion independent of the psoralen. Rotation about double bonds where the spin label group is conjugated to the psoralen π-system would be hindered. This is the approach that Hopkins and coworkers used in synthesizing a spin-labeled thymidine analog that could be incorporated into chemically synthesized DNA oligomers (Spaltenstein *et al.*, 1989). Unfortunately, functional groups that can conjugate with the psoralen nucleus dramatically decrease the photoreactivity of the compound. In most cases the reactivity toward nucleic acids is eliminated. To avoid free rotation of the spin label about these single bonds, we chose short linker arms to let the steric bulk of the DNA restrict independent motion (see above).

The synthesis and chemistry of nitroxide spin labels has been comprehensively reviewed by Keana (Keana, 1978) and Gaffney (Gaffney, 1976). The syntheses of the six spin-labeled psoralen derivatives is shown in figures 1.8 and 1.9. Mesylpyrrolinyl

Figure 1.7 The six psoralen derivatives synthesized in this study and their parent compounds

1

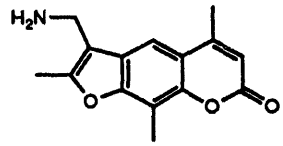

Spin labelled AMT derivatives on 4'-aminomethyl side

2

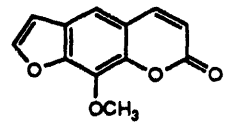

Spin labelled 8-hydroxypsoralen derivatives on 8-hydroxy side

3

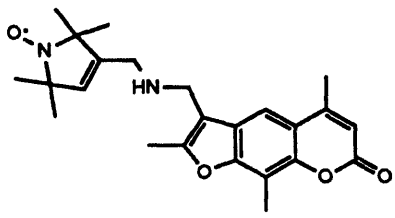

6

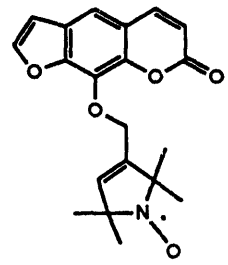

4

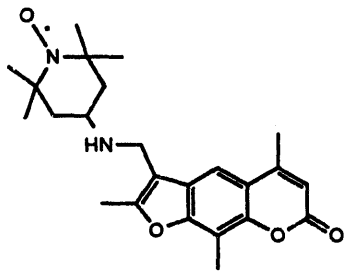

7

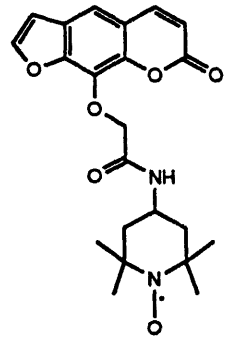

5

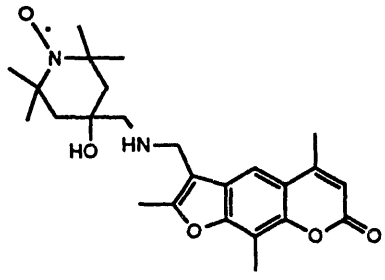

8

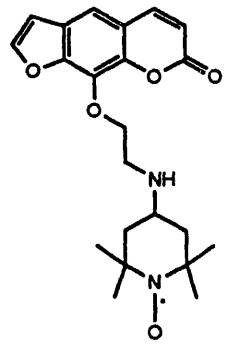

Figure 1.8 Synthetic pathway to the three spin-labeled AMT derivatives

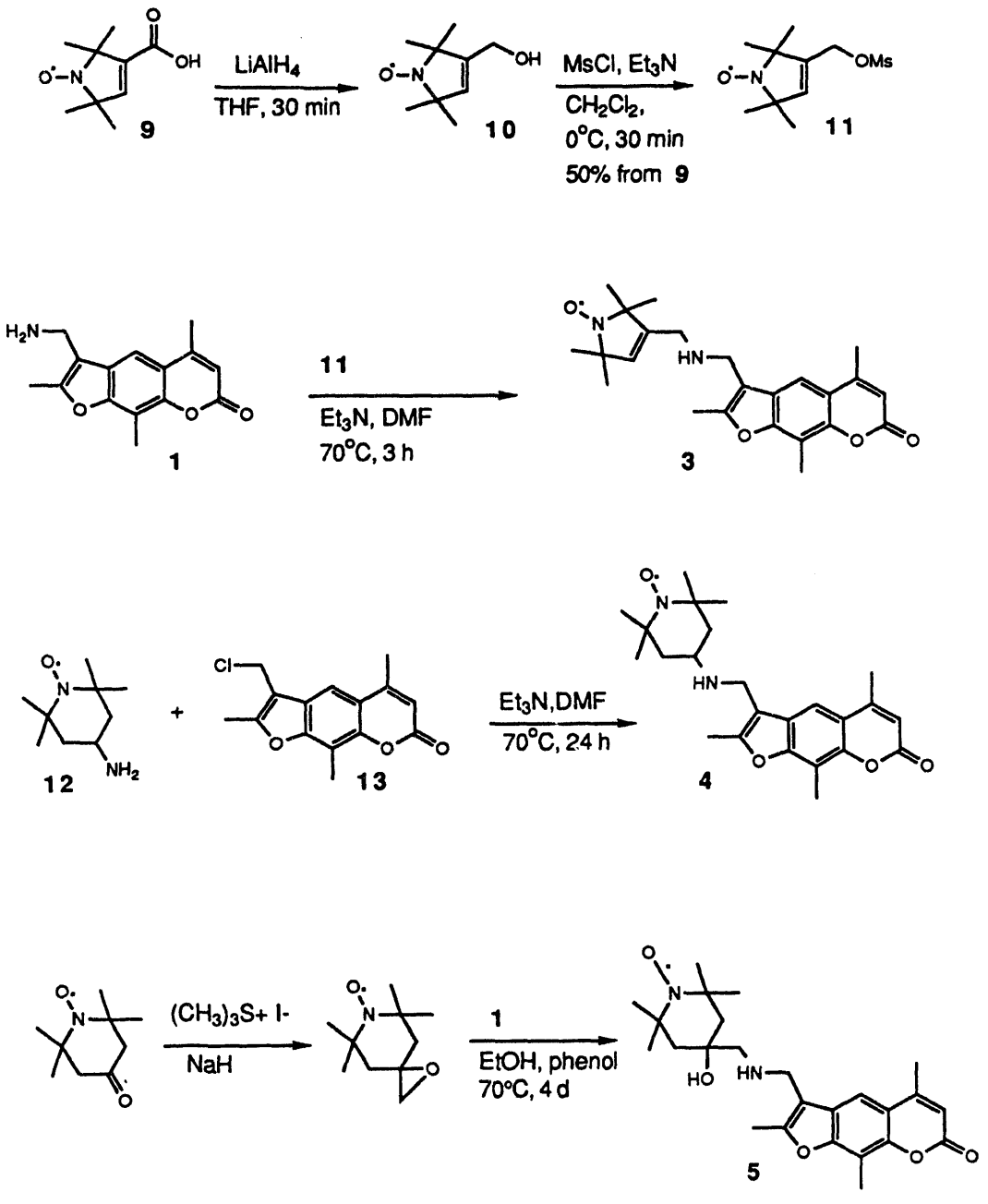

Figure 1.9 Synthetic pathway to the three spin-labeled 8-MOP derivatives

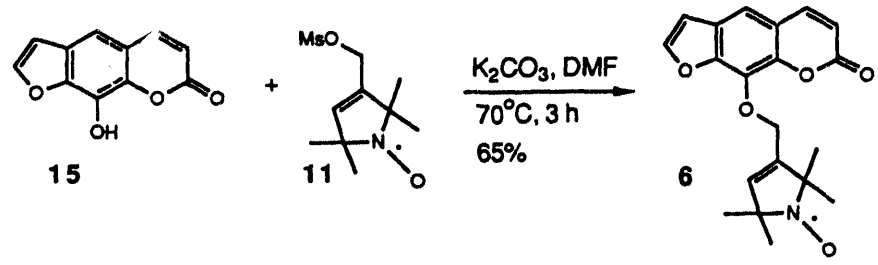

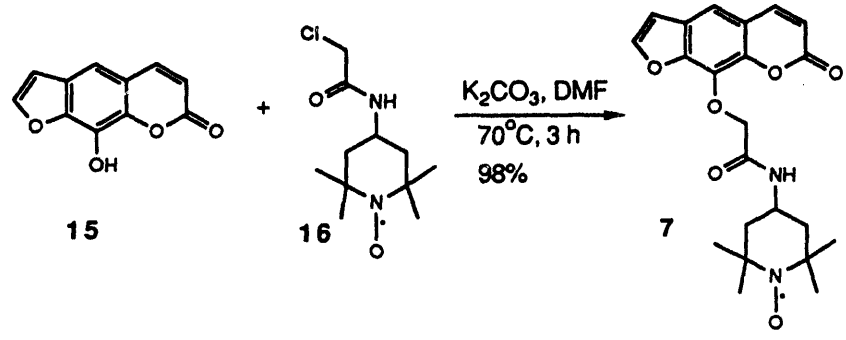

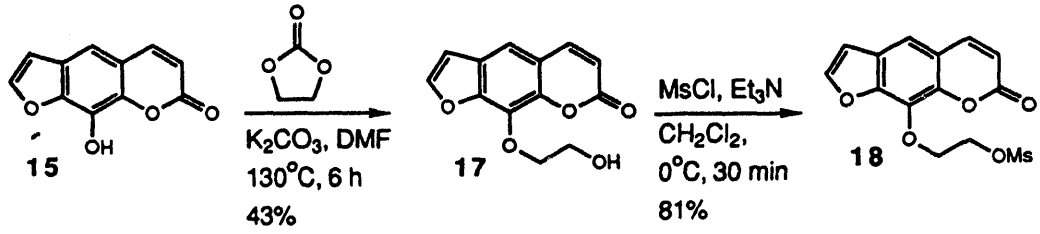

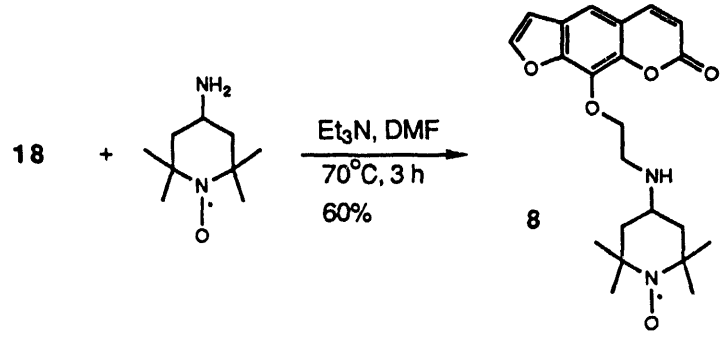

nitroxide **11** was prepared from carboxylic acid **9** by reduction (Rauckman and Rosen, 1976a) and mesylation in 50% overall yield. The displacement reaction of mesyl nitroxide by AMT in DMF (*N, N*-dimethylformamide) at 70°C for 3 h provided spin-labeled AMT derivative **3** in the 55% yield. Similar derivative **4** was prepared from TEMPAMINE **12** and 4'-chloromethyl-4,5',8-trimethylpsoralen (CMT, **13**) in 80% yield. Epoxide **14** (Rauckman *et al.*, 1976b)was ring opened by AMT in the presence of phenol slowly at 70°C, giving hydroxyamino psoralen in the 50% yield. 8-Hydroxypsoralen **15** was prepared from 8-MOP by demethylation with BBr_3 (57%, (Issacs *et al.*, 1982)). The displacement reaction of mesylpyrrolinyl nitroxide **11** by the phenoxide of **15** in DMF at 70°C for 3 h gave spin-labeled 8-MOP derivative **6** in good yield. Amido-8-MOP compound **7** was prepared in a similar manner as **6** from 8-hydroxypsoralen and TEMPO chloroacetamide in high yield (98%). Spin-labeled 2-aminoethoxypsoralen **8** was synthesized by displacement reaction from corresponding mesylate **18** and TEMPAMINE **12**. Treatment of a mixture of 8-hydroxypsoralen and ethylene carbonate with base provided the precursor alcohol **17** of mesylate **18**.

Photoreactivity of Spin-Labeled Psoralens with Double-Stranded DNA

The photoreactivity of the spin-labeled psoralens **3-8** were tested by reacting them with the double-stranded DNA formed by the self-complementary oligonucleotide 5'-GGGTACCC-3' (8-mer). This oligonucleotide contains a central 5'-TpA site that is especially reactive toward psoralen photo-cross-linking (Gamper *et al.*, 1984). An ethanolic solution of the spin-labeled psoralen was added to a solution of 5'(^{32}P)-labeled 8-mer, cooled to 0°C, and irradiated with 300 mW/cm^2 broadband 320-380 nm light (Cimino *et al.*, 1986). Under these irradiation conditions, there was no degradation of the ESR signal (data not shown). The resulting mixture of products was loaded onto a 20% polyacrylamide gel and electrophoresed. Under these conditions, cross-linked 8-mer

migrates much slower than the unmodified DNA. Quantitative measurement of the extent of reaction can be obtained by excising the gel bands and measuring the ^{32}P counts of each. Table 1.1 shows the results for the cross-link formation between the double-stranded 8-mer and the six spin-labeled psoralen derivatives as well as 8-MOP, AMT, and HMT (4'-hydroxymethyl-4,5',8-trimethylpsoralen). All six of the new psoralen derivatives except **8** have lower photoreactivity than 8-MOP, AMT, and HMT. At least two factors are responsible for this lower photoreactivity, lowered solubility in aqueous solution and unfavorable steric interactions between the intercalated psoralen and the DNA. Another possible cause of the lowered photoreactivity is quenching of the excited psoralen by the nitroxide. The cross-linking efficiency depends on the initial intercalative noncovalent binding of a psoralen to the DNA, and is sensitive to the solubility of the psoralen, the size of the substituents, and the substitution pattern on the psoralen. An attempt was made to use 389 nm light to form only the furan-side monoadducted oligonucleotide with psoralen **3**. With HMT, and AMT furan-side monoadduct is formed preferentially to cross-link under these conditions. This is due to the relative extinction coefficients of the psoralen and furan-side monadduct (figure 1.4). The wavelength dependency of this photochemistry is discussed in more detail in chapter 2. Only cross-linked molecules resulted from the reaction between the DNA and spin-labeled psoralen **3**. This can be rationalized if the quantum yield for the initial reaction to form furan-side monoadduct is much lower than the quantum yield for subsequent cross-link formation. The bulk of the spin-label group attached to the 4'-position of the psoralen seems to interfere with the intercalation geometry, slowing the rate of monoaddition. The aliphatic amino substituents greatly increase the solubility because they are charged in aqueous solution at neutral pH. This positive charge also stabilizes the binding of the psoralen by electrostatic interaction with the negatively charged phosphates of the DNA backbone. Of psoralens **3**, **4**, and **5**, the longer the linker is, the better the photoreactivity, in the order **4**, **3**, **5**, with **5** having an

Table 1.1 Amount of cross-link formation between the double-stranded 8-mer 5'-GGGTACCC-3' and the six spin-labeled psoralen derivatives and controls

Psoralen	% cross-link
3	13
4	9
5	23
6	9
7	31
8	44
HMT	53
AMT	43
8-MOP	38

Each reaction was performed by irradiating a 50 µl volume containing 10 µg/ml of the appropriate psoralen, 10 ng of 5'-^{32}P labeled 5'-GGGTACCC-3', 150 mM NaCl, 10 mM $MgCl_2$, 10 mM Tris-HCl pH 7.5 for 10 min with 300 mW/cm^2 320-380 nm light. The DNA was isolated by ethanol precipitation and the crosslinked species were separated by electrophoresis on a 20% denaturing PAGE. The the unmodified DNA and the bands that contained the cross-links were located by autoradiography, excised and counted with fluor in a scintillation counter.

Figure 1.10: Compound **3** in solution gave a symmetric ESR spectrum characteristic of fast motion (A), the cross-link formed between the 8-mer 5'-GGGTACCC-3' and compound **3** gave a ESR spectrum indicative of restricted slow motion of the spin bound in the double-stranded DNA helix. The interpretation of the EPR spectrum obtained from the cross-link 8 mer is discussed in the text.

A.

B.

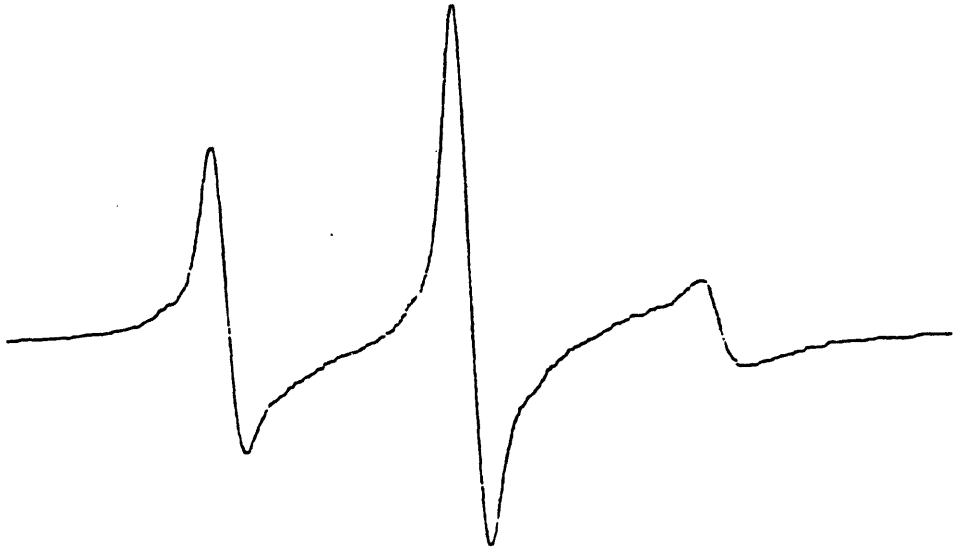

extra hydroxyl group to further increase solubility. A similar pattern is seen in compounds **6**, **7**, and **8**. We have also found out that psoralens with substituents at the 8-position are more reactive than those with substituents at the 4'-position. For this reason, compound **6** has the same reactivity as compound **4**, even though it is uncharged and extremely insoluble in water

We chose to continue our investigations with compound **3**. As mentioned above, the DNA may be locally kinked at the site of photoaddition (Kim *et al.*, 1983), thus bending the helix into the major groove and opening the minor groove around the psoralen. The spin label in compound **3** is attached to the 4'-position of the psoralen, thus placing it into the major groove. We chose to proceed with psoralen **3** because experience with the photochemistry of psoralens indicates that AMT derivatives form less pyrone-side adduct than do 8-MOP derivatives. Because we needed to make a preparative amount of cross-linked DNA oligomer, we wanted to have as high a level of photoreactivity and photocross-linking as possible. Although psoralen **8** gave the highest photoreactivity of the new psoralens, its longer linker arm between the psoralen nucleus and the spin label reporter group give the nitroxide more degrees of freedom than the free radical in psoralen **3**. With these predicted steric constraints, the spin label in the psoralen would be expected to have restricted motion, thus giving an ESR spectrum different from that of the free spin. Figure 1.10 shows this is the case. While the free spin in compound **3** in solution gave a symmetric ESR spectrum characteristic of fast motion, the cross-link formed between the 8-mer and compound **3** gave a ESR spectrum indicative of restricted slow motion of the spin bound in a double-stranded DNA helix. The interpretation of the EPR spectrum obtained from the cross-link 8 mer is discussed in more detail below.

Experimental Section

Materials and Methods. Pyridine and Tetrahydrofuran (THF) were distilled from sodium benzophenone ketyl. N,N-Dimethylformamide (DMF) was distilled from phosphorus pentoxide. Column chromatography was done by Flash chromatography with 40-63 μm silica gel 60 (EM Reagents (17)), High-performance liquid chromatography (HPLC) was performed using a 10 mm x 25 cm 5 μm Ultrasphere ODS preparative column (Altex). HMT, AMT, and CMT were gifts from HRI Associates Inc. (Concord, CA). Nitroxide spin label starting materiels were purchased from Molecular Probes Inc. (Portland, OR) The oligonucleotides were synthesized on an automated DNA synthesizer using the phosphoramadite method. After synthesis, the oligonucleotide was deprotected in concentrated ammonia solution at 55°C for 5-16 h and purified by electrophoresis on a 20% polyacrylamide-7 M urea gel followed by EtOH precipitation. The purification gel (40 cm x 40 cm x 0.12 cm) had a composition of 19:1 acrylamide/bis(acrylamide) and was run at 45 W with an aluminum plate clamped on the gel plate. [γ-^{32}P]ATP was purchased from Amersham. T4 polynucleotide kinase and T4 ligase were bought from Bethesda Research Laboratories. All other chemicals were purchased from Aldrich corp. or Sigma corp.

^{1}H NMR spectra were obtained with the UCB 250-MHz and UCB 200-MHz spectrometers and are reported in part per million downfield from internal tetramethylsilane reference. Elemental analyses were performed by the Analytical Laboratory, College of Chemistry, University of California, Berkeley, CA. Mass spectrometry was performed by the Mass Spectrometry facility, College of Chemistry, University of California, Berkeley, CA.

Chemical Synthesis

1-Oxyl-3-hydroxymethyl-2,2,5,5-tetramethyl-3-pyrroline **10**. Carboxylic Acid **9** (921 mg, 5 mmol) was dissolved in 25 mL of flash distilled THF. Lithium aluminum hydride (230 mg, 6 mmol) was added slowly. After being stirred for 20 min at room temperature, the reaction mixture was carefully quenched with 10% aqueous NH_4Cl solution. Sodium chloride and $CHCL_3$ (30 ml) were added and the mixture was filtered. The chloroform solution was dried (Na_2SO_4) and evaporated to dryness giving 500 mg (59%) of yellow crystalline **10** (This crude crystal was used for the following mesylation reaction without further purification): ^1H NMR of 1-hydroxy-3-hydroxymethyl-2,2,5,5-tetramethyl-3-pyrroline (200 MHz, $CDCL_3$) δ 1.36 (s, 6, $2CH_3$), 1.39 (s, 6, $2CH_3$), 3.4-4.0 (bs, 1, OH), 4.20 (s, 2, CH_2), 5.62 (s, 1, CH); mass spectrum (70eV), m/z (relative intensity) 170 (M^+, 42), 155 (10), 140 (34), 125 (20), 122 (14), 107 (100). Anal. Calcd for $C_9H_{16}NO_2$: C, 63.50; H, 9.47; N, 8.23. Found: C, 63.33; H, 9.50; N, 8.07.

1-Oxy-3-methanesulfonyloxymethyl-2,2,5,5-tetramethyl-3-pyrroline **11**. The alcohol **10** (494 mg, 2.9 mmol) was dissolved in dichloromethane (8.5 ml) and triethylamine (411 mg, 4.1 mmol) was added. The solution was cooled to -5°C. Methanesulfonyl chloride (332 mg, 2.9 mmol) was added dropwise. After being stirred for 30 min, the reaction mixture was quenched with the aid of more dichloromethane and with ice. The organic layer was washed with cold water and 5% aqueous sodium bicarbonate and dried (Na_2SO_4). Removal of solvent in vacuo and flash chromatography gave 567 mg (79%) of yellow solid of mesylate **11**; 1H NMR of 1-hydroxy-3-methanesulfonyloxy-methyl-2,2,5,5-tetramethyl-pyrroline (200 MHz, $CDCL_3$) δ 1.35 (s, 6, $2CH_3$), 1.38 (s, 6, $2CH_3$), 3.05 (s, 3, SCH_3), 4.73 (s, 1, CH); UV (EtOH) start absorb from 260nm; mass spectrum (70 eV), m/z (relative intensity) 248 (M^+, 36), 233 (12), 218 (3), 153 (5), 138

(9), 122 (18), 107 (100). Anal. Calcd for $C_{10}H_{18}NO_4S$: C, 48.37; H, 7.31; N, 5.64; S, 12.91. Found: C, 48.63; H, 7.42; N, 5.65; S, 12.54.

4'-[N-(1-Oxy-2,2,5,5-tetramethyl-3-pyrrolinyl)methylamino]methyl-4,5',8-trimethylpsoralen **3**. Mesylate **11** (330 mg, 1.13 mmol) and 4'-aminomethly-4,5'8-trimethylpsoralen (AMT) (490 mg, 1.28 mmol) were placed in two-neck flask with a reflux condenser under a nitrogen stream. After adding DMF (3 ml) and triethylamine (279 µl, 1.7 mmol) the solution was kept at 60°C for 5h with stirring. Then the DMF was evaporated in vacuo and the residue was partitioned between 5% aqueous sodium bicarbonate and dichloromethane. The organic layer was dried (Na_2SO_4) and evaporated in vacuo, giving the crude product. Flash chromatography (silica gel, 4% EtOH/CH_2Cl_2) and crystallization with EtOH yielded orange crystals of **3** (254 mg, 55%); ^1H NMR of 4'-[N-(1-hydroxy-2,2,5,5-tetramethyl-3-pyrrolinyl)methlamino]methyl-4,5',8-trimethylpsoralen 250 MHz, $CDCL_3$) δ 1.31 (s, 12, $4CH_3$), 2.49 (s, 3, CH_3), 2.51 (s, 3, CH_3), 2.58 (s, 3, CH_3), 3.31 (s, 2, pyrroline ring-CH_2N), 3.94 (s, 2, NCH_2-psoralen), 5.58 (s, 1, C3-H), 7.73 (s, 1, C5-H); UV (EtOH) λ max 340, 290, 250 nm; mass spectrum (70eV), m/z (relative intensity) 409 (M^+, 33), 395 (5), 379 (11), 256 (6), 240 (100), 212 (10), 138 (10). Anal. Calcd for $C_{24}H_{29}N_2O_4$: C, 70.39; H, 7.14; N, 6.84. Found: C, 70.18; H, 7.13; N, 6.73.

4'-[N-(1-Oxyl-2,2,6,6-tetramethyl-4-piperidinyl)amino]methyl-4,5',8-trimethylpsoralen**4**

To anhydrous N,N-dimethylformamide (DMF, 3 ml) was added 4'-chloromethly-4,5'8-trimethylpsoralen (CMT) (55.3 mg, 0.2 mmol), TEMPAMINE (34 mg, 0.2 mmol), and triethylamine (20.2 mg, 0.4 mmol) with stirring. The solution was heated at 70°C for 16 hr and turned dark brown. The solvent was evaporated. The residue was dissolved in 15 ml $CHCl_3$ and extracted once against 10 ml 5% HCl. The organic layer was discarded. 8M NaOH was added to the aqueous layer to pH 14 and extracted 3 x 10ml $CHCl_3$. The

combined organic extracts were dried over Na_2SO_4 and evaporated. The residue was applied to a 20 cm x 20 cm x 2 mm silica gel TLC plate and developed with 5% MeOH/$CHCl_3$. The major UV absorbing band was scraped off and eluted with 3 X 20 ml 10% EtOH/$CHCl_3$. The organics were evaporated to give 70 mg orange solid (85% yield). ^1H NMR of 4'-[N-(1-hydroxy-2,2,6,6-tetramethyl-4-piperidinyl)amino]methyl-4,5',8-trimethylpsoralen (250MHz, $CDCl_3$), δ 1.13 (s, 8, $2CH_3$), 1.23 (s, 8, $2CH_3$), 2.49 (s, 3, CH_3), 2.51 (s, 3, CH_3), 2.53 (s, 3, CH_3), 1.91 (m, 4, piperdine CH_2), 3.87 (s, 2, NCH_2-psoralen), 6.26 (s, 1, C3-H), 7.69 (s, 1, C5-H); UV (EtOH) λmax 340, 296, 250 nm; mass spectrum (70eV), m/z (relative intensity) 412 (M^+, 6), 411 (8), 379 (9), 338 (10), 282 (12), 256 (12), 241 (100), 212 (21), 155 (38), 141 (28), 124 (41), 98 (93), 58 (84). Anal. Calcd for $C_{24}H_{31}N_2O_4$: C, 70.05; H, 7.59; N, 6.80. Found: C, 70.04; H, 7.58; N, 6.62.

4'-[N-(1-Oxyl-4-hydroxy-2,2,6,6-tetramethyl-4-piperidinyl)methylamino]methyl-4,5',8-trimethylpsoralen **5**. 5,5,7,7-Tetramethyl-6-oxyl-1-oxa-6-azaspiro[2,5]-octane (**14**) was prepared from TEMPONE and trimethylsulfonium iodide with sodium hydride (Rauckman *et al.*, 1976b). AMT (**1**, 613 mg, 2.38 mmol) and epoxide (**14**, 354 mg, 1.92 mmol) were dissolved in ethanol (25 ml) and 10 mg phenol was added as catalyst. The solution was heated at 70°C for 4 days. After removal of ethanol, the residue was participated with dichloromethane and water. The organic layer was washed with 5% aqueous solution of sodium bicarbonate, dried (Na_2SO_4), and evaporated to give a orange red solid (837 mg). Flash chromatography on silica gel (5% EtOH/CH_2CL_2) provided **5** (420 mg, 50%): (recrystallized in EtOH/hexane); ^1H NMR of 4'-[N-(1-hydroxy-4-hydroxy-2,2,6,6-tetramethyl-4-piperidinyl)methylamino]methyl-4,5',8-trimethylpsoralen (250MHz, $CDCL_3$) δ 1.38 (s, 6, $2CH_3$) 1.50 (s, 6, $2CH_3$), 2.49 (s, 3, $2CH_3$), 2.51 (s, 3, $2CH_3$), 2.56 (s, 3, $2CH_3$), 2.60 (s, 2, piperidine ring-CH_2N), 3.97 (s, 2, NCH_2-psoralen), 6.24 (s, 1, C3-H), 7.67 (s, 1, C5-H); UV (EtOH) λmax 340, 297, 250 nm; mass spectrum

(70eV), m/z (relative intensity)441 (M^+, 3), 423 (2), 408 (6), 393 (23), 391 (23), 269 (17), 256 (19), 241 (60), 212 (42), 168 (37), 156 (32), 151 (29), 128 (61), 98 (65), 83 (68). Anal. Calcd for $C_{25}H_{33}N_2O_5$: C, 68.01; H, 7.53; N, 6.34. Found: C, 67.97; H, 7.64; N, 6.32.

8-(1-Oxyl-2,2,5,5-tetramethyl-3-pyrrolinyl)methoxypsoralen **6**. To anhydrous N,N-dimethylformamide (DMF, 3 ml) was added 8-hydroxypsoralen **15**, (55 mg, 0.27 mmol), mesylate **11** (79 mg, 0.27 mmol), and potassium carbonate (68 mg, 0.49 mmol) with stirring. The solution was heated at 70°C for 3 hr. The solvent was evaporated. The residue was dissolved in dichloromethane and passed through short silica/Na_2SO_4 column. The solvent was evaporated, providing a yellow solid **6** (46 mg, 48%) (recrystallized from ethanol); ^1H NMR of 8-(1-hydroxy-2,2,5,5-tetramethyl-3-pyrrolinyl)methoxypsoralen (250 MHz, $CDCl_3$) δ 1.23 (s, 6, $2CH_3$), 1.44 (s, 6, $2CH_3$), 5.02 (s, 2, OCH_2-psoralen), 5.83 (s, 1, pyrroline-H), 6.40 (d, 1, J =9.6 Hz, C3-H), 6.83 (peaks of C4'-H were overlapped with the peaks of phenylhydrazine), 7.47 (s, 1, C5-H), 7.75 (d, 1, J = 9.7 Hz, C4-H), 7.80 (s, 1, C5'-H) UV (EtOH) λmax 297, 262 (sh), 248 nm;

8-[2-(1-Oxy-2,2,6,6-tetramethyl-4-piperidinyl)amino-2-oxolethoxypsoralen **7**. To anhydrous N,N-dimethylformamide (DMF, 1 ml) and benzene (1 ml) was added 8-hydroxypsoralen (**15**, 55 mg, 0.27 mmol), TEMPO chloracetamide (**16**, 0.295 mmol), and potassium carbonate (68 mg, 0.49 mmol) with stirring. The solution was heated at 70°C for 1 h and turned dark brown. The solvent was evaporated. The residue was dissolved in dichloromethane and passed through short silica/Na_2SO_4 column, providing a yellow orange solid **7** (110 mg, 98%): (recrystallized from ethanol); ^1H NMR of 8-[2-(1-hydroxy-2,2,6,6-tetramethyl-4-piperidinyl)amino-2-oxo]ethoxypsoralen (250 MHz, $CDCl_3$) δ 1.47 (s, 6, $2CH_3$), 1.62 (s, , $2CH_3$), 2.04-2.32 (m, 4, $2CH_2$), 4.41-4.49 (m, 1, CH), 4.87 (s, 2, CH_2), 6.40 (d, 1, J =9.6 Hz, C3-H), 6.85 (peaks of C4'-H were

overlapped with the peaks of phenylhydrazine), 7.46 (s, 1, C5-H), 7.80 (d, 1, J = 9.7 Hz, C4-H), 7.88 (s, 1, C5'-H). UV (EtOH) λmax 297, 262 (sh), 248 nm; mass spectrum (70eV), m/z (relative intensity) 413 (M^+, 20), 399 (26), 384 (20), 327 (31), 260 (70), 215 (62), 202 (59), 154 (72), 140 (70), 126 (100), 109 (78), 84 (95). Anal. Calcd for $C_{22}H_{25}N_2O_6$: C, 63.91; H, 6.09; N, 6.78. Found: C, 63.77; H, 6.11; N, 6.67.

8-(2-Hydroxy)ethoxypsoralen **17**. A mixture of hydroxypsoralen **15** (600 mg, 2.97 mmol), ethylene carbonate (436 mg, 4.95 mmol), and K_2CO_3 (820 mg, 5.93 mmol in DMF (40 ml) was heated at 130°C under N_2. After 6 h, DMF was evaporated in vacuo and residue was partitioned between 30 ml of water and dichloromethane (3 x 30 ml). The combined organic layer was washed with 1 N sodium hydroxide solution, dried (Na_2SO_4), and evaporated in vacuo. Flash chromatography (silica gel, 5% EtOH/CH_2Cl_2) gave 485 mg (66.4%) of colorless crystalline **17**: ^{1}H NMR (200 MHz, $CDCl_3$) δ 2.04 (bs, 1 OH), 3.97 (t, 2, J = 4.5 Hz, CH_2OH), 4.59 (t, 2, J = 4.5 Hz, OCH_2CH_2OH), 6.39 (d, 1, J = 9,6 Hz, C3-H), 6.84 (d, 1, J = 2.2 Hz, C4'-H), 7.41 (s, 1, C5-H) 7.70 (d, 1, J = 2.2 Hz, C5'-H), 7.78 (d, 1, J = 9.6 Hz, C4-H); mass spectrum (70 eV), m/z (relative intensity) 246 (M^+, 36), 202 (100), 174 (55), 89 (27): exact mass (HR-EIMS) calcd for $C_{14}H_{10}O_5$ 246.0528, found 246.0521.

8-(20Methanesulfonyloxy)ethoxypsoralen **18**. The mesylation was performed in a manner similar to the method of compound **11**. The alcohol **17** (27 mg, 0.11 mmol), triethylamine (24.3 mg, 0.24 mmol), methanesulfonyl chloride (18.3 mg, 0.16 mmol) and dichloromethane (2 ml) were used. The organic layer was passed through neutral alumina (1/2 inch) and sodium sulfate (1/2 inch) and removal of solvent gave 35 mg (98%) of colorless crystals of mesylate **18**; (recrystallized in CH_3CN, almost recovered); ^{1}H NMR (200 MHz, $CDCl_3$) sigma 3.25 (s, 3, CH_3), 4.66 (t, 2, J = 2.6 Hz, CH_2), 4.75 (t, 2, J = 2.6 Hz, CH_2), 6.39 (d, 1, J = 9.7 Hz, C3-H), 6.85 (d, 1, J = 2.2 Hz, C4'-H), 7.42 (s, 1,

C5-H), 7.70 (d,1, J = 2.2 Hz, C5'-H), 7.78 (d, 1, J = 9.6 Hz, C4-H); mass spectrum (70 eV), m/z (relative intensity) 324 (M^+, 14), 202 (13), 201 (14), 173 (15), 123 (100), 107 (15), 89 (19), 79 (35), 73 (31). Anal. Calcd for $C_{14}H_{12}O_7S$: C, 51.84; H, 3.73; S, 9.89. Found: C, 51.88; H, 3.66; S, 9.76.

8-[2-(1-Oxy-2,2,6,6-tetramethyl-4-piperidinyl)aminolethoxypsoralen **8**. A solution of mesylate **18** (160 mg, 0.49 mmol), TEMPAMINE (101 mg, 0.52 mmol), and triethylamine (75 mg, 0.74 mmol) in DMF (5 ml) was stirred at 90°C for 40 h. The solvent was evaporated in vacuo and the residue was extracted by dichloromethane and water. The organic layer was washed with 5% aqueous sodium bicarbonate, dried (Na_2SO_4), and evaporated to provide crude mixture of **8**. preparative TLC (20 x 20 cm, 2 mm, 5% EtOH/CH_2Cl_2, developed twice) gave 8 (118 mg, 60%) as a reddish crystal: (recrystallized in CH_3CN); ^1H NMR of 8-[2-(1-hydroxy-2,2,6,6-tetramethyl-4-piperidinyl)amino]-ethoxypsoralen (250 MHz, $CDCl_3$) δ 1.23 (s, $2CH_3$), 1.32 (s, $2CH_3$), 1.80 (m, 4, piperidine ring-CH_2), 3.34-3.37 (bs, 2, CH_2N), 4.78-4.85 (bs, 4, OCH_2), 6.38 (d, 1, J = 9.7 Hz, C3-H), 6.85 (peaks of C4'-H were overlapped with the peaks of phenylhydrazine), 7.43 (s, 1, C5-H), 7.71 (m, 1, J = 2.3 Hz, C5'-H), 7.79 (d, 1, J = 9.7 Hz, C4-H); UV (EtOH) λmax 298, 262 (sh), 248 nm; mass spectrum (70 eV), m/z (relative intensity) 400 (M^++1, 12), 399 (M^+, 4), 385 (5), 384 (2), 396 (6), 326 (66), 312 (53), 298 (75), 202 (48), 183 (33), 169 (73), 112 (59), 98 (90), 96 (82), 84 (100). Anal. Calcd for $C_{22}H_{27}N_2O_5$: C, 66.15; H, 6.81; N, 7.01. Found: C, 66.23; H, 6.79; N, 7.02.

5'-End Labeling of DNA Oligonucleotides. The oligonucleotides were 5'-end labeled with [γ-^{32}P]ATP and T4 polynucleotide kinase according to standard procedures (Maniatis *et al.*, 1982). The amount of enzyme in each aliquot used in the following experiments was approximately equal to the amount required to completely phosphorylate the 5'-end of the oligonucleotide, which was estimated on the basis of the amount of DNA

present, the incubation time (usually 2-5 h), and the assumption that 1 unit of enzyme will kinase 1 nmol of oligonucleotide in 0.5 h at 37°C. A 1X linker kinase buffer (70 mM Tris-HCl, 10 mM $MgCl_2$, 5 mM dithiothreitol, pH 7.6) containing the oligonucleotide to be labeled, [γ-^{32}P]ATP, and an aliquot of kinase was incubated at 37°C for a few hours. The reaction was then chased to completion by adding cold ATP to a final concentration of 1mM, another aliquot of enzyme, 10X linker kinase buffer to maintain a 1X buffer concentration and incubating at 37°C. To ensure complete kinasing, a third aliquot of kinase was added, and the solution was incubated again at 37°C. The mixture either was used directly or was EtOH-precipitated (10mM $MgCl_2$, 0.2 N NaCl, 2.5 v/v EtOH). After EtOH precipitation, the DNA was then dissolved in water or the appropriate buffer and stored at -20°C.

Preparation of Psoralen 3 Cross-Linked Double-Stranded 5'-GGGTACCC-3'. The cross-link was prepared following the procedures of Cimino et al. (Cimino *et al.*, 1986). A total of 400 µg of 5'-GGGTACCC-3' was dissolved in 700 ml of irradiation buffer (50 mM Tris-HCl, 0.1 mM EDTA, 150 mM NaCl, 10 mM $MgCl_2$, pH 7.6) after kinasing and EtOH precipitation. 15 µl of concentrated Psoralen 3/DMSO solution was added to the reaction mixture (final psoralen 3 concentration was 1.5 x 10^{-4} M). The mixture was irradiated in a 4 ml 1 cm pathlength quartz cuvette for 10 min at 4°C with broad-band light from a 2.5-kW Hg/Xe lamp, which was filtered through Pyrex glass and an aqueous cobaltous nitrate solution [1.7% $Co(NO_3)_2$, 2% NaCl, 9-cm path length] (320-380 nm, 300 mW/cm^2; (Cimino *et al.*, 1986)). The irradiated DNA was EtOH-precipitated and electrophoresed on a 20% polyacrylamide-7 M urea gel (40 cm x 40 cm x 0.05 cm, 35 W for 3-4 h). The cross-link and the unmodified DNA bands were located by autoradiography, excised, and eluted from the gel with a solution of 50 mM NaCl-1 mM EDTA. The unmodified DNA and cross-link were finally EtOH precipitated, washed, and dissolved each in 200 µl of H_2O. The unmodified DNA was stored at -20°C and the cross-link at 4°C.

Synthesis of modified oligonucleotides using the Argon laser: Irradiations were carried out a SpectraPhysics 2045 Argon laser operating in broad band mode centered at 366 nm at a power of 5.0 W. The 5'-OH oligonucleotides were dissolved in 35 ml of 150 mM NaCl, 10 mM $MgCl_2$,1 mM EDTA, 15 mM azide, $3.5X10^{-5}$ M of the desired spin labeled psoralen. This solution was flowed through a 1cm path length quartz flow cell cuvette at a rate of 1.5 ml/min. The cuvette was placed in the laser beam and irradiated for 40 min. After the irradiation was complete, the solution was brought to 200 mM NaCl with 6.1 M NaCl, and 3 volumes of absolute EtOH were added. Solution was cooled overnight at -20°C and the precipitate collected by centrifugation at 25,000 x g for 2 hours. The supernatant was removed and the pellet washed with 95% EtOH and dried in vacuo. The precipitated DNA was loaded a 15% 8 M urea denaturing polyacrylamide gel (40 cm x 40 cm x 0.05 cm) and electrophoresed at 45 W for 3 hours. The cross-link and the unmodified DNA bands were located by autoradiography, excised, and electroeluted from the gel. The unmodified DNA and cross-link were finally EtOH precipitated, washed, and dissolved each in 600 µl of TE.

Ligation of the cross-linked 21 mers and 24 mers. The gel purified cross-linked 21 mer or 24 mer oligonucleotides were kinased as above. The DNA strands were phenol extracted, once with phenol, once with phenol:chloroform, and once with chloroform, precipitated twice, resuspended in 0.5× TE, and the ligase reaction components were added. The final 600 µl reaction contained 66 mM TrisHCl, pH 7.6, 6.6 mM $MgCl_2$, 10 mM DTT, 50 µg/ml BSA, 1 mM ATP, and 4000 U T4 DNA ligase. The reaction was incubated for 16 hrs at 16 °C. The reaction mixture was then adjusted to 200 mM NaCl and precipitated with ethanol. The precipitate was collected by centrifugation, washed, dried, and loaded onto an 8% polyacrylamide denaturing gel, and electrophoresed at 50 W. The multimerized DNA bands were located by autoradiography, excised, and electroeluted from the gel. The individual multimerized cross-linked molecules were finally EtOH precipitated, washed, and dissolved each in 10 µl of TE.

Klenow reaction to fill in the 5' overhanging ends of the multimerized 21 mers. The individual multimers isolated from the ligation reaction of the 21 mer XL were dissolved in 20 µl Klenow reaction buffer (40 mM potassium phosphate pH 7.5, 6.6 mM $MgCl_2$, 1 mM DTT, 0.25 mM each dCTP, dGTP, dTTP and 40 µCi 600 Ci/mmol $\alpha^{32}P$ dATP). The reaction was initiated by adding 10 units of the Klenow fragment of DNA polymerase. After 4 hr the reaction was diluted with 20 µl 10 M urea, heat/cooled, and loaded onto a 12% 8 M urea denaturing PAGE. The filled in multimerized DNA bands were located by autoradiography, excised, and electroeluted from the gel. The individual multimerized cross-linked molecules were finally EtOH precipitated, washed, and dissolved each in 10 µl of TE.

Photochemical characterization of the psoralens

Figure 1.11 is an autoradiogram of cross-link reactions between the self-complementary DNA oligomer 5'-GGGTACCC-3' and the six spin labels **3-8** (structures in figure 1.7). Lanes 1-12 are cross-linking reactions with the psoralens **3-8** in pairs. The first lane in each pair is one addition of the psoralen followed by irradiation for 5 minutes with light transmitted through a $Co(NO_3)_2$ band pass filter (300 mW by uranium oxalate actinometry), and the second lane in each pair is a second addition of the psoralen followed by irradiation for an additional 5 minutes. Lanes 13-16 are control reactions. Lane 13 is the reaction of the oligomer with one addition of HMT; lane 14 is reaction with one addition of AMT; lane 15 is reaction with one addition of 8-MOP; and lane 16 is the DNA irradiated without any psoralen. Reaction with psoralen **3** yields three products that have mobility indicating a cross-link reaction has occurred. There are also 4 bands that indicate formation of monoadducts. Reaction with psoralen **4** (lanes 3 and 4) yield two products that have mobility indicating a cross-link reaction has occurred. There are two bands that indicate formation of monoadducts. Reaction with psoralen **5** (lanes 5 and 6) yield two main

Figure 1.11: Shown is an autoradiogram of cross-link reactions between the self-complementary DNA oligomer 5'-GGGTACCC-3' and the six spin labels **3-8** (structures in figure 1.7). Lanes 1-12 are cross-linking reactions with the psoralens **3-8** in pairs. The first lane in each pair is one addition of the psoralen followed by irradiation for 5 minutes with light transmitted through a $Co(NO_3)_2$ band pass filter (300 mW by uranium oxalate actinometry), and the second lane in each pair is a second addition of the psoralen followed by irradiation for an additional 5 minutes. Lanes 13-16 are control reactions. See the text for a more detailed interpertation of these data.

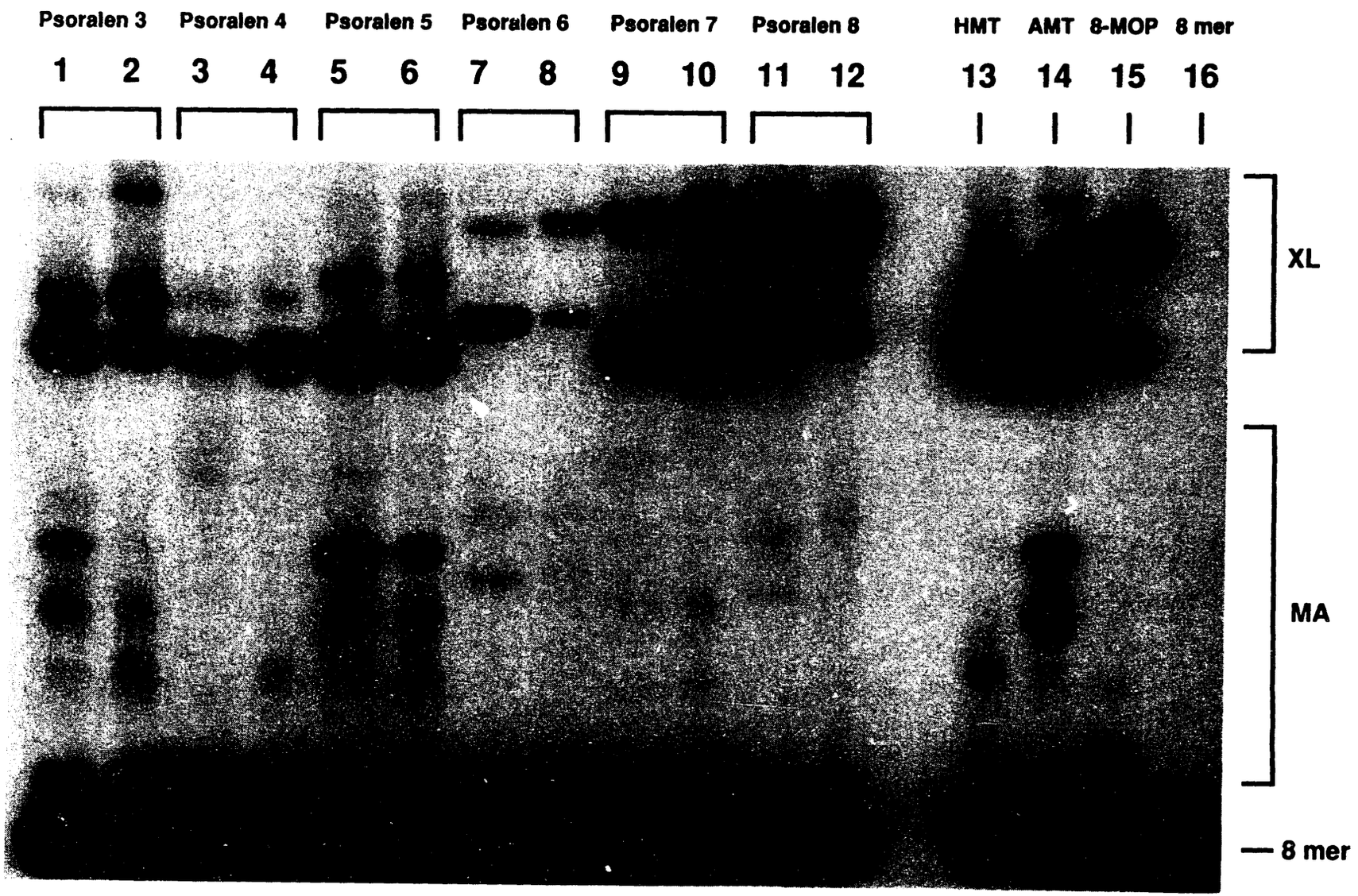
Psoralen 3
Psoralen 4
Psoralen 5
Psoralen 6
Psoralen 7
Psoralen 8
HMT
AMT
8-MOP
8 mer
1 2 3 4 5 6 7 8 9 10 11 12 13 14 15 16
XL
MA
8 mer

products that have mobility indicating a cross-link reaction has occurred. There are four bands that indicate formation of monoadducts. Reaction with psoralen **6** (lanes 7 and 8) yield two products that have mobility indicating a cross-link reaction has occurred. There are two bands that indicate formation of monoadducts. Reaction with psoralen **7** (lanes 9 and 10) yield two products that have mobility indicating a cross-link reaction has occurred. There are four bands that indicate formation of monoadducts. Reaction with psoralen **8** (lanes 11 and 12) yield two products that have mobility indicating a cross-link reaction has occurred. There are two bands that indicate formation of monoadducts. Reaction with HMT (lane 13) yielded two main cross-link species and two monoadducts. Reaction with AMT (lane 14) yielded one cross-linked species and two monoadducted oligos. Reaction with 8-MOP (lane 15) yielded two main cross-linked species and two monoadducted oligos. The control DNA in lane 16 was unaffected by the irradiation.

To further characterize the reaction of these novel psoralens, the major bands that corresponded to cross-links were excised and eluted from the gel and subject to conditions that photoreverse psoralen cross-links to monoadducts and unmodified DNA. The monoadducts that were formed during the forward cross-linking reaction were not further characterized. The eluted cross-links were divided into two portions; one that was reserved in the dark, and the other was photoreversed. To photoreverse the cross-links, they were irradiated under a germicidal lamp with its maximum emission at 254 nm for 2.5 minutes at a distance of 10 cm from the lamp to the surface of the solution. Following photoreversal, the products of the reaction were isolated and loaded onto a gel to compare the products with the unphotoreversed parent material.

Figure 1.12 is an autoradiogram of the photoreversal of the major bands that corresponded to cross-links for psoralens **3-5**. These are AMT derivatives. The lanes of the gel are photoreversal reactions of the major bands that formed in the reactions with the psoralens in pairs. The first lane in each pair is cross-linked oligomer photoproduct photoreversed with 254 nm light and the second lane in each pair is the parent material.

Figure 1.12: Shown is an autoradiogram of the photoreversal of the major bands that corresponded to cross-links for psoralens **3-5** shown in figure 1.11. These are AMT derivatives. The lanes of the gel are photoreversal reactions of the major bands that formed in the reactions with the psoralens in pairs. The first lane in each pair is cross-linked oligomer photoproduct photoreversed with 254 nm light and the second lane in each pair is the parent material. Lanes 15 and 16 are the reaction of the AMT cross-link control. See the text for a more detailed interpertation of these data.

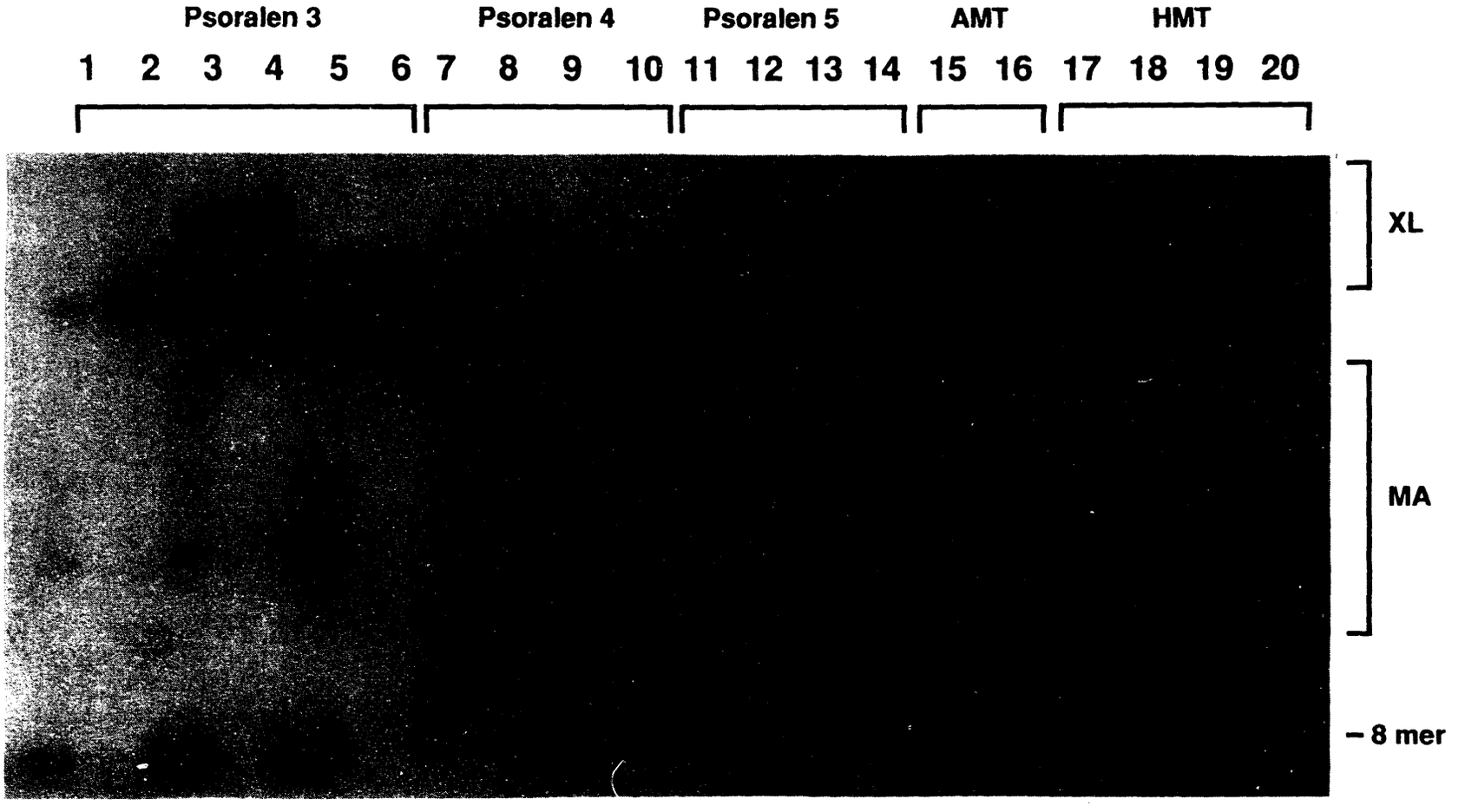
Psoralen 3
Psoralen 4
Psoralen 5
AMT
HMT
1 2 3 4 5 6 7 8 9 10 11 12 13 14 15 16 17 18 19 20
XL
MA
– 8 mer

Lanes 15 and 16 are the reaction of the AMT cross-link. Reversal of this cross-link gives two monoadducts and the unmodified DNA. Lanes 17-20 are photoreversal reactions of the two HMT cross-links. Lane 17 is photoreversal of the upper HMT cross-link. It gives two monoadducts; the unmodified DNA and a band with a mobility that corresponds to the lower cross-link (lane 20). This can be rationalized as a cross-link plus a monoadduct making up the modification on the upper band. Lane 19 is the photoreversal of the lower HMT cross-link. It gives two monoadducts and the unmodified DNA. These three photoreversal reactions constitute the control reactions. Lane 1 is the photoreversal of the upper most of the three cross-link bands formed by photoreaction with psoralen **3**. After elution from the initial cross-linking gel, it has the same mobility as the lower of the three cross-link bands (compare lanes 2 and 6). It gives two bands that correspond to monoadducts and the unmodified DNA. Lane 5 is the lower most of the three cross-link bands formed with psoralen **3** and it produces the same pattern as the uppermost band (compare lanes 1 and 5). This indicates that the uppermost and lower band in the cross-linking gel are the same material. One explanation for the different mobilities in the initial gel is that the two cross-linked species adopted different conformations during electrophoresis. The most likely alternate conformation is that of the ring open form of the pyrone-side of the cross-link. Lane 3 is the photoreversal reaction of the middle band formed by photoreaction with psoralen **3**. It is not a homogeneous material. There are at least four bands in the unphotoreversed parent material one of which has the same mobility as the materiel in lanes 2 and 6 (lane 4). Photoreversal of this material gave four monoadduct bands plus the unmodified oligomer. Two of these monoadduct bands were the same as the monoadducts formed in lanes 1 and 5. The simplest explanation for these results is the presence of multiple psoralen adducts in the middle band. Lane 7 is the photoreversal of the upper most of the two cross-link bands formed by photoreaction with psoralen **4**, and lane 9 is the photoreversal of the lower of the two. The upper band is contaminated with a small amount of materiel that has the same mobility as the lower band.

Lane 7 indicates that four monoadducts are formed from this mixture. Lane 9 indicates that the lower cross-linked materiel gives two different monoadducts. Two of the monoadduct bands in lane seven are the same as those in lane nine. Lane 11 is the photoreversal of the upper most of the two cross-link bands formed by photoreaction with psoralen **5**, and lane 13 is the photoreversal of the lower of the two. The upper band is contaminated with a small amount of materiel that has the same mobility as the lower band. Two monoadduct bands and the unmodified oligomer are produced by photoreversal in lane 13. Photoreversal of the upper band yields four monoadducted oligonucleotides, two of which have the same mobility as the adducts in lane 13 (lane 11).

Figure 1.13 is an autoradiogram of the photoreversal of the major bands that corresponded to cross-links for psoralens **6-8**. These are 8-MOP derivatives. The lanes of the gel are photoreversal reactions of the major bands that formed in the reactions with the psoralens in pairs. The first lane in each pair is cross-linked oligomer photoproduct photoreversed with 254 nm light and the second lane in each pair is the parent material. Lanes 13-16 are photoreversal reactions of the two 8-MOP cross-links. Lane 13 is photoreversal of the upper 8-MOP cross-link. It gives two monoadducts; the unmodified DNA. Lane 15 is the photoreversal of the lower 8-MOP cross-link. It gives two monoadducts and the unmodified DNA. Lanes 13 and 15 show products with identical electrophoretic mobility. The different mobilities of the two products in the initial gel reflects two different conformations that the cross-linked species adopt during electrophoresis. The most likely alternate conformation is that of the ring open form of the pyrone-side of the cross-link. These two photoreversal reactions constitute the control reactions. Inspection of the gel indicates that the pairs of upper and lower bands that were excised from the gel in figure 1.11 (lanes 1 and 3 for psoralen **6**, lanes 5 and 7 for psoralen **7**, and lanes 9 and 11 for psoralen **8**) give the same distribution of photoreversal products. The explanation for this is the same as that given above for the 8-MOP cross-links.

Figure 1.13: Shown is an autoradiogram of the photoreversal of the major bands that corresponded to cross-links for psoralens **6-8** shown in figure 1.11. These are 8-MOP derivatives. The lanes of the gel are photoreversal reactions of the major bands that formed in the reactions with the psoralens in pairs. The first lane in each pair is cross-linked oligomer photoproduct photoreversed with 254 nm light and the second lane in each pair is the parent material. Lanes 13-16 are photoreversal reactions of the two 8-MOP cross-links. See the text for a more detailed interpertation of these data.

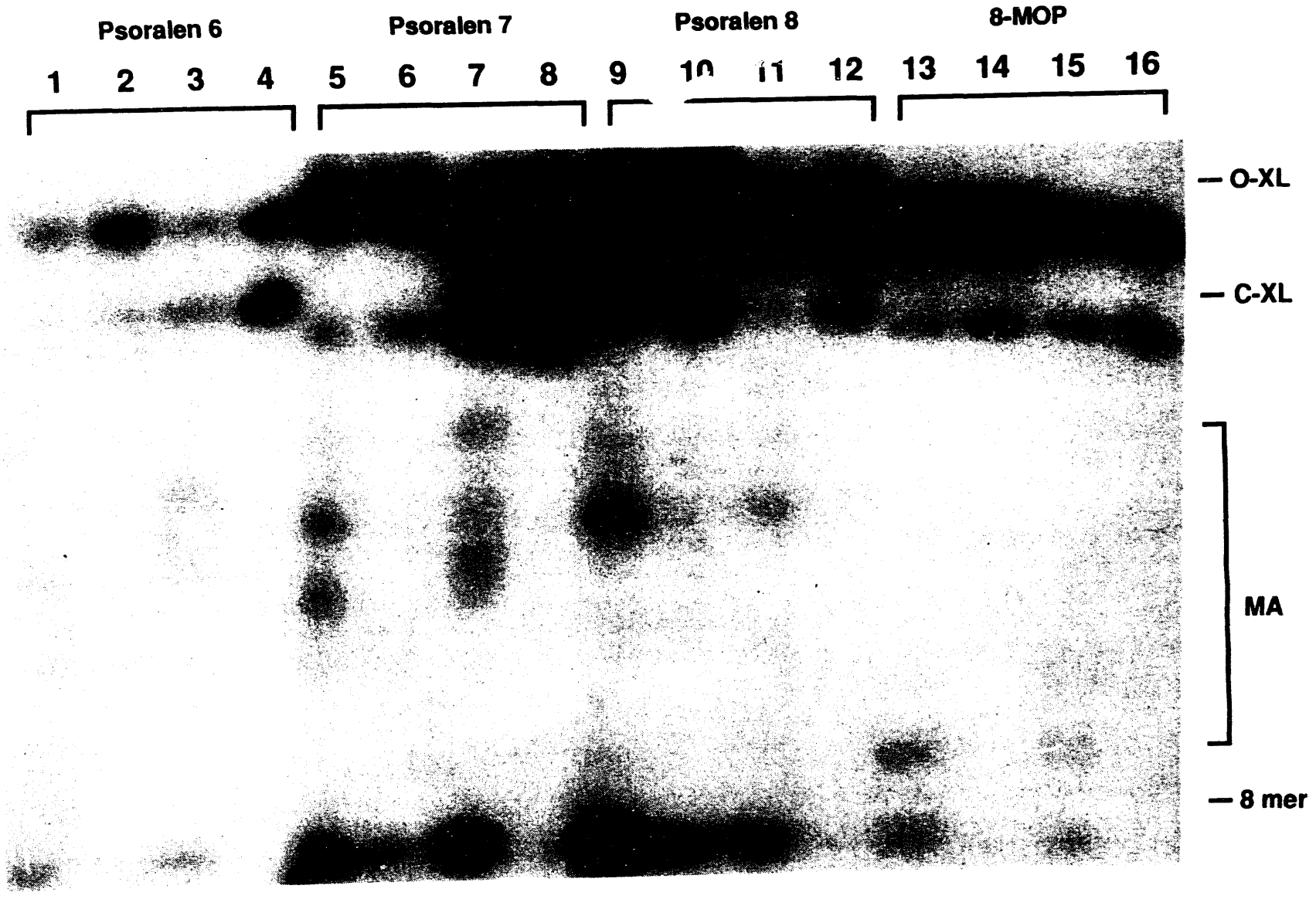
Psoralen 6
Psoralen 7
Psoralen 8
8-MOP
1 2 3 4 5 6 7 8 9 10 11 12 13 14 15 16
— O-XL
— C-XL
MA
— 8 mer

In order to investigate the length dependence of the DNA oligomer to which the spin-label was photobound, we investigated the reaction between compounds 3 and 4 and two sets of DNA oligomers. The first set of DNA oligomers were a pair of complementary 21 mers that formed a helix of 17 base pairs with four base overhangs on each end. The second set of DNA oligomers were a pair of complementary 24 mers that formed a helix 20 base pairs long with four base overhangs on each end. Both ends of the duplex have a Bam H1 restriction site. There is a central 5'-TpA-3' site in both of the duplexes. The sequences are shown below.

```
5'-GAT-CCG-AGC-TCG-GTA-CCC-GGG-AGC-3'          24 mers
     3'-GC-TCG-AGC-CAT-GGG-CCC-TCG-CTA-G-5'

 5'-AAT-TCG-AGC-TCG-GTA-CCC-GGG-3'             21 mers
      3'-GC-TCG-AGC-CAT-GGG-CCC-CTA-G-5'
```

A solution of the two 21mers or two 24 mers and psoralen 3 or 4 were irradiated in a flow cell using an argon-ion laser emitting at 366 nm to form cross-linked molecules. The DNA was isolated from the reaction mixture and the cross-linked isolated by preparative electrophoresis on denaturing polyacrylamide gels. This material was then multimerized by treatment with T4 DNA ligase. The multimerized 21 mers or 24 mers from the ligation mixture were separated from each other by preparative electrophoresis on denaturing polyacrylamide gels (Figure 1.14). The right-hand autoradiogram in figure 1.14 shows the ligation mixture run out on a 5% native polyacrylamide gel from the 24 mers. It can be seen that the majority of the material was ligated into pieces of DNA that were larger than could be resolved by the gel. Multimers of 1-8 24 mer duplexes were isolated by electrophoresing on a 1 mm x 40 cm x 40 cm denaturing gel. The left-hand autoradiogram in figure 1.14 shows the multimerized 21 mers made up of 1-8 units run out on a 12% denaturing gel as a final purification step. After elution of the individual multimerized cross-linked oligomers from the gel and purification and concentration, the DNA was placed in the ESR spectrometer and spectra of the spin-labeled DNAs were

Figure 1.14: The right-hand autoradiogram in this figure shows the products of the ligation of the 24 mers cross-linked with psoralen **4** run out on a 5% native polyacrylamide gel. It can be seen that the majority of the material was ligated into pieces of DNA that were larger than could be resolved by the gel. The left-hand autoradiogram shows the multimerized 21 mers made up of one to eight 21 mers crosslinked with psoralen **3** run out on a 12% denaturing gel as a final purification step. See text for further details.

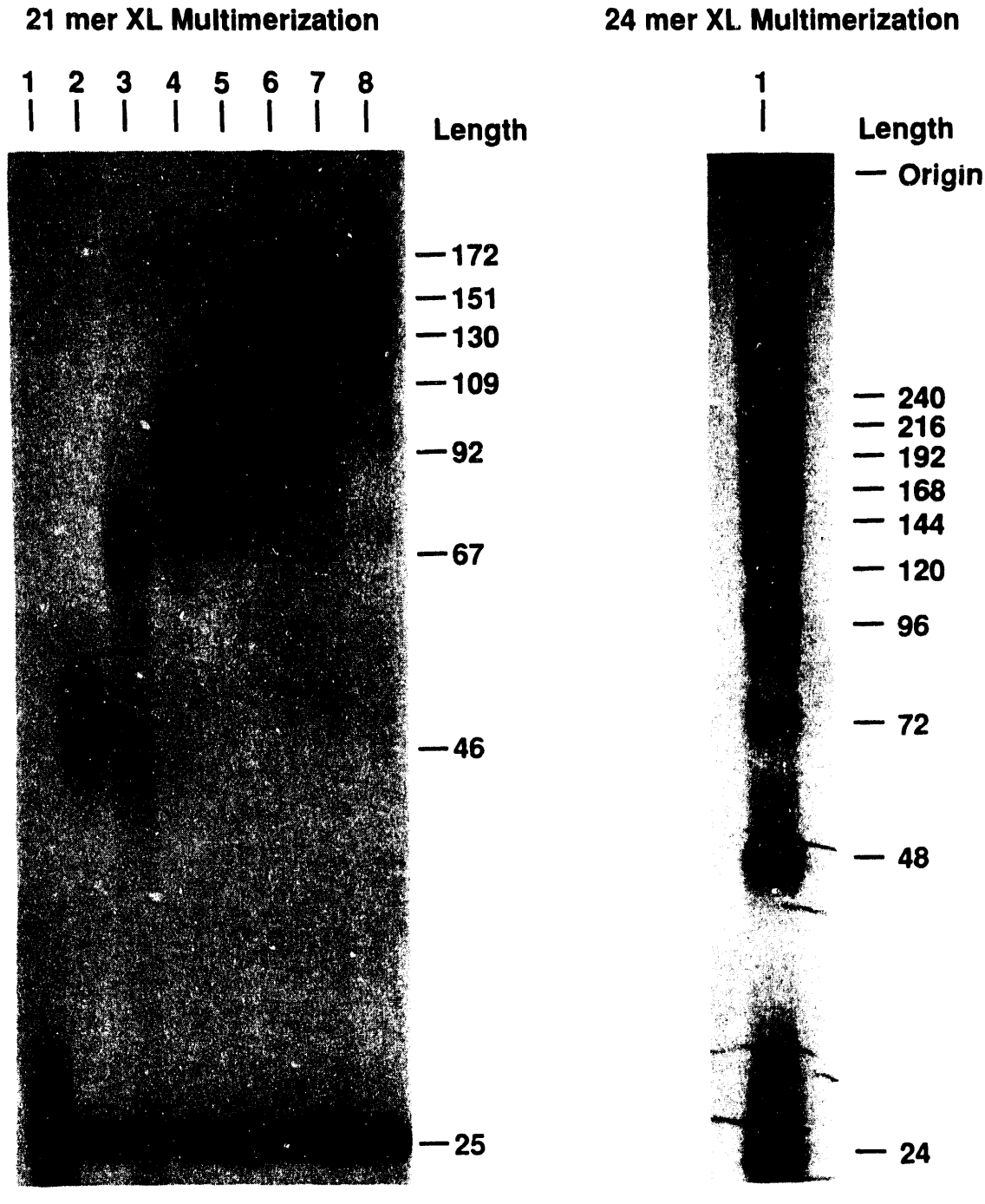
21 mer XL Multimerization
1 2 3 4 5 6 7 8
Length
172
151
130
109
92
67
46
25
24 mer XL Multimerization
1
Length
Origin
240
216
192
168
144
120
96
72
48
24

acquired. A number of technical difficulties appeared during this process. First, to insure that all the 5'-ends of the oligos were phosphorylated and therefore substrates for ligase, the oligomers had to be kinased. Secondly, recovery of the oligomers and multimerized oligomers from the gels was a inefficient process. Typically, only 50-80% of the DNA loaded onto a gel was recovered. The 21mers proved to be poor substrates for DNA ligase, giving a low yield of the desired multimers. On the other hand, the cross-linked 24 mers proved to be excellent substrates for DNA ligase with the majority of the material forming products of lengths greater than ten 24 mers ligated together. After the DNA was isolated from the gel, the remaining single stranded overhangs were filled in using the Klenow fragment of DNA polymerase and dNTP's to give blunt ended DNA fragments. In order to acquire a good EPR signal, a minimum of 10^{14} spins is necessary. This works out to be approximately 3 μg of cross-linked DNA 21 or 24 mers. Much larger quantities than this of each of the multimers 1-4 were synthesized. However, very little EPR signal was observed. This was ascribed to photodestruction of the spin-label by the intense laser light. When the psoralen itself was subject to irradiation by the 366 nm laser light, in aqueous solution, no degradation of the signal was observed. When the psoralen was cross-linked into DNA, signal was destroyed. Attempts were made to reoxidize the nitroxide using copper II and hydrogen peroxide; however, these failed. It is known that photochemically excited nitroxides in the appropriate geometry can either photoreduce or photochemically insert themselves into sigma bonds. If the psoralen-DNA-spin label complex was photoreduced, copper catalyzed reoxidation of the nitroxide should be possible. If the nitroxide had photo-inserted itself into the surrounding DNA molecule, then no reoxidation and recovery of the EPR signal would be possible. A further experimental difficulty encountered was the destruction of the EPR signal over time after the DNA had been introduced into the sample tubes. We sealed the EPR tubes containing our samples with a silicon based vacuum grease which destroyed spin label signal. After losing a spin label DNA sample to this phenomenon, we found that TEMPONE in aqueous

Tris buffer was destroyed by the vacuum grease as well with a half life of 11 hours. In spite of all these difficulties, EPR spectra were obtained for DNA molecules of length 8, 24, 46, and 92 base pairs long (figures 1.15 through 1.19). In all cases, the spectra can be interpreted to indicate that the nitroxide spin label that survived photodestruction and handling is faithfully reporting the motion of the DNA. Cross-linked and multimerized molecules of length 96, 109, 120, 130, 144, 151, and 172 base pairs were also successfully isolated, however there was not enough materiel available to acquire an adequate EPR spectrum.

Flow chart

1. Kinase the mixture of oligomers
2. Reaction of 21T and 21B with psoralen X in the laser.
3. Run a prep gel to separate XL away from MAp and UM 21mer
4. Electroelute the XL in an elutrap device, and then ppt the oligomer.
5. Ligate the recovered XL molecules together (Big loses)
6. Run a prep gel to separate the multimers 1-8
7. Electroelute the individual multimers in an elutrap device, followed by precipitation
8. Use the Klenow fragment and NTP's to fill in the ends of the fractions. label lightly with α^{32}P ATP.
9. Run a gel with the various fractions to further purify the multimers

   Electroelute the individual multimers in an elutrap device, followed by precipitation.
10. Take up the purified multimers in 10λ 150 mM NaCl, 100 mM Tris-HCl pH 7.3, and 5mM EDTA
11. acquire EPR spectra.

Results of purification

Multimer	Length	Cpm ^{32}P	cpm*(SL/molecule)	Ratio
1	24	142881	142881	35.5
2	46	24891	49782	12.0
3	67	60152	180456	43.6
4	88	25596	102384	24.8
5	109	9870	49350	12.0
6	130	4570	27420	6.6
7	151	1879	13153	3.2
8	172	517	4136	1.0

Multimer refers to the number of 21 mers ligated together. Length is in base pairs. Cpm was measured by cherenkov counting. cpm*(SL/molecule) normalizes the cpm to the number of spin labels in a molecule. Only the ends of a molecule are labeled with ^{32}P. Ratio refers to the anticipated EPR signal relative to the amount of 172 mer.

Interpretation of EPR Spectra

Electron paramagnetic resonance (EPR) is very similar in principle to NMR. The technique is not as well known as NMR because the signal arises from unpaired electron spins rather than nuclear spins. This limits the applicability of the technique to free radicals and certain metals and metal ions.

Since the electron magnetic moment is three orders of magnitude larger than typical nuclear magnetic moments, EPR spectrometers usually operate at higher frequencies than NMR instruments. All our experiments were performed at fixed frequencies on the order

of 9.2 GHz, in the microwave region. The larger magnetic moment and higher frequency also result in a sensitivity advantage over NMR. With our instrument we can easily detect as few as 10^{12} spins, this is approximately 1.7×10^{-12} moles.

While in NMR the signal is collected as a function of frequency at fixed magnetic field, all our data was taken at fixed frequency as a function of magnetic field. For technical reasons, the data collected and displayed is $d\chi/dH$, the first derivative of the absorption of the sample with respect to field, rather than the absorption itself.

We wish to use EPR to obtain information on the dynamics of DNA. Unfortunately DNA has no unpaired electrons. In order to study it by EPR, we need to attach a spin-label. Nitroxides are the free radicals of choice for spin-labeling due to their relative stability. In using a spin-label to study DNA dynamics, it is important to establish that the spin-label is rigidly attached to the DNA. If the spin-label is not rigidly attached, it will wobble independently of the DNA and will give an EPR spectrum indicative of faster motion than the DNA is actually undergoing.

The EPR spectrum of a nitroxide spin-label is determined by the interaction between the unpaired electron and the external field (fine structure interaction) and the interaction between the electron and the neighboring nitrogen nucleus (hyperfine interaction). The hyperfine interaction can be decomposed into two parts - the anisotropic hyperfine interaction (a.h.i.), which depends on the orientation of the spin-label with respect to the external magnetic field; and the isotropic hyperfine interaction, which does not depend on the spin-label's orientation. The a.h.i. may be partially or completely averaged out by rotation and tumbling of the spin-label. The extent of this averaging depends on the rate of rotation and determines the shape of the EPR spectrum. The spectrum may also be affected by the type of rotation the spin-label undergoes: anisotropic rotation results in different spectra than isotropic rotation.

The isotropic hyperfine interaction does not depend on the orientation of the spin-label and is therefore not affected by any motion of the spin-label. For ^{14}N nuclei, I = 1

and the EPR spectrum is a superposition of (2I + 1) = 3 lines, each corresponding to a different value of m_I, where m_I is the z-component of the nuclear spin. In the fast-motion limit, the a.h.i. is averaged out and results only in a slight difference in the line widths and heights for the 3 narrow lines in the spectrum. This limit occurs when the rotational correlation time, τ_c, is short compared to the inverse of the EPR transition frequency, typically 100ps. The rotational correlation time is the average time it takes a molecule to change its orientation by one radian. For 10^{-11} s $< \tau_c < 2\text{x}10^{-9}$ s , the a.h.i. is not completely averaged out and has a larger effect on the heights of each of the 3 lines. In this range of τ_c, the value of τ_c can be calculated from the EPR spectrum by taking ratios of line-heights (Likhtenshtein, 1974):

$$\tau_c = ((h_0/h_{-1})^{1/2} - 1)\, \Delta H_0 / 3.6\text{x}10^9$$

where h_0 is the height of the $m_I = 0$ line, h_{-1} is the height of the $m_I = -1$ line, ΔH_0 is the width of the m_I=0 line in Gauss. τ_c is in seconds. For $\tau_c > 2\text{x}10^{-9}$ s, each of the 3 lines broadens to the extent that they begin to overlap, and the rotational correlation time must be inferred from a more detailed comparison of the spectrum with simulated spectra calculated for different rotational correlation times.

The rigid-limit spectrum occurs for τ_c longer than 1/A, where A is the magnitude of the hyperfine splitting in Hertz. Our experimental data was acquired using continuous wave (CW) EPR. The CW EPR spectrum of nitroxides does not change with increasing τ_c beyond about 10^{-7} s. Dynamic information can still be extracted by other EPR techniques, as long as the rotational correlation time is not longer than $4T_1T_2\gamma dH_{res.}/d\theta$, where T_1 is the spin-lattice relaxation time, T_2 is the spin de-phasing time, γ the magnetogyric ratio, $H_{res.}$ the value of applied field at EPR resonance, and θ is the orientation angle of the nitroxide with respect to the applied field, **H** (see Future work, below).

Molecules in solution, in addition to diffusing in space, will diffuse in orientation. A roughly spherical molecule (e.g. most globular proteins) tumbles in solution with a rotational correlation time of $\eta V / k T$, where η is the viscosity and V the volume of the molecule. Cantor and Schimmel give a rule-of-thumb number of 1 nsec for each 2400 daltons of molecular weight.

A molecule which is not spherical will re-orient with more than one characteristic time. Cantor and Schimmel give expressions for prolate and oblate ellipsoids (p. 562 - 3)(Cantor and Schimmel, 1980). Intuitively, one would expect that a prolate ellipsoid (i.e. a football) or a rod will rotate more rapidly about its long axis than it will end-over-end. Since short (< 500Å, 150 base pairs) pieces of DNA are rod-like, they will have one rotational correlation time for rotation about their long axis and a longer time for end-over-end motion.

EPR spectra of nitroxides for isotropic rotation (such as that of spheres) are different from anisotropic rotation (such as for rods). With sufficient effort, orientational anisotropy can be incorporated into the analysis of EPR spectra. In our analysis of EPR spectra for spin-labelled DNA (see below), we have stuck to the simpler case of isotropic rotational motion. This may account for some of the differences between experimental and simulated spectra and also for differences between expected and observed rotational correlation times.

Results and Simulations of CW EPR spectra

For EPR spectra in the fast-tumbling region where the three lines of the nitroxide spectrum are well-separated and narrow, the rotational correlation time was calculated using the formula given above. These spectra for spin labeled psoralen **3** and for the self-complementary 8 mer 5'-GGGTACCC-3' cross-linked with psoralen **3** are shown in figure 1.10. The rotational correlation times are for these two molecules are 7×10^{-11} s and 2.5 x

10^{-9} s, respectively. These compare with times of 1.5 x 10^{-10} s and 2.1x10^{-9} s, calculated by applying Cantor and Schimmel's rule-of thumb for spherical molecules. This is a fairly good agreement for the two methods for calculating τ_c. An 8 mer duplex DNA is roughly spherical, being approximately 27Å in length, and 20Å in width. This result indicates that the rotational freedom of the nitroxide reporter group covalently bound to the DNA is indeed limited by its interaction with the surrounding molecule.

The spectra that we acquired for molecules larger than the 8 mer cross-link were too complex to be analyzed by simple application of the line height equation. This result in and of itself indicates that the independent rotation and/or reorientation of the nitroxide bound to the molecules was on a longer time scale than 3 nano-seconds. To get rotational correlation times for the larger molecules, we compared our experimental spectra with simulated spectra generated by a set of programs provided by Schneider and Freed (Schneider and Freed, 1989). All simulated spectra used the parameters g_{xx} = 2.00747, g_{yy} = 2.00581, g_{zz} = 2.00310, A_{xx} = 6.24 G, A_{yy} = 10.05 G, A_{zz} = 32.29 G, where the g-tensor couples the field H to the electron spin, and the A-tensor couples the electron and nuclear spins. For a more detailed discussion of the physics of EPR, see Wertz and Bolton.

The top panel of figure 1.15 is the experimentally acquired spectrum for the two 24 mers cross-linked with psoralen **4**. The top panel of figure 1.16 are the same DNA molecules except cross-linked with psoralen **3**. The top panel in figure 1.17 is the same molecule as in figure 1.15 except that it is 10 times more concentrated. The top panel of figure 1.18 is the spectrum aquired from a 46 mer cross-linked with psoralen **3** with two psoralen cross-links per molecule separated by 21 base pairs. It is unlikely that the spins on any individual molecule would interact with each other, because the vast majority of the nitroxides in this sample were destroyed in the photochemical cross-link formation step. The best simulated spectra for each of these are shown in the bottom panel of figures 1.15 through 1.19. The fit to the spectrum in figure 1.15 gives a τ_c of 5ns. The spectrum in figure 1.16 also has a reasonable resemblance to a 5ns simulation, although it seems to

Figure 1.15 EPR spectrum of 24 mer cross-linked with psoralen **3**

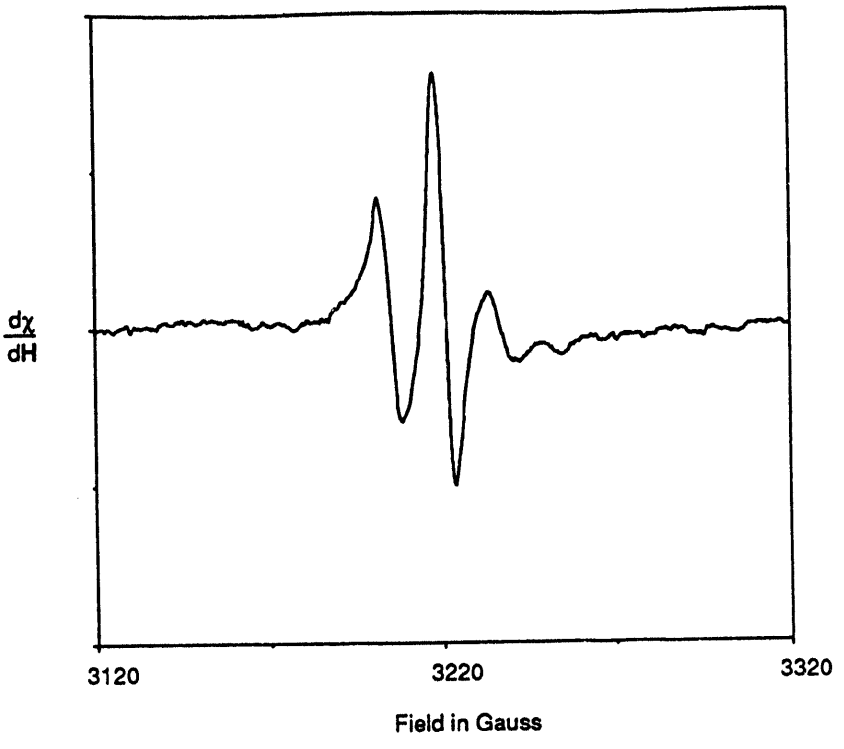

Best simulated spectrum

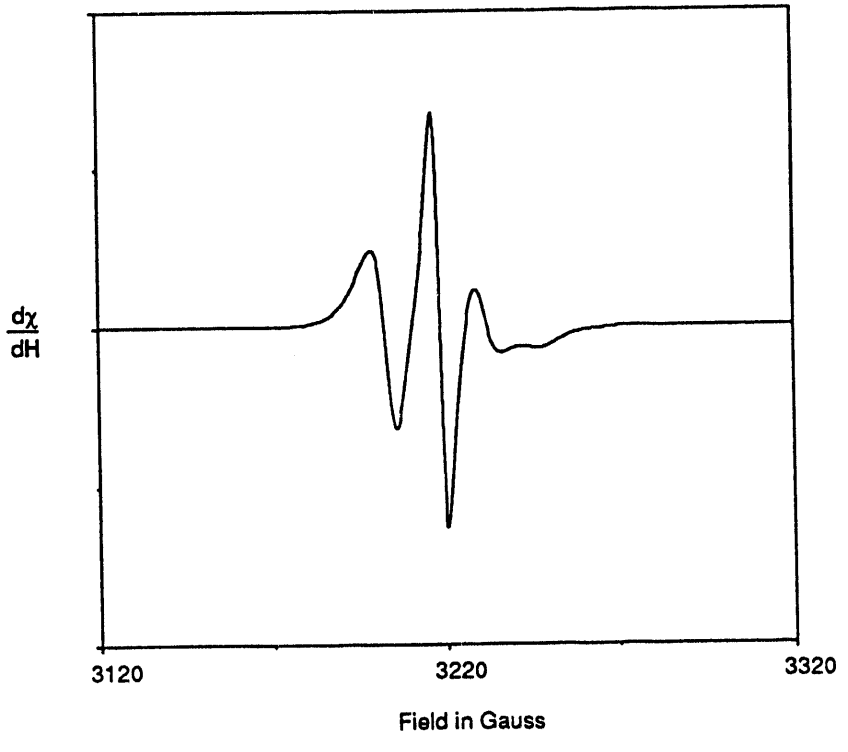

Figure 1.16 EPR spectrum of 24 mer cross-linked with psoralen **4**

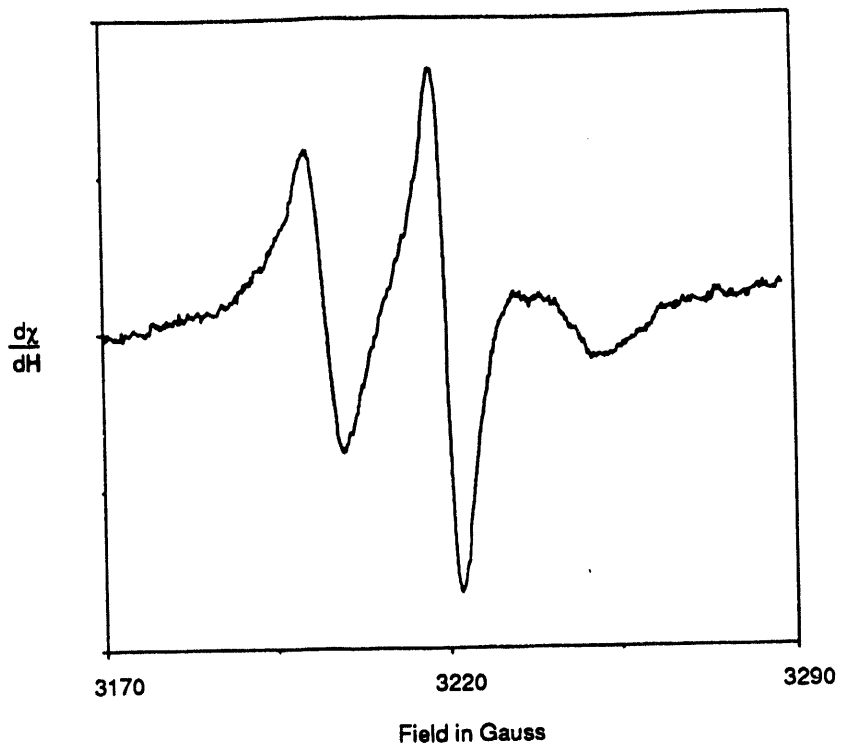

Best simulated spectrum

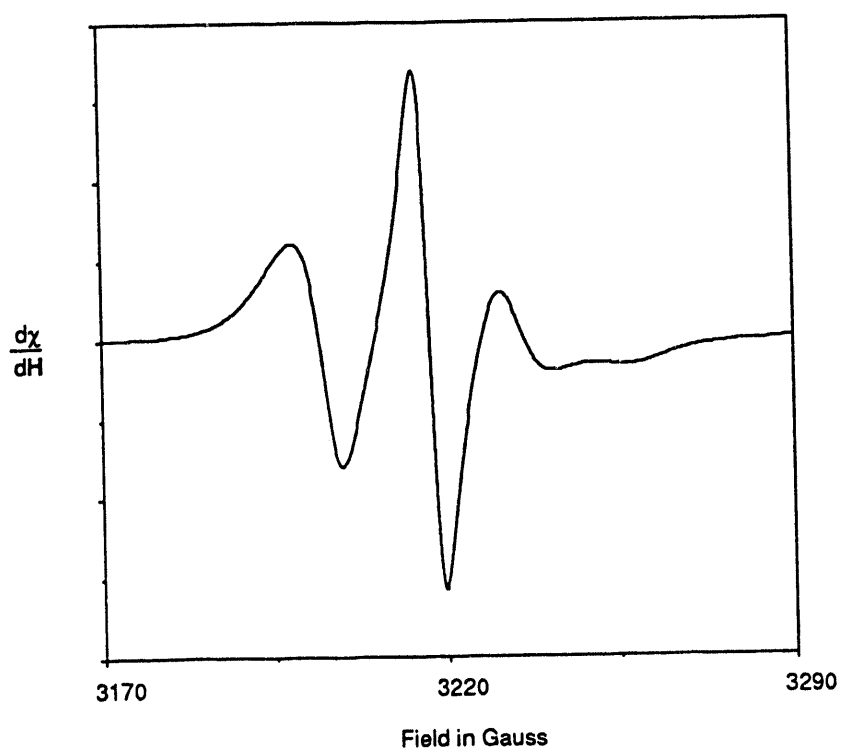

Figure 1.17 EPR spectrum of 24 mer cross-linked with psoralen **3**

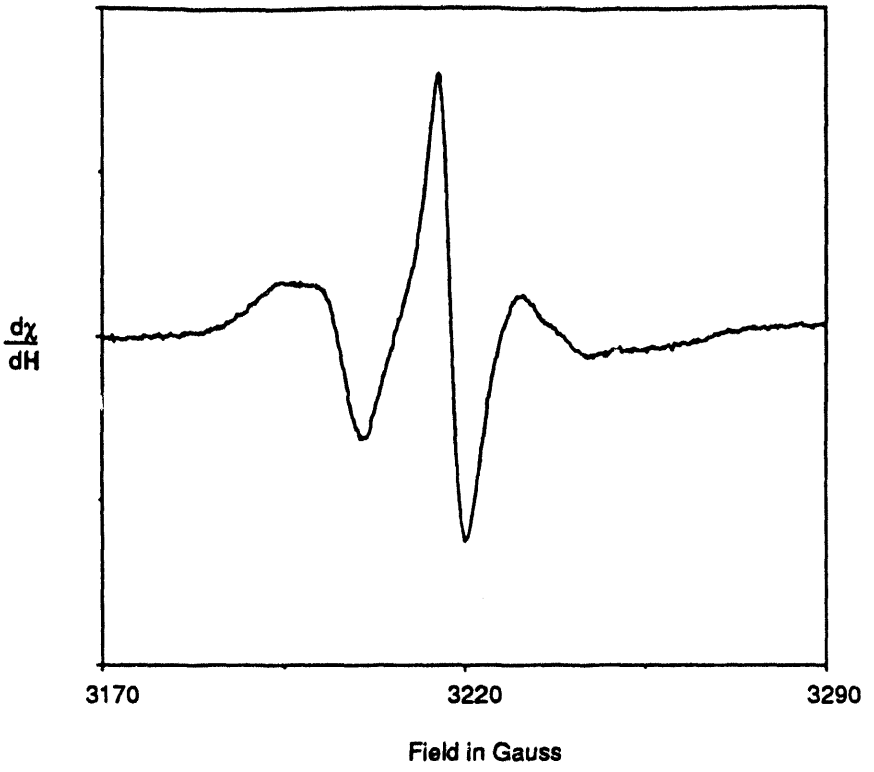

Best simulated spectrum

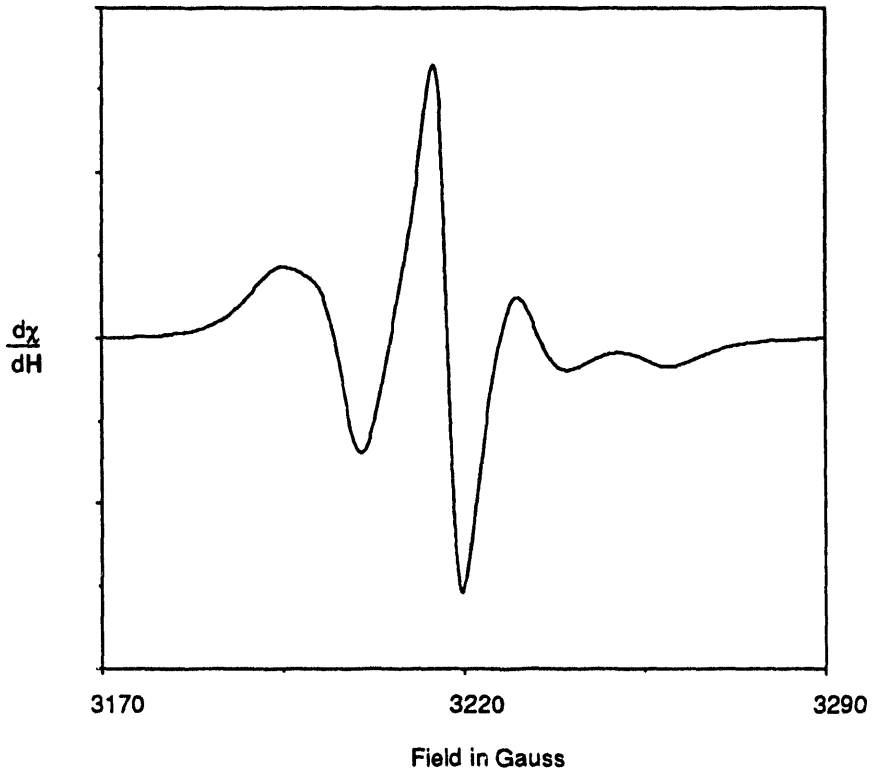

Figure 1.18 EPR spectrum of 46 mer cross-linked with psoralen 3

Best simulated spectrum

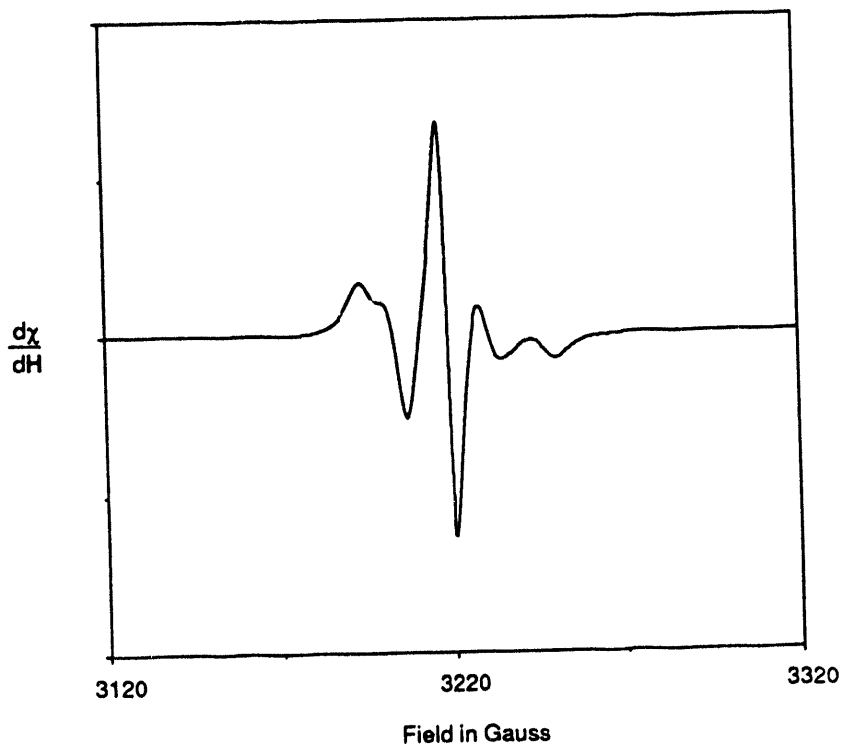

Figure 1.19 EPR spectrum of 88 mer cross-linked with psoralen **3**

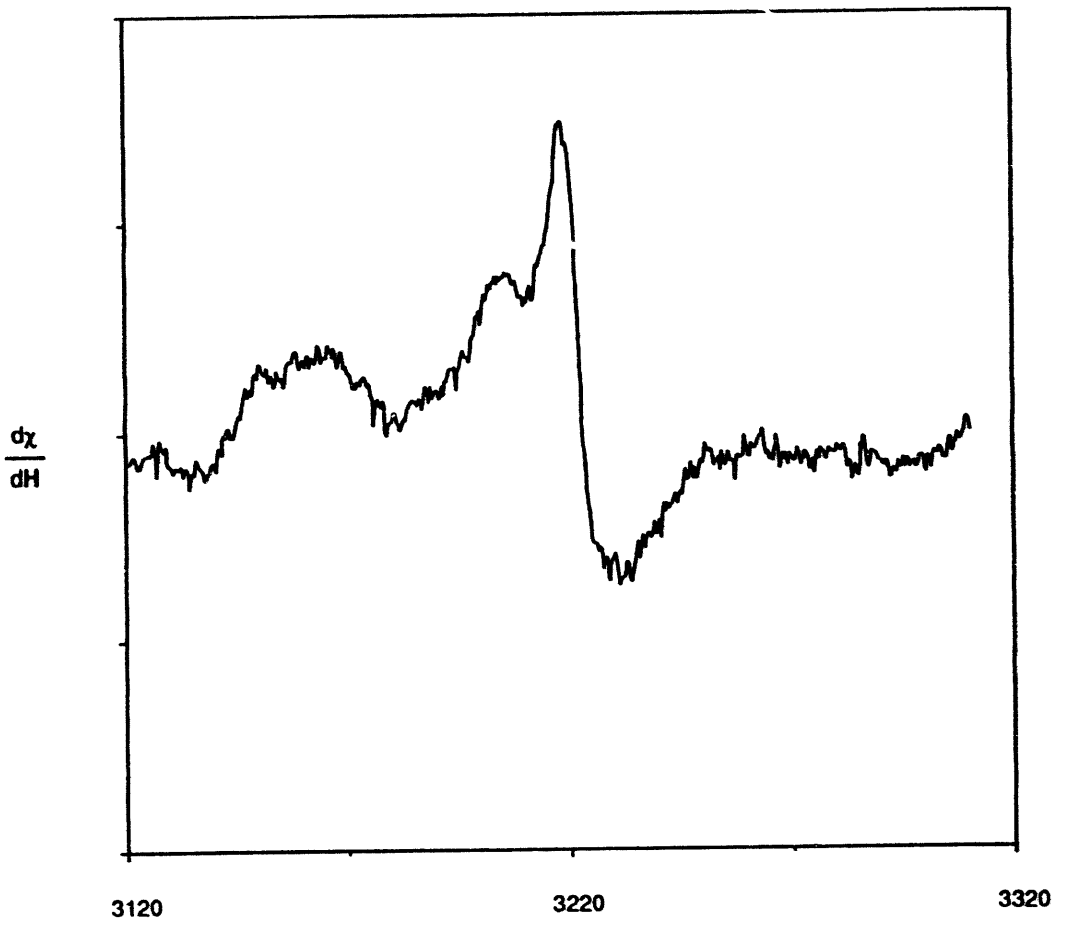

indicate slightly slower motion than the spectrum in figure 1.15. There are three sigma bonds between the psoralen and the spin label ring in compound **4**, while there are four sigma bonds separating the components in molecule **3**. This extra sigma bond and the increased freedom of motion that it may allow could account for the longer correlation time seen in the 24 mer cross-linked with psoralen **4**. The rule-of-thumb for molecules of this size gives a τ_C of 6.4ns. Thus if our spin-labels are moving independently of the DNA, the motion is small. The spectrum for a concentrated solution of the 24 mers (figure 1.17) best resembles a simulation with τ_C of 6.7 ns. Because the concentration of DNA in this solution was 10 times higher than the sample which yielded the spectrum in figure 1.15, the increase in the correlation time may be due intermolecular interactions. The spectra for the 46 base pair fragment (figure 1.18) and for the 96 base pair fragment (figure 1.19) are more problematic because of the combination of low signal-to-noise and the presence of a background signal in the EPR cavity. All that can be said is that the 46 base pair fragment data is consistent with simulations with τ_C of 8.3ns, as well as simulations with much longer τ_C, e.g. 16.7 ns. The spectrum in figure 1.19 of a 96 base pair fragment cannot be matched well with simulated spectra.

It is possible to do more detailed simulations of the EPR spectra by varying all the parameters in the simulation (A-tensor, g-tensor, rotational correlation time, rotational anisotropy). All these parameters can be adjusted to find an optimal fit to the spectra. Calculations of this type require a supercomputer and can give very nice fits. We decided to just use published values of the A- and g-tensors for nitroxides, vary the rotational correlation time, and leave out the effects of rotational anisotropy. The simulations resemble our spectra closely enough that we can determine rotational correlation time to within 20%. The rotational correlation times we obtained agree with Cantor and Schimmel's rule-of-thumb for τ_C within 20%.

Conclusions and Potential Future Applications of Spin-Labeled Psoralens

The CW EPR spectra that we acquired in this study indicate that our spin-labels faithfully report the over-all tumbling of DNA oligomers. The spin-labels therefore do not wobble with respect to the DNA on the time-scales investigated, i.e. up to about 10ns. In studies of synthetic DNA oligomers, the Hopkins spin-labeled thymidine EPR probe is clearly superior to these spin-labeled psoralens. Because it does not cross-link the nucleic acid, the modified thymidine does not introduce nearly as large a structural perturbation as the psoralens. It also does not suffer loss of signal during its introduction into the nucleic acid because there is no photochemical step. However, if the dynamics of native nucleic acids such as chromatin and whole nuclei are to be studied, then a probe such as our spin-labeled psoralens is ideal for delivery of the nitroxide reporter group. Also, psoralen damaged DNA is recognized by repair enzyme complexes. Nitroxide labeled psoralens can be used to study the dynamics of this system both by EPR directly and by line-broadening of NMR resonances. In order to study the slower DNA dynamics characteristic of large-scale DNA bending and twisting, we will study DNA molecules large enough so that the over-all tumbling of the molecule is negligible.

As noted above, CW EPR is capable of measuring motion for τ_c as long as 10^{-7} s. To study slower motions using EPR, non-linear techniques must be used. The two most important ones are saturation transfer EPR, reviewed by Hemmings and de Jager (Hemmings and De Jager, 1989), and electron-electron double resonance (ELDOR), reviewed by Hyde and Feix (Hyde and Feix, 1989). With these techniques one can obtain information on motions as slow as 1msec.

We have described here the synthesis of several spin-labeled psoralen derivatives and their photoreactivity with double-stranded DNA fragments. We have demonstrated that the spin labels (nitroxides) can survive at some level the UV irradiation required to bind the

probe to the target DNA. There are some potential strategies for overcoming the problem of photochemical destruction of the nitroxide. The most obvious approach is a more extensive investigation of the photofixation of nitroxides to oligomers using the spin labeled 8-MOP derivatives. It is possible that the excited-state photochemistry available to the nitroxide in the major groove is quite different than that available in the minor groove. Another potential solution is to do the photochemistry with reduced spin labeled psoralen and then to re-oxidize the cross-linked molecules. The use of longer wavelength light to drive the photochemistry is another possibility. A reduction in the intensity of the cross-linking light can also be investigated. The light from the argon-ion laser used had an intensity of approximately 25 W/cm^2 which is 100X the intensity of the light source used to investigate the photocross-linking of the 8-mer $d(GGGTACCC)_2$. With the well-characterized photochemistry of psoralen with double-stranded nucleic acids, the capability to place a spin label at any specific site in a nucleic acids molecule to faithfully report the motion of the macromolecule should become possible. With different techniques involving spin labels, we will be able to gain information on the dynamic motion within a wide range of time scale (from micro- to millisecond). This will allow us to study the motion of nucleic acid molecules free in solution and even in a biochemical process such possible DNA rotations during transcription and replication. These spin-labeled psoralens should also prove useful in studying the secondary and tertiary structure of RNA by their ability to paramagnetically broaden NMR lines.

Chapter 2

Nucleotide Excision Repair in Human Cell-Free Extracts

DNA is the repository of an organism's genetic makeup, RNA viruses excepted. A variety of DNA repair mechanisms exist and are active and available to the cell to ensure that the genetic information and the physical functionality of the genome are not compromised. The kinds of DNA damage that we are concerned with are the loss of information at modified or deleted bases and interference with the processes of replication and transcription in the case of interstrand cross-links. There are many types of DNA damage, alkylation, single stranded nicks, double strand breaks, interstrand cross-links, hydrolysis, radiolysis and oxidation to name a few.

To ensure that genetic information is properly passed on to the next generation, the error frequency of DNA replication in a cell is very low. One in 10^7 nucleotides is incorrectly copied by DNA polymerase and the attendant accessory proteins that enhance the fidelity of replication. Post-replication mismatch repair pathways further reduce the error frequency to one in 10^{10} nucleotides. Errors in replication are not the only challenges faced by an organism attempting to maintain the integrity of its genome. DNA can be damaged in a number of ways. Spontaneous chemical changes to the bases include deamination of deoxycytidine to give deoxyuridine, tautomerization which may affect basepairing, and depurination. The environment subjects the cell to a variety of chemical and physical agents that can adversely affect both the bases and the sugar-phosphate backbone (Friedberg, 1985).

Cellular DNA repair processes have been investigated in both prokaryotic and eukaryotic systems. Progress towards understanding excision repair in *Escherichia coli*, yeast and mammalian systems has been recently reviewed (Friedberg, 1987; Friedberg, 1988; Myles and Sancar, 1989; Smith, 1988). Cellular repair of DNA damage is best understood in *E. coli*. In *E. coli*, a number of DNA repair pathways have been identified. Some types of damage to DNA can be reversed directly, as in the photolyase-mediated monomerization of *cis-syn* pyrimidine dimers (Sancar and Sancar, 1988) or the ligation of single-stranded breaks by DNA ligase. Other lesions must be excised from the genome or somehow replicatively or transcriptionally bypassed. Replicative bypass is usually a mutagenic process. DNA glycosylases that hydrolyze the N-glycosidic bond between the base and the sugar-phosphate backbone mediate base excision repair. Apurinic/apyrimidinic (AP) endonucleases recognize the absence of a base and hydrolyze the adjacent 5′ and 3′ phosphodiester bonds (Friedberg, 1985). Mismatched basepairs can also be corrected through excision repair pathways (Friedberg, 1985; Modrich, 1989; Myles and Sancar, 1989). In nucleotide excision repair, the damaged base or bases are typically removed as part of a small oligonucleotide. Nucleotide excision repair is a mechanism by which lesions are removed from DNA in the form of a short oligonucleotide with the concomitant filling in of the resulting gap by DNA polymerase and nick closure by DNA ligase (Sancar and Sancar, 1988). This process can be either error free or error prone. An *in vitro* model for the error free repair of psoralen cross-linked DNA has recently been proposed (Cheng *et al.*, 1991). The incorporation of nucleotides by DNA polymerase into this patch is termed repair synthesis. Nucleotide excision repair restores the integrity of the DNA molecule. In *E. coli* mutations in any of three genes, *uvrA*, *uvrB* and *uvrC*, make the cells extremely sensitive to killing by UV and UV-mimetic agents such as psoralen and cisplatin. Biochemically these mutants fail to incise DNA damaged with these and other agents.

In the yeast *Saccharomyces cerevisiae*, at least twelve genetic loci have been implicated in excision repair. The RAD3 group defines ten of the twelve genetic loci that are unique to the nucleotide excision repair epistasis group. Mutations in any one of the genes or combination of genes in this group result in the same degree of sensitivity to UV radiation or chemical agents by the yeast. The *RAD1*, *RAD2*, *RAD3*, *RAD4*, and *RAD10* genes are absolutely required for nucleotide excision repair. All of these genes have been isolated and sequenced.

Recombinational repair (RAD52 group) and mutagenic repair (RAD6 group) are two other major repair systems that have been identified in *S. cerevisiae*. Recombinational repair and mutagenic repair in *E. coli* are activated during the SOS response to environmental stresses. As in *E. coli*, activation of these yeast genes are implicated as cellular responses to psoralen monoadducts and cross-links in addition to the excision repair pathways. Recombination between sister chromatids may play a role in repair in mammalian cells as well. Glycosylase activities have been identified in *E. coli* and human cells (Boorstein *et al.*, 1989; Doetsch *et al.*, 1987; Weiss *et al.*, 1989), and in *S. cerevisiae* (Gossett *et al.*, 1988). All three of these systems (bacterial, yeast, and human) have demonstrated a limited ability for replicative bypass of psoralen monoadducts. Evidence from both *E. coli* and *S. cerevisiae* suggests that an intermediate in the excision repair pathway can serve as a common substrate for other repair processes. (Moustacchi, 1988)

The cellular responses of mammalian systems to DNA damage represent yet another level of complexity. Cell lines derived from the autosomal recessive disorders Fanconi's anemia (FA) and xeroderma pigmentosum (XP) are two human cell lines that have been used in the study of DNA excision repair. XP cells are deficient in nucleotide excision repair, and FA cells exhibit a heightened sensitivity to agents which form interstrand cross-links (Averbeck *et al.*, 1988a; Moustacchi *et al.*, 1988). Chinese hamster ovary (CHO) mutants sensitive to UV radiation and deficient in excision repair have been used in the

isolation of human repair genes (Friedberg, 1987; Thompson *et al.*, 1988). In man the genetics of nucleotide excision repair is more complicated than that of either *E. coli* or yeast. Mutations in any of the nine xeroderma pigmentosum (XP) genes render cells sensitive to these same DNA-damaging agents. It is generally agreed that patients suffering from this disease have a defect in nucleotide excision repair and, as with the *E. coli uvr* mutants, the biochemical defect is at or before the incision step.

The focus of this study was to determine whether psoralen interstrand cross-links are also removed from damaged DNA during the *in vitro* repair reaction with HeLa human cell-free extracts. In *E. coli,* excision repair of a psoralen cross-link is a complex multistep mechanism requiring homologous DNA and the activity of RecA in addition to the uvrABC excinuclease complex, helicase, polymerase I and ligase (Cheng *et al.*, 1988b; Sladek *et al.*, 1989; Van Houten *et al.*, 1986a). The repair of psoralen monoadducts and interstrand cross-links has been reported for normal human cells (Vos and Hanawalt, 1987). ABC excinuclease is the multisubunit enzyme which mediates nucleotide excision repair in *E. coli* (Myles and Sancar, 1989; Sancar and Sancar, 1988). Both psoralen monoadducts and cross-links are among the various lesions targeted in this process. ABC excinuclease recognizes and excises adducts to DNA formed by the drug CC-1065 (Selby and Sancar, 1988) numerous other alkylating agents, *cis*-Pt(II)NH_2Cl_2, as well as UV irradiation-induced pyrimidine dimers and 6-4 photo-products (Sancar and Sancar, 1988). One possible basis for the recognition of such lesions is a distortion of the DNA helix. A psoralen monoadduct induces a greater distortion in the structure of the DNA helix than that induced by a thymine dimer. Thymine glycol, AP sites (Lin and Sancar, 1989), the N^2-guanine adduct formed by anthramycin (Walter *et al.*, 1988) and O^6-methylguanine (Voigt *et al.*, 1989) are lesions that do not induce significant distortions of the DNA helix. Incision at a site-specifically placed psoralen monoadduct, thymine dimer, and O^6-methylguanine correlate with the degree of resulting helical distortion induced by the lesion (Voigt *et al.*, 1989). ABC excinuclease will also recognize damage at lesions that do not

cause significant distortion of the DNA helix at a lower efficiency. Repair of DNA damage sites may be targeted through a process in which lesions alter helix dynamics and thus influence binding of the excinuclease rather than through recognition of a particular static structural distortion of the helix (Lin and Sancar, 1989; Pu *et al.*, 1989).

ABC excinuclease typically makes two specific incisions, one at the seventh or eighth phosphodiester bond on the 5′ side, and one at the fourth or fifth bond on the 3′ side of a lesion, leaving a gap with 3′-OH and 5′-P termini that is then filled in by polymerase and sealed by ligase (Sancar and Sancar, 1988). The short repair patch pathway that predominates nucleotide excision repair is characterized by repair patches of 10-30 nucleotides (Peterson *et al.*, 1988; Smith *et al.*, 1989). Van Houten and co-workers found that following incision of a uniquely monoadducted duplex, 83% of the repair patches were 12 nucleotides long. This was precisely the size of the gap between the two (A)BC incision sites. An additional 10% of the patches were 12-20 nucleotides long, and no patches longer than 45 nucleotides were detected (Van Houten *et al.*, 1988). Several studies on the mechanism of (A)BC excinuclease have utilized substrates containing site-specifically placed psoralen adducts (Cheng *et al.*, 1991; Jones and Yeung, 1988; Van Houten *et al.*, 1986a; Van Houten *et al.*, 1986b; Yeung *et al.*, 1987). Both furan- and pyrone-side psoralen monoadducts are recognized and are incised at the eighth phosphodiester bond 5′ and the fifth bond 3′ to the adduct (Van Houten *et al.*, 1986a). (A)BC excinuclease incises DNA at a site-specific HMT cross-linked 40-basepair duplex only on the furan-side strand. The incision takes place at the ninth phosphodiester bond on the 5' side and the third phosphodiester bonds on the 3' side of the cross-link (Van Houten *et al.*, 1986b).

We desired to demonstrate excision repair of DNA damage in the human system. We decided to use a DNA substrate that was randomly damaged with psoralen for this study. The work reported here was done in conjunction with Dr. Joyce Reardon and Dr. Aziz Sancar at the University of North Carolina, Chapel Hill. The design and construction

of the psoralen photochemicaly modified plasmids were caried out by me, while the enzymatic assays were carried out by the U.N.C. group.

The details of DNA excision repair that have been elucidated in *E. coli* can serve as a foundation for constructing models of the more complicated eukaryotic mechanisms. Strong parallels in biochemical processes such as replication have previously been found among bacteria, yeast, and mammalian cells (Kornberg, 1980). Although this excision repair mechanism has been well-characterized in prokaryotes it remains biochemically ill-defined in mammalian cells.

An important step towards characterization of nucleotide excision in humans was the development of a cell-free extract (CFE) system capable of carrying out repair synthesis on damaged DNA substrates (Heiger-Bernays *et al.*, 1990; Sibghat-Ullah *et al.*, 1989; Wood, 1989; Wood *et al.*, 1988). Previous reports have demonstrated that cell-free extracts prepared from human cells contain a repair activity which acts on DNA damaged by UV light, psoralen and platinum. This activity was detected in a DNA damage-dependent repair synthesis assay and was interpreted as true repair in a biological sense in that it restored the sensitivity of site-specific psoralen damaged DNA to a restriction enzyme (Sibghat-Ullah *et al.*, 1989) or reactivated platinum-modified DNA templates for *in vitro* replication (Heiger-Bernays *et al.*, 1990). Because the damage-dependent DNA synthesis activity was greatly reduced or absent in all tested XP cell lines, it was concluded that the activity was due to repair synthesis following removal of the various adducts.

Although this *in vitro* system has been used extensively (Cheng *et al.*, 1988b; Manley *et al.*, 1980; Sladek *et al.*, 1989; Van Houten *et al.*, 1986a; Vos and Hanawalt, 1987), the repair synthesis that can be accomplished utilizing this system under optimal conditions corresponds to removal of only 1-10% of total adducts assuming a "repair patch" size of 20 nucleotides (Manley *et al.*, 1980; Wood *et al.*, 1988). Therefore it has not been possible to directly demonstrate that the *in vitro* system is capable of removing the damaged nucleotides. Indirect evidence for excision repair mediated removal of DNA

lesions have been presented in these reports. Indeed, it could be argued that the so-called "repair synthesis" is actually damage induced aberrant DNA synthesis which does not result in repair. Repair of the damaged DNA is defined as the removal of the modified base adduct and its replacement with a normal nucleotide.

We have used DNA containing psoralen adducts to directly address the question of whether all or part of the damage-induced DNA synthesis is associated with adduct removal and is therefore genuine repair synthesis. We found that all DNA synthesis in our HeLa cell-free extracts induced by psoralen monoadducts or cross-links is associated with adduct removal and therefore qualifies as bona fide repair synthesis. In this cell free extract system we also found that psoralen cross-links elicited a higher level of DNA synthesis when compared with psoralen monoadducts, and that this higher level of synthesis was associated with removal of the interstrand cross-links.

MATERIALS AND METHODS

Materials. HeLa S3 cells were from the stock of Lineberger Cancer Center (University of North Carolina). The radioisotopes, [α-^{32}P]dCTP (6000 Ci/mmole) and [γ-^{32}P]ATP (7000 Ci/mmole) were obtained from New England Nuclear-DuPont (Boston, MA) and ICN Radiochemicals (Irvine, CA), respectively. ATP, dNTPs, pyruvate kinase, and phosphoenolpyruvate were obtained from Pharmacia (Piscataway, NJ) or Sigma Chemical Company (St. Louis, MO). Restriction enzymes, kinase, ligase and PolI were from Bethesda Research Laboratories (Gaithersburg, MD) and 4-hydroxymethyl-4,5'8-trimethylpsoralen (HMT) was a gift from HRI Associates (Concord, CA).

Repair Systems. HeLa cell free extract (CFE) capable of damage-induced DNA synthesis was prepared from HeLa S3 cells by the method of Thomas *et al.* (Thomas *et al.*, 1985) as described by Sigbhat-Ullah *et al.* (Sibghat-Ullah *et al.*, 1989). Typically, the yield was 7-10 mg total protein per liter of cells; each batch of extract was tested to

determine the optimal protein concentration to be used in the repair synthesis assays. The amount of protein which gave optimal signal-to-noise ratio in these assays varied somewhat from extract to extract. The CFE was stable for at least 6 months when stored at -80°C and retained its activity after one cycle of thaw-and-refreeze. The subunits of E. coli (A)BC excinuclease were purified as described previously (Hansson and Wood, 1989).

Substrates. pBR 322 DNA damaged by UV or psoralen (HMT) was our substrate for these reactions. The plasmid was purified through two CsCl-ethidium bromide density gradients, dissolved in TEN 7.4 (10 mM Tris HCl, pH 7.4, 10 mM NaCl, 1 mM EDTA) and stored at 4°C. For UV damage, the DNA was exposed to 375 J/m^2 of 254 nm radiation from a 15 W Westinghouse Germicidal Sterilamp. The DNA was at a concentration of 20 μg/ml and in the form of 5 μl droplets during irradiation. We have established that under these conditions 12.5 J/m^2 introduces 1 UV pyrimidine dimer per plasmid. No nicks were introduced into DNA during irradiation with 254 nm light.

Psoralen adducted DNA containing either exclusively monoadduct or mostly diadducts (interstrand cross-links) were prepared by taking advantage of the unique spectral properties of DNA, psoralen, and the psoralen-pyrimidine monoadduct. In order to test for the presence of excision repair of psoralen-DNA adducts in Human HeLa cell-free extracts we needed to synthesize the appropriately adducted molecules. Since we expected only 1-10% of the psoralen adducts to be repaired under the conditions of our assay, we decided to use a randomly damaged plasmid substrate with multiple psoralen lesions to increase our signal-to-noise ratio. We also wanted to determine if there was any difference between repair of monoadducts and that of cross-links by the HeLa CFE. Previous methods for the synthesis of monoadducted DNA required irradiation of duplex DNA with free psoralen at 365 nm, and then photoreversal of the crosslinked product with short wavelength light (254 nm) to give a mixture of pyrone-side and furan-side monoadducts. This procedure is impractical with any DNA except for relatively short oligonucleotides. In a plasmid system that is being created to test for the repair activity of cell-free extracts it is undesirable to

expose the DNA to 254 nm light because of the formation of pyrimidine dimers and other DNA photo-damage products (Cimino *et al.*, 1986). In addition, the pyrone-side fraction of the monoadducts produced in this fashion are unable to be re-cross-linked efficiently. Furan-side monoadduct cannot be isolated directly from initial irradiation performed under conditions that produce cross-linked molecules because the quantum yield for formation of monoadduct is smaller than the quantum yield for driving a monoadduct on to cross-link.

We used an improved method for the preparation of furan-side monoadduct which only requires irradiation of duplex DNA and HMT at wavelengths ≥ 389 nm (Kodadek and Gamper, 1987). Figure 1.4 is a comparison of the absorption spectra of DNA, furan-side monoadducted DNA and psoralen. DNA effectively stops absorbing light at wavelengths longer than 310 nm. The psoralen furan-side monoadduct stops absorbing light at wavelengths greater than 390 nm. Psoralen has an absorption to at least 410 nm. We have exploited the wavelength dependence of this chemistry to produce HMT furan-side monoadducted plasmids for this study of DNA excision repair. The monoadducts formed by this method are about 98% furan–side. The irradiation device we used produced very high initial intensities of light with wavelengths shorter than 389 nm requiring the use of an extensive filtering system. Cross-linking light for these reactions was produced by filtering the output of a 2200 W Hg/Xe arc lamp through a 9 cm path length 1.7 % $Co(NO_3)_2$/ 2 % NaCl filter which produced 300 mW/cm^2 of 320-380 nm light (Cimino *et al.*, 1986). For long wavelength irradiations we used a 1/4″ thick glass–Pyrex filter with about 50% transmission at 365 nm and a 3 mm 350 nm cutoff filter followed by a 389 nm bandpass filter. Multiple filters were necessary to remove the strong 365 nm mercury emission line and to protect the bandpass filter from overheating. This filter train resulted in 5 mW/cm^2 of 389 nm (monoadducting) light. Filters for long-wavelength UV irradiations were purchased from Oriel or Baird Atomic.

The distribution of furan-side monoadducts and cross-links in a molecule will depend on the rate of furan-side monoadduct formation relative to rate at which the

monoadduct goes on to cross-link. This rate is directly proportional to the extinction coefficient of HMT (ε_1) and the furan-side monoadduct (ε_2) at the wavelength that the irradiation takes place according to the following equations:

$$k_1 = I\sigma_1\phi_1$$

$$k_2 = I\sigma_2\phi_2$$

$$\sigma = 2303\varepsilon / N_A$$

$$k_1 / k_2 = (\varepsilon_1\phi_1) / (\varepsilon_2\phi_2)$$

Where k_1 is the rate of monoadduct formation, k_2 is the rate of cross-link formation from furan-side monoadduct, I is the intensity of the light irradiating the sample, ϕ_1 and ϕ_2 are the quantum yields for furan-side monoadduct and cross-link formation respectively, ε_1 and ε_2 are the extinction coefficients for HMT and furan-side monoadduct respectively, N_A is Avogadro's number, and σ_1 and σ_2 are respectively the absorption cross-sections of HMT and furan-side monoadduct. σ is directly proportional to the extinction coefficient of the molecule at that wavelength. The quantum yield ϕ_1 for the formation of furan-side monoadduct of 8-MOP by irradiation at 397.5 nm is 0.0065, and the quantum yield ϕ_2, for the conversion of furan-side monoadduct to cross-link by irradiation at 341 nm is 0.028 (Tessman *et al.*, 1985). The quantum yield for conversion of HMT furan-side monoadduct to cross-link has been measured to be 0.024 by irradiation at 334 nm (Shi and Hearst, 1987b). The quantum yields for the formation of cross-link from furan-side monoadduct are the same for these two psoralens within experimental error. It is safe to assume that the quantum yields for formation of monoadducts from the two psoralens will also be similar. The quantum yield measured for driving a furan-side monoadduct on to cross-link is four times larger than the quantum yield for the initial formation of furan-side monoadduct. This explains why furan-side monoadduct does not accumulate in the reaction mixture when a HMT / DNA solution is irradiated at 365 nm where both HMT and the furan-side monoadduct have a relatively large extinction coefficient. The unfavorable ratio of quantum yields can be overcome to make furan-side monoadduct by exploiting the difference in

extinction coefficients at longer wavelengths. If the plasmid is irradiated with light in a region of the spectrum where the extinction coefficient for the furan-side monoadduct is substantially lower than the extinction coefficient for the free psoralen, monoadduct can then accumulate in the reaction mixture. The extinction coefficients for HMT and the HMT furan-side monoadduct at 389 nm can be estimated from their UV absorption spectra. The extinction coefficient for HMT at this wavelength is about 40 (l $mole^{-1}$ cm^{-1}), and for the furan-side monoadduct, it is less than 1 (l $mole^{-1}$ cm^{-1}).

The human HeLa cell-free extract excision repair activity can be saturated at a fairly low level of DNA damage. The average total number of psoralen adducts in a plasmid was required to be in a relatively narrow range, and could not be too high, or too low. If the number of adducts in a plasmid were too high, the signal to noise ratio in our assay would go down because more than one psoralen adduct would be present in any given restriction fragment of the plasmid (see below for a discussion of how the results of CFE repair assays were interperted). If the level of psoralen addition to the plasmid was too low, then background synthesis in the assays would swamp out any signal. There are two ways to control the total number of photobound psoralen adducts in a randomly adducted plasmid. The first is to limit the total amount of psoralen in the sample, and drive all of it into a photobound state, and the second is to limit the amount of light that a sample with excess psoralen is exposed to. The total number of psoralens photobound to a plasmid is much easier to control in the first case, because one simply irradiates the sample until no further reaction between the DNA and psoralen is possible. The disadvantage to this method is that with increasing light dose, more monoadducts can absorb light and be driven on to cross-link. This is a fine approach if a crosslinked sample is what is desired. To generate plasmid DNA molecules where furan-side monoadducts are the predominant form of photoadduct, the second, light limiting method is much more desirable. In order to predict what light dose will give a certain level of photoaddition, a light dose vs. number of adducts per plasmid calibration curve was required. It was also necessary to determine the

Figure 2.1 Time couse of photoaddition of HMT to pUC 19 by irradiation with 389 nm light

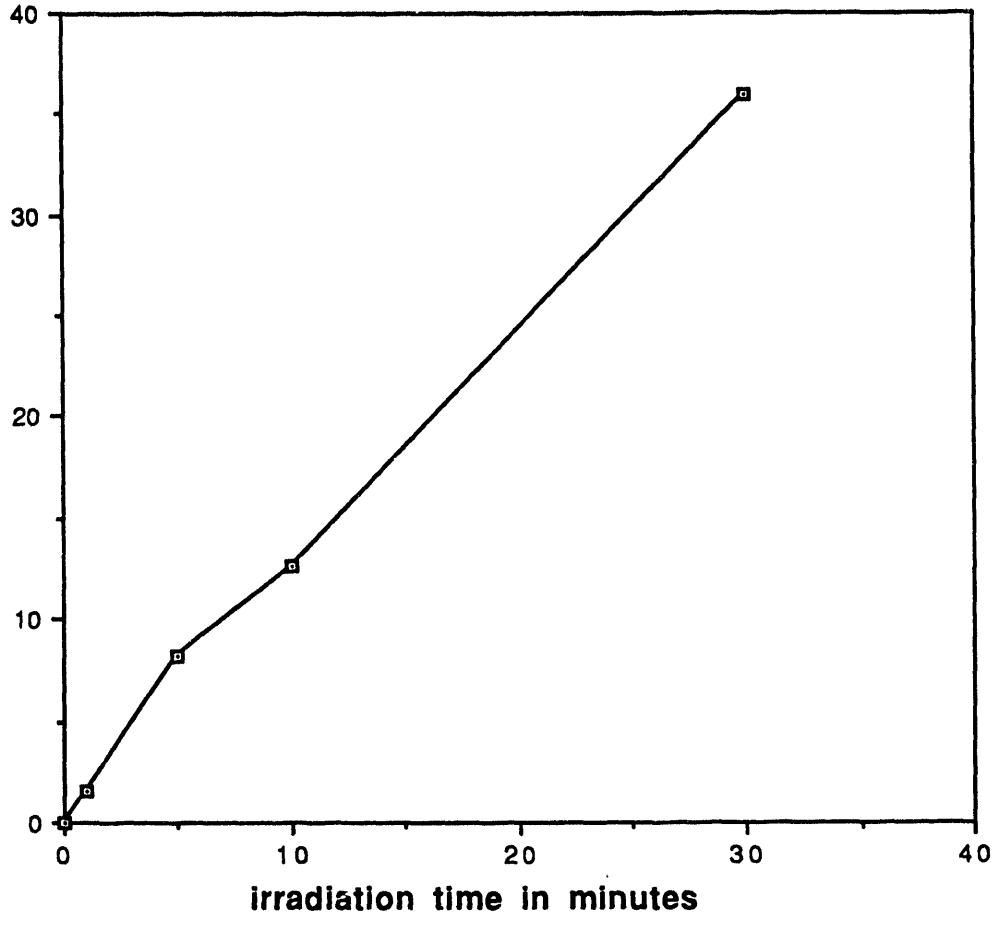

distribution of adducts produced under the irradiation conditions. This is especially true before any preparative scale production of randomly modified plasmid was to be undertaken.

1.5 µg pUC 19 (9×10^{-13} moles) was taken up in 25 µl 150 mM NaCl in which 45 µCi ^{3}H HMT (5×10^{-9} moles) were dissolved. This mixture was [illegible] 5 mW/cm^2 389 nm light using the apparatus described above. The ar[illegible] intersecting the beam was 1/4 cm^2 with a pathlength of 0.2 cm. 5 µl aliquots were withdrawn from the reaction mixture at 1, 5, 10, and 30 minute intervals. The plasmid was precipitated from the mixture with ethanol to remove most of the unreacted HMT. The DNA pellet was resuspended in 50 µl water and the total amount of DNA in each aliquot was determined by UV absorbance. The bound HMT was quantified by counting a fraction of each aliquot in a scintillation counter. The time course of photoaddition of HMT to pUC 19 using 389 nm irradiation [illegible]wn in figure 2.1. It shows that under light limiting conditions, photoaddition of H[illegible]ow adduct to base pair ratios is linear in light dose. The remainder of each of the samples was digested to nucleosides, and analyzed by reverse phase HPLC.

Adducted DNA was enzymatically digested essentially as described (Kanne *et al.*, 1982a; Straub *et al.*, 1981). Samples were treated with DNase II, phosphodiesterase II, and alkaline phosphatase and analyzed by reverse–phase HPLC as follows: Precipitated DNA was resuspended in 2 ml of 15 mM NaOAc, pH 5.0. We added 0.1 % NaN_3 to prevent bacterial growth and reaction mixture was adjusted to pH 5.0 with a few microliters of 50% acetic acid. Approximately 0.5 mg (500-1500 Kunitz units) Type IV DNase II was added and the reaction was incubated for 24 hr at 37 °C. The solution was neutralized to pH 7 with ~12 µl 1 M Tris base, 0.4 U Type 1-S phosphodiesterase II was added (the lyophilized enzyme is resuspended before use to 10-15 µ/ml in 15 mM NaOAc, pH 7), incubation at 37 °C was continued for 24 hr, a second 0.4 U aliquot of enzyme was added, and incubation was continued for a further 24 hr. The pH was then adjusted to 8.1

Figure 2.2 HPLC elution profile of enzyme hydrolyzed pUC 19
DNA monoadducted and cross-linked with Tritiated HMT

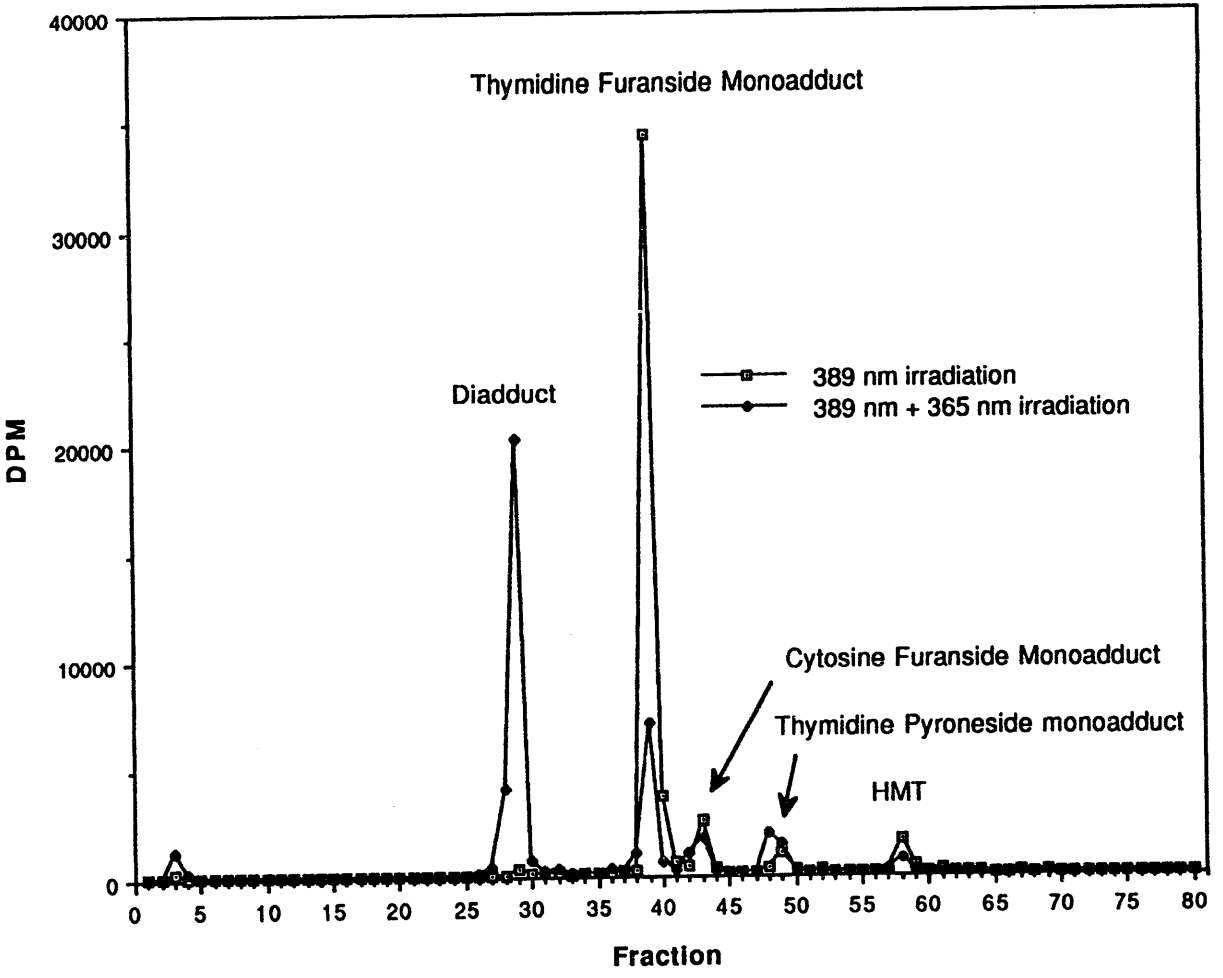

with ~ 5 µl 1 M Tris base (and 1 M pH 5 NaOAc if necessary), 20 µl (20-30 U) of Type VII-S alkaline phosphatase in $(NH_4)_2SO_4$ suspension was added, and incubation was continued for 24 hr at 37 °C. The sample was adjusted to pH 2.9 with 3 M or 6 M H_3PO_4 and the solution was allowed to sit at room temperature for 30 min. This ensures that the pyrone ring of the psoralen adduct is closed; the phenolic lactone is unstable to base after the 3,4 double bond is saturated by photoreaction. Before analysis by HPLC, the solution was filtered through 0.45 µm filters (Millipore). HPLC was done using a 4.6 mm ID × 25 cm Dynamax 60 Å pore size 8 µm C_{18} column (Rainin). Mobile phase A was 10 mM H_3PO_4, pH 2.2 and mobile phase B was MeOH; the gradient was 100 % A from 0 to 10 min followed by 0 to 100 % B over 70 min, at a flow rate of 1.4 ml/min. Fractions were collected at 1 minute intervals and assayed for tritium by scintillation counting with 5 ml of Ecolume fluor (ICN) in an LKB 1209 scintillation counter. Charged molecules elute in the void volume, so the peak at 3-5 min corresponds to any incompletely digested ^3H–nucleotides in this solvent system. HMT-DNA diadducts elute between fractions 28 and 33, furan side thymidine adducts elute between fractions 38 and 41 , furan side cytosine adducts elute between fractions 41 and 44, pyrone side thymidine adducts elute between fractions 48 and 50 using this system. The position of the adducts in the chromatogram was determined by comparison with known standards.

The chromatograms of the various digests all gave similar results. A representative chromatogram is shown in figure 2.2. All of the peaks were identified by comparison with authentic standards. The peak that elutes at minute 58 was identified as HMT, and represents just 4.2% of the total counts in the digestion reaction. The vast majority of the unreacted HMT is removed by ethanol precipitation. Three sequential ethanol precipitations remove all unreacted HMT (data not shown). After correction for background, and un-photobound psoralen, the following distribution of adducts in the plasmid was calculated.

Monoadducted pUC 19	%
Diadduct	0.5
Furan side thymidine adduct	82.6
Furan side cytosine adduct	6.3
Pyrone side thymidine adduct	3.3

An aliquot of this monoadducted pUC 19 was re-precipitated to remove the small amount of unbound psoralen and irradiated with 500 mW/cm^2 of 320-380 nm light to drive the MAf onto XL. This material was digested to nucleosides and the resulting products separated by HPLC as described above. After correction for background, the following distribution of adducts in the plasmid was calculated.

Crosslinked pUC 19	%
Diadduct	60.9
Furan-side thymidine adduct	20.6
Furan-side cytosine adduct	7.1
Pyrone-side thymidine adduct	8.7

After it was demonstrated that plasmids could be made which contained mostly furan-side psoralen monoadducts, that the level of photoaddition could be controlled and that the monoadducts could be driven onto cross-links, a preparative scale reaction using the plasmid pBR 322 was performed.

0.625 mg pBR 322 was taken up in 2.2 ml of 150 mM NaCl, 10 mM tris pH 7.5, 1mM EDTA, and made to 41μg/ml 150 Ci/mole ^{3}H-HMT with 4 μl ^{3}H-HMT stock in DMSO. This was divided into two portions, and each portion was irradiated in a 4 ml quartz cuvette for two minutes with 389 nm light in the device described above. The sample

Figure 2.3 HPLC elution profiles of enzyme hydrolyzed pBR 322 DNA monoadducted and cross-linked with Tritiated HMT

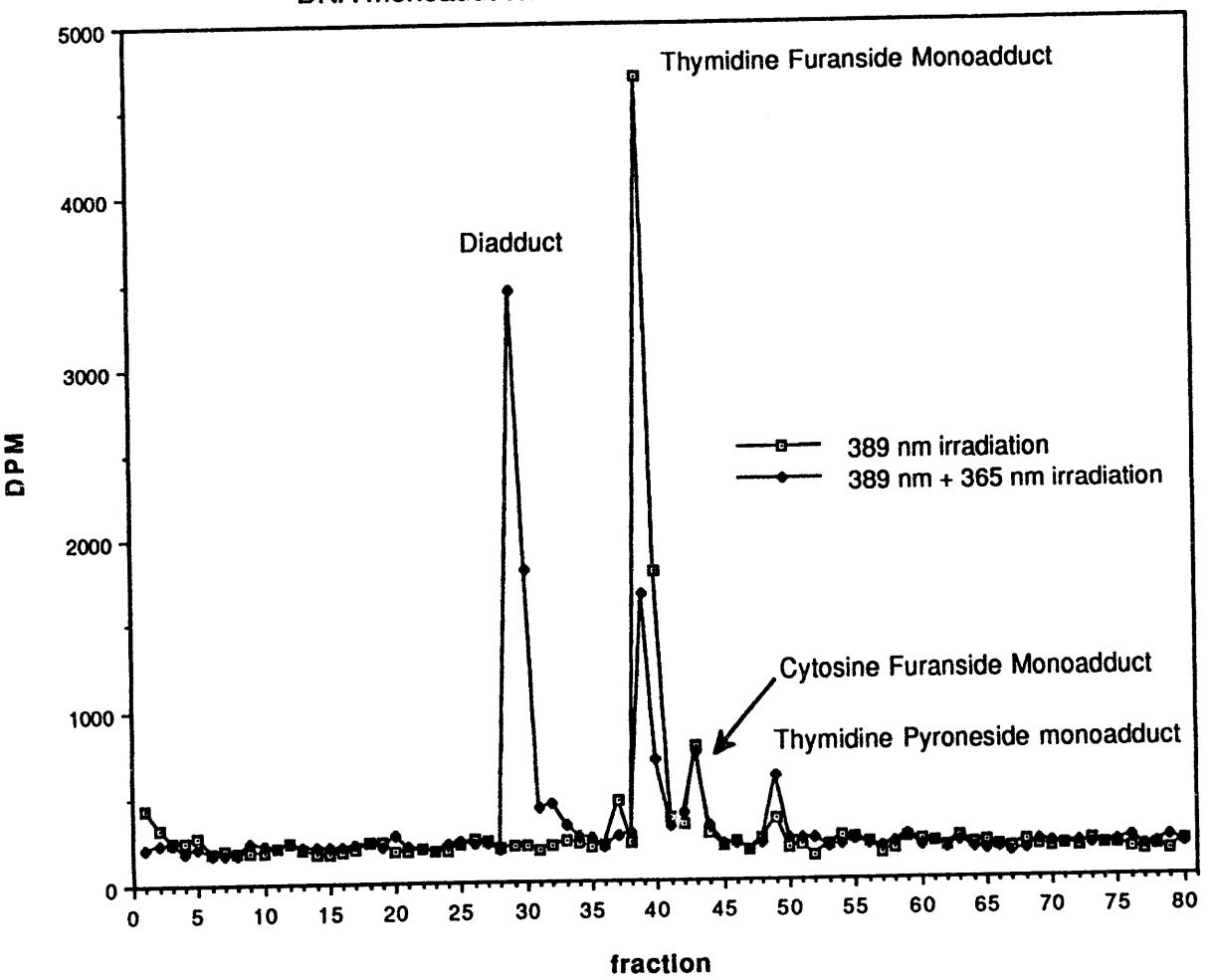

Figure 2.4 HPLC elution profiles of enzyme hydrolyzed pBR 322 DNA with an average of 40 HMT monoadducts and an average of 8 HMT monoadducts

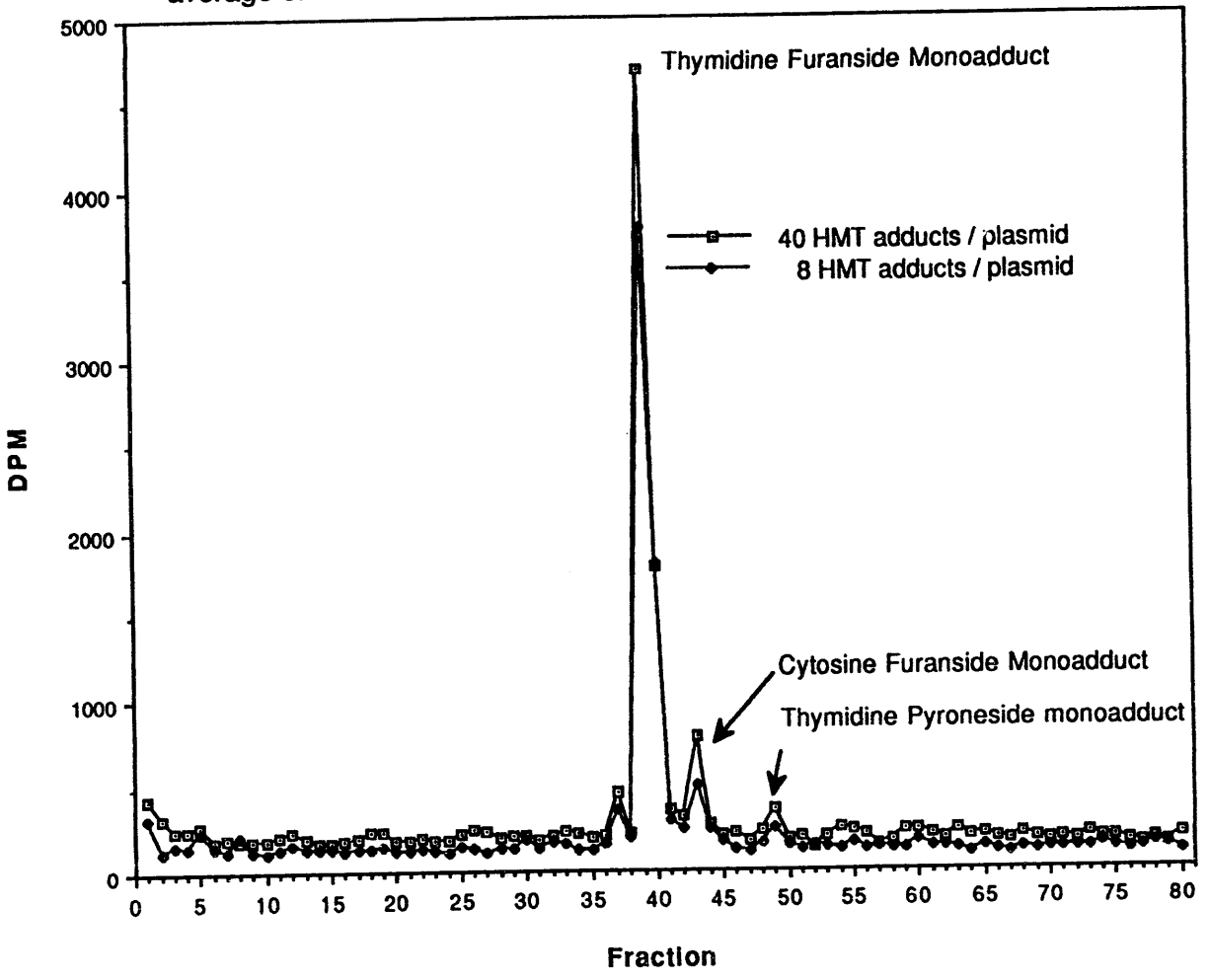

was precipitated three times with ethanol. This treatment removes any unbound psoralen from the DNA. The DNA was dissolved in TE and divided into two portions. The first was reserved in the dark, and the second was irradiated for ten minutes with 300 mW/cm^2 320-380 nm light. An aliquot of the singly and doubly irradiated DNA's were removed and assayed for DNA concentration and bound tritium. There were an average of 40 HMT adducts per plasmid. Approximately 192 μg monoadducted plasmid and 184 μg crosslinked plasmid were created in this way. To produce HMT modified pBR 322 with fewer adducts per plasmid, the initial irradiation time was reduced to 27 seconds. When assayed for psoralen incorporation as above, an average of 8 HMT adducts were in each plasmid.

An aliquot of each of these two solutions was digested to nucleosides and analyzed by reverse phase HPLC. After correction for background,the following distribution of adducts in the plasmids was calculated. The chromatograms comparing these digests are shown in figure 2.3.

Monoadducted pBR 322	%
Diadduct	none
Furan-side thymidine adduct	77.2
Furan-side cytosine adduct	10.5
Pyrone-side thymidine adduct	2.2

Crosslinked pBR 322	%
Diadduct	58.0
Furan-side thymidine adduct	22.0
Furan-side cytosine adduct	9.2
Pyrone-side thymidine adduct	4.4

The same distribution of adducts was found in both the 40-adduct and 8-adduct furan-side monoadducted plasmids (Figure 2.4). The average number of psoralen adducts in the monoadducted and cross-linked plasmids did not change, indicating that there was no photoreversal of the adducts out of the DNA. Not all of the furan-side monoadducts in the plasmid were converted to diadducts under the conditions used in the second irradiation. There are two possible explanations for this failure, either the sample was exposed to an insufficient dose of crosslinking light, or that many of the adducts are in non-cross-linkable sites in the plasmid. The slight decrease in the amount of cytosine furan-side monoadducts seen indicates that some of these adducts are also being driven on to cross-link. The doubling of the amount of pyrone-side adduct in the cross-linked sample relative to the monoadducted sample is due to in-helix photoisomerization of furan-side monoadducts in cross-linkable sites (Tessman *et al.*, 1985). This is in contrast to the results of Shi & Hearst (Shi and Hearst, 1987b) where no in-helix photoisomerization was observed for HMT furan-side monoadducted oligomers subject to 334 nm light. This discrepancy is probably due to the relative sensitivities of the assays used in the two studies. The conversion of MAf to MAp under these conditions involves only 2% of the furan-side adducts, an amount easily overlooked when analyzing an autoradiogram. The singly and doubly irradiated plasmids were run on a 0.8% agarose gel in TBE along with stock pBR 322 and visualized with ethidium staining (data not shown). There was a significant amount of nicked plasmid in both the monoadducted and crosslinked samples. This nicking was probably due to formation of singlet oxygen during the irradiation, and handling of the plasmid through the precipitations. In order for the modified plasmids to be useful as substrates for repair activity assays, there had to be no nicks in them. The assay involves the incorporation of radioactive label into the putative excision patch. Any nicks in the DNA substrate would act as sites for incorporation of label by the polymerases in the extracts by either nick translation or strand displacement synthesis. Covalently closed circular (CCC) adducted plasmids were purified away from nicked (relaxed) plasmid by a

ethidium bromide, CsCl gradient. Only psoralen adducted DNA with greater than 95% superhelical molecules was used in the repair synthesis assay.

Repair Synthesis Assay. This assay which measures the incorporation of a radiolabeled nucleotide into damaged DNA was performed as previously described (Sibghat-Ullah *et al.*, 1989) except that the concentration of KCl was increased to 75 mM and undamaged M13RFI was not included as an internal control. Repair synthesis with (A)BC excinuclease was conducted essentially as described elsewhere (Wood, 1989). Following repair synthesis DNA was either linearized with EcoRI or digested into several fragments with HpaII or a combination of BamHI, BstYI, EcoRI, HincII, PstI and PvuII and the fragments were separated on either 1% agarose gel or 5% native polyacrylamide gel. When indicated, the fragments were excised from the gels, electroeluted and processed further. When UV, psoralen monoadducted or psoralen cross-linked DNA was used in the repair synthesis assay with CFE, we observed a stimulation of radiolabeled nucleotide incorporation relative to that observed in unmodified pBR 322. Nonspecific synthesis in undamaged DNA, which had an average value of 60 ± 14 fmol, was subtracted from the total incorporation in modified DNA to determine the damage-specific incorporation (Table 2.1).

Table 2.1 Nucleotide Incorporation (fmol dCMP) During Repair Synthesis by Human and *E.coli* Systems on DNA Damaged by UV or Psoralen

Repair System	Type Damage/Number of Adducts Per Plasmid	
	HeLa CFE	UvrABC + PolI
UV/8	149 ± 19	n.d.
UV/20	198 ± 33	382 ± 14
Pso MA/8	83 ± 38	429 ± 109
Pso MA/40	134 ± 24	309 ± 52
Pso XL/40	298 ± 58	95 ± 24

The Pso XL substrate contains both monoadducts (17) and crosslinks (23). For the human system, plasmid pBR322 (200ng) containing the indicated type of damage and number of adducts was incubated at 30°C for 150-180 mins in 50µl repair synthesis buffer containing 2µCi[a-^{32}P]dCTP and the optimal amount of CFE, typically 40µg. For the *E. coli* system, 200ng randomly damaged pBR322 was incubated at 37°C for 60 mins in 100µl repair synthesis buffer containing 2µCi[a-^{32}P]dCTP, UvrA (10nM), UvrB (100nM), UvrC (50nM), DNA polymerase I (20 units) and T4 DNA ligase (2 units). Following repair synthesis, the DNA was linearized with Eco RI, resolved on 1% agarose gels, located by autoradiography and then cut out of the gel for quantitation of DNA synthesis by liquid scintillation or Cerenkov counting. Levels of incorporation were determined after normalizing for DNA recovery and subtracting the nonspecific synthesis into undamaged pBR322 which was incubated and processed as described for damaged DNA and used as a control in all experiments. The values given (fmol ± s.e.m.) are the averages of 3-9 experiments using HeLa CFE (6 extract preparations) or 2 experiments using the *E. coli* system.

Assays to Detect Removal of Psoralen Adducts. The fraction of DNA labeled by repair synthesis which no longer contained psoralen was measured. The assay measures the relative amount of psoralen in DNA restriction fragments radiolabeled as a result of damage induced DNA synthesis compared to the amount of psoralen in fragments labeled by kinasing the total DNA.

For measuring removal of psoralen monoadducts, pBR 322 containing on average 8 HMT monoadducts was subjected to repair synthesis and digested with a mixture of restriction enzymes and then the fragments were separated on a 5% polyacrylamide gel. A total of five fragments ranging in size from 276 bp to 454 bp were excised from the gel, purified by electroelution, precipitated with ethanol and resuspended in TEN 7.4 buffer. Aliquots of these labeled fragments were irradiated with 7.5×10^4 J/M^2 of 366 nm from 15 W GE Black Light lamp to convert all cross-linkable psoralen monoadduct (70-80%) into cross-links. To measure the level of psoralen adducts in total DNA, a sample of pBR 322 with 8 monoadducts (as measured scintillation counting) was digested with the same mixture of restriction enzymes, kinased, and these same fragments were isolated and subjected to the above irradiation treatment. The DNA fragments labeled by either damage induced synthesis or terminally labeled by kinasing were then denatured by heating at 95°C for 15 min and allowed to renature at 23°C for 5 min and then separated on 5-8% polyacrylamide gels. The gels were autoradiographed and the autoradiograms were scanned by densitometry to estimate the fractions of single-stranded (~ psoralen-free) and double stranded DNA.

The same method was employed to measure the removal of psoralen cross-link except the irradiation step to convert monoadducts to cross-links was omitted. Again fragments labeled either as a result of damage induced synthesis or kinasing were subjected to denaturation-renaturation and then separated on native polyacrylamide gels and the fractions of single stranded DNA in the two DNAs were compared to find out whether

DNA labeled by damage induced synthesis contained a greater fraction of single strand compared to total DNA (labeled by kinasing).

Data Analysis. The rationale of our assay is as follows: Since only 1-10% of the DNA is repaired it would be difficult to detect a 1-10% decrease in the number of adducts if total DNA were used in the repair assay. However if one analyzes only those molecules which have undergone damage-induced DNA synthesis then the background signal from unrepaired molecules is eliminated. Psoralen chemistry allows one to estimate psoralen adducts in the repair synthesis radiolabeled subpopulation and therefore determine if DNA synthesis is associated with loss of the adduct. Psoralen at low doses reacts with thymidines in 5'-TpA-3' sequences and these monoadducts can be converted into cross-links with 70-80% efficiency by irradiation with 366 nm. Thus, following repair synthesis if one exposes DNA to 366 nm and then looks at the fraction of the labeled DNA which becomes single stranded upon denaturation by heating at 95°C, only the amount of psoralen in radiolabeled DNA is measured. By conducting the same type of treatments on terminally labeled DNA (kinased) the level of psoralen in total DNA can be similarly determined. From a comparison of these levels it can be determined whether DNA labeled by repair synthesis contains lower a frequency of psoralen photoproducts. Since the psoralen damage is more-or-less randomly distributed, the data must be analyzed using the Poisson formula. A DNA fragment containing an average (M) of one psoralen adduct per molecule will have a fraction, P(0), of 37% with no adduct at all and a fraction of 13% with two adducts and so on. In applying Poisson statistics to this specific problem it is expected that the P(0) class will not be labeled and that the P (> 2) class will remain as duplex even if one of the psoralens has been removed by repair. The possibility of removal of two adducts from a plasmid in this low efficiency repair system is considered to be negligible. Therefore only the removal of psoralen from the P(1) class is assumed to contribute to an increase in single-stranded DNA [P(O) class]. The P(0) class of total DNA is measured by analyzing kinased (unrepaired) fragments, and from this value M is calculated knowing that

the various classes of psoralen adducts are estimated from $P(k) = e^{-m} m^k/k!$ where k = frequency class. We assumed (1) damage induced DNA synthesis always results in elimination of one adduct, (2) the probability of repairing more than one adduct in a fragment is zero and (3) the probability of repair synthesis in a fragment is directly proportional to the number of adducts present in that fragment. With these assumptions then for a fragment with an average of M psoralen monoadducts, the fraction of single strand after denaturation is expected to be $P(0)=e^{-m}$ while the fraction that becomes single stranded in repaired DNA should be P(1)/[1-P(O)] that is the ratio of P(1) class to the rest of the classes of adducted fragment as P(O) is assumed not to contribute to labeling and the labeling into P(>1) does not result in generation of single strand. Thus, for any given M in total DNA determined experimentally from analysis of kinased fragments, P(1)/[1-P(O)]is calculated. If damage induced DNA synthesis is not associated with repair the fraction of ssDNA should be equal to P(0) for both kinased and internally labeled DNA; however, if all damage induced DNA synthesis is associated with adduct removal then the fraction that becomes ssDNA in the repair synthesis reaction should be P(1)/[1-P(O)]. By comparing the fraction of single stranded DNA in the kinased and "repaired" DNAs we were able to tell whether the "repaired" DNA was indeed repaired. The analysis for repair of cross-linked DNA was identical.

RESULTS

Repair Synthesis with DNA-MA and DNA-XL. Previous work (Sancar and Sancar, 1988; Wood *et al.*, 1988) has shown that psoralen damaged DNA elicits DNA synthesis by HeLa CFE. The previous work was conducted with substrate containing mostly MA and an unknown level of cross-links. We wished to determine the relative efficiencies of the two forms of adducts as substrates for repair synthesis. We used short wavelength UV-damaged DNA as our reference substrate since its dose response is well characterized. In

agreement with earlier reports at modification levels of 8 adducts per molecule UV damaged or psoralen adducted DNA give comparable repair signals. At higher doses the UV signal appears to measure linearly up to 20 adduct per molecule while the signal with psoralen adducted DNA starts to level off. However, when the monoadducts are converted to cross-links the signal more than doubles. This is in contrast with what is observed with the E. coli nucleotide excision repair system. Conversion of monoadducts to cross-links drastically reduces the repair signal in this system which was reconstituted with purified UvrA, UvrB, UvrC proteins, DNA polymerase I and ligase. The result with the E. coli system was not unexpected. Even though (A)BC excinuclease incises psoralen monoadducts and cross-links with near-equal efficiency the cross-link cannot be further processed by the enzyme and the two nicks generated on the furan-side of the cross-link do not function as primers for PolI (Cheng *et al.*, 1991; Cheng *et al.*, 1988a; Sladek *et al.*, 1989; Van Houten *et al.*, 1986a). Whether the increased repair synthesis observed with HeLa CFE constitute true repair synthesis will be addressed later.

Removal of Psoralen MA by HeLa CFE. While the results presented above as well as several previous reports clearly show damage-induced DNA synthesis by HeLa CFE, it has not been shown unambiguously that this synthesis is the result of filling-in of the single strand gaps generated by nucleotide excision nuclease. To demonstrate that adducts were removed from DNA we took advantage of a unique property of psoralen photochemistry: The psoralen furan-side thymine monoadduct can absorb a second ultraviolet photon to form an interstrand cross-link with an adjacent thymidine on the opposite strand. Psoralens preferentially react at 5'-TpA-3' sequences in DNA. At low adduct to base pair ratios, such as with these substrates, most of the furan-side monoadducts will be in cross-linkable sites. Psoralen monoadducts can be converted with 80-90% efficiency to interstrand cross-links by a second round of irradiation with 366 nm light. Following repair synthesis the frequency of psoralen adducts remaining in radiolabeled DNA can be determined easily by measuring the fraction of rapidly renaturable radioactive DNA following heat denaturation-

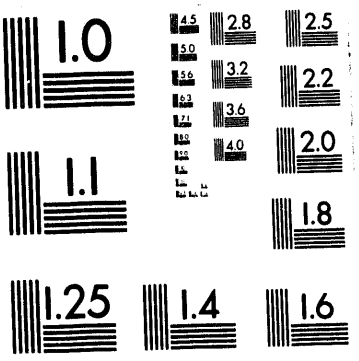
1.0
1.1
1.25
1.4
1.6
1.8
2.0
2.2
2.5
2.8
3.2
3.6
4.0
4.5
5.0
5.6
6.3
7.1
8.0
9.0

2 of 3

rapid renaturation. By comparing this fraction with that obtained with unrepaired DNA (5'-terminally labeled) a quantitative estimate between label incorporation and adduct removal can be made.

The fraction of DNA that remains single stranded in DNA labeled by repair synthesis is higher than the fraction of single stranded DNA in total DNA and thus the repair-labeled DNA must have fewer psoralen adducts compared to the remainder of DNA.

To establish whether all repair synthesis was associated with adduct removal, five fragments ranging in size from 276 bp to 454 bp were isolated from pBR322/MA8 which had been subjected to repair synthesis. If "repair synthesis" was not the result of adduct removal then the P(0) class (single-stranded fraction) of kinased DNA would be the same as the DNA labeled by "repair synthesis". Since the P(0) class does not contribute to "repair synthesis" and since repair synthesis in P(>1) class does not contribute to ssDNA formation, all synthesis associated with adduct removal in the fraction of ssDNA in "repair DNA" would be $P(1)/\Sigma P\ (>1)k$. The results obtained with these five fragments are summarized in Table 2.2. Several conclusions can be drawn from the data in this table. First, the P(0) class of the individual fragments does not decrease uniformly with fragment size as would have been expected if psoralen adducts were uniformly distributed in pBR322. As a result, in calculating $P(1)/\Sigma Pk\ P(>1)$ the M values for individual fragments obtained experimentally must be used rather the M value obtained from the total number of adducts in pBR322 and fragment size. Secondly, the calculated $P(1)/\Sigma P(>1)k$ is significantly different than P(0) indicating the importance of this type of analysis rather than comparing P(0) values. Finally, the experimentally determined single stranded DNA fraction, with the exception of the 295 bp fragment, is in good agreement with the calculated $P(1)/\Sigma P(>1)k$ which was calculated assuming that all synthesis is the result of adduct removal. We therefore conclude that HMT furan-side monoadduct damage induced DNA synthesis in our system is true repair synthesis resulting from the filling in of gaps generated by adduct removal.

Table 2.2 Fraction of Fragments that Migrate as Single-Stranded DNA Following Repair of Psoralen Monoadducted DNA by HeLa Cell-Free Extract

Fragment Size (bp)	Observed Damaged DNA	Expected Repaired DNA	Observed Repaired DNA
454	0.34	0.49	0.61
400	0.60	0.75	0.76
377	0.50	0.66	0.66
295	0.78	0.90	0.77
276	0.69	0.83	0.84

Repair of Psoralen Monoadducted (MA) DNA by HeLa CFE. Plasmid pBR322 containing 8 MA per molecule was incubated as described in Table 1 except each reaction mixture contained 300ng DNA and 5μCi [α-^{32}P]dCTP. Following incubation a total of 5.4μg repaired DNA was restricted and the BamHI-HincII$_{(276bp)}$ fragment was gel purified. One half of the repaired and thus internally labelled DNA, was irradiated with a black light (+366nm) and one half was left untreated (-366nm). Damaged DNA, which was not repaired but which was 5' end-labelled with T4 polynucleotide kinase and [γ-^{32}P]ATP, was similarly irradiated or not. Prior to resolution on a 5% polyacrylamide gel, one half of each sample was heat denatured or left in its native state. The relative amounts of single-stranded DNA in each lane were determined by scanning the resulting autoradiographs with a Zeineh Soft Laser Scanning Densitometer. The values reported for observed fraction single-stranded DNA are the averages of 2-5 experiments. The values for expected fraction single-stranded DNA following repair synthesis were determined from the average values observed for damaged DNA, as described in the text.

Removal of Psoralen Cross-links. In a manner analogous to that for psoralen monoadducts we reasoned that analysis of radiolabeled DNA following repair synthesis with cross-linked substrate would reveal whether "repair synthesis" resulted in cross-link repair. The rationale and method of analysis were the same as for the monoadducts except that there was no post-repair irradiation to convert monoadducts to cross-links. Furthermore, in calculating the cross-link induced radiolabel incorporation, the signal from monoadducts present in cross-linked DNA was taken into account. In the cross-linked DNA we only looked at the average signal from cross-link repair. With these corrections, the fraction of single-stranded DNA in repair-labeled and total (terminally labeled) DNA of eight fragments can be compared to find out whether there was cross-link removal. The quantitative analysis for 8 fragments is summarized in Table 2.3. In all fragments analyzed the fraction of repair-labeled DNA that become single stranded upon denaturation-rapid renaturation was higher for repair labeled DNA than terminally labeled DNA. In most cases the fraction that became single stranded equaled the fraction that was calculated assuming all labeling resulted from the elimination of cross-links.

Table 3. Fraction of Fragments that Migrate as Single-Stranded DNA Following Repair of Psoralen Cross-Linked DNA by HeLa Cell-Free Extract

Fragment Size (bp)	Observed Damaged DNA	Expected Repaired DNA	Observed Repaired DNA
309	0.28	0.46	0.37
217	0.20	0.37	0.23
160	0.61	0.78	0.76
147	0.47	0.67	0.64
122	0.52	0.71	0.76
110	0.50	0.69	0.72
76	0.58	0.76	0.78
67	0.73	0.88	0.79

Repair of Psoralen Cross-Linked DNA (XL) DNA by HeLa CFE. Plasmid pBR322 containing 23 XL per molecule (+17 MA) was incubated as described in Table 1 except each reaction mixture contained 300ng DNA and 5 μCi[α-^{32}P]dCTP. Following incubation a total of 1.4μg repaired DNA was restricted and the HpaII-HpaII$_{(309bp)}$ fragment was gel purified. The repaired samples contain an internal label introduced during incubation with CFE. Undamaged or damaged DNA which was not repaired were 5' end-labelled with T4 polynucleotide kinase and [γ-^{32}P]ATP. Prior to resolution on a 5% polyacrylamide gel, one half of each sample was heat denatured or left in its native state. The relative amounts of single-stranded DNA in each lane were determined by scanning the resulting autoradiographs with a Zeineh Soft Laser Scanning Densitometer. The values reported for observed fraction single-stranded DNA are the averages of 3-7 experiments. The values for expected fraction single-stranded DNA following repair synthesis were determined from the average values observed for damaged DNA, as described in the text.

In E. coli cross-links are incised efficiently by the excision repair enzyme (A)BC excinuclease but the two incisions made on the furan-side adducted strand do not constitute an efficient primer site for PolI in the absence of the recombination protein RecA. A stronger "repair synthesis" signal is obtained with monoadducted DNA relative to cross-linked substrate, in a defined E. coli system consisting of (A)BC excinuclease, PolI, RecA, ligase and the necessary substrates and cofactors. It was therefore surprising that HeLa CFE yielded a stronger repair synthesis signal with X-linked DNA. We considered the possibility that the 2-3-fold increase in repair synthesis associated with cross-linked DNA may actually result from aberrant synthesis initiated at a nick either on the 5' or 3' side of the cross-link, which is then either ligated to the fragment without cross-link removal or continues in the form of strand displacement synthesis, or nick translation. Neither of these cases is expected to yield uniform size single strand-labeled fragments free of cross-links upon denaturation. We analyzed the fragments of pBR 322 which were labeled by repair synthesis on DNA sequencing gels. When the monoadducts in the substrate are converted to cross-link prior to inclusion of the modified DNA into the reaction mixture, the intensity of the signal from the radioactive label incorporated into fragments of defined size decreases for the *E. coli* exinuclease repair synthesis system while it increases for the HeLa CFE. The most likely explanation of these data for HeLa CFE is that cross-linked DNA induces repair synthesis which results in the removal of the cross-link from at least one strand and closure of the gap following repair synthesis. Whether the cross-link is totally eliminated from DNA or one of the strands remains attached to the cross-linked adduct while the other is filled in by translesion synthesis cannot be ascertained from our data.

DISCUSSION

Nucleotide excision repair involves several formal steps: incision, excision, resynthesis, and ligation. In theory any of the first three could be used to quantify DNA repair. In the incision assay either conversion of superhelical DNA to open circular form is measured or agarose gel electrophoresis or the average molecular weight of linear DNA of non-uniform size is determined by alkaline sucrose gradient following treatment with the nicking enzyme. In the excision assay the removal of a radiolabeled adduct is measured in the form of acid soluble oligonucleotides. Although these assays could be quite sensitive when conducted properly, in general they are insensitive to levels of incision/excision below 0.05 per kbp. In contrast, a repair synthesis assay under appropriate conditions can be quite sensitive. Assuming that a DNA adduct forming-chemical, such as psoralen, and an dNTP of the same specific activity are available and assuming that the repair patch is about 20 nucleotides in length the repair synthesis assay would be 20 / 4 = 5 times more sensitive than the excision assay. In practice dNTPs are available in much higher specific activities than psoralen, 4-nitroquinoline, acetylaminofluorene or other chemicals which make base adducts excised by nucleotide excision nucleases. The sensitivity of the resynthesis assay is routinely 50-100-fold higher than the incision or excision assays (see Sibghat-Ullah, 1989 #69].

Because of its high sensitivity the resynthesis assay was successfully applied to a human cell-free system to demonstrate nucleotide excision repair (Sibghat-Ullah *et al.*, 1989; Wood, 1989; Wood *et al.*, 1988) under conditions where neither the incision nor the excision assays could provide any convincing signal (Sibghat-Ullah *et al.*, 1989). The lack of repair synthesis signal in extracts from XP cell lines known to be defective in nucleotide excision repair provided strong evidence that this was indeed repair synthesis (Wood *et al.*, 1988).

Despite this advantage in sensitivity, the repair synthesis assay suffers an important disadvantage in specificity. It can be argued that the increased DNA synthesis observed with damaged DNA merely reflects the increased susceptibility to nicking of damaged DNA by non-specific nucleases to generate primers for DNA polymerases which may incorporate radiolabel 5' or 3' to the adducted nucleotide without ever removing the adduct.

The unique photochemistry of psoralen enabled us to address the question of specificity in the *in vitro* repair synthesis assay. Psoralen preferentially intercalates into 5'-TpA-3' sites in DNA. Furan-side monoadduct is formed by absorption of a long wavelength UV light (310 - 410 nm) photon by the psoralen. This monoadduct is the result of a covalent cycloaddition reaction between the 4',5' double bond of the furan ring and the 5,6 double bond of thymidine. The monoadduct can then be driven on to an interstrand cross-link by absorbing a second photon that forms a cyclobutane ring between the 3,4 double bond of the psoralen and the pyrimidine on the opposite strand. By controlling the wavelength and dose of irradiation, one can obtain psoralen modified DNA containing only monoadducts which can later be converted into cross-links with high efficiency by a second round of irradiation.

Utilizing the unique properties of psoralen photochemistry we have increased the specificity of the repair synthesis assay. Three main conclusions can be made from our results. First, the distribution of psoralen adducts in a plasmid the size of pBR 322 is non-random. When we measured the adduct frequency in fragments ranging in size from about 100 to 500 bp we found some fragments contained either higher or lower numbers of adducts than determined from the numbers predicted from the total number of adducts present in the plasmid. A non-random distribution of adducts in these fragments is not surprising because psoralen has high affinity for 5'-TpA-3' sites and still higher affinity 5'-$(ApTp)_n$-3' stretches. However, inspection of the sequences of the "hot spot" and "cold spot" fragments failed to yield any unusual distribution of such sequences. Perhaps more

subtle sequence modifiers are responsible for the observed non-random distribution of psoralen adducts.

The most significant conclusion to be made from this work, however, is that "damage-induced DNA synthesis" observed with psoralen adducted DNA in cell free extract is "repair synthesis" in that it is associated with removal of psoralen monoadducts. In general, all P(1) class repair-labeled DNA is no longer cross-linkable upon a second round of UV-irradiation. As the adducts are distributed according to Poisson distribution within the fragments some of the repair labeled DNA is converted into cross-links by UV irradiation. However, the fraction which is convertible to cross-links is in good agreement with the fraction of fragments expected to have more than one adduct. There are two exceptions to this observation. In one case a higher fraction of repair labeled DNA is converted than would be predicted from random distribution of adducts. In the second case a lower fraction than expected became single-stranded upon denaturation-renaturation. We expect that these are due to non-Poisson adduct distribution in the two cases, having a single hot spot for photo adduction in the former and two or more hot spots in the latter case.

Finally, and quite unexpectedly, we found that psoralen cross-links induced a higher level of repair synthesis compared to monoadducts. A trivial explanation of this phenomenon would be that upon conversion to a cross-link a psoralen monoadduct becomes a diadduct and in a sense the adduct level in DNA doubles and therefore it is to be expected that the "repair synthesis" signal should go up. However, at the level of short wavelength UV damaged DNA and psoralen adducts (40 monoadducts per pBR322) used in these experiments, the adduct level is near saturating and two-fold increase in monoadducts would not result in two-fold increase in signal. The increase in repair synthesis upon conversion of monoadducts to cross-links is more than two-fold. It is clear that a cross-link induces more repair synthesis than two monoadducts. Whether this is because a cross-link is a better substrate than monoadduct or the "repair patch" induced by

cross-link is larger, remains to be determined. Differential repair of psoralen cross-links and monoadducts in eukaryotic systems has been observed *in vivo* . In *S. cerevisiae*, (Averbeck, 1988b; Averbeck *et al.*, 1988a) noted that a mixture of cross-links and monoadducts was more mutagenic than a population of monoadducts alone, and that bifunctional psoralen derivatives were more mutagenic than monofunctional ones. TMP monoadducts can interfere with the efficiency of cross-link repair in normal human fibroblast cells, as measured by incision of the DNA (Papdopoulo *et al.*, 1988). In the repair-deficient FA cells, this effect was even more significant (Averbeck *et al.*, 1988a). The variations in the efficiencies of repair of adducts formed by TMP, 8-MOP, and 5-MOP have been attributed to the different levels of monoadduct versus cross-link damage induced by 365 nm light (Averbeck, 1988b; Papdopoulo *et al.*, 1988).

Our data provide strong evidence that the repair synthesis induced by psoralen cross-link is associated with the disappearance of that cross-link and might legitimately be considered as cross-link repair. There are at least two possible ways how an interstrand cross-link may disappear from a DNA with a repair synthesis patch. In one mechanism the cross-link is totally removed by first incising one strand, filling in the gap and then removing the "dangling-cross-linked oligomer" (Van Houten *et al.*, 1986b) from the other strand. A second mechanism involves bypass DNA synthesis following two incisions made on both sides of the adduct in one strand. Which mechanism is operative in our system remains to be established. The apparent disappearance of the psoralen cross-link in this system opens new possibilities for studying cross-link repair in mammalian cells.

Chapter 3

The Large Scale Synthesis of Site-Specifically Psoralen Adducted DNA Molecules

In chapter 1 of this dissertation, psoralens were used as probes for DNA dynamics. They have been used to study RNA secondary and tertiary structure. Cross-linking by psoralens is a sensitive probe for DNA conformation *in vivo*. In chapter 2, we used psoralen modified DNA as a model for the study of DNA repair enzyme systems. There is something about the structure of psoralen damaged DNA which is recognized by the repair enzyme complex as not normal. We are interested in the investigation of the detailed molecular structure dynamics and interactions of these repair proteins with damaged DNA. Psoralen adducts in DNA also interfere with processes of replication and transcription. Despite the fact that repair enzymes recognize psoralen adducted DNA as unusual, a furan-side monoadduct stabilizes the helix by 1.6 kcal/mol, a pyrone-side monoadduct stabilizes the helix by 0.7 kcal/mol and an interstrand cross-link prevents the denaturation of the strands. We wish to understand the structural basis for these stabilizing interactions. To investigate these and other phenomena, large quantities of each of these three types of adducts are necessary. In order to study the structures of these adducts by NMR and X-ray crystallographic methods, they must be homogeneous and very pure. Both the forward and the reverse photochemistry of all three adducts have been extensively investigated (Figure 1.2). The structures of the three main adducts are shown in Figure 1.3.

You can't study it if you can't make it. Reported below are methods to make very pure micromole quantities of all three main psoralen-DNA adducts. This chapter is divided into four parts. The first part is the preparation of furan-side monoadducted DNA. The second part is the preparation of cross-linked DNA. The third part is the preparation of pyrone-side monoadducted DNA and the fourth part is an application of the site-specifically psoralen modified oligonucleotides synthesized in the first three parts.

Part I: The Preparation of Furan-side Monoadducted DNA

Figure 1.4 is a comparison of the absorption spectra of DNA, furan-side monoadducted DNA and psoralen. DNA effectively stops absorbing light at wavelengths greater than 310 nm. The psoralen furan-side monoadducted DNA stops absorbing light at wavelengths greater than 395 nm, and psoralen continues to absorb light out to at least 410 nm. We have exploited the wavelength dependence of this chemistry by irradiating psoralen-DNA mixtures with a krypton ion laser operating at 406.7 nm to produce micromole quantities of HMT furan-side monoadducted oligomers for physical studies (NMR and X-ray crystallography) and as substrate to investigate various aspects of DNA repair. The absorption coefficient of psoralen at wavelengths longer than 400 nm is only between 1 and 20 (l $mole^{-1}$ cm^{-1}). In order to get efficient photochemistry at these wavelengths, a high intensity monochromatic light source is necessary. We have used a krypton ion laser that emitted light at 406.7 nm and 413 nm as our light source. The laser radiation specifically excites the psoralen to form furan-side monoadducts with DNA. The resulting monoadducts do not absorb light at the irradiation wavelength allowing it to accumulate in the reaction (see discussion in chapter 2). A laser is desirable for this procedure because of its high intensity light, low beam divergence and most importantly, the monochromaticity of the beam. Because psoralen has such a low extinction coefficient

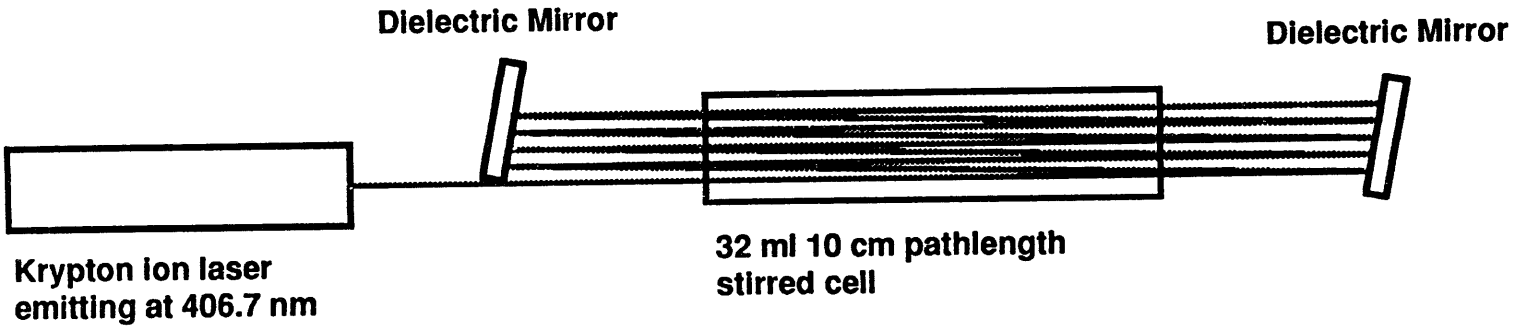

Figure 3.1 Schematic of Krypton ion laser set up to perform monoaddition reactions at long wavelengths and at high light flux

at this wavelength, a long path length reaction cell is necessary to maximizes the efficient use of the photons generated. A laser is ideal for long path length irradiations because the light that is emitted is highly collimated, so that there is little loss of light intensity due to beam divergence. To maximize the efficient use of photons, a multipass irradiation set-up was used (Figure 3.1, for a complete description of this apparatus, see experimental section).

Using a DNA 12 mer (5'-GAA-GCT-ACG-AGC-3'), a complementary DNA 8 mer (5'-TCG-TAG-CT-3') and HMT (4' - hydroxymethyl - 4, 5', 8 - trimethylpsoralen) yields of 14% 12 mer furan-side monoadduct and 10% 8 mer furan-side monoadduct after HPLC purification were achieved. Using a self complementary DNA 8 mer (5'-GCG-TAC-GC-3') and HMT, a yield of 30% (1.21 micromoles) 8 mer furan-side monoadduct after HPLC purification was achieved. Because of the large amounts of DNA used in these reactions, yields and quantities of the various reaction components were determined with high precision using UV absorption spectrophotometry. There is a theoretical maximum yield of 50% in the case of a self complementary oligonucleotide because only one monoadduct can form per duplex. The theoretical maximum yield for non-self complementary oligomers is also 50% monoadduct on each strand because there is an equal statistical probability that the psoralen will be oriented in the duplex with its furan end intercalated into either strand.

A time course of the reaction between the HMT and the 8 mer / 12 mer duplex irradiated with 350 mW of 406.7 nm and 413 nm light from the krypton laser was performed. The reaction plateaued after 120 minutes of irradiation time. The reaction was tested out to irradiation times of 300 minutes (data not shown). When the krypton laser was used, there was no detectable formation of cross-linked DNA if the sample was handled with respect (i.e. minimal exposure to fluorescent room light, and sunlight). Production of monoadduct using a 389 nm band pass filter and an arc lamp yielded some monoadducted oligonucleotide but not in nearly as high a yield as when a high intensity krypton laser was employed. The experimental set up for irradiations with 389 nm light is

Figure 3.2: This is a comparison of the reaction between the self-complemtary 8mer 5'-GGGTACCC and AMT using light transmitted by a $Co(NO_3)_2$ filter and light transmitted through a 389nm band pass filter. Lanes 1, 2 and 3 are a time course of the reaction irradiated through the $Co(NO_3)_2$ filter with time points of 5, 15 and 30 minutes. Lane 2 did not load well. Lanes 4, 5, and 6 are a time course of the reaction irradiated through the 389nm band pass filter with time points of 20, 60 and 130 minutes. The difference between lanes 1 and 3 is the disappearance of the band that corresponds to the 8MAf. The major product produced in these reaction is the crosslinked molecule. A side product is the 8mer MAp. The 8mer MAf grows in in lanes 4, 5 and 6. There is also the appearance of 8mer MAp and 8mer XL. Both of these grow in slower than the 8mer MAf.

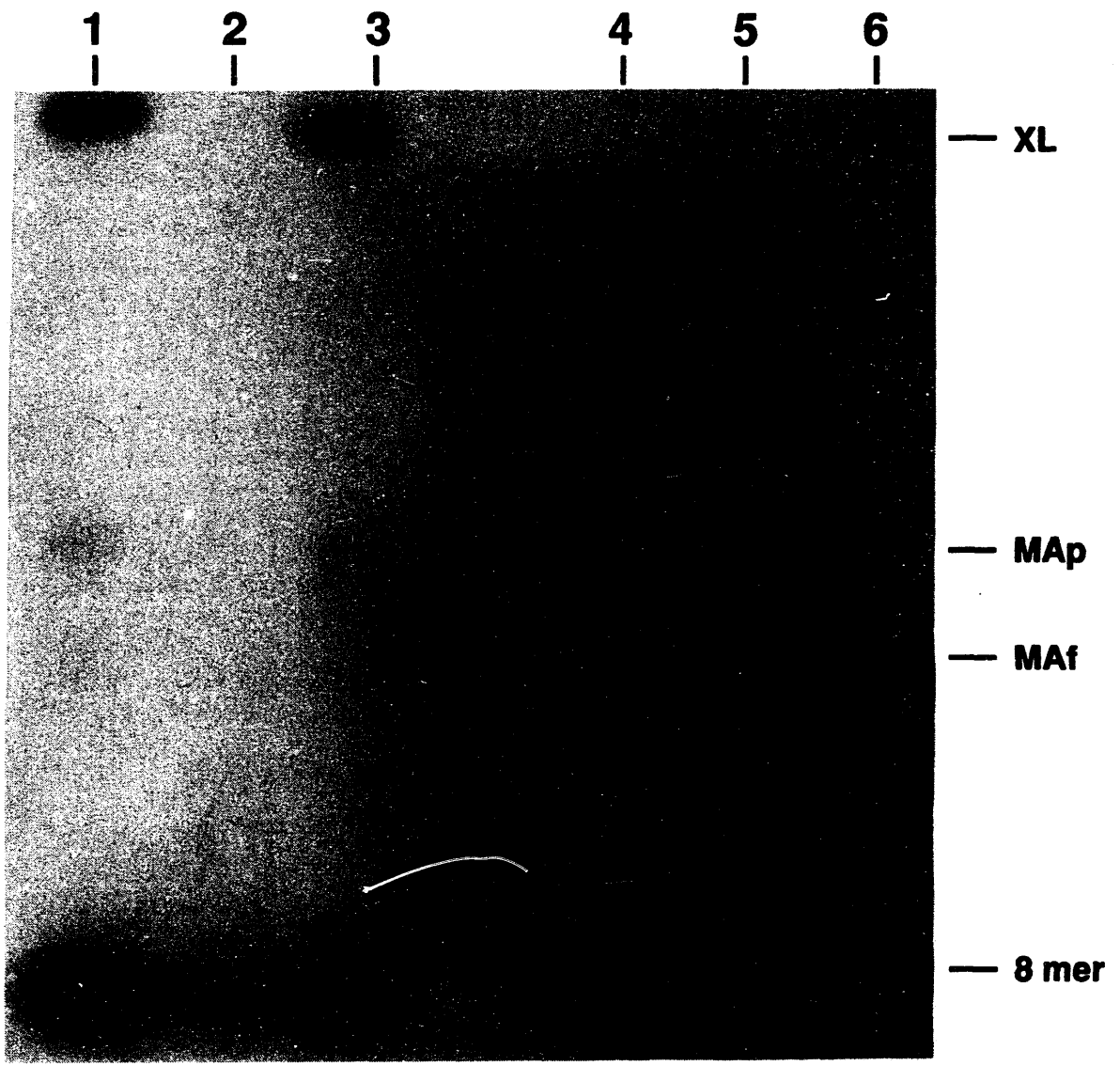
1
2
3
4
5
6
XL
MAp
MAf
8 mer

described in the previous chapter (Kodadek and Gamper, 1987). Figure 3.2 is an autoradiogram that compares light transmitted by a $Co(NO3)2$ 320 - 380 nm bandpass liquid filter with light transmitted through a 389 nm band pass filter upon the photoreaction of the self-complementary 8 mer 5'-GGGTACCC-3' and AMT. Lanes 1, 2 and 3 are a time course of the reaction irradiated through the $Co(NO3)2$ filter with time points of 5, 15 and 30 minutes. Lane 2 did not load well. Lanes 4, 5, and 6 are a time course of the reaction irradiated with 5 mW of 389 nm light with time points of 20, 60 and 130 minutes. The difference between lanes 1 and 3 is the disappearance of the band that corresponds to the 8 mer MAf. The major product produced in these reaction is the cross-linked molecule. A side product is the 8 mer MAp. The 8 mer MAf grows in in lanes 4, 5 and 6. There is also the appearance of 8 mer MAp and 8 mer XL. Both of these products grow in slower than the 8 mer MAf. By irradiation of a duplex DNA mixture and psoralen with light filtered through a 389 nm band pass filter it is possible to make furan-side monoadducted oligonucleotides. However, synthesis of monoadducted oligonucleotides using the band pass filter always resulted in formation of some cross-link and pyrone-side adduct. The possible explanation for this is that 389 nm light is of a short enough wavelength that the furan-side monoadduct can absorb light and go on to cross-link and that excitation of the psoralen at this wavelength allows pyrone-side adduct to form. Short wavelength light leakage through the filter train can be discounted as a mechanism for cross-link formation because the optical density of the filters used was greater than 5 ODU for wavelengths shorter than 375 nm. Because of the low intensity of the light through the filter, reaction times were quite long. Since the light was from an arc lamp and divergent, it was not possible to use an efficient multi-pass set up to maximize the use of the photons.

Formation of the desired monoadducted oligonucleotide is not the only problem to be faced when large scale production of these modified DNA's is undertaken. Purification of the resulting furan-side adducted molecules away from the rest of the reaction mixture must also be successfully performed. HPLC has been used to separate short DNA

Figure 3.3 Chromatogram of the HMT furan-side monoaddition reaction of the DNA oligomers 5'-GAAGCTACGAGC-3' AND 5'-TCGTAGCT-3'.

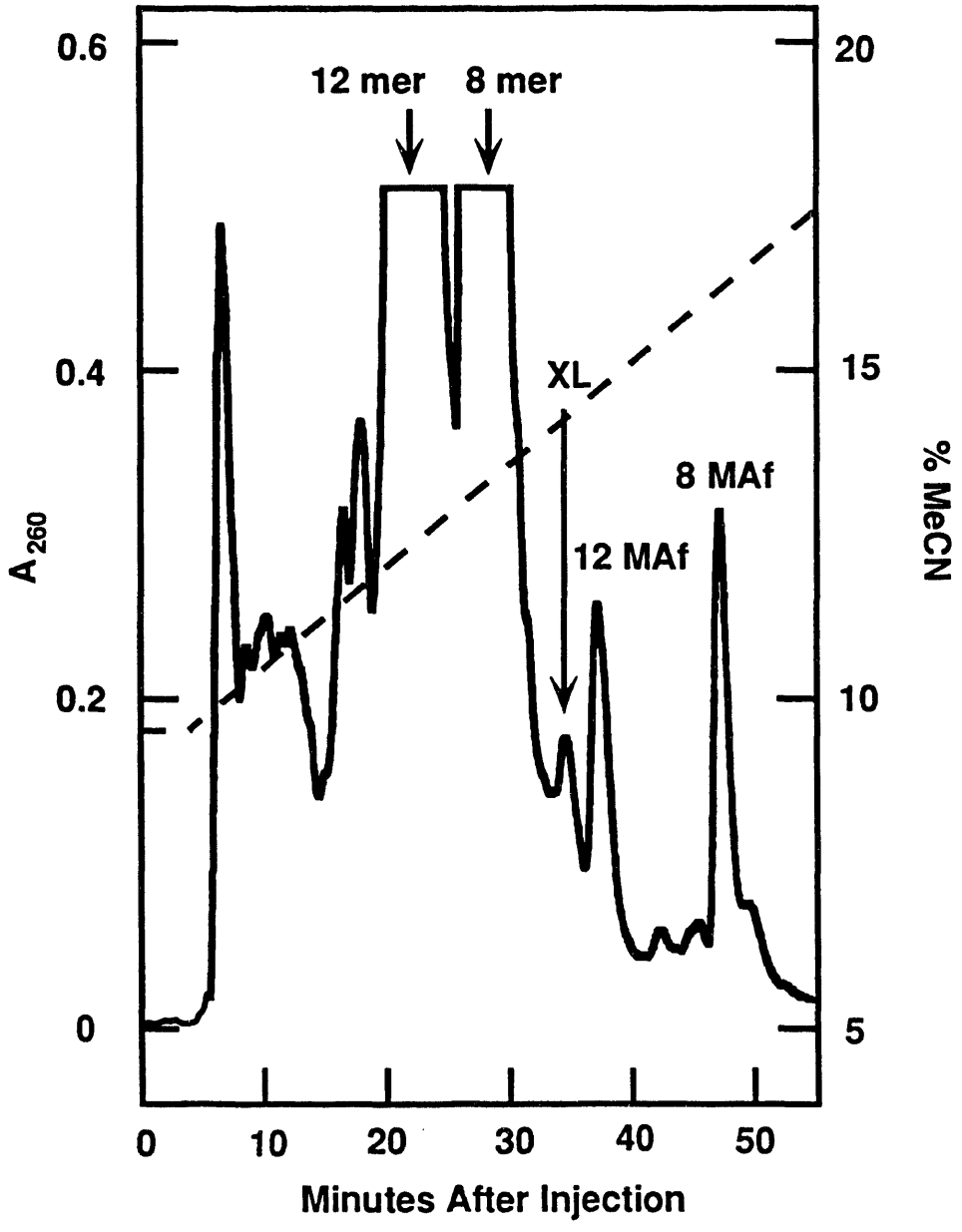

Figure 3.4: This is an autoradiogram of kinased HPLC fractions from the reaction between the 12 mer 5'-GAA-GCT-ACG-AGC-3' and its complementary 8 mer 5'-TCG-TAG-CT-3' with HMT irradiated at 406.7 nm. Lane 1 corresponds to fraction 28 and is the 8 mer. Lane 2 corresponds to fraction 48 and is the furan-side monoadducted 8 mer. Lane 3 corresponds to fraction 23 and is the unmodified 12 mer. Lane 4 corresponds to fraction 37 and is the furan-side monoadduct of the 12 mer. Lane 5 corresponds to fraction 35 and is the HMT cross-link 8 mer and 12 mer. Lane 6 is the control reaction where the 8 mer and 12 mer are irradiated in the presence of HMT with 365 nm light. This forms an interstrand cross-link between the two DNA molecules. A faint band can be seen in this lane that has the same electrophoretic mobility as the 12 mer MAf and 8 mer MAf. These are the pyrone-side adducts of the 12 mer and 8 mer.

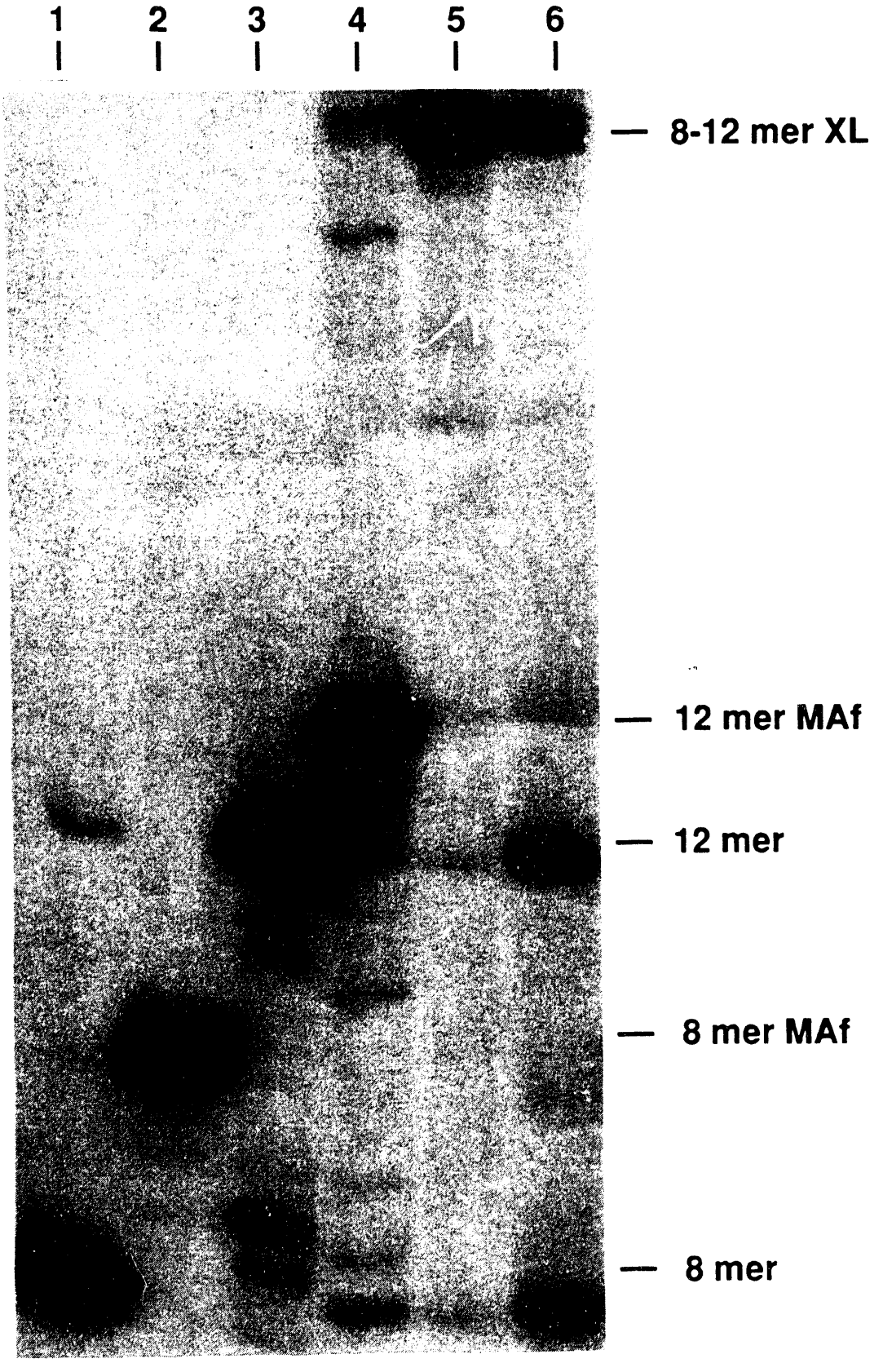
1
2
3
4
5
6
— 8-12 mer XL
— 12 mer MAf
— 12 mer
— 8 mer MAf
— 8 mer

oligomers that have been modified with 2-(acetylamino)fluorene and 4-aminobiphenyl from their parent DNA (Johnson *et al.*, 1986; Lasko *et al.*, 1987). The monoadducted oligonucleotides have a significantly different retention time from the parent oligonucleotides on C_{18} reverse phase HPLC. This is primarily due to the increased hydrophobicity of the psoralen containing oligonucleotide. Cross-linked oligonucleotides also exhibit a longer retention time than the parent oligonucleotides, although, it is shorter than that for the monoadducted oligonucleotides. This is most likely due to the fact that the psoralen in a cross-linked oligonucleotide is unable to interact with the column packing because it is sequestered in the helix. Figure 3.3 is the chromatogram of the monoaddition reaction between the 12 mer (5'-GAA-GCT-ACG-AGC-3'), it's complementary DNA 8 mer (5'-TCG-TAG-CT-3') and HMT. Figure 3.4 is an autoradiogram where various fractions from that HPLC run were kinased with ^{32}P and identified. The retention time on the HPLC column for the HMT cross-linked 8 mer and 12 mer is between that of the unmodified oligonucleotides and the furan-side monoadducted molecules. This relationship between the chromatographic retention time of the cross-link and the monoadducted oligonucleotides does not always hold up, for it is dependant on the sequence of the oligonucleotides involved in the reaction. As the chain length of the oligonucleotide increases, the difference between a monoadducted oligo and its parent decreases. This is discussed in greater detail below. Another HPLC technique that can be used to separate the components of a monoaddition reaction is anion exchange chromatography. This method separates molecules based on their charges. Preparative polyacrylamide gel electrophoresis can also be employed in the purification of these modified oligonucleotides. However, there are limitations and problems associated with this technique. These two methods, HPLC (both reverse phase and anion exchange) and gel electrophoresis, are compared in the discussion section in greater detail. The practical limit for separating monoadducted oligos from their parent compound is about 30 nucleotides in length.

Materials and methods:

Synthesis of modified oligonucleotides using the krypton laser: Irradiations were carried out using a SpectraPhysics 2020 krypton laser operating in broad band mode at 406.7 nm and 413 nm at 350 mw. The oligonucleotides were dissolved in 35 ml of 150 mM NaCl, 10 mM $MgCl_2$, 1 mM EDTA, 15 mM azide, $5.6X10^{-4}$ M HMT. This solution was introduced into a 10 cm path length quartz cuvette. The cuvette was placed in the laser beam and between two dielectric mirrors optimized for reflectivity at 406.7 nm with stirring. The mirrors were adjusted to cause the beam to be reflected for a total of eight passes through the sample. Aliquots for analysis were withdrawn from the cuvette during the irradiation. These aliquots were typically 5 µl. After the irradiation was complete, the solution was brought to 200 mM NaCl with 6.1 M NaCl, and 3 volumes of absolute EtOH were added. Solution was cooled overnight at -20°C and the precipitate collected by centrifugation at 25,000 x g for 2 hours. The supernatant was removed and the pellet washed with 95% EtOH and dried in vacuo.

HPLC Analysis: The pellet of modified DNA was dissolved in 1 ml 9.5% acetonitrile and 100 mM triethylammonium acetate (TEAA) pH 6.5 and applied to a 4.6 mm x 25 cm reverse phase C_{18} column. The products of the reaction were eluted with a linear acetonitrile gradient in 100 mM triethylammonium acetate (TEAA) pH 6.5 over a period of 80 minutes (flow rate = 1.0 ml/min). The percentage acetonitrile was changed from 9.5% to 17.5% from time 5 minutes to time 85 minutes. The fractions of interest were collected and evaporated in a speed vac. The residue was resuspended in a minimum volume of TE and adjusted to 200 mM NaCl, 10 mM $MgCl_2$ and 3 volumes of absolute ethanol were added. The solution was cooled overnight at -20°C and the precipitate collected by centrifugation at 16,000 x g for 35 minutes. The supernatant was removed and the pellet washed with 95% EtOH and dried in vacuo.

Gel Analysis of HPLC fractions: The oligonucleotide fractions isolated by HPLC were resuspended in 0.5 ml TE. 1 µl of each of these fractions was 5' ^{32}P end labeled using T4 polynucleotide kinase and γ^{32}P-ATP. An aliquot of each of these reactions was loaded onto a 20 cm x 40 cm x 0.4 mm 24% 19:1 acrylamide:bis 7 M urea gel and electrophoresed until BPB was at the bottom of the gel. The results of this electrophoresis were visualized by autoradiography.

Synthesis of the furan-side monoadducted oligomer 5'-GCGTACGC-3': The self complementary 8 mer 5'-GCGTACGC-3' was reacted with HMT as described above in the materials and methods section. The oligomer was synthesized on a 10 µmole scale, and purified by reverse phase HPLC before it was used in the photo reaction. After the reaction was worked up, a small aliquot of the precipitated DNA was analyzed by reverse phase HPLC. The pellet of modified DNA was dissolved in 1 ml 11% acetonitrile and 100 mM triethylammonium acetate and applied to a 4.6 mm X 25 cm reverse phase C_{18} column. The products of the reaction were eluted with a linear acetonitrile gradient in 100 mM triethylammonium acetate (TEAA) pH 6.5 over a period of 55 minutes (flow rate = 1.0 ml/min). The percentage of acetonitrile was changed from 11% to 17.5% from time 5 minutes to time 60 minutes. Under these conditions, the unmodified 8 mer eluted in a broad asymmetric peak at 18 minutes, and the 8 mer MAf eluted as a sharp symmetric peak at 28 minutes. The remainder of the DNA was injected onto the column in two batches, the first injection was monitored at 300 nm where all DNA components would absorb, and the second injection was monitored at 330 nm where only the furan-side monoadducted molecules absorbed. This overloaded the column, but a good initial separation was effected. The unmodified 8 mer eluted as a broad band from minute 13-22, where the 8 mer MAf band began to come off the column. The 8 mer MAf eluted as a broad peak from minute 23-34. The 8 mer MAf band was collected and concentrated, and reinjected onto the column to separate the unmodified molecules away from the modified ones (Figure 3.5). The unmodified 8 mer containing fractions 22-24 were combined together, and

Figure 3.5 HPLC Chromatogram showing the separation of HMT Monoadducted and Unmodified 5'-GCGTACGC-3'

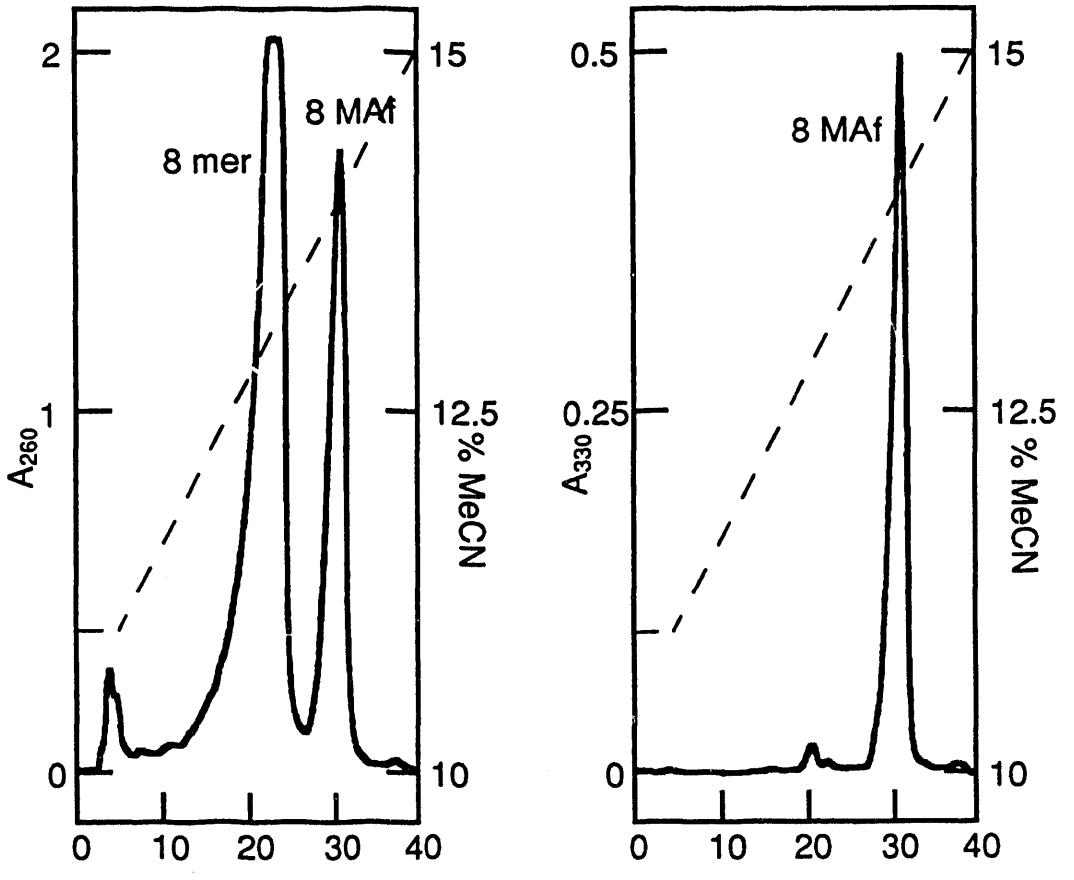

fractions 30-32 which contained the furan-side monoadduct were pooled. An aliquot of each of these column cuts was kinased with $\gamma^{32}P$ ATP and polynucleotide kinase and electrophoresed on a 24% denaturing PAGE. Inspection of the autoradiogram indicated that each cut was greater than 95% homogeneous (data not shown). The fractions were lyophilized, and then each was taken up in 400 µl 200 mM NaCl, 10 mM $MgCl_2$, and precipitated by the addition of 3 volumes of ethanol. The precipitate was collected by centrifugation, and redissolved in water. UV spectrophotometry indicated that 1.21 µmoles of 8 mer MAf were isolated in this fashion, for an overall yield based on the starting 8 mer of 30%.

Preparation of 8 mer MAf DNA samples for NMR. The single stranded monoadducted oligomer was taken up in 80 µl 1 M NaCl and the unmodified oligomer was taken up in 200 µl 20 mM deuteratedTris-HCl (d_{11}) pH 7.0 and 14 µl 1 M NaCl and lyophilized. The two salt and oligomer residues were then each taken up in 200 µl 99.96% D atom D_2O and lyophilized. This was repeated a total of three times. The 8 mer MAf was dissolved in 400 µl and the unmodified 8 mer was dissolved in 70 µl 99.996% D atom D_2O. The final Na^+ and deuterated Tris concentrations in these two solutions was 200 mM and 10 mM respectively. The single stranded 8 mer MAf was then titrated with the more concentrated unmodified 8 mer to give duplex DNA. The titration was monitored by observing the appearance of two resonances assigned to the adenine C2-H protons in the ^1H NMR at 600 MHz.

Synthesis of 30 mer 5'-TTT-GCC-GAT-CCC-CCC-CTT-GCC-ATA-GAC-CGA furan-side monoadduct: The 30 mer and its 12 mer complement 5'-TCG-GTC-TAT-GGC-3' were synthesized on an applied biosystems DNA synthesizer on a one µmole scale. The DNA was removed from the support by treating the column with concentrated ammonia solution for one hour at room temperature. The resulting solution was then heated to 55°C for 18 hours. The ammonia was evaporated and the DNA taken up in 400 µl 200 mM NaCl and precipitated with two volumes of ethanol. These crude oligos were then used in

the subsequent photoreaction. By UV spectrophotometry , there was 6.36 X 10^{-7} moles of the 30 mer, and 6.62 X 10^{-7} moles of the 12 mer complement. These were combined in 32 ml of 100 mM NaCl, 10 mM $MgCl_2$, 1 mM EDTA, 10 mM Tris pH 7.5, 13 mM NaN_3, and 40 μg/ml HMT ($5X10^{-6}$ moles) in a 10 cm path length quartz reaction cell. The azide was present as a dynamic singlet oxygen quencher. This mixture was irradiated with a model 171 spectra physics Kr^+ ion laser set to broad band emission at the 406 nm and 413 nm wavelength lines, for 210 minutes with a power of 1 watt. The reaction products were analyzed by kinasing an aliquot of the reaction mixture using $\gamma^{32}P$ ATP and running the resulting mixture out on a 15% 8 M urea PAGE. This indicated approximately 20% of the 30 mer had been converted to furan-side HMT monoadduct. The reaction mixture was adjusted to 200 mM NaCl and the DNA was precipitated by the addition of 2.5 volumes of ethanol and cooled to -20°C overnight. The DNA was taken up in 1.8 ml 200 mM NaCl and 10 mM $MgCl_2$ and ethanol precipitated one more time, before the 5' hydroxl groups were kinased.

Separation of 30 mer MAf from unmodified 30 mer: The DNA pellet was kinased in a 2.4 ml volume using 13.5 μmoles ATP. A small fraction of the DNA was labeled with $\gamma^{32}P$ ATP, and combined with the cold kinase. The enzyme in the mixture was heat killed for 15 min at 70°C, adjusted to 200 mM NaCl and precipitated with 2.5 volumes of ethanol at -70°C for 2 hours. The isolated DNA was taken up in 10 M urea/dyes and loaded onto a 1 mm x 40 cm x 40 cm 15% prep PAGE run at 60 W, until BPB was at the bottom. The band containing the 30 mer MAf co-migrated with the unmodified 30 mer. This band was cut out of the gel and electroeluted in an elutrap device at 10 V/cm for 4 hours. The eluent was adjusted to 200 mM NaCl, 10 mM $MgCl_2$ and precipitated by adding 2 volumes of ethanol and cooling to -20°C for 6 hours. The precipitated DNA was isolated by centrifugation, taken up in 0.8 ml 10 M urea and dyes, and loaded onto a 0.8 mm x 40 cm x 40 cm 15%, 7 M urea PAGE, and electrophoresed until xylene cyanole was 10 cm from the bottom. An autoradiogram of the gel showed that the 30 MAf was separated from the

30 mer. Both of these bands were cut out and subject to the same elutrap conditions that are described above. The purity of each of the isolated bands was determined by running an aliquot of each of the isolated DNA's out on a 15% 8M urea PAGE. The following yields were estimated from UV spectrophotometry: 30 MAf mw = 9389, total 195 μgr, $2.07X10^{-8}$ moles. 30 mer unmodified mw = 9133, total 624 μgr, $6.83X10^{-8}$ moles.

Discussion

We wanted to develop a method to easily synthesize large quantities of site specifically modified oligomers to be used in the investigation of DNA structure, function, and dynamics. We require psoralen modified DNA oligomers of many lengths, from 8 mers for structural studies, to plasmid sized molecules to investigate the action of DNA damage repair systems. Previous methods for the preparation of site specifically modified oligomers longer than 15 nucleotides relied upon the ligation of shorter oligomers together to form the molecule of desired length. Ligation reactions are extremely variable in their efficiency with different substrate molecules. This poses a synthetic block to the production of large quantities of the desired modified molecule. Often times there are situations where it is desirable to have oligomers that are site-specifically modified that are under 30 nucleotides in length (cf. cross-linkable PCR primers, short photo-cross-linkable DNA probes for reverse southern hybridization assays, direct production of short psoralen modified restriction fragments). We desired a simpler path that would lead to such oligomers under 30 nucleotides, bypassing the need for ligation. To reduce the number of steps in the production of such target molecules we approached the problem from the point of view of; 1) how many nucleotides long can one make a site specifically modified oligomer directly, 2) how well can one direct the specificity of the monoaddition reaction, and 3) on how large of a scale can these molecules conveniently be made.

DNA oligomers are easily synthesized using phosphoramadite technology on an automated DNA synthesizer. They are typically synthesized on the 0.2 μmole, 1.0 μmole, or 10.0 μmole scale. The DNA oligomers are synthesized using a solid support method that adds a single base with each round of the synthesis from the 3' to 5' end. The efficiencies of each coupling reaction is typically better than 97% when synthesizing a molecule on the 0.2 or 1.0 μmole scale because a ten-fold molar excess of the monomer reagent over the amount bound to the solid support is used. Coupling efficiency in the 10.0 μmole scale synthesis is somewhat lower because only a three-fold molar excess of the monomer is used, due to the expense of the reagents. There are always shorter molecules, called failure sequences, than the target molecule in any synthesis because each step of an oligomer synthesis does not go with 100% efficiency. In this study we also investigated whether it was important to remove these failure sequences before the monoaddition or cross-linking reactions were performed.

The DNA sequence requirements for the synthesis of site specifically furan-side monoadducted oligonucleotides are a 5'-TpA-3' site in a region of double stranded DNA in the oligomer, with a minimum number of other thymidines on the target strand. The procedure that seems to work best is to anneal the two complementary oligos together and then irradiate them in the presence of saturating HMT (41 μg/ml) with 406.7 nm light. The DNA is then concentrated from the reaction mixture by precipitation with ethanol. This removes any excess psoralen and psoralen degradation products from the DNA. The modified DNA is then separated from the unmodified DNA components of the reaction mixture by using C_{18} reverse phase HPLC. This type of chromatography separates mixtures based on differences in the hydrophobicity of the individual components. The addition of a HMT furan-side monoadduct increases the hydrophobicity of the parent molecule. Often times it is necessary to run a second reverse phase separation on the fractions of interest because of co-elution of different species, or partial overlap of the elution of different molecules. In cases where reverse phase chromatography does not give

an adequate separation between species, ion exchange chromatography using a DEAE HPLC system may be required. This type of chromatography separates molecules on the basis of charge. This is particularly useful in separating the two complementary DNA components of a monoaddition reaction if they are of different lengths because the charge of a DNA molecule is due to the phosphate groups of the backbone, and therefore directly proportional to the molecule's length. The practical size limit for separating modified oligonucleotides is about 25 bases. The separation of the modified oligomers from their parent compounds becomes much more difficult as their lengths increase. With reverse phase chromatography, the difference in hydrophobic moment between the modified molecule and the parent compound gets smaller as the chain length increases. The efficiency of any separation is also affected by the nucleotide sequence of the oligomers involved. For example, the molecules 5'-TCC-GGG-TAC-C-3', 5'-GGT-ACC-CGG-A-3', and 5'-GCT-CGG-TAC-C-3' are 10 mers and have retention times on reverse phase chromatography of 9, 11, 18 minutes respectively under the same conditions (described below). The purity of the starting oligos is a major factor in the efficient isolation of the desired monoadducted product. In most cases, the purer the starting materials, the easier the subsequent purification of the reaction products from the reactants becomes. The best results are obtained when the starting oligomers are HPLC purified before they are used in a monoaddition reaction.

Figure 3.6 shows the chromatogram from the monoaddition reaction of a 24 mer and its 10 mer complement with HMT. There are two main peaks that absorb at 330 nm, the 24 mer MAf which elutes at 29-30 minutes and the 10 mer MAf which elutes at 18 minutes. The parent 24 mer elutes in a broad band from 19-21 minutes and the 10 mer complement elutes at 18 minutes. Only furan-side monoadducted oligomers absorb at 330 nm. The chromatography conditions for separating this mixture into its components was elution with 10% acetonitrile in 0.1 M triethylammonium acetate (TEAA) from 0-5 minutes followed by a gradient of 10-20% acetonitrile in TEAA over 55 minutes at a flow rate of 1

Figure 3.6 HPLC Chromatogram showing the separation of HMT Monoadducted and Unmodified 24 mers and 10 mer complements

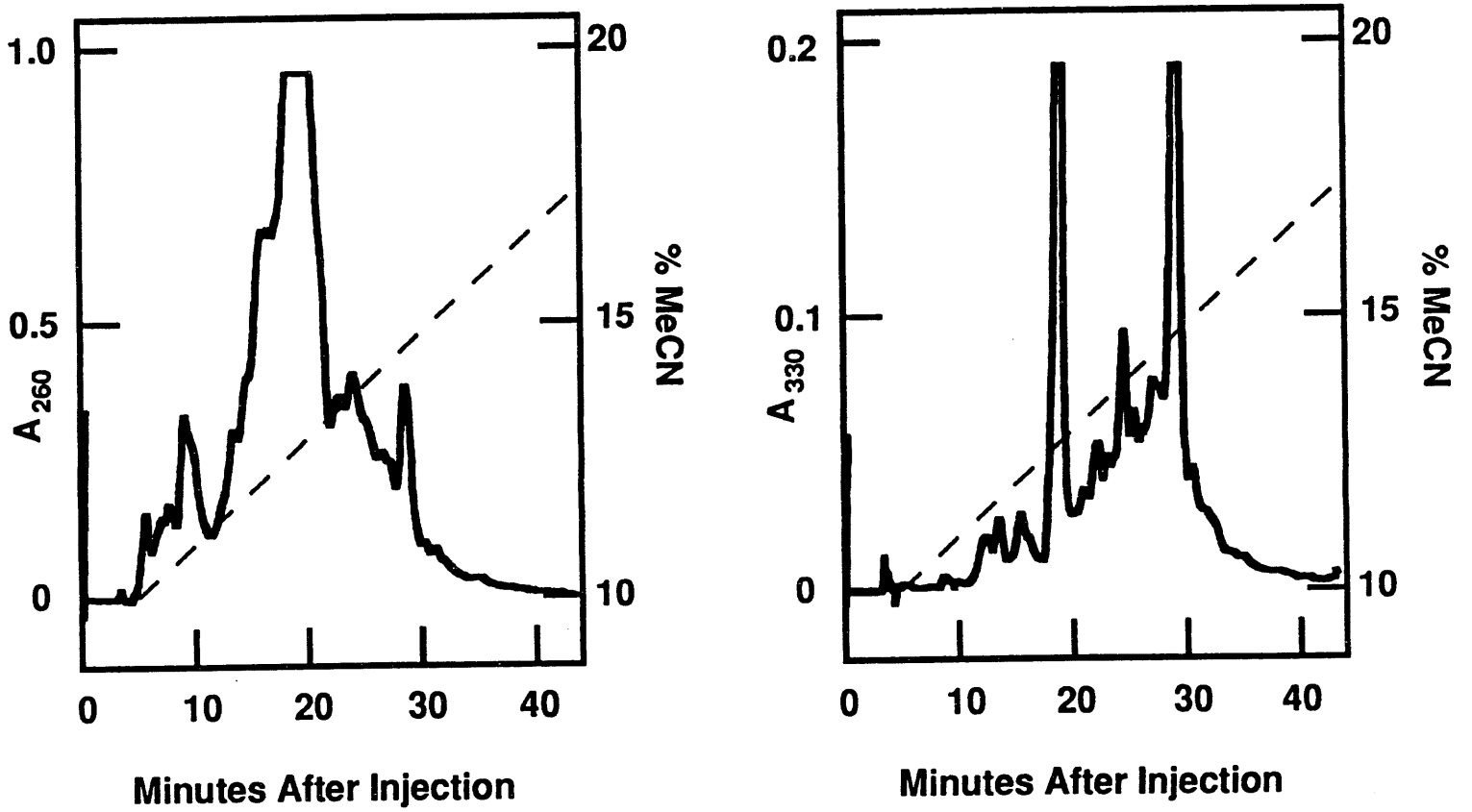

Figure 3.7: This is an autoradiogram of kinased HPLC fractions from a reaction between the 21 mer 5'-CGG-AAT-TCC-GGG-TAC-CGG-CCG-3' and its complementary 10 mer 5'-GGT-ACC-CGG-A-3' (lanes 1-13), and the 24 mer 5'-GAT-CGC-TCC-CGG-GTA-CCG-AGC-TCG-3' and its complementary 10 mer 5'-GCT-CGG-TAC-C-3' (lanes 14-24), with HMT irradiated at 406.7 nm. Lanes 1, 2 and 3 correspond to fractions 14, 15, and 16 and is the unmodified 21 mer. Lanes 4-10 correspond to fractions 20-26 and are a mixture of the unmodified 21 mer and 21 mer MAf, with the monoadducted DNA predominating. Lane 11 corresponds to fraction 30 and is a mixture of 21 mer MAf and what appears to be a diaddition product. Lanes 14,15, 16, and 17 correspond to fractions 15,16,17 and 18 of the 24 mer/10 mer reaction. They contained the unmodified 10 mer and the 10 mer MAf (not shown). Lanes 18-20 correspond to fractions 19-21 and are the 24 mer. Lanes 21-22 correspond to fractions 29 and 30 and are the 24 mer MAf. Lane 23 is the reaction mixture before irradiation and lane 24 is the reaction mixture after irradiation. The HPLC chromatogram monitored at 290 nm shows absorbance for all these species. The chromatogram monitored at 330 nm shows absorbance only for the furan-side monoadducted molecules.

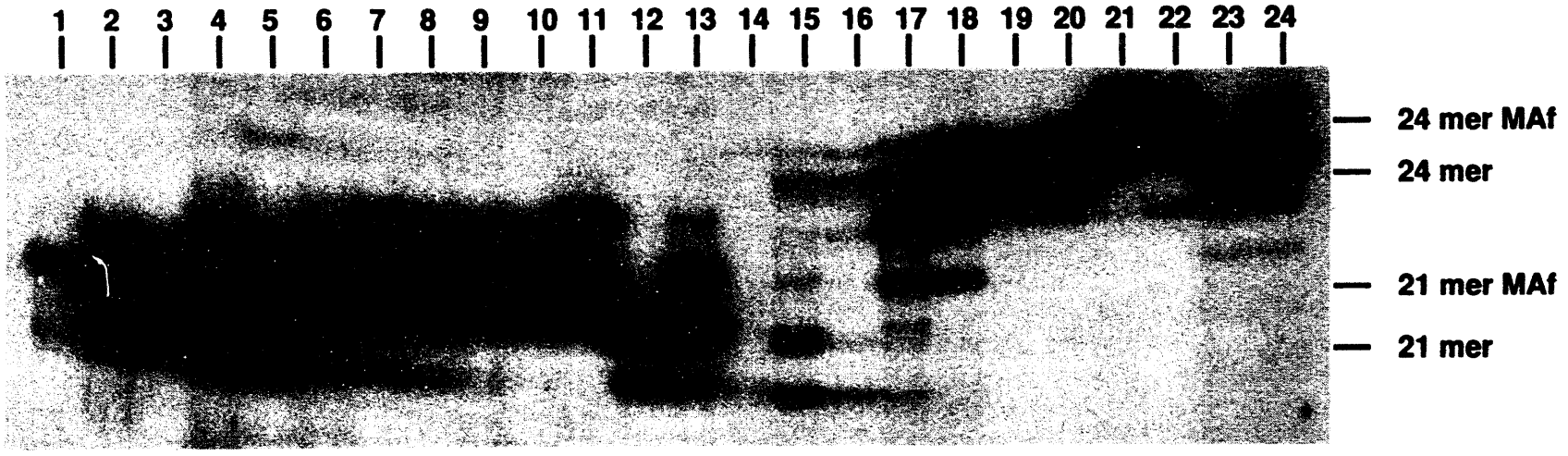
1 2 3 4 5 6 7 8 9 10 11 12 13 14 15 16 17 18 19 20 21 22 23 24
24 mer MAf
24 mer
21 mer MAf
21 mer

Figure 3.8 HPLC Chromatogram showing the separation of HMT Monoadducted and Unmodified 21 mers and 10 mer complements

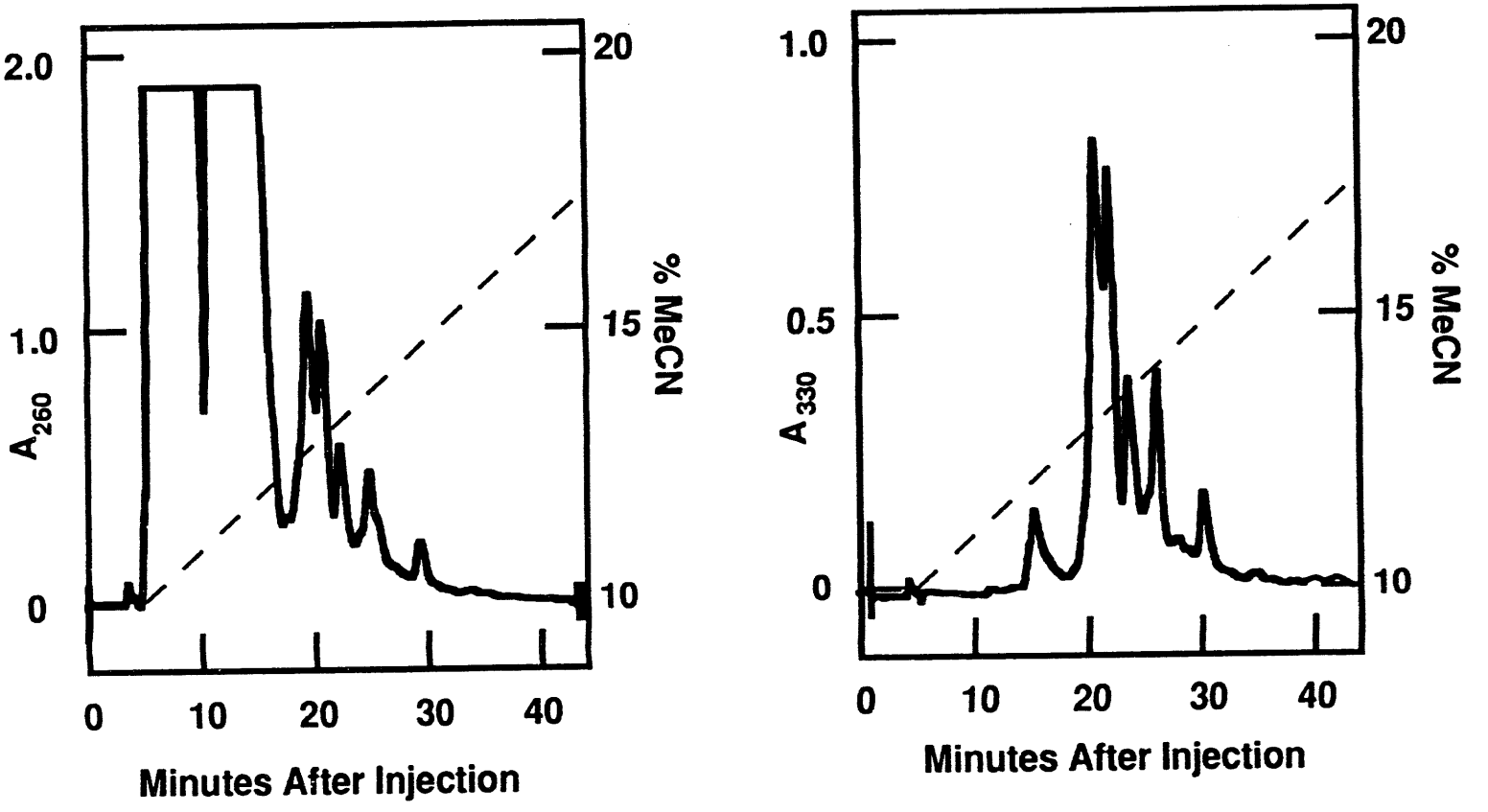

ml/minute on a 4.6 mm x 25 cm 300 Å pore size C_{18} reverse phase HPLC column. Figure 3.7 shows kinased aliquots of fractions 19-21 in lanes 18-20 and fractions 29-30 in lanes 21-22. The addition of a monoadduct to the oligomer retards its electrophoretic mobility on the gel by about one base.

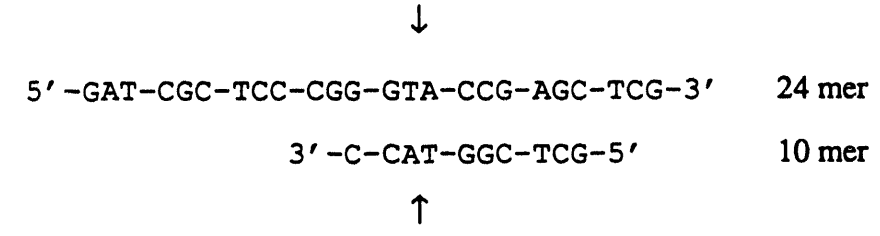

There is only one thymidine on the 24 mer that is in duplex DNA and therefore accessible for monoaddition by HMT. The thymidine at position 22 of the 24 mer would probably not be reactive to psoralen in this particular duplex because even if a psoralen were to stack onto the end of a helix, there are no geometric constraints onto how the thymidine is oriented relative to the psoralen. Recall that one of the requirements for psoralen photoreactivity is intercalation into a duplex. Inspection of the 24 mer/10 mer duplex indicates that there are two sites for monoaddition on the 10 mer complement, however, only one species of 10 mer MAf is observed to be created.

Figure 3.8 shows the chromatogram from the monoaddition reaction of a 21 mer and its 10 mer complement with HMT. The 21 mer chromatogram shows four peaks in the region of the 21 mer that absorb at 330 nm. Under these conditions, the 21 mer co-elutes at 15-16 minutes with the complementary 10 mer used to form the duplex where the psoralen can react. There is only one 5'-TpA-3' site in this molecule, so to a first approximation there should be only one monoadducted molecule. There is a strong sequence dependance for the specificity of psoralen photobinding to DNA. 5'-TpA-3' sites are preferred over 5'-ApT-3' sites by 100 fold, and that alternating $(AT)_n$ sites are the most reactive to psoralen. Adjacent thymines make better targets than thymidines in a GC environment, although both of these sites have a much lower reactivity than the others just described(Boyer *et al.*, 1988; Sage and Moustacchi, 1987). Take for an example the case

of the 24 mer and 10 mer just described. There are only two thymidines in the 24 mer, one in a 5'-TpA-3' site and one completely surrounded by GC bases. Only the thymidine at the 5'-TpA-3' site reacts with HMT under these conditions. The 21 mer MAf molecules elute as four peaks with retention times of 20, 22, 24, and 26 minutes. Inspection of the sequence of the 21 mer annealed to its 10 mer complement shows that there are multiple sites on the 21 mer for psoralen monoaddition, indicated by the arrows.

```
      ↓↓↓       ↓
5'-CGG-AAT-TCC-GGG-TAC-CGG-CCG-3'   21 mer
      3'-AGC-CCC-ATG-G-5'           10 mer
                  ↑
```

In the central 5'-TpA-3' site and the 5'-TpC-3' site at the 3' end of the 10 mer complement, the HMT can be fully intercalated. HMT can react with either face of the thymidine across from the 3' terminal adenosine of the 10 mer complement. In this case the HMT would be stacked onto the end of the helix. The ends of helicies are hot spots for the photoaddition of psoralens stacked onto them (Cimino *et al.*, 1985). Although the thymidine at position 6 of the 24 mer is unconstrained by hydrogen bonding interactions, HMT photoaddition to it is the most likely source of the fourth peak in the chromatogram. All four peaks when kinased have the same rf value when electrophoresed on a denaturing 24% polyacrylamide gel. This is illustrated in lanes 4-10 of figure 3.7. This is not surprising because the monoadducted molecules have the same overall basic shape, and gel electrophoresis separates molecules based on their shapes, sizes and charge. The addition of a monoadduct to an oligomer retards its mobility on a denaturing PAGE by approximately one base. In other words, a 21 mer MAf appears to run as a 22 mer. By reverse phase chromatography, however, the hydrophobic moment of individual monoadducted molecules will be different depending on the position of the adduct. There is a peak in the chromatogram at 30 minutes (lane 11 of figure 3.7) that we are assigning to a di-monoadducted 21 mer. It runs on denaturing PAGE as a 23 mer. So it stands to reason that there are two adducts in this

Figure 3.9 HPLC Chromatograms showing the separation of HMT Monoadducted and Unmodified 25 mers and 10 mer complements

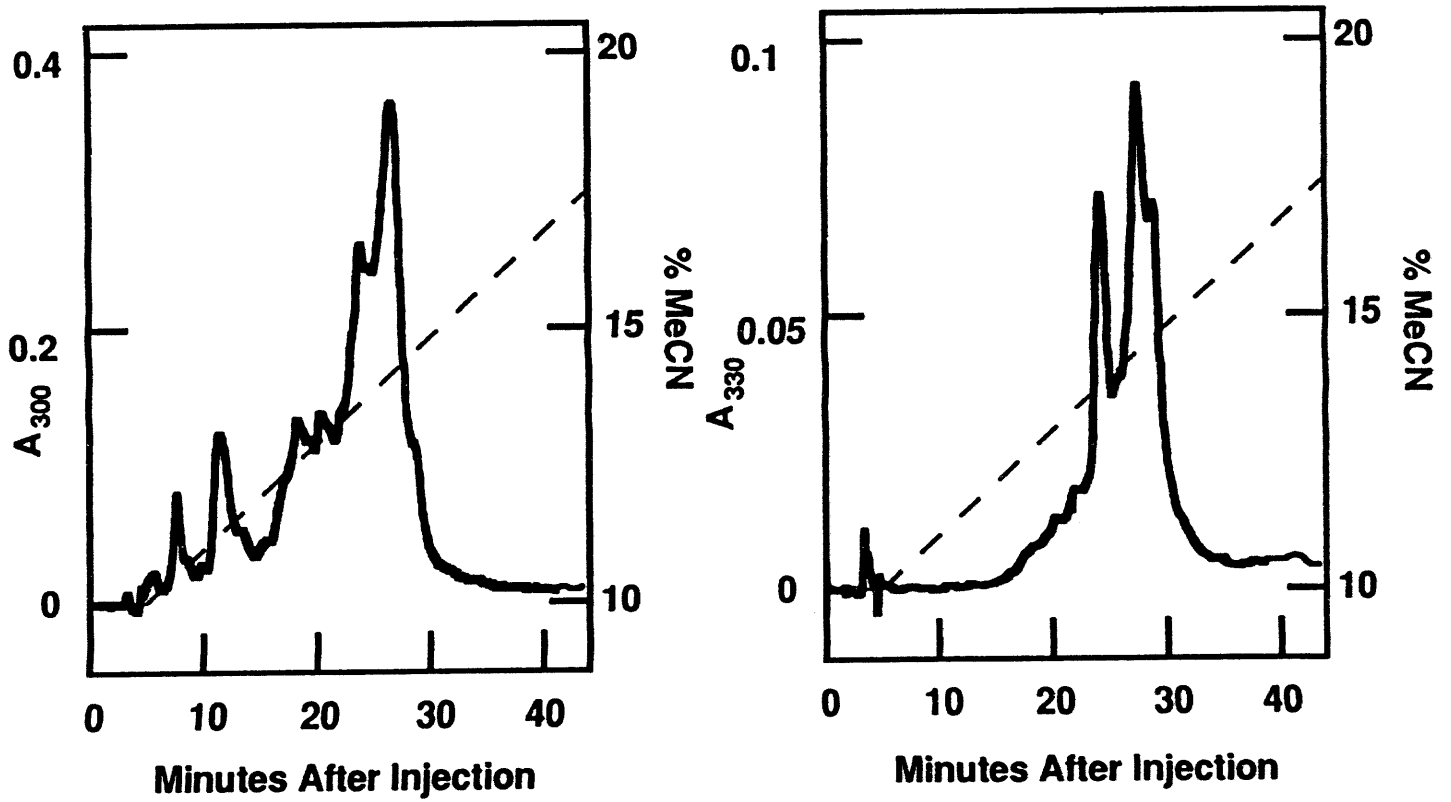

Figure 3.10: This is an autoradiogram of kinased HPLC fractions from the reaction between the 25 mer 5'-GAT-CCG-GCC-GGT-ACC-CGG-AAT-TCC-G-3' and its complementary 10 mer 5'-TCC-GGG-TAC-C-3' with HMT irradiated at 406.7 nm. The 10 mer used in this reaction was quite impure. It had a substantial fraction of 8 mer and 9 mer failure sequences. Lane 1 corresponds to fraction 12 and is a mixture of the unmodified 8, 9 and 10 mers. Lane 2 corresponds to fraction 13 and is a mixture of the unmodified 9 and 10 mers. Lane 3 corresponds to fraction 25 and is a mixture of unmodified 25 mer and 9 mer and 10 mer MAf. Lanes 4, 5, and 6 correspond to fractions 26, 27, and 28, and are unmodified 25 mer. Lanes 7 and 8 correspond to fractions 29 and 30 and are mixtures of the unmodified 25 mer and 25 mer MAf. Lane 8 is the reaction mixture before irradiation and lane 9 is the reaction mixture after irradiation. The HPLC chromatogram monitored at 290 nm shows absorbance for all these species. The chromatogram monitored at 330 nm shows absorbance only for the furan-side monoadducted molecules.

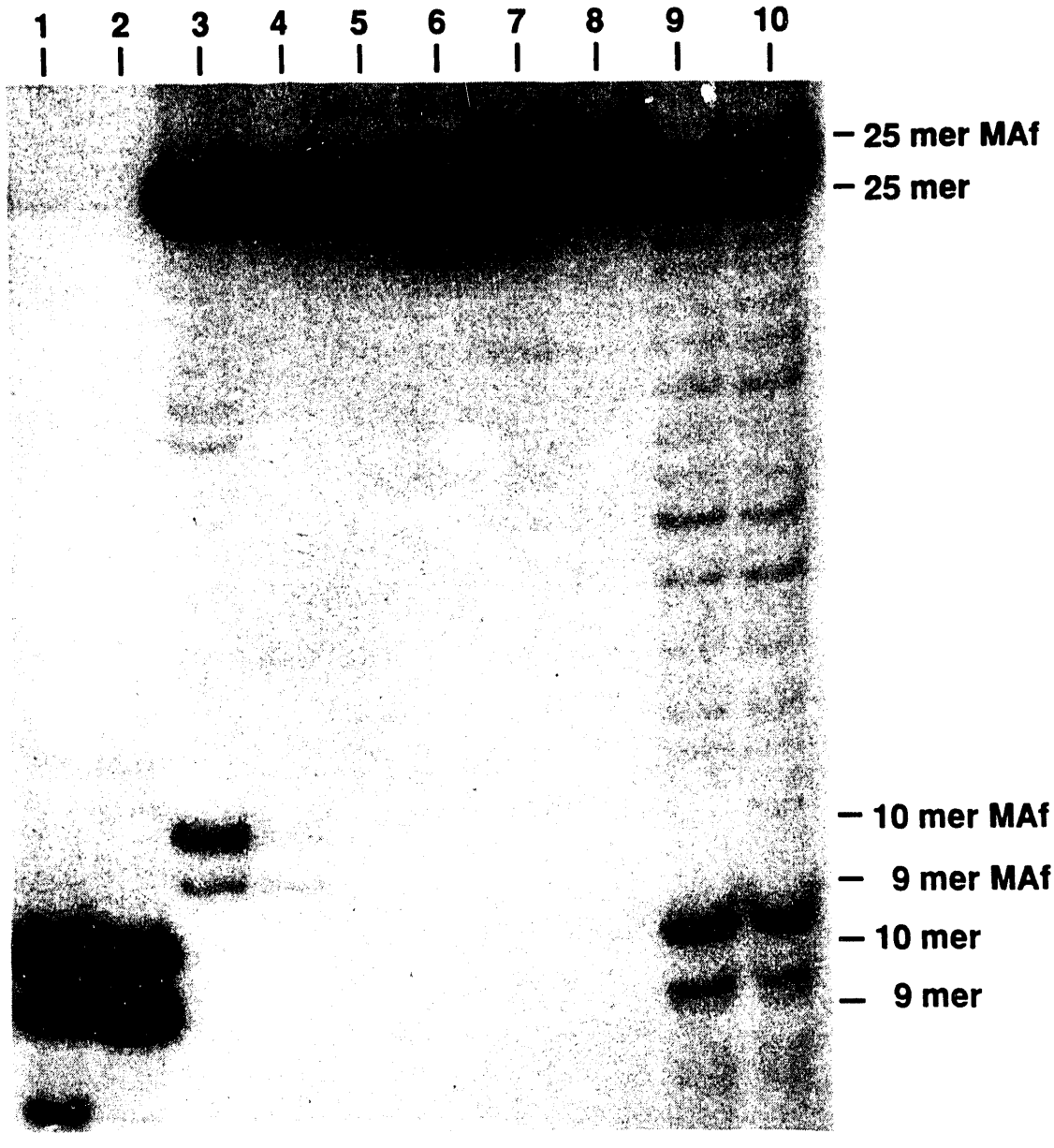
1
2
3
4
5
6
7
8
9
10
25 mer MAf
25 mer
10 mer MAf
9 mer MAf
10 mer
9 mer

molecule. The chromatogram when monitored at 290 nm, where all DNA components absorb is complicated. This is because the 21 mer and 10 mer complement were used as a crude mixture and not purified after the DNA synthesis.

Figure 3.9 shows the chromatogram of the reaction between HMT and a 25 mer and its 10 mer complement. The initial purification showed two peaks when the chromatogram is monitored at 330 nm, one of which was split. The first peak eluted with a retention time of 25 minutes and the second over the period of 27-30 minutes. The kinase of aliquots of these fractions is shown in figure 3.10. The 10 mer complement that was used in this reaction was heavily contaminated with a 9 mer failure sequence. Lanes 1 and 2 of figure 3.10 show that the 9 mer and 10 mer eluted in fractions 12 and 13. There was a broad absorbance over fractions 24-28 when the chromatogram was monitored at 300 nm, where all DNA components in the reaction mixture absorb. Lanes 3-6 correspond to fractions 25-28, and are predominantly unmodified 25 mer. In lane 3, which corresponds to fraction 25, there are the 9 mer and 10 mer MAfs. Lanes 7 and 8 correspond to fractions 29 and 30 and are predominantly 25 mer MAf. These two fractions were combined and re-injected to separate out the contaminating unmodified 25 mer. Fractions 29 and 30 were combined and reinjected onto the reverse phase HPLC column and an adequate separation of the unmodified 25 mer and the 25 mer MAf was effected. The 25 mer MAf eluted in a broad peak with a retention time of 32 minutes. Inspection of the 25 mer and its 10 mer complement's sequences indicate that there is only one thymidine on the 25 mer that is available for photoadduction by HMT indicated by the arrows.

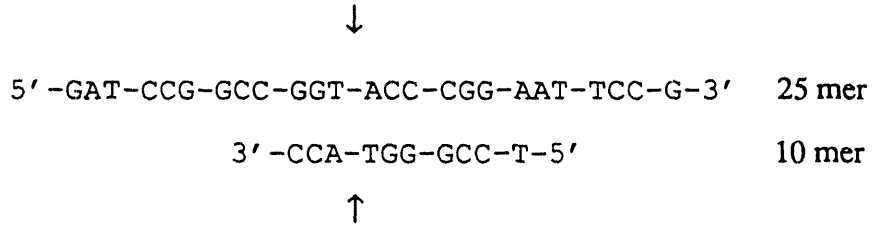

Figure 3.11 shows the chromatogram from the monoaddition reaction of a 19 mer and its 11 mer complement with HMT. The chromatography conditions for separating

Figure 3.11 HPLC Chromatograms showing the separation of HMT Monoadducted and Unmodified 19 mers and 11 mer complements

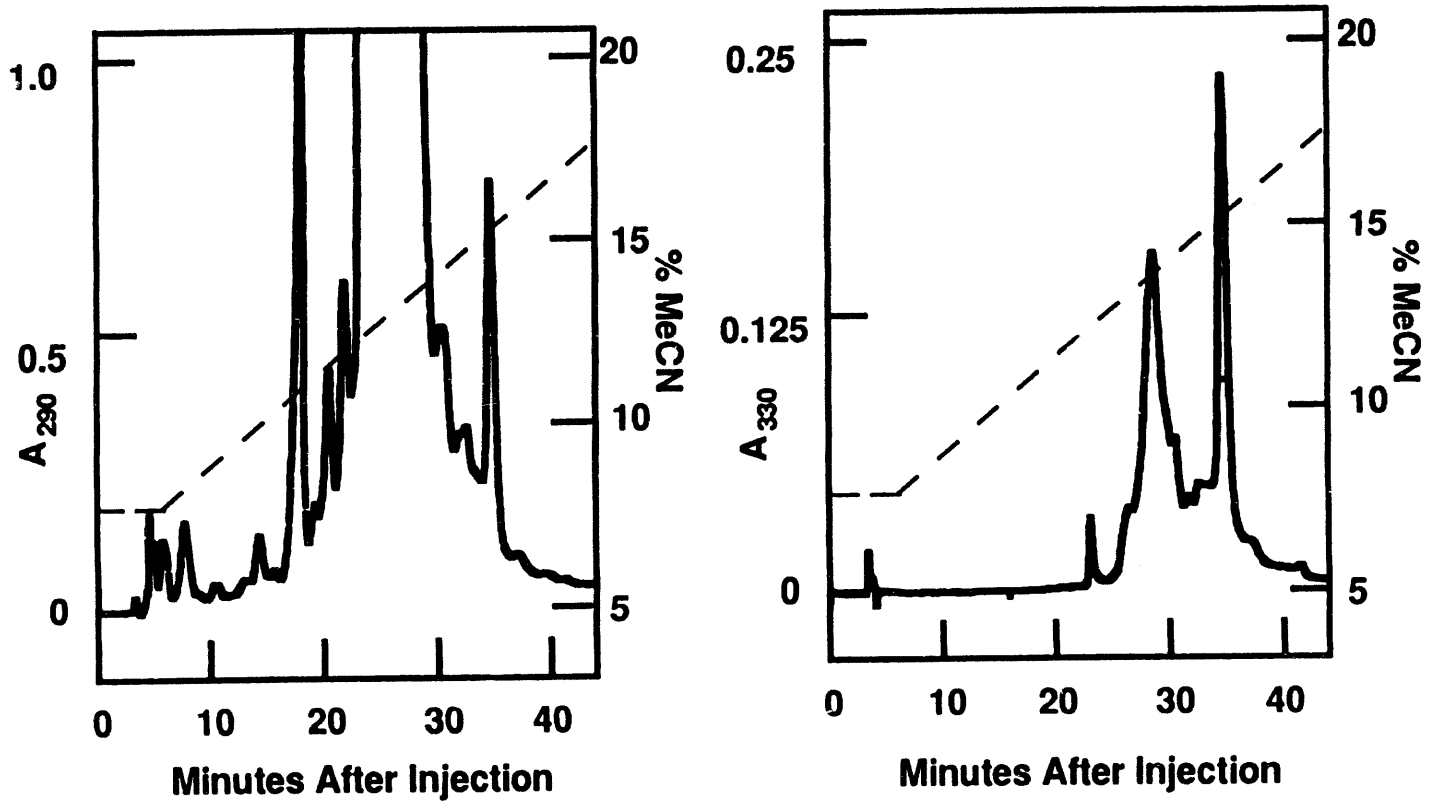

Figure 3.12: This is an autoradiogram of kinased HPLC fractions from a reaction between the 19 mer 5'-GAT-CCC-CGG-GTA-CCG-AGC-T-3' and its complementary 11 mer 5'-CGG-TAC-CCG-GG-3' with HMT irradiated at 406.7 nm. This is an example where reverse phase chromatography fails in separating the products of a monoaddition reaction. The 11 mer used in this reaction was impure. It had a substantial amount of 8 mer failure sequence. Lane 1 corresponds to the reaction mixture after irradiation. Lanes 2 and 3 correspond to fractions 25 and 26 and are a mixture of 11 mer and 8 mer. Lane 4 corresponds to fraction 27 and is a mixture of 19 mer, 17 mer failure sequence, 11 mer and 8 mer failure sequence. There was no absorbance at 330 nm in this fraction. Lane 5 corresponds to fraction 28 and is a mixture of 19 mer, 17 mer, a small amount of 11 mer MAf and 11 mer. Lanes 6, 7, and 8 correspond to fractions 29, 30 and 31 and are a mixture of 19 mer, and 11 mer MAf. Lane 9 corresponds to fraction 32 and is a mixture of 19 mer and various failure sequenced from the 19 mer synthesis. Lane 10 corresponds to fraction 36. This is pure 19 mer MAf.

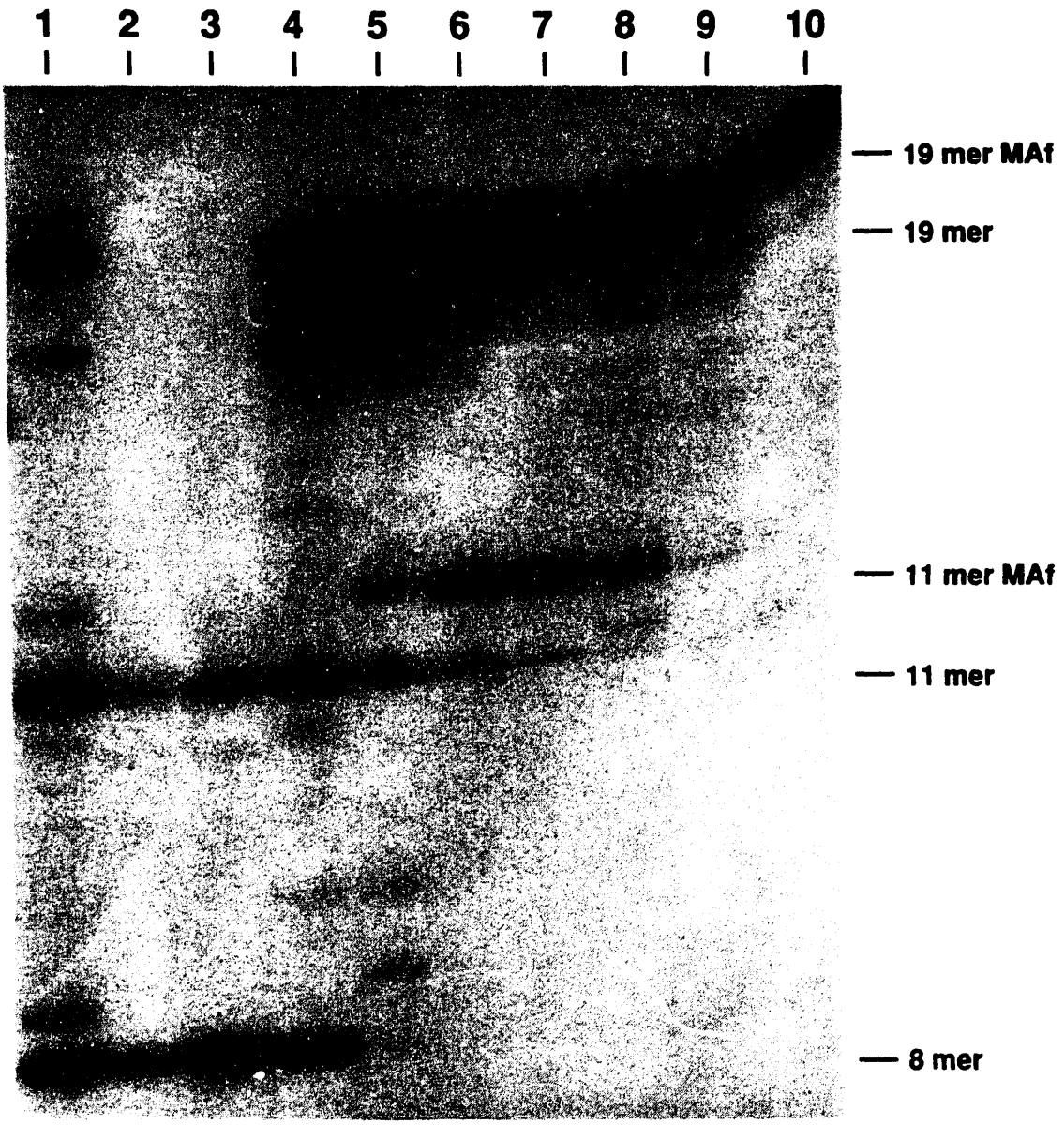
1
2
3
4
5
6
7
8
9
10
19 mer MAf
19 mer
11 mer MAf
11 mer
8 mer

this mixture into its components was elution with 8% acetonitrile in 0.1M triethylammonium acetate (TEAA) from 0-5 minutes followed by a gradient of 2-20% acetonitrile in TEAA over 55 minutes at a flow rate of 1 ml/minute on a 4.6 mm x 25 cm 300 A pore size C_{18} reverse phase HPLC column. Under these conditions, the 19 mer MAf elutes as a well separated and resolved peak with a retention time of 36 minutes (lane 10 of figure 3.12). The synthesis of the 11 mer complement contained a large amount of a failure sequence that ran as an 8 mer on denaturing PAGE. The synthesis of the 19 mer contained a large amount of a failure sequence that ran as an 17 mer on denaturing PAGE. These contaminants contributed to the complexity of the chromatogram. The only component of this reaction mixture which separated cleanly was the 19 mer MAf. The unmodified 11 mer elutes in a broad band over fractions 25-28 (lanes 2-5 of figure 3.12). The 11 mer MAf elutes in fractions 29-31 (lanes 6-8, figure 3.12). Both of these components co-elute with the unmodified 19 mer, which elutes in a broad band over fractions 27-32 (lanes 4-9, figure 3.12). Fractions 29-31 combined and reinjected onto a C_{18} reverse phase column, and eluted with 8% acetonitrile in 0.1M triethylammonium acetate (TEAA) from 0-5 minutes followed by a gradient of 8-20% acetonitrile in TEAA over 55 minutes at a flow rate of 1 ml/minute, but this gave no improvement in the resolution of the components. The 11 mer and the 11 mer MAf are resolvable from each other using C_{18} reverse phase chromatography, however they co-elute with the unmodified 19 mer. This is a case where an initial separation of the components of the reaction mixture by ion exchange, followed by reverse phase chromatography was necessary. The anion exchange chromatography separates the 19 mers from the 11 mers, and the reverse phase chromatography was then able to separate the monoadducted molecules away from the unmodified molecules. Inspection of the sequence of the 19 mer / 11 mer duplex reveals that there is only one thymidine that is base-paired and available for photoreaction with the psoralen indicated by the arrows.

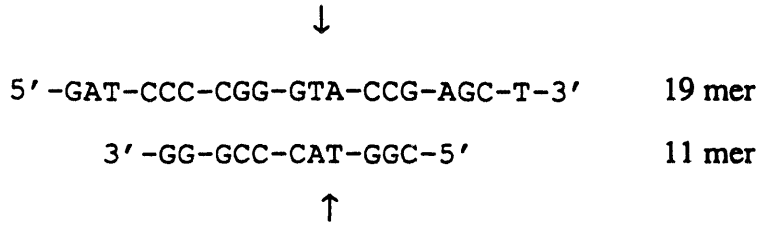

A 30 mer MAf was synthesized using a 30 mer and a 12 mer complement to it. The 12 mer formed a duplex in a region where there was a 5'-TpA-3' site. Inspection of the double stranded DNA duplex reveals that there is only one thymidine on the 30 mer target that is in the duplex. A reaction on either face of the thymidine with HMT at position 23 gives a cross-linkable molecule. By analogy with the 21 mer described above, denaturing PAGE probably would not be able to separate the two species into distinct bands. There are multiple thymidines on the 12 mer complement, but they are of little concern for the specificity of the reaction because the target molecule was the 30 mer. The only drawback to the multiple thymidines on the complement, is that photoaddition to these sites decreases the overall yield of 30 mer MAf. The potential monoaddition sites are indicated by the arrows.

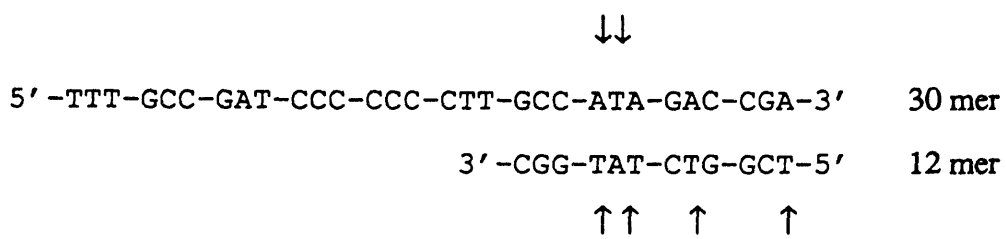

The DNA oligomers were annealed together and irradiated in the presence of HMT with 406.7 nm light from a Kr^+ laser. The isolated DNA was electrophoresed on a 1 mm x 40 cm x 40 cm 15% prep denaturing PAGE. The 30 mer MA co-migrated with the unmodified 30 mer under these conditions, because the gel was overloaded. The monoadducted 30 mer migrates slower than the unmodified oligomer under these conditions, therefore the broad band of DNA that contained the 30 mer and 30 mer MAf was cut from the gel into upper and lower sections. The upper section was enriched in monoadduct relative to the lower (faster moving) section. These bands cut out of the gel

were electroeluted from the gel matrix and then the DNA was concentrated from the eluent by precipitation with ethanol. The precipitated DNA from the upper band was electrophoresed on a second 0.8 mm x 40 cm x 40 cm 15%, denaturing PAGE. An autoradiogram of the gel showed that the 30 MAf was separated from the 30 mer. Both of these bands were cut out and subject to the same electroelution conditions that are described above. The purity of each of the isolated bands was determined by running an aliquot of each of the isolated DNA's out on a 15% 8 M urea denaturing PAGE (data not shown).

We investigated the monoadduction reaction of HMT with a duplex formed by a 39 mer and a 35 mer. Inspection of the sequence shows that there are four thymidines in the 39 mer sequence and five thymidines in the 35 mer sequence. As noted above, when there are multiple thymidines available for photoreaction, many products can result. Only one of the thymidines in each strand is in a 5'-TpA-3' site. It was hoped that the primary site of photoaddition would be the 5'-TpA-3' site, with minor reaction at some of the other thymidines. The 5'-TpA-3' site is indicated with arrows.

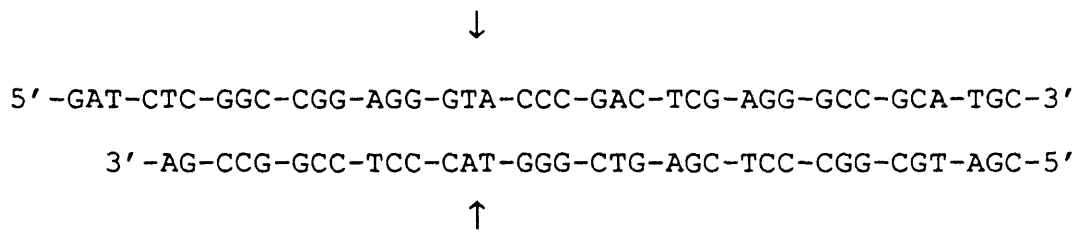

As noted above, a 30 mer MAf was successfully separated from it's parent 30 mer by denaturing PAGE, and it was hoped that the two monoadducts produced in this reaction (35 MAf and 39 MAf) could also be separated in this fashion. After photoreaction, aliquots of the reaction mixture were run out on a denaturing PAGE and showed broad unresolvable smears where the 35 mer and 39 mer would have normally run. The difference between the modified and the unmodified DNA was insufficient to give any resolution on 10%, 15% or 20% denaturing polyacrylamide gels. The DNA was demonstrated to be monoadducted by exposing it to 365 nm light which drove the monoadducts onto cross-link (data not shown). In light of the results with the 21 mer and it's 10 mer complement,

what happened was that there were a multitude of psoralen addition products in the reaction mixture. Attempts were made to use ion exchange and reverse phase HPLC to separate the mixture, but these met with no success. The conclusion that we drew from our experience with this system was that the oligomer length was too long for HPLC purification methods, and that without directed addition of the psoralen to one site in the molecule using a short oligonucleotide, gel electrophoresis and HPLC purification methods were of little use in separating the products. With only a single species of monoadduct at the 5'-TpA-3' site, denaturing PAGE probably would have been successful in giving separation.

In the reaction between the 13 mer, 5'-GCT-CGG-TAC-CCG-G-3' and it's complementary 8 mer 5'-GGG-TAC-CG-3' and HMT to produce 13 mer MAf and 8 mer MAf, a different problem with the choice of the two complementary oligomers arose. When the photoreaction was analyzed, there was twice as much 8 mer MAf as there was 13 mer MAf (data not shown). The reason for the disparity in the amounts of photo product was probably due to the formation of duplex between the 8 mer and itself in competition with duplex between the 13 mer and the 8 mer. When the 8 mer forms duplex with itself there are two GG mismatches at the ends of the helix. While there are no data for terminal mismatches for DNA, GG mismatches are a common motif in RNA. The lesson from this result is to choose two complementary molecules of which neither one can form a self-complementary duplex (unless of course, the required monoadduct is from a self-complementary molecule).

The isolated yields of the 10 furan-side monoadducted oligonucleotides successfully synthesized in these 8 reactions is summarized in table 3.1.

An advantage of HPLC methods over denaturing PAGE is that there is a much larger loading capacity of the HPLC columns relative to a gel. Another advantage is that the time required to run a separation procedure is much shorter for HPLC. The work up of the fractions of interest is also much simplified and speeded up when using HPLC. The buffer system that is used in reverse phase HPLC is a volatile salt. When the fractions

Table 3.1 Furan-side monoadducts synthesised

	Oligomer	moles	% yield
8 MAf (NMR)	5'-GCG-TAC-GC-3'	1.21 µmoles	30.0
8 MAf (13 comp)	5'-GGG-TAC-CG-3'	14.0 nmoles	6.0
13 MAf	5'-GCT-CGG-TAC-CCG-G-3'	7.0 nmoles	3.0
8 MAf (12 comp)	5'-TCG-TAG-CT-3'	0.5 µmoles	10.0
12 MAf	5'-GAA-GCT-ACG-AGC-3'	0.7 µmoles	14.0
19 MAf	5'-GAT-CCC-CGG-GTA-CCG-AGC-T-3'	21.0 nmoles	16.0
21 MAf	5'-CGG-AAT-TCC-GGG-TAC-CGG-CCG-3'	90.0 nmoles	19.4
24 MAf	5'-GAT-CGC-TCC-CGG-GTA-CCG-AGC-TCG-3'	26.0 nmoles	4.1
25 MAf	5'-GAT-CCG-GCC-GGT-ACC-CGG-AAT-TCC-G-3'	10.0 nmoles	9.3
30 MAf	5'-TTT-GCC-GAT-CCC-CCC-CTT-GCC-ATA-GAC-CGA-3'	20.7 nmoles	20.0

containing the oligomer of interest are evaporated, the TEAA evaporates with the water and acetonitrile. With a gel all of the salts that are present in the slab of material containing the oligomer of interest remain with the DNA after evaporation. This means that some de-salting step is required. In addition to unwanted salts, there are always some particulates left over from the acrylamide. The salt problem is also present when doing DEAE chromatography. This can be circumvented to some extent by elution of the DNA from the column with a LiCl gradient. DNA oligomers can be precipitated directly from 4 M LiCl solutions by the addition of ethanol. A very important consideration is the recovery of the modified oligomer in high yield from a purification of a reaction. Recovery of DNA oligomers from gels is a variable business. As the length of the oligomer goes up, the yield of oligomer recovered goes down. In fact, it is impossible to recover 100% of any one band of DNA from a denaturing PAGE, and quite often it is substantially lower. HPLC has the advantage here because virtually all of the oligo that goes onto the column comes off again. The detection of the individual species of molecules that elute from the column using these chromatographic methods also has an effect on the synthetic utility of the method. UV absorption is the method of choice for visualizing an HPLC chromatogram. The drawback to this method is that it is not particularly sensitive to small amounts of material, but our concern is with a method that produces micromole quantities of material anyway. The ability to observe the chromatography and record a chromatogram at different wavelengths is also an important feature of HPLC purification. When the monoadducted oligomer co-elutes, or is buried under the shoulder of another peak, comparison of the chromatograms monitored at 290 nm and 330 nm, can tell you in what fractions the peak of interest is. Eventually, an aliquot taken from all of the fractions of interest need to be kinased and run down an analytical denaturing PAGE in order to unambiguously assign them. The visualization of where a molecule of interest is on a preparative denaturing PAGE is somewhat more complicated. UV shadowing of the bands of interest is undesirable, because photoreversal of the monoadduct and/or photo-cross-linking of the

monoadducted molecules can occur. Nucleic acid stains such as ethidium bromide and toluidine blue cannot be removed completely enough to prevent photodegradation of the DNA under our irradiation conditions. Oligomers may be labeled with ^{32}P on their 5'-OH group with T4 polynucleotide kinase, and their positions on a gel determined by autoradiography. To perform a preparative separation by this method, all of the 5' ends of the molecules must be kinased, because 5'-OH and 5'-phosphate molecules have different electrophoretic mobilities. This presents difficulties and disadvantages to subsequent manipulations of the modified oligomer. The first is that the DNA is now radioactive, and must be handled in a more restricted manner, and secondly, if there is a requirement for a free 5'-OH, then the 5'-phosphate must be removed by alkaline phosphatase, yet another enzymatic manipulation.

These eight examples of synthesis of site-specifically monoadducted oligo nucleotides indicate how important it is to choose the complement of the desired strand so that there are as few reactive thymidines as possible engaged in base pairing, that the complement cannot itself form duplex in the absence of the target, and that the target itself does not also form structure which competes with the formation of the desired photo-reaction directing duplex.

Part II: The Preparation of Cross-linked DNA

The production of preparative quantities of cross-linked HMT-DNA was the second type of adduct that we investigated. Use of an argon ion laser as a high intensity light source allowed us to efficiently synthesize psoralen-DNA cross-links (diadducts). We used an argon ion laser operating at 366 nm to synthesize micromole quantities of psoralen cross-linked DNA oligomers for structural studies. Figure 3.13 is a schematic of the experimental set up that we used in these experiments. Both HMT and the furan-side monoadduct formed from it absorb light efficiently at this wavelength. The furan-side monoadduct is an intermediate on the path to interstrand diadduct (see figure 1.2). The furan-side monoadduct does not accumulate in the reaction mixture because the quantum yield for its conversion to cross-link is four times larger than the quantum yield for formation of monoadduct from HMT. The high intensity radiation from the laser allows for short reaction times and high yields of cross-linked molecules. Utilizing this laser light source, we have prepared 2 μmoles of purified cross-link (8 XL) formed between the DNA octanucleotide d(5'-GCGTACGC-3') and HMT. The solution NMR structure for this molecule is currently being solved. The 2D ^{1}H NOESY and COSY spectra for this molecule have been fully assigned, and the ^{1}H homonuclear NOE build up curves for this molecule have been acquired and are currently being interpreted. Data from X-ray diffraction quality crystals from this cross-linked molecule is currently being accumulated. This work was done with Dr. Srinivas Sastry. The ^{1}H NMR was done with Dr. Tammy Dwyer and Dr. David Wemmer.

Using a DNA 12 mer (5'-GAA-GCT-ACG-AGC-3'), a complementary DNA 8 mer (5'-TCG-TAG-CT-3') and HMT yields of 50% 12 mer / 8 mer cross-link after HPLC purification were achieved. Using a self complementary DNA 8 mer (5'-GCG-TAC-GC) and HMT, yields of between 36-80% 8 mer cross-link after HPLC purification were

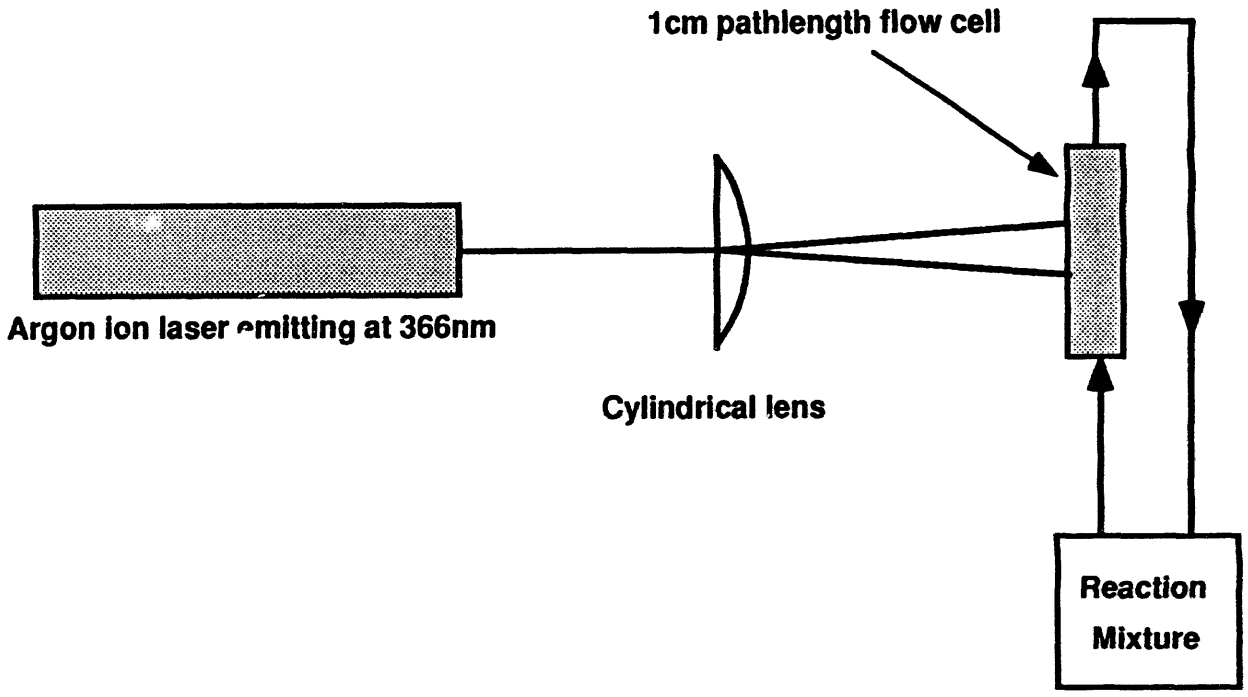

Figure 3.13 Schematic drawing of the Argon ion laser set up to perform crosslinking reactions at high light flux

achieved depending upon the purity of the starting material. Under conditions of high levels of photoaddition, multiple psoralen additions to the oligomers were observed. The extremely high intensity of the irradiating light allowed us to convert large quantities of DNA into cross-link by using a flow system in a reasonable amount of time. The absorbance of a saturated HMT solution at the wavelength of irradiation is 0.36 optical density units for a 1 cm path length. Under these conditions, the entire sample is exposed to an adequate amount of light for conversion to cross-link. The purification of such large quantities of cross-linked material away from other components in the reaction mixture is efficiently achieved by employing reverse phase and anion exchange HPLC. These two techniques are discussed in more detail in part I of this chapter. Anion exchange chromatography is especially useful in the separation of cross-linked molecules from single stranded DNA. The higher charge density of a cross-linked molecule from the phosphate groups cause it to have significantly different chromatographic characteristics than single stranded DNA from which it is made.

Materials and Methods

The oligonucleotides were synthesized on either a 10 μmole or 1 μmole scale on an Applied Biosystems Synthesizer using the phosphoramadite method. The oligomers were deblocked with ammonia and used either as crude preparations or purified by reverse phase HPLC with the trityl group on. Following separation of the tritylated material from the failure sequences, the full length oligomer was detritylated and purified on HPLC. For the 8 mer several batches of 10 μmole syntheses were necessary to obtain several mgs of the final psoralen-DNA cross-link. The sequence of the self - complementary 8 mer was 5'- GCGTACGC -3'. An average 10 mmole synthesis yielded 18 - 22 mgs of total DNA. It was determined by gel electrophoresis and autoradiography that the amount of 8 mer (5'- GCGTACGC -3') that was present in the various syntheses varied considerably. Most

preparations contained significant amounts of shorter oligos such as 6 mers and 7 mers. Since the final product (8 mer cross-link) was purified on denaturing gels or by HPLC, these failure sequences in the initial syntheses did not affect our ability to generate the required product.

Annealing of the DNA strands: After deprotection with ammonia, the oligonucleotides (an average of 20 mg) were taken up in 10 to 20 ml of annealing buffer which consisted of 50 mM Tris - Cl (pH 7.5) + 10 mM $MgCl_2$ + 100 mM NaCl + 1 mM EDTA for the 8 mer DNA. The DNA solutions were heated at 95^0C for 30 min in a waterbath and cooled slowly over a period of 3 - 6 hrs to room temperature. After the DNA had cooled to room temperature, the volume of the solution was increased to 200 ml (~ 0.1 mg DNA / ml final concentration) by diluting with annealing buffer for the respective oligonucleotides. EDTA was added to 7 mM (final) for the 8 mer duplex preparations. It was found that increasing the EDTA concentrations before the addition of HMT (for dark binding) increased the final yield of the cross link.

HMT additions : A stock solution of HMT was prepared in DMSO at a concentration of 14.5 mg / ml. HMT was added to 80 µgs per ml, and the solutions were kept at 4^0C in the dark overnight (dark binding). This concentration of HMT is above the saturation limit of HMT in water. Greater than saturation (40 µg / ml) quantities of HMT were added because we found that in the course of these experiments more than 50% of the HMT was being photodestroyed by the high - intensity laser light (data not shown).

Laser irradiation: The HMT + DNA solution was pumped through a jacketed quartz flow cell (NSG Precision Cells, Inc, N.Y.; 10 mm path length) that was positioned in the path of the laser light (Fig. 3.13). The output of the laser was adjusted between 5 and 6 watts. A cylindrical quartz lens was used to focus the light beam such that the entire area of the flow cell received the maximum amount of laser light. The intensity of the light at the surface of the cell was approximately 25 W/cm^2. The pumping was done at a constant rate of 1 ml / min using a peristaltic pump. For the 8 mer self - complementary duplex,

irradiation was done while cooling the jacket of the flow cuvette with ice water. We observed that irradiation at 0-5°C for the 8 mer increased the formation of only a single species of cross link. In this case, the sample (DNA + HMT) reservoir was also maintained on ice during the course of the irradiation. After one cycle of irradiation, additional HMT was added to 80 µgs per ml and the DNA + HMT solution was pumped through the laser beam for a second cycle of photoreaction.

Sample concentration: The reaction mixture volume was reduced to 50 ml by lyophilization. These samples were then dialyzed extensively (42 hrs) against 500 to 1000 fold excess water with 3 - 4 changes of water. This removes most of the salts and unreacted and / or photodamaged HMT from the sample. The samples were then concentrated to dryness by lyophilization.

Preparative gel purification : The DNA was resuspended in 2 ml of Tris - Borate Buffer (pH 8.0) + 8M urea and dyes. The DNA sample was denatured by heating to 95^{0}C and cooling rapidly on ice. The DNA was electrophoresed on preparative denaturing 20% polyacrylamide gels (19:1 acrylamide:bis) until the bromophenol blue dye was half way down the gel. The cross-link band which migrated sufficiently far away from the unmodified 7 and 8 mers, was identified by careful UV shadowing with a hand held UV lamp from a distance of 1 - 2 ft from the gel. The gel was scanned very quickly with the UV lamp to avoid any significant photoreversal of the DNA cross link. Gel slices which contained the cross link band were excised from the gel and cut into many smaller pieces. DNA from these gel pieces was passively eluted by repeatedly soaking the gel pieces in water. A total volume of 20 ml of water was used for a 10 mmole starting DNA synthesis. The efficiency of the elution of 8 mer cross link (8XL) DNA was ~ 85% of the DNA that was present in the gel slices (data not shown). The cross-linked DNA molecules were then dialyzed extensively (50 - 90 hrs) against water as described above. The DNA samples were then passed through a Nalgene 0.45 micron filter to remove debris and residual particulate polyacrylamide. The DNA was then lyophilized to dryness.

HPLC purification: Both reverse phase and anion exchange chromatography were used for the purification of the 8 mer cross link DNA. See part I of this chapter for a description of the general reverse phase purification method. For ion exchange chromatography a Nucleogen 60 - 7 DEAE anion exchange HPLC set up (column dimensions 4 mm x 125 mm) was used. The pellet of modified DNA was dissolved in 1 ml 30% acetonitrile and 20 mM sodium acetate pH 5.5 and applied to the anion exchange column. The products of the reaction were eluted with a linear KCl gradient over a period of 200 minutes (flow rate = 1.0 ml/min). The concentration of KCl was changed from 0.0 to 1.0 M from time 5 minutes to time 205 minutes. The fractions of interest were collected and concentrated in a speed vac. The cross-linked DNA molecules were then dialyzed extensively (50 - 90 hrs) against water as described above. The DNA was then lyophilized to dryness. The residue was resuspended in a minimum volume of TE and adjusted to 200 mM NaCl, 10 mM $MgCl_2$ and 3 volumes of absolute ethanol were added. The solution was cooled overnight at -20°C and the precipitate collected by centrifugation at 16,000 x g for 35 minutes. The supernatant was removed and the pellet washed with 95% EtOH and dried in vacuo. Both types of chromatography used in conjunction with each other yielded extremely pure 8XL DNA as verified by denaturing polyacrylamide gels and autoradiography of the labeled cross-linked molecules.

Gel Analysis of HPLC fractions: The oligonucleotide fractions isolated by HPLC were resuspended in 0.5 ml TE. 1 µl of each of these fractions was 5' ^{32}P end labeled using T4 polynucleotide kinase and $\gamma^{32}P$-ATP. An aliquot of each of these reactions was loaded onto a 20 cm x 40 cm x 0.4 mm 24% 19:1 acrylamide:bis 7 M urea gel and electrophoresed until BPB was at the bottom of the gel. The results of this electrophoresis were visualized by autoradiography.

Synthesis of the HMT cross-linked 8 and 12 mer oligonucleotides using the Argon laser: Irradiations were carried out a SpectraPhysics 2045 Argon laser operating in broad band mode centered at 366 nm at a power of 5.0 W. The oligonucleotides were dissolved

in 35 ml of 150 mM NaCl, 10 mM $MgCl_2$,1 mM EDTA, 15 mM azide, $5.6X10^{-4}$ M HMT. This solution was flowed through a 1 cm path length quartz flow cell cuvette at a rate of 1.5 ml/min. The cuvette was placed in the laser beam and irradiated for 40 min. After the irradiation was complete, the solution was brought to 200 mM NaCl with 6.1 M NaCl, and 3 volumes of absolute EtOH were added. Solution was cooled overnight at -20°C and the precipitate collected by centrifugation at 25000 X g for 2 hours. The supernatant was removed and the pellet washed with 95% EtOH and dried in vacuo.

Results and Discussion

Efficiency of cross link formation and cross link purification by HPLC : Aliquots of the photoreactions were kinased with γ^{32}P-ATP and the resulting mixtures loaded onto denaturing PAGE and electrophoresed. We quantified the efficiency of cross-link formation by cutting and counting the ^{32}P radiolabeled DNA bands from gels. We found that the yield of cross link formation ranged from 36% to 80% of the starting DNA material. The yield depended on the relative purity of the starting material DNA. As described for the formation of furan-side monoadducts above, the purity of the starting DNA has a dramatic effect on the extent of photoreaction. A profile of an 8 mer preparation that was purified by reverse phase HPLC is shown in the left hand panel of figure 3.15. The 8 mer eluted as a single peak showing that the initial C_{18} purification effectively removed almost all of the synthetic oligos that were shorter than 8 nucleotides. The presence of the shorter oligos was confirmed in the crude oligonucleotide by gel electrophoresis (data not shown). In the case of synthetic 8 mer preparations, which were initially purified on reversed phase C_{18} columns before subjecting them to cross linking reactions, the yield of HMT - 8 mer cross-link (8XL), after argon laser irradiation, was approximately 50 %.

Figure 3.14: This is a anion exchange chromatogram of an argon laser cross linking reaction of a crude 8 mer preparation with HMT. A multitude of species eluted with retention times between 30 to 100 min. Some of these can be rationalized as photodamaged 8 mer and failure sequences, and various monoadducted species. The major peak (111 - 113 mins) contained at least two species of cross-linked material (upper and lower bands shown in the inset). Purified 8 mer and 5'-TpA-3' 8 mer cross-link (8XL) standards, shown on the left hand side of the inset, indicate that the lower band contained the 5'-TpA-3' 8 mer cross-link (8XL).

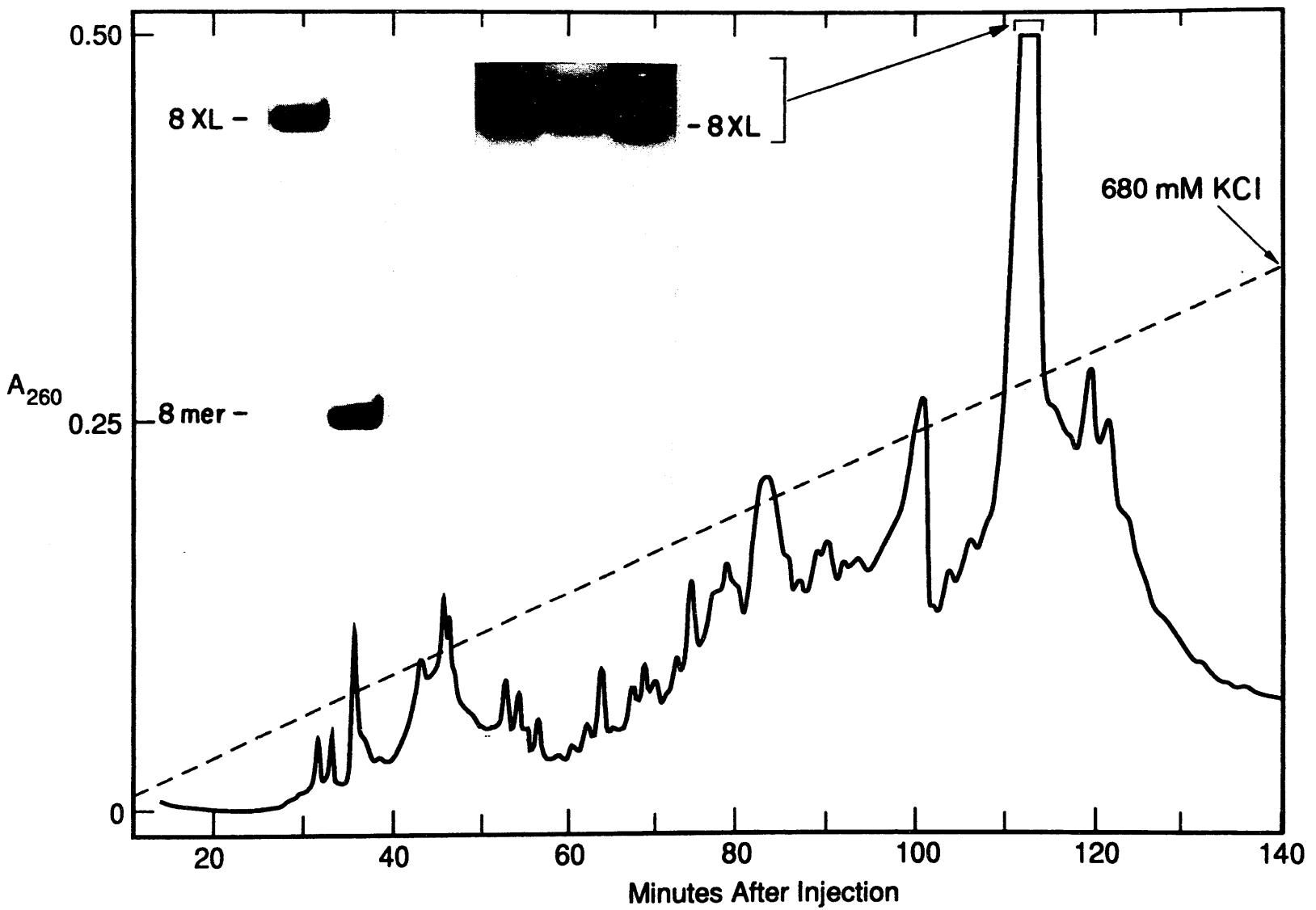
0.50
0.25
0
A_{260}
8 XL –
– 8XL
8 mer –
680 mM KCl
20
40
60
80
100
120
140
Minutes After Injection

Figure 3.15: Panel A is a reverse phase chromatography elution profile of the 8 mer 5'-GCGTACGC-3'. Panel B is a reverse phase chromatogram of the main cross-link containing fractions described in figure 3.14. This material was resolved into three main peaks. Analysis of these peak fractions by denaturing gel electrophoresis (upper panel of figure 3.15) revealed that the 8 mer cross-linked at the 5'-TpA-3' site eluted as a single peak (# 3) and was greater than 95% pure. Peak #1 consisted of a different cross-link species that had a retention time longer than that of the 5'-TpA-3' 8 mer cross-link (# 1 upper panel). The material that eluted in peak #2 contained two components, one of which co-migrates with the 5'-TpA-3' 8 mer cross-link when electrophoresed on a denaturing PAGE, but has a significantly different retention time from the 5'-TpA-3' 8 mer cross-link on reverse phase HPLC. See text for a disscussion of the origin of these other cross-linked species.

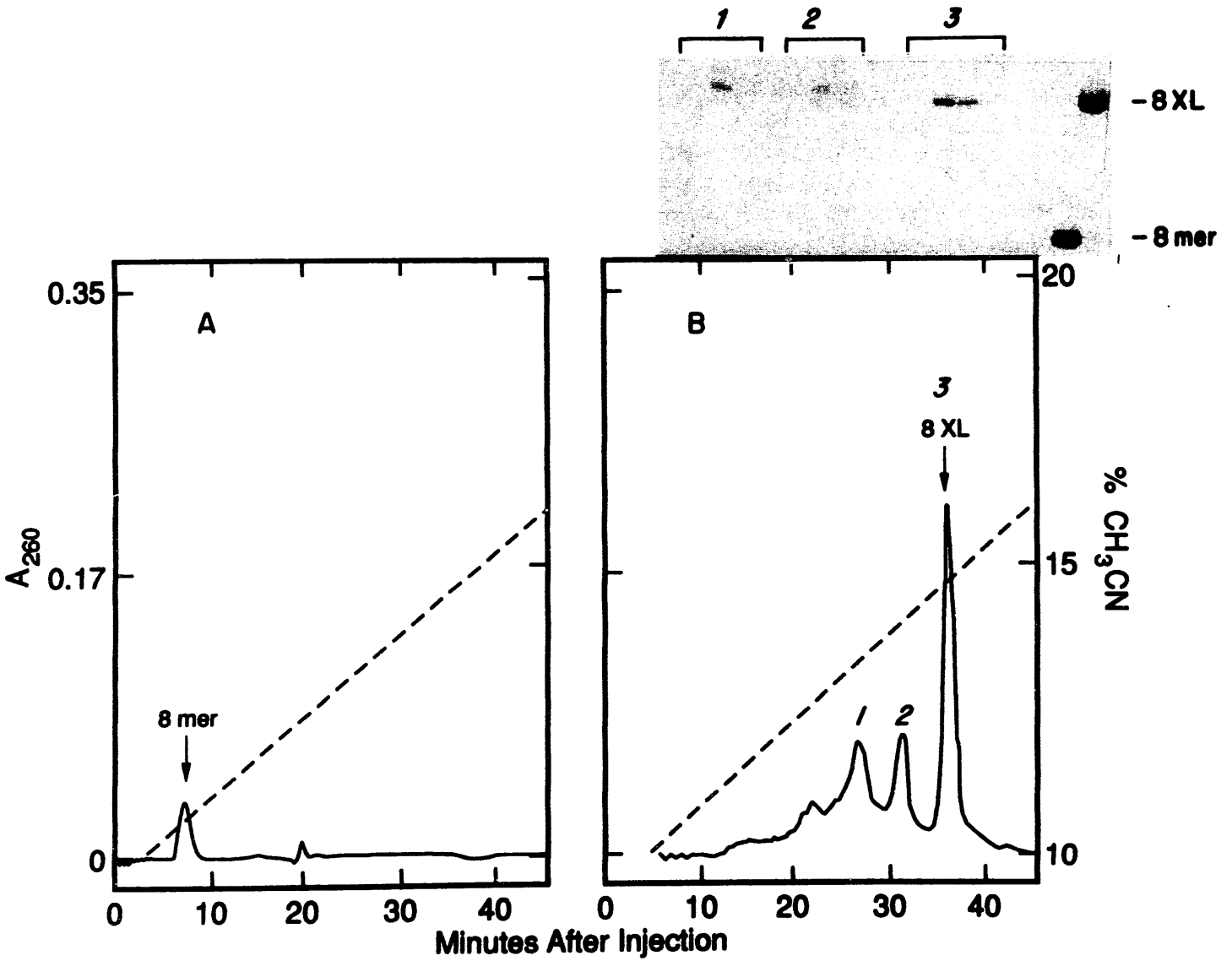
1
2
3
-8XL
-8mer
0.35
A
0.17
0
8 mer
A_{260}
0
10
20
30
40
B
3
8 XL
1
2
20
15
10
% CH_3CN
Minutes After Injection

An example of a direct cross linking reaction without initial HPLC and/or gel purification of the 8 mer preparation is shown in figure 3.14. The DNA was removed from the support column, deprotected, and subjected to argon laser irradiation in the presence of HMT. The resulting material was injected onto a Nucleogen DEAE ion-exchange column on an analytical scale. A multitude of species eluted with retention times between 30 to 100 min . Gel electrophoresis (not shown) of these fractions revealed the presence of many smaller species of oligos, the corresponding cross link material, and 8 mer single - stranded DNA. Some of these DNA molecules had mobilities on this PAGE with retention times longer than that of the parent 8 mer. Some of these can be rationalized as photodamaged 8 mer and failure sequences, and various monoadducted species. The major peak (111 - 113 mins) contained at least two species of cross-linked material (upper and lower bands shown as inset to Fig.3.14). Using purified 8 mer and 8 mer cross-link (8XL) as standards, (shown on the left hand side of the inset) it was determined that the lower band contained the 8 mer cross-link (8XL). The upper band may represent an 8 mer cross-link species containing an additional adduct on one of the deoxycytidine residues in the 8 mer or cross-linking at a site in the molecule other than in the central 5'-TpA-3' site. The origin of the upper band is discussed in further detail below. To resolve these species, we reinjected these fractions on to a reversed phase analytical C_{18} column. This material was resolved into three main peaks, shown in the right hand panel of figure 3.15. Analysis of these peak fractions by denaturing gel electrophoresis (upper panel of figure 3.15) revealed that the 8 mer cross-linked at the 5'-TpA-3' site eluted as a single peak (# 3) and was greater than 95% pure. Peak #1 consisted of a different cross-link species that had a retention time longer than that of the 5'-TpA-3' 8 mer cross-link (# 1 upper panel). The material that eluted in peak #2 contained two components, one of which co-migrates with the 5'-TpA-3' 8 mer cross-link when electrophoresed on a denaturing PAGE, but has a significantly different retention time from the 5'-TpA-3' 8 mer cross-link on reverse phase HPLC. The yields of 5'-TpA-3' 8 mer cross-link, based on total DNA absorbance, was substantially

Figure 3.16: This is a anion exchange chromatogram of the repurification of an argon laser cross linking reaction of a crude 8 mer preparation with HMT that was initialy cleaned by gel electrophoresis. The 8 mer 5'-TpA-3' cross link (8XL) eluted as single peak (# 1) away from other contaminants (#2). The extent of purification was monitored by denaturing gel electrophoresis. The major peak was the 5'-TpA-3' 8 mer cross-link and was at least 95 % pure (inset of figure 3.16, lane 1) . The minor peak (#2) consisted of a mixture of cross links, including both material that co-migrates with the 5'-TpA-3' 8 mer cross-link and a species that ran slower than it on denaturing PAGE. See text for a disscussion of the origin of these other cross-linked species.

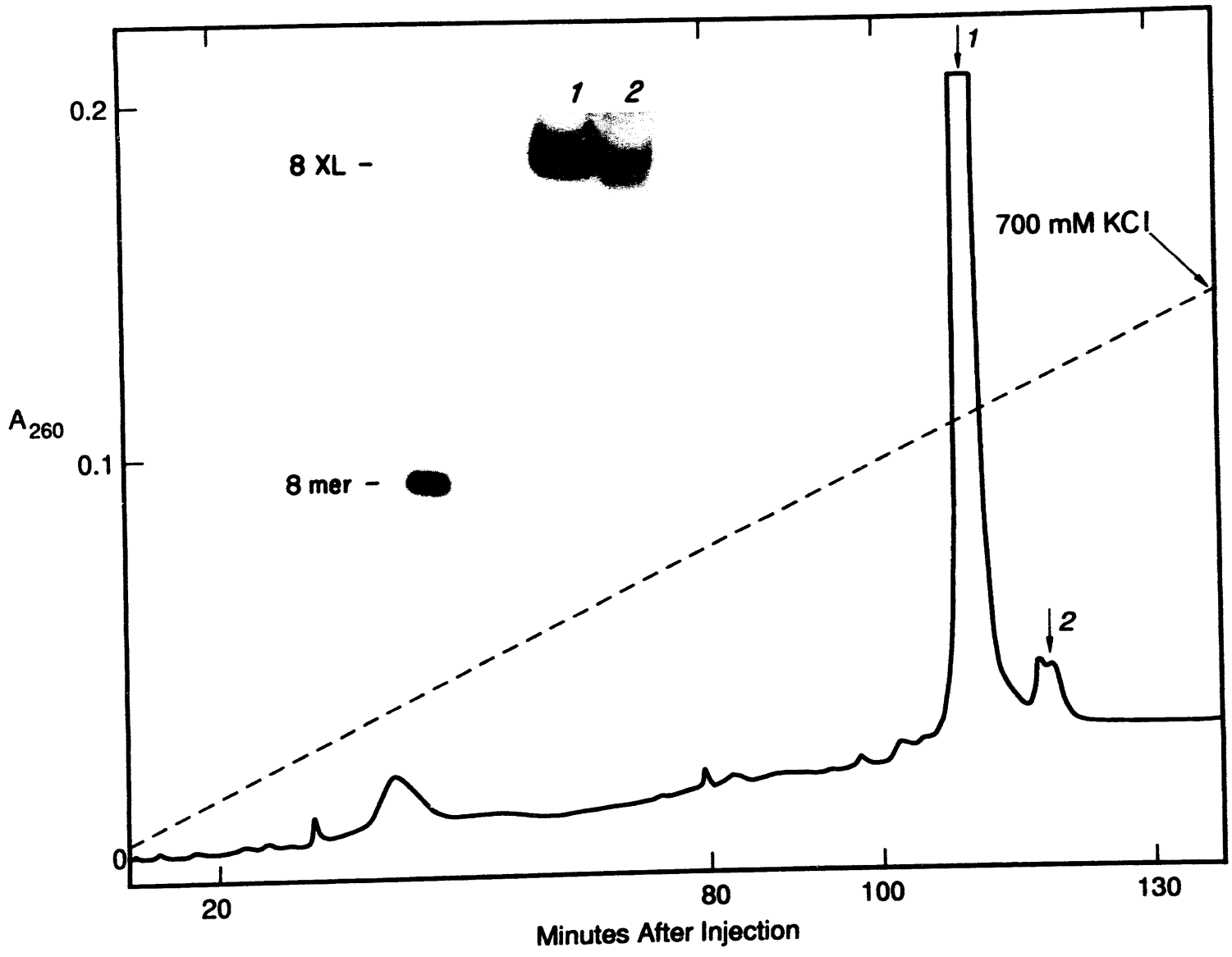
1
2
8 XL –
8 mer –
700 mM KCl
1
2
0.2
0.1
0
A_{260}
20
80
100
130
Minutes After Injection

lower (approximately 36 %) with crude preparations of 8 mer that were not subjected to initial HPLC purification.

We have also successfully purified HMT - DNA cross-links prepared on the μmole scale by employing denaturing polyacrylamide gel electrophoresis. The DNA component of a laser cross-linking reaction was subject to electrophoresis on a denaturing 20% polyacrylamide gel. The different adducted molecules were located on the gel either by autoradiography in the case of ^{32}P labeled DNA, or by careful UV shadowing of the bands. The cross-linked DNA was recovered from the gel by excising the appropriate gel slices and eluting the DNA into water (see materials and methods). To further purify the eluted cross-links, we chromatographed the eluted cross-link on to a Nucleogen DEAE HPLC column. Figure 3.16 shows the results of this purification procedure. The 8 mer 5'-TpA-3' cross link (8XL) eluted as single peak (# 1) away from other contaminants (#2). The extent of purification was monitored by denaturing gel electrophoresis. The major peak was the 5'-TpA-3' 8 mer cross-link and was at least 95 % pure (inset of figure 3.16, lane 1) . The minor peak (#2) consisted of a mixture of cross links, including both material that co-migrates with the 5'-TpA-3' 8 mer cross-link and a species that ran slower than it on denaturing PAGE.

As discussed above in part I, denaturing polyacrylamide gel electrophoresis separates molecules based on their overall shapes, sizes and charge, reverse phase HPLC is sensitive to the hydrophobic moment of the molecules, and anion exchange HPLC is sensitive to their charge density. The retention times and order of elution relative to the 5'-TpA-3' 8 mer cross-link of the three contaminating cross-linked species is reversed when the mixture is separated by reverse phase or anion exchange chromatography. These results can be rationalized if these three HPLC peaks are composed of either a T-HMT-C or C-HMT-C cross-linked molecule in addition to the main T-HMT-T species (5'-TpA-3' 8 mer cross-link). The molecules in the three cross-link containing peaks all have the same overall charge because they were derived from the same 8 mer. The structural distortion

induced in the molecule depends on the site of psoralen addition, and this influences the particular charge density, hydrophobic moment and overall shape of an individual cross-linked species. A cross-linked molecule that is electrophoresed under denaturing conditions presumably adopts an extended X shaped conformation. This significantly retards its progress through the gel matrix relative to single stranded molecules. In this symmetric self-complementary 8 mer, a cross-link at the central 5'-TpA-3' site and a cross-link at the flanking 5'-GpT-3' site would have the same essential X shape while being electrophoresed. The only other sites available for photoreaction in this molecule are a 5'-GpC-3' and a 5'-CpG-3' site. Photoreaction at either of these sites would give molecules that have a significantly different shape under these electrophoresis conditions. It is likely that such a C-HMT-C cross-linked molecule is the upper band identified as peak #1 in figure 3.15 A mixture of T-HMT-C and a C-HMT-C cross-linked molecules are likely the components that make up peak #2 in figure 3.15 with the C-HMT-C cross-link as the molecule in the upper band. This explanation accounts for the four cross-link species seen in the autoradiogram in figure 3.15. The main peak (#3) has been unambiguously determined to be the HMT cross-linked molecule at the 5'-TpA-3' site by ^{1}H NMR. The reported structure for the AMT cross-linked self-complementary 8 mer d(5'-GGGTACCC-3') determined by ^{1}H NMR contained a persistent contaminant that hindered the analysis of the data (Tomic *et al.*, 1987). The cross-link used in this study was purified by gel electrophoresis. In light of the analysis of the products of psoralen photo-cross-linking of short oligomers given above, it is possible that the contaminating species in the NMR was a cross-link at the 5'-GpT-3' site.

Our experience with these reactions allowed us to make 1 μmole (5.1 mg) of greater than 95% pure 8 mer cross-linked with HMT from which X-ray diffraction quality crystals have been grown. The procedure for producing these large quantities of modified molecules is as follows: A mixture of HMT and the 8 mer was irradiated with UV light and the modified DNA were concentrated as described in the experimental section. The

Figure 3.17: This is an autoradiogram of kinased HPLC fractions run on a 24% 7 M urea denaturing polyacrylamide gel from the second round of reverse phase HPLC purification of a HMT cross-linking reaction with the 8 mer 5'-GCGTACGC-3'. Most of the unmodified 8 mer was removed in the first round of purification. Lanes 1-4 correspond to HPLC fractions 9-12 and are the unmodified 8 mer. Lanes 6-7 correspond to HPLC fractions 19 and 20 and they are pyrone-side monoadduct. The pyrone-side monoadduct is contaminated with a small amount of cross-link. Lanes 8-12 correspond to HPLC fractions 21-25 and are the cross-linked 8 mer. Lane 13 is unmodified 8 mer standard, and lane 14 is cross-linked 8 mer standard.

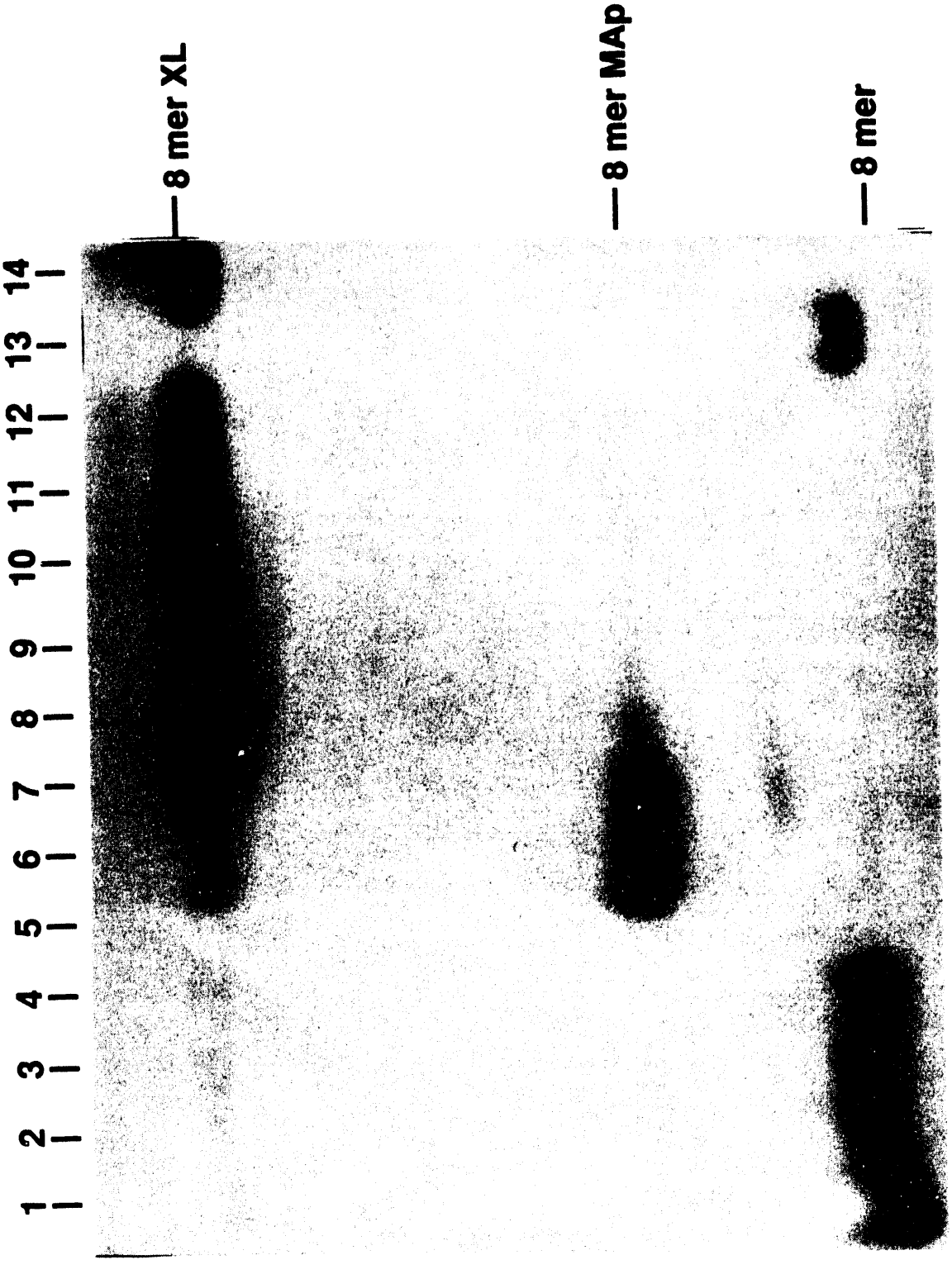
8 mer XL
8 mer MAp
8 mer
1
2
3
4
5
6
7
8
9
10
11
12
13
14

majority of the unmodified 8 mer was separated from psoralen adducted DNA by an initial round of reverse phase chromatography. In this system, both the cross-linked molecules and pyrone-side adduct co-eluted in a broad band. This was a function of column overloading. The psoralen containing peak was collected and subject to a second round of reverse phase HPLC. It contained a small amount of unmodified 8 mer along with the pyrone-side adduct and the cross-links. Figure 3.17 is an autoradiogram of kinased HPLC fractions run on a 24% 7 M urea denaturing polyacrylamide gel from the second round of reverse phase HPLC purification. In the second round of chromatography, the amount of material loaded on the column was much smaller and separation was effected between the three species in the mixture. Lanes 1-4 correspond to HPLC fractions 9-12 and are the unmodified 8 mer. Lanes 6-7 correspond to HPLC fractions 19 and 20 and they are pyrone-side monoadduct. The pyrone-side monoadduct is contaminated with a small amount of cross-link. Lanes 8-12 correspond to HPLC fractions 21-25 and are the cross-linked 8 mer. Lane 13 is unmodified 8 mer standard, and lane 14 is cross-linked 8 mer standard. The fractions 21-25 were pooled and chromatographed using anion exchange HPLC. This completed the separation of all of the components of the reaction mixture. The unmodified 8 mer was removed in the initial reverse phase HPLC steps and the various cross-link isomers were separated from each other and the single stranded pyrone-side adduct was separated uncontaminated with unmodified DNA in the anion exchange HPLC step.

Part III: The preparation of Pyrone-side Adduct

The third type of common psoralen DNA photochemical adduct is the pyrone-side monoadduct. Pyrone side adducts do not absorb light at wavelengths greater than 310 nm. Under typical UVA conditions they do not absorb light and go on to form cross-links. They are formed in relatively low yield during the forward photochemical cross-linking reaction (see figure 1.2). In fact, the pyrone-side adduct is not detected when the krypton laser is used to synthesize monoadducts at long wavelengths (data not shown). When the argon laser is used to make cross-link, pyrone-side monoadducted oligomers only account for less than 5% of the total modified DNA. We have developed a method for producing micromole quantities of pyrone-side adduct using a base catalyzed reversal of the furan-side cyclobutane ring of psoralen cross-linked DNA. While investigating the pH dependence of the photoreversal of psoralen cross-linked DNA, we found that under certain alkaline conditions, the cross-link could undergo reversal without exposure to actinic UV light to produce the unmodified DNA and the pyrone ring opened and closed forms of the pyrone-side monoadducted DNA (Shi *et al.*, 1988; Yeung *et al.*, 1988). We have found that, in contrast to photoreversal, base-catalyzed reversal of the cross-link yields only the pyrone-side monoadducted and unmodified DNA. No furan-side monoadducted DNA was detected under the base-catalyzed conditions. The photoreversal with short wavelength UV light of cross-linked double stranded oligonucleotides yields mostly the furan-side monoadducted oligonucleotide (Shi and Hearst, 1987b). The pyrone-side monoadducted oligonucleotide is a minor product of this photo-reversal reaction. Parts of this work were done in conjunction with Dr. Yun-Bo Shi and have been published previously (Shi *et al.*, 1988).

The cross-link used in the discovery of this reaction was formed by the cycloaddition of HMT to the two thymidine residues in the DNA helix formed by the self

complementary oligonucleotide 5'-GGGTACCC-3'. When this cross-link was incubated in the absence of UV light at 60°C at pH 10.1 in the presence of 3 M urea it was reversed into the unmodified oligonucleotide and the pyrone-ring opened (O-MAp) and pyrone-ring closed (C-MAp) forms of the pyrone-side monoadducted oligonucleotide (Cimino *et al.*, 1986). No furan-side monoadducted oligonucleotide was generated under these conditions. The amount of the product increased with increasing incubation time. No reversal of the cross-link was observed when urea was omitted or the pH of the incubation solution was lowered to pH 8.5. These results suggest that the reversal of the cross-link under these conditions is a base-catalyzed reaction. The requirement for urea implies that the reaction only occurs if the cross-linked helix is denatured. We have observed that the cross-linked HMT-DNA molecule could be reversed upon incubation at pH 12 at 37°C in the absence of urea and that the cross-link formed between the psoralen derivative AMT (4'-aminomethyl-4,5',8-trimethylpsoralen. **1**) and the oligonucleotide 5'-GGGTACCC-3' could be reversed upon incubation in concentrated ammonia solution at room temperature or higher temperatures. The cross-linked DNA helix would be expected to be denatured under these conditions and the pyrone ring of the psoralen moiety in the cross-link would be opened (Cimino *et al.*, 1986) at such high pH.

The properties of the reversal reaction are characteristic of a light-independent chemical reaction. First, increasing incubation time in the absence of actinic light results in more product formation. Secondly, increasing the concentration of the catalyst (OH^-) (see discussion of the proposed mechanism below) concentration by increasing the pH from 10 to 10.5, and 12, increases the reaction rate. The amount of product formed at pH 10.5 in the absence of urea is comparable to that formed at pH 10 in the presence of 3M urea. (data not shown) even though little reaction was observed at pH 10 in the absence of urea (Figure 3.18). Thirdly, raising the temperature of the reaction from 60°C to 65°C increases the reversal rate (data not shown).

Figure 3.18: Base-catalyzed reversal of the cross-link. Lane C: XL photoreversed with 254 nm light. Lanes 1, 2, 3, and 4: XL in 10 mM $NaBO_3$ and 3 M urea, pH 10, incubated at 60°C for 0, 0.5, 1, and 2 h, respectively (Less products were produced here as compared to those in Figure 3.19. This is most likely due to the pH difference under the two reaction conditions.) Lanes 5, 6, 7, and 8: XL in 10 mM $NaBO_3$, pH 10, incubated at 60°C for 0, 0.5, 1, and 2 h, respectively. Lanes 9, 10, 11, and 12: XL in 10 mM $NaBO_3$ and 3 M urea, pH 8.5, incubated at 60°C for 0, 0.5, 1, and 2 h, respectively. After incubation, 75 µl of 0.2 M succinate (pH 4) was added to each sample (350 µl) (final pH, 4-5). The samples were then incubated at 37°C for 30 min. EtOH precipitated in the presence of carrier tRNA, and analyzed on a polyacrylamide-urea gel. Abbreviations: XL, HMT-DNA cross-link; Mfu, furan-side monoadducted oligonucleotide; C-Mpy, pyrone ring closed form of the pyrone-side monoadducted oligonucleotide; O-Mpy, pyrone ring opened form of the pyrone-side monoadducted oligonucleotide; UM, unmodified oligonucleotide.

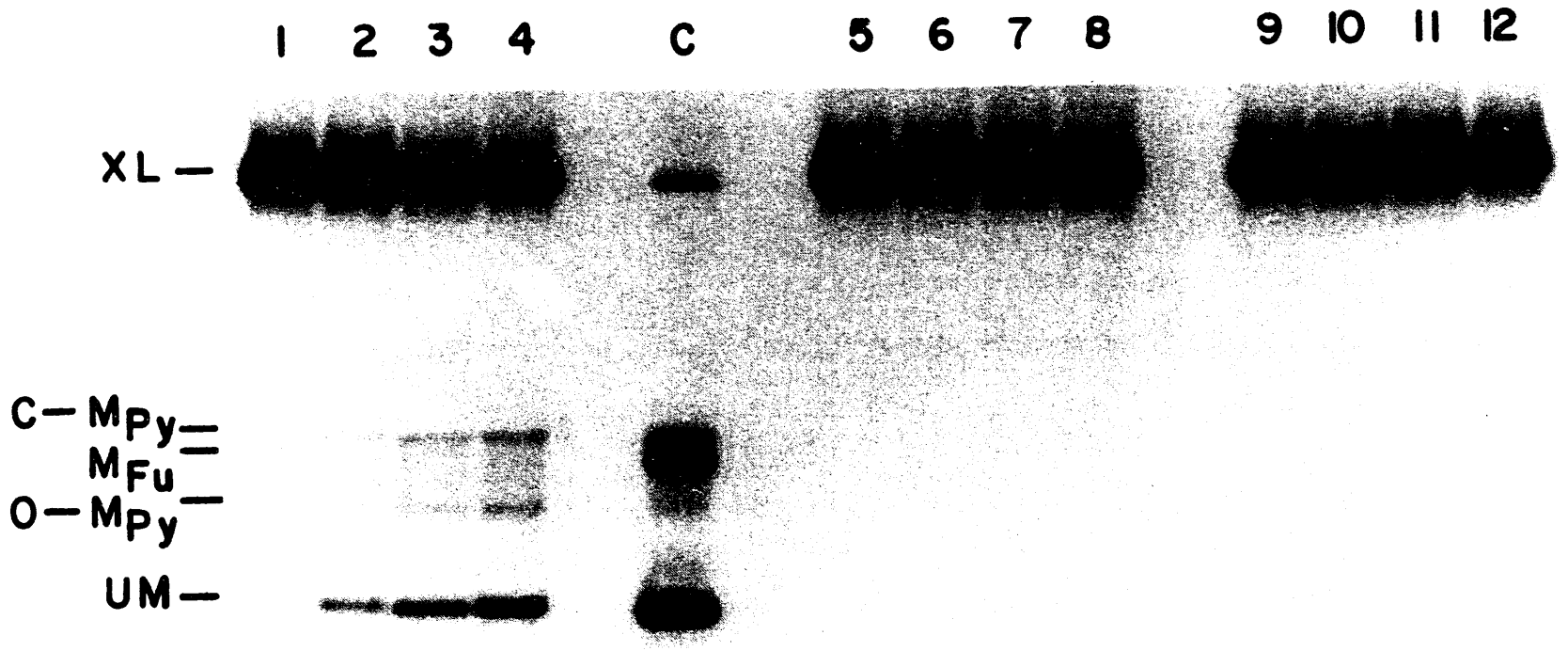
1 2 3 4 C 5 6 7 8 9 10 11 12
XL
C—MPy
MFu
O—MPy
UM

Materials and Methods

Materials. HMT and [^{3}H]HMT were gifts from HRI Associates Inc. (Berkeley, CA). The oligonucleotide 5'-GGGTACCC-3' was synthesized on an automated DNA synthesizer. After synthesis, the oligonucleotide was deprotected in concentrated ammonia solution at 55°C for 5 h and purified by electrophoresis on a 20% polyacrylamide-7 M urea gel followed by EtOH precipitation. The purification gel (40 cm x 40 cm x 0.12 cm) had a composition of 30:1 acrylamide/bis(acrylamide) and was run at 45 W with an aluminum plate clamped on to the gel plate. [γ-^{32}P]ATP was purchased from Amersham. T4 polynucleotide kinase was bought from Bethesda Research Laboratories.

Isolation of DNA from Polyacrylamide Gels. DNA bands on a gel were identified by autoradiography and excised, and the DNA was eluted into a solution of 50 mM NaCl and 1 mM EDTA by soaking at room temperature overnight. The DNA solutions were then adjusted to 0.2 M NaCl and 10 mM $MgCl_2$ followed by precipitation with 2.5 volumes of EtOH.

Preparation of HMT-DNA Cross-link. (A)5'-^{32}P-Labeled HMT-DNA Cross-link. The cross-link (1-20 μg) was prepared as described by (Cimino *et al.*, 1986) and stored frozen in 1 mM EDTA. See materials and methods, chapter 1.

(B)5'-^{32}P-Labeled [^{3}H]HMT-DNA Cross-link. Large amounts of [^{3}H]HMT-DNA cross-link were required for the HPLC analysis of the products of the base-catalyzed reversal. For this purpose, 560 μg of the self-complementary oligonucleotide 5'-GGGTACCC-3' was 5'-^{32}P-labeled with [γ-^{32}P]ATP and T4 polynucleotide kinase followed by a chase of the kinase reaction with unlabeled ATP to phosphorylate all the 5'-ends (Shi and Hearst, 1986). The labeled DNA was then irradiated with 320-380 nm light in the presence of 0.15 mM [^{3}H]HMT (1.2 Ci/mmol) according to the procedures of Shi and Hearst (Shi and Hearst, 1986). The cross-linked DNA was separated from the unmodified DNA by electrophoresing the sample on a 20% polyacrylamide-7 M urea gel.

This gel and all other analytical gels in this work were identical with the purification gel described earlier except the thickness was 0.05 cm. The cross-link was isolated from the gel. Two hundred thirty micrograms of the ^{3}H-labeled cross-link was thus generated.

Base-Catalyzed Reversal of the HMT-DNA Cross-link. The base catalyzed reversal of the cross-link was performed under a variety of conditions in the absence of UV light to avoid the possibility of photochemistry. Appreciable reversal of the cross-link was observed at 37°C and pH 12 (1 mM Na_3PO_4), at 60°C and pH 10.5 (10 mM Na_3BO_3), and at 60°C and pH 10.0 (10 mM Na_3BO_3) in the presence of 3M urea. Following the incubations at alkaline pH and elevated temperatures, the cross-link samples were adjusted to pH 4-5.5 with 0.2 M succinate (pH 4.0) with or without further incubation at 37°C. The samples were then adjusted to 0.2 M NaCl, 10 mM NaCl, and 40 μg/ml carrier tRNA followed by precipitation with 2.5 volumes of EtOH. The products were then analyzed by electrophoresis on a denaturing polyacrylamide gel.

HPLC Analysis of Products of the Base-Catalyzed Reversal. EtOH-precipitated ^{3}H-labeled cross-linked oligonucleotide (230 μg) was dissolved in 1.5 ml of 10 mM Na_3BO_3 and 3 M urea, pH 10.5, split into six 1.5 ml Eppendorf tubes, and incubated at 65°C for 2 h. One hundred microliters of 0.2 M succinate (pH 4.0) was then added to each tube, and the mixture was incubated at 37°C for 1.5 h. The DNA was EtOH precipitated and electrophoresed on a polyacrylamide gel. The products were isolated and digested to nucleosides by sequential treatment with DNase II, phosphodiesterase II, and alkaline phosphatase according to published procedures (Kanne *et al.*, 1982a). See materials and methods, chapter 2.

Characterization of Products of the Base-Catalyzed Reversal. The pyrone-side monoadducted DNA can exist in either the pyrone ring open form (O-MAp) or the pyrone ring closed form (C-MAp). The two forms have different mobilities on a denaturing polyacrylamide gel (Figures 3.18 and 3.19) and are interconvertable. Basic conditions (pH 10) open the pyrone ring, and acidic conditions (pH 4) close the ring ((Cimino *et al.*, 1986)

Figure 3.19: Base-catalyzed reversal and photoreversal of the HMT-DNA cross-link. The HMT-DNA cross-link after EtOH precipitation was dissolved in 700 μl of 10 mM $NaBO_3$ and 3 M urea, pH 10.1. Lane 1: Cross-link solution (130 μl) kept in the dark at room temperature as the control. Lane 2: Cross-link solution (350 μl) incubated at 60°C for 2 h. Lane 3: Cross-link solution (220 μl) photoreversed with 254-nm light from a low pressure germicidal lamp for 5 min at a distance of 2.5 inches from the lamp. After treatment, all samples were adjusted to ca. pH 4.5 with 0.2 M succinate (pH 4), EtOH precipitated in the presence of carrier tRNA, and then analyzed on a polyacrylamide-urea gel.

1
2
3
XL
C-MPy
MFu
O-MPy
UM

Figure 3.20: Lane 1: XL photoreversed with 254 nm light. Lanes 2-4, 5-7, and 8-10: XL, gel-purified O-Mpy, and gel-purified C-Mpy, respectively. Lanes 2, 5, and 8: untreated control samples. Lanes 3, 6, and 9: Samples (250 μl each) in 10 mM $NaBO_3$ and 3 M urea (pH 10.5) incubated at 60°C for 2 h, followed by addition of 100 μl of 0.2 M succinate (pH 4) and EtOH precipitation in the presence of carrier tRNA before gel analysis. Lanes 4, 7, and 10: Same as lanes 3, 6, and 9, respectively, except hat they were incubated in the acidified solution at 37°C for 1 h before EtOH precipitation.

1 2 3 4 5 6 7 8 9 10
XL
UM
O-MPy
C-MPy
MFu

Figure 3.21: Characterization of the products of base-catalyzed reversal. 5'-Labeled UM, O-Mpy, and C-Mpy were isolated from the gel shown in Figure 1. Lane 1: XL was photoreversed with 254 nm light from a germicidal lamp for 4 min at a distance of 2.5 in. Lanes 2, 4, and 6: Dark controls of C-Mpy, O-Mpy, and UM respectively. Lanes 3 and 5: C-Mpy and O-Mpy, respectively, in 750 µl solution containing 4 µg of unlabeled unmodified oligonucleotide, 10 mM $MgCl_2$, and 100 mM NaCl, was irradiated at 2°C with 249 nm light (4.6×10^{17} photons), dried in a Speedvac concentrator, redissolved in 300 µl of H_2O, and EtOH precipitated in the presence of carrier tRNA. Lane 7: UM generated from base-catalyzed reversal was irradiated for 3.5 min with 320-380 nm light from a 2.5 kW Hg/Xe lamp (Cimino et al., 1986) in 100 µl of 10mM $MgCL_2$ and 100 mM NaCl in the presence of 4 µg of unlabeled UM and 0.15 mM HMT, extracted with chloroform and ether, and EtOH precipitated in the presence of carrier tRNA. All the samples were analyzed on a polyacrylamide gel. Due to the overexposure of the film, the silver grains of the lower part of one side of the X-ray film were removed before making the print.

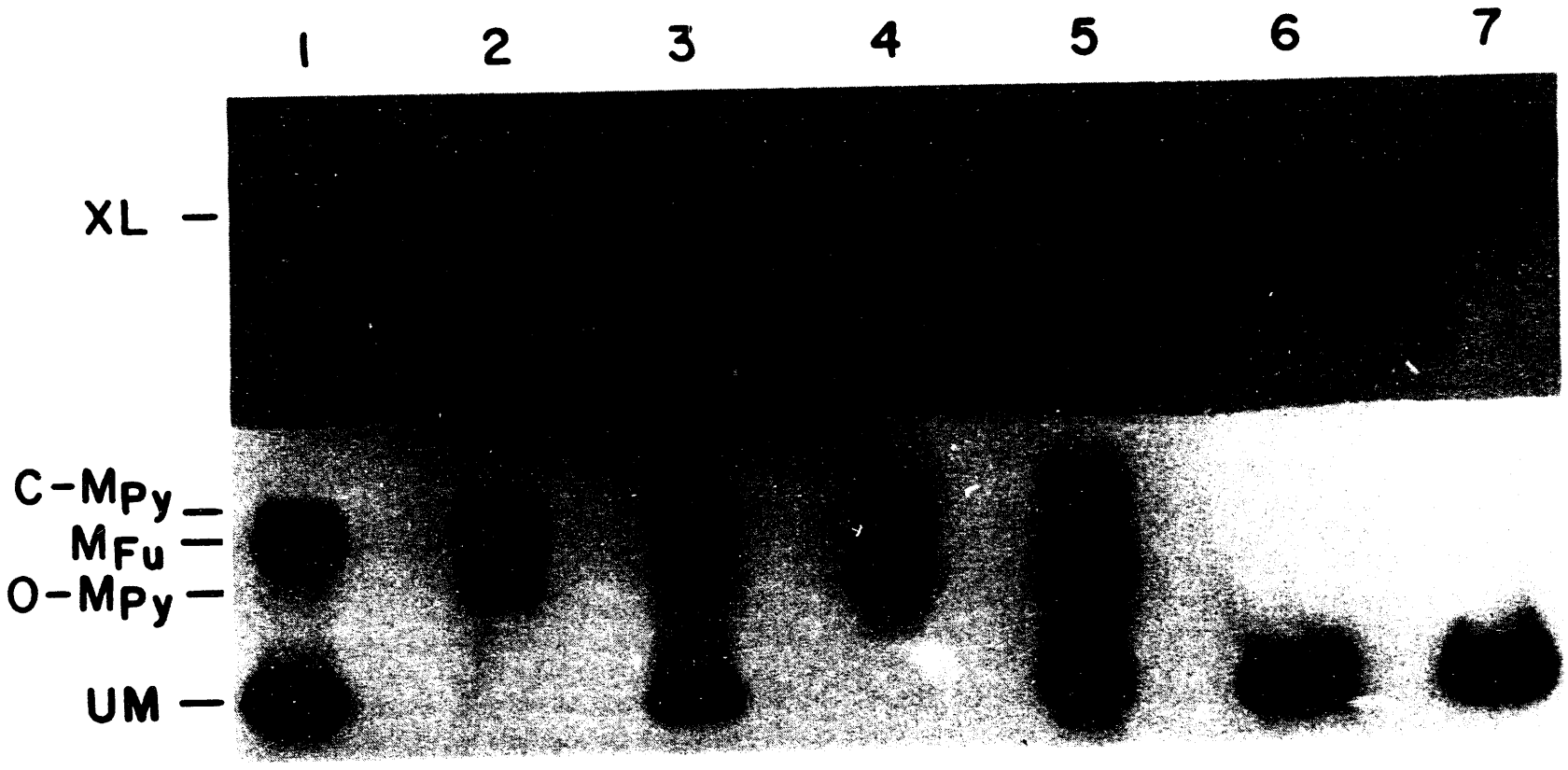
1
2
3
4
5
6
7
XL
C-MPy
MFu
O-MPy
UM

also, see below). Analysis of the base-catalyzed samples without acidic incubation on a denaturing polyacrylamide gel yielded mostly O-MAp (Figure 3, lane 3.20). Acidic incubation of the same sample before gel analysis increased the amount C-MAp with concurrent loss of O-MAp (compare lanes 3 and 4 in Figure 3.20). These results indicate that the initial product of the base-catalyzed reversal is O-MAp and subsequent acidic incubation converts the O-MAp into C-MAp.

The interconversion of C-MAp and O-MAp is also demonstrated in Figure 3.20. Incubation of gel-purified C-MAp in basic solution (pH 10) converted most of the C-MAp into O-MAp (lane 9). An acidic incubation of the base-treated C-MAp *before gel analysis* converted all the O-MAp in the C-MAp sample back into C-MAp (lane 10). However, incubation of the gel-purified O-MAp under acidic conditions (pH 4, 60-65°C, or pH 2.2, 37°C) did not convert it back to C-MAp (Figure 3.20, lane 7, and data not shown) even though upon storage, O-MAp could be partially converted into C-MAp (see lane 5 of Figure 3.20 and lane 4 of Figure 3.21). These results suggest that a modification of O-MAp occurred during gel electrophoresis and this modification is irreversible under the acidic conditions described above.

To further characterize the products, [^{3}H]HMT-DNA cross-link was prepared and reversed as described under Materials and Methods, and the products were purified by polyacrylamide gel electrophoresis. The O-MAp and C-MAp as well as the cross-link were enzymatically digested to nucleosides and analyzed by HPLC (data not shown). With authentic T-HMT adducts as standards, it was found that the cross-link digest gave T-[^{3}H]HMT-T diadduct. The ^{3}H label in the digest of C-MAp co-eluted with that of authentic T-HMT pyrone-side monoadduct. In addition, the absorption spectrum of this HPLC-purified ^{3}H-labeled product is within experimental error identical with that of the authentic T-HMT pyrone-side monoadduct (Shi and Hearst, 1987a), indicating that C-MAp contains T-HMT pyrone-side monoadduct. The HPLC profile of the digested O-MAp gave two major peaks, with one corresponding to T-HMT pyrone side monoadduct, generated

by the conversion of O-MAp to C-MAp during storage and/or enzyme digestion, and the other corresponding to none of the known T-HMT adducts, it cannot be further characterized at the present time.

The photochemical properties of the products were also investigated. The gel-purified C-MAp and O-MAp from the base-catalyzed reversal were irradiated with 249 nm monochromatic light from a 2.5k-kW Hg/Xe lamp (Cimino *et al.*, 1986) at 2°C in t presence of the unlabeled oligonucleotide 5'-GGGTACCC-3'. The unlabeled DNA wa. expected to form double-stranded DNA with itself as well as with the pyrone-side monoadducted oligonucleotide since the stability of the pyrone-side monoadducted double helix is 0.7 kcal/mole greater than that of the unmodified helix (Shi and Hearst, 1986). The results in Figure 3.21 show the characteristic photochemistry of a pyrone-side monoadducted oligonucleotide (Shi and Hearst, 1987a; Shi and Hearst, 1987b). The irradiation resulted predominantly in photoreversal of the monoadducted oligonucleotide with formation of very little cross-link (a longer expos e gel definitely showed the presence of the cross-link band in lanes 3 and 5; data no

The unmodified oligonucleotide generated from the base-catalyzed reversal was irradiated at 2°C with the broad-band near-UV light (320-380 nm; Cimino, 1986 #25) in the presence of a large excess of unlabeled 5'-GGGTACCC-3' and HMT. The labeled DNA generated from base-catalyzed reversal would be expected to form double-stranded DNA with the unlabeled oligonucleotide and be cross-linked by HMT if the thymidine residue on each strand is intact. The formation of the cross-link (Figure 3.20, lane 7) shows that the DNA generated from the base-catalyzed reversal reaction is indeed the unmodified 5'-[^{32}P]GGGTACCC-3'. Three additions of HMT (35 μg/ml) each of which was followed by near-UV irradiation with 320-380 nm light could cross-link essentially all the labeled DNA (data not shown).

These results demonstrate that a psoralen-DNA interstrand cross-link can be reversed in the absence of UV irradiation under denaturing alkaline conditions at elevated

temperatures. The initial products of the reversal reaction are unmodified DNA and the pyrone ring opened form of the pyrone-side monoadducted DNA. The O-MAp can be subsequently converted to the ring closed form (C-MAp) by treatment with mild acid. Upon gel electrophoresis on a denaturing polyacrylamide gel, O-MAp is converted to a form that cannot be converted back to C-MAp under the acidic conditions tested. This unknown and uncharacterized product can be avoided by incubating the base catalyzed reversal (BCR) mixture under acidic conditions prior to gel electrophoresis to convert all of the O-MAp to C-MAp.

This reaction has been exploited by us to produce preparative amounts of the third main type of psoralen adduct the pyrone-side monoadduct. Structural studies similar to those for the furan-side monoadduct and cross-link are being performed.

Preparative Experimental Method

BCR: 1 X 10^{-8} moles of HPLC purified 12-HMT-8 cross-link was dissolved in 200 µl of 0.1 N NaOH or KOH and heated to 90°C for 30 min. The reaction mixture was cooled to room temperature and 10 µl 2 N HCl added along with 50 µl Tris pH 7.5.

HPLC Analysis and preparative purification: The modified DNA was applied to a 4.6 mm x 25 cm reverse phase 60Å pore size C_{18} column. The products of the reaction were eluted with a linear acetonitrile gradient in 100 mM triethylammonium acetate (TEAA) pH 6.5 over a period of 80 minutes (flow rate = 1.0 ml/min). The percentage acetonitrile was changed from 9.5% to 17.5% from time 5 minutes to time 85 minutes. The fractions of interest were collected and lyophilized. The residue was resuspended in a minimum volume of TE and adjusted to 200 mM NaCl, 10 mM $MgCl_2$ and then 3 volumes of absolute ethanol were added. The solution was cooled overnight at -20°C and the precipitate collected by centrifugation at 16,000 X g for 35 minutes. The supernatant was

removed and the pellet washed with 95% EtOH and dried in vacuo. Quantification of the main products was done by UV spectrophotometry.

Gel Analysis of HPLC fractions: The oligonucleotide fractions isolated by HPLC were resuspended in 0.5 ml TE. 1 µl of each of these fractions was 5' end labeled using T4 polynucleotide kinase and γ^{32}P ATP. An aliquot of each of these reactions was loaded onto a 20 cm x 40 cm x 0.4 mm 24% 19:1 acrylamide:bis(acrylamide) 7 M urea gel and electrophoresed until BPB was at the bottom of the gel. The results of this electrophoresis was visualized by autoradiography.

A DNA 12 mer (5'-GAA-GCT-ACG-AGC-3'), a complementary DNA 8 mer (5'-TCG-TAG-CT-3') and HMT as the psoralen were irradiated using and argon ion laser operating at 366 nm to form cross-linked molecules in 50% yield after HPLC purification (see above). This cross-link was heated to 90°C in 0.1 N NaOH for 30 minutes. The reaction mixture was neutralized and applied to a reverse phase C_{18} HPLC column and the pyrone-side adducts separated from unmodified DNA and cross-link.

Figure 3.22 is the chromatogram from the base catalyzed reversal reaction of the 12 mer cross-linked to the 8 mer. The reaction was performed by mixing HPLC purified 12/8-XL with 0.1N KOH and heating to 90°C for 30 minutes. The reaction was neutralized with Tris-HCl and applied to a reverse phase HPLC column. This reaction should yield four products if it goes to completion, the unmodified 12 mer and 8 mer, and the pyrone ring open forms of the 12 mer and 8 mer pyrone-side adducts. The identity of the peaks in the chromatogram was determined by kinasing an aliquot of each fraction that corresponded to the peaks with γ^{32}P ATP and then running the kinase reaction mixture out on an denaturing polyacrylamide gel. The autoradiogram for this reaction is shown in figure 3.23, and it is an overexposure to show minor products. Lane 15 is the BCR reaction mixture before chromatography. Lanes 16 and 17 correspond to fractions 25-30, the first peak. This is the unmodified 12 mer as can be seen by comparison with the standard in lane 3. Lane 18 is fraction 34 and this corresponds to the unmodified 8 mer as

Figure 3.22 Chromatogram of Base Catylzed Reversal Reaction of the HMT Crosslinked 12 mer and 8 mer

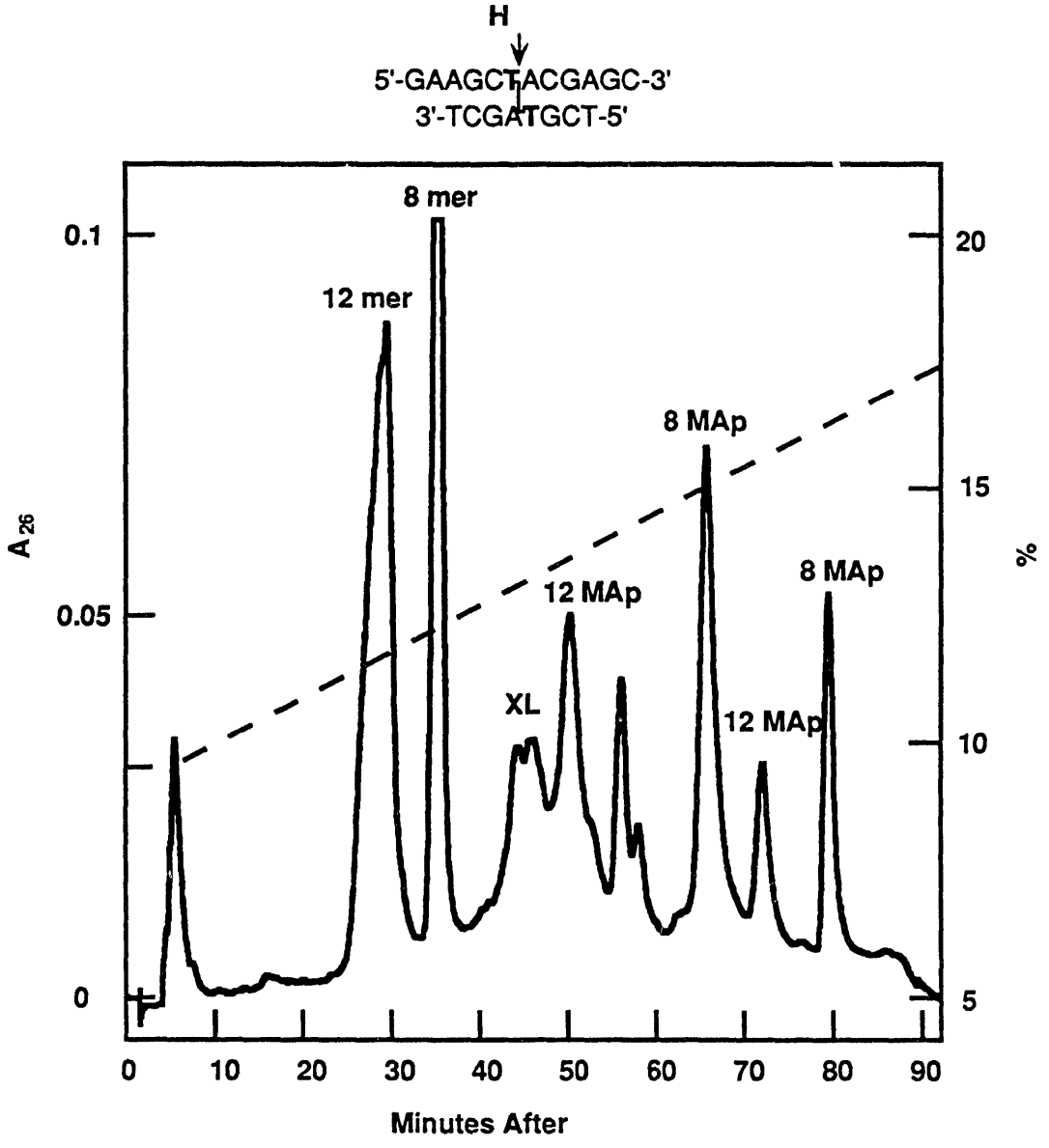

Figure 3.23: This is the autoradiogram of kinased HPLC fractions for two BCR reactions, and it is an overexposure to show minor products. Lanes 1-5 are controls. Lane 1 is unmodified 8 mer, lane 2 is 8 mer MAf, lane 3 is unmodified 12 mer, lane 4 is 12 mer MAf, and lane 5 is 8 mer / 12 mer XL. Lane 7 is the BCR reaction mixture using NaOH as the catalyst prior to chromatography. The 12 mer pyrone-side adduct elutes in fractions 46 and 65 (lanes 10 and 12). The 8 mer pyrone-side adduct elutes in fractions 68 and 76 (lanes 13 and 14). An unknown materiel elutes in fraction 52 (lane 11)(see text for a discussion of the possible origin of this material). Unmodified 8 mer eluted in fraction 31 (lane 8). 8/12-XL eluted in fraction 39 (lane 9). Lane 15 is the BCR reaction mixture using KOH as the catalyst before chromatography. Lanes 16 and 17 correspond to fractions 25-30, the first peak, and are unmodified 12 mer. Lane 18 is fraction 34 and is the unmodified 8 mer. Lanes 19 and 20 correspond to the two peaks at fractions 42 and 44 and these are the ring open form of the two isomers of the cross-link. In comparison to the cross-link standard in lane 5, they run slower. The pyrone open form of psoralen DNA adducts run slower than the closed form on denaturing polyacrylamide gel electrophoresis. Lane 21 corresponds to the peak at fraction 49 and is the pyrone-side monoadduct in the closed form. Lane 22 corresponds to fraction 55 in the chromatogram and is of unknown origin. Lane 24 corresponds to the peak at fraction 65, and is 12 mer O-MAp. Lanes 25 and 26 correspond to fractions 71 and 79 respectively, and are identified as the ring closed and ring opened form of the 8 mer MAp.

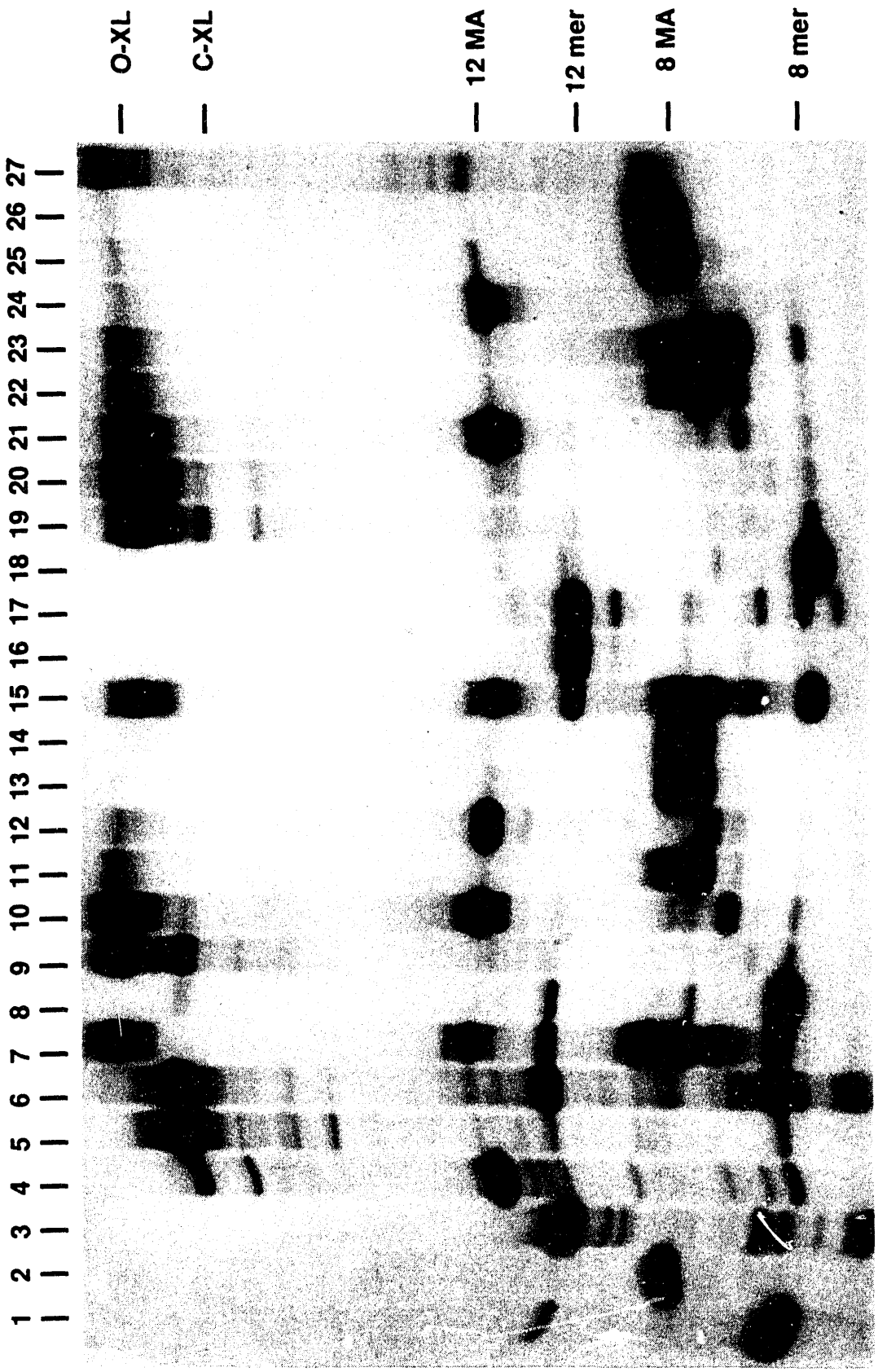
O-XL
C-XL
12 MA
12 mer
8 MA
8 mer
1 2 3 4 5 6 7 8 9 10 11 12 13 14 15 16 17 18 19 20 21 22 23 24 25 26 27

can be seen by comparison with the standard in lane 1. Lanes 19 and 20 correspond to the two peaks at fractions 42 and 44 and these are identified as the ring open form of the two isomers of the cross-link. In comparison to the cross-link standard in lane 5, they run slower. It has been observed that the pyrone open form of psoralen DNA adducts run slower on denaturing polyacrylamide gel electrophoresis. Lane 21 corresponds to the peak at fraction 49 and is a product whose mobility is similar to that of the furan-side monoadducted 12 mer standard in lane 4. This peak is identified as the the pyrone-side monoadduct and is in the closed form. Lane 22 corresponds to fraction 55 in the chromatogram. It has a mobility in between that of the unmodified 8 mer and the 8 MAf. Lane 23 corresponds to the peak at fraction 57 in the chromatogram. This is a minor amount of material and runs with a mobility between that of the unmodified 8 mer and the 8 MAf. These peaks are of unknown origin and were not characterized further. It is possible that these peaks in the chromatogram correspond to the unknown product that was observed in the enzymatic digestion of the ^{3}H-HMT BCR product formed from the oligomer 5'-GGG-TAC-CC-3'. Lane 24 corresponds to the peak at fraction 65. This peak corresponds to a molecule that has the same mobility on a gel as the material in fraction 49. On the HPLC, it is most likely 8 O-MAp, but after work up, the pyrone ring closes and it has identical mobility to the closed form of the monoadduct. Lanes 25 and 26 correspond to fractions 71 and 79 respectively, and are identified as the ring closed and ring opened form of the 8 mer MAp.

Lanes 7-14 of figure 3.23 represent the same sort of analysis for a BCR reaction that was done by substituting 0.1N NaOH as the catalyst. The chromatogram was essentially identical to the chromatogram obtained for the KOH case, as would be expected if the cation was only acting as a spectator ion. Briefly, lane 7 is the BCR reaction mixture prior to chromatography, The 12 mer pyrone-side adduct elutes in fractions 46 and 65 (lanes 10 and 12). The 8 mer pyrone-side adduct elutes in fractions 68 and 76 (lanes 13

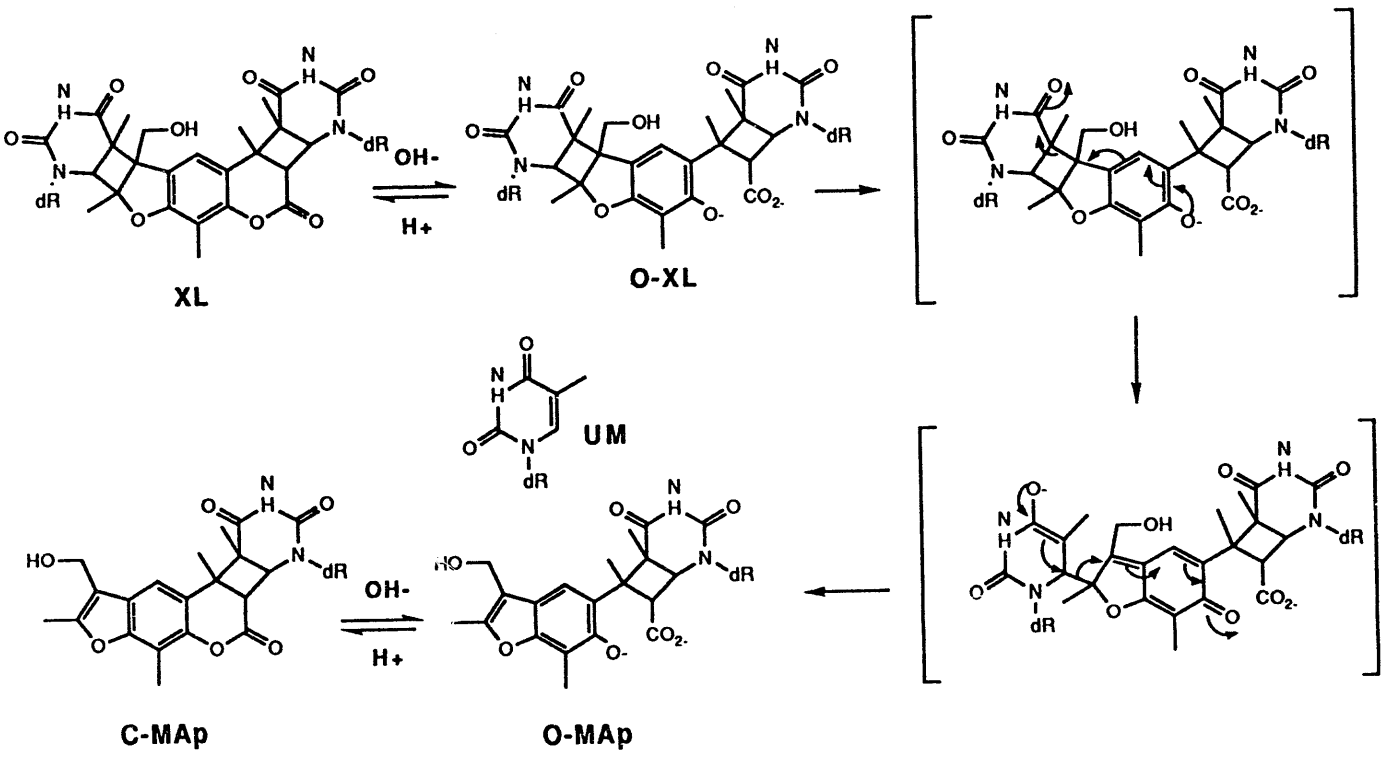

Figure 3.24 Proposed mechanism for the base-catalyzed reversal of an HMT-DNA cross-link.

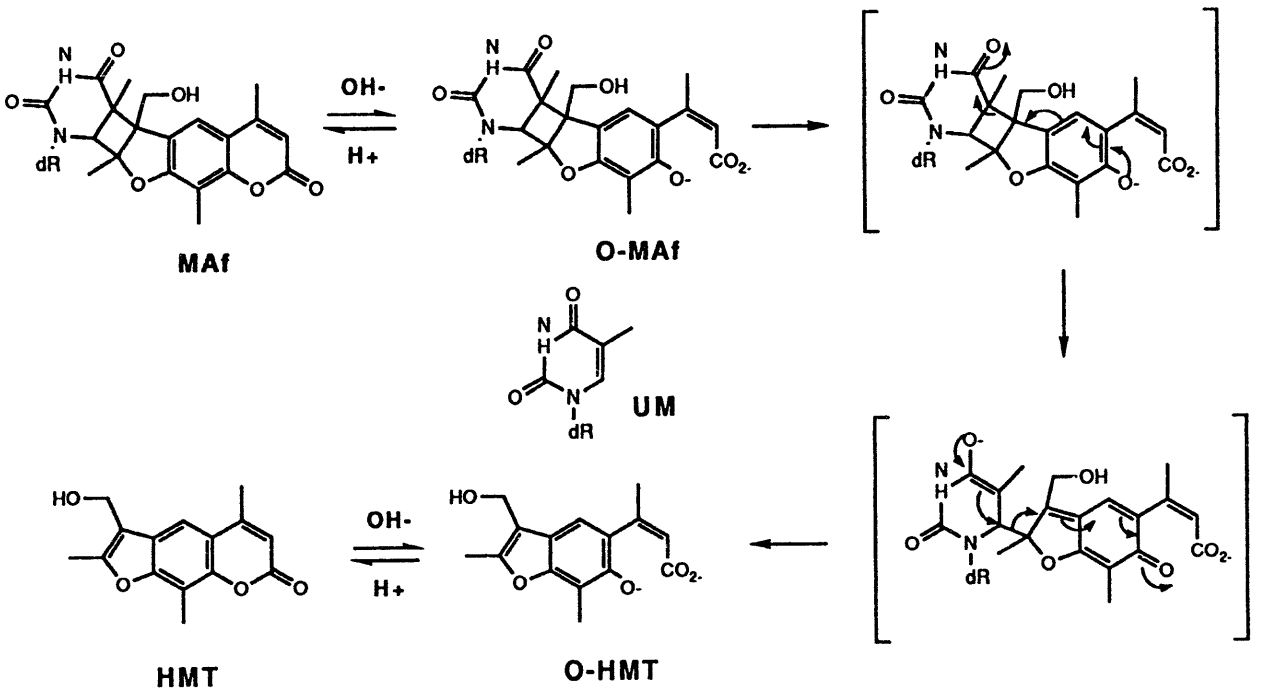

Figure 3.25 The proposed mechanism for the base-catalyzed reversal of an HMT-DNA furan-side monoadduct

and 14). The unknown materiel elutes in fraction 52 (lane 11). Unmodified 8 mer eluted in fraction 31 (lane 8). 8/12-XL eluted in fraction 39 (lane 9).

We propose the following mechanism for the base catalyzed reversal reaction (Fig.3.24). The first step of the reaction is the basic hydrolysis of the pyrone ring of the cross-link. The phenolate anion can then undergo a through-phenyl-ring retro-aldol condensation, breaking the bond between C(5) of the thymidine and C(4') of the psoralen. This intermediate enolate can then undergo a retro-Michael reaction, yielding the unmodified DNA and the ring opened form of the pyrone-side monoadducted DNA. Upon acidification the pyrone ring can close. This mechanism predicts that a furan-side monoadducted oligonucleotide would undergo a similar base-catalyzed reversal to yield the pyrone ring opened psoralen and the unmodified oligonucleotide if treated under strong alkaline conditions (figure 3.25). Yeung and co-workers report that when a furan-side monoadducted oligonucleotide is subject to BCR, it is reversed to the unmodified DNA (Yeung *et al.*, 1988). The fate of the psoralen was not investigated.

There were two psoralen monoadduct containing peaks eluting from the column for each strand. This can be explained as the pyrone-open and pyrone-closed forms of the monoadducts. The pyrone ring open form carries one more negative charge than does the pyrone ring closed form. This is a synthetically useful reaction, and it is currently being exploited to produce micromole quantities of the pyrone-side adduct to the thymidine in the DNA octamer 5'-GCGTACGC-3'.

The presence of the unknown products in the chromatogram of the 12 mer / 8 mer BCR reaction mixture, and the unusual and uncharacterized nucleoside adduct in the DNA digestion reactions present a challenge to the proposed mechanism. One possible explanation for these products is the alkali cleavage of the DNA strands at the site of psoralen reaction. The saturation of the 5,6 double bond of the thymidine causes the glycosidic bond of the adducted thymidine to become labile. If the glycosidic bond is cleaved during the reaction, then an apurinic site is created in the strand. Under the

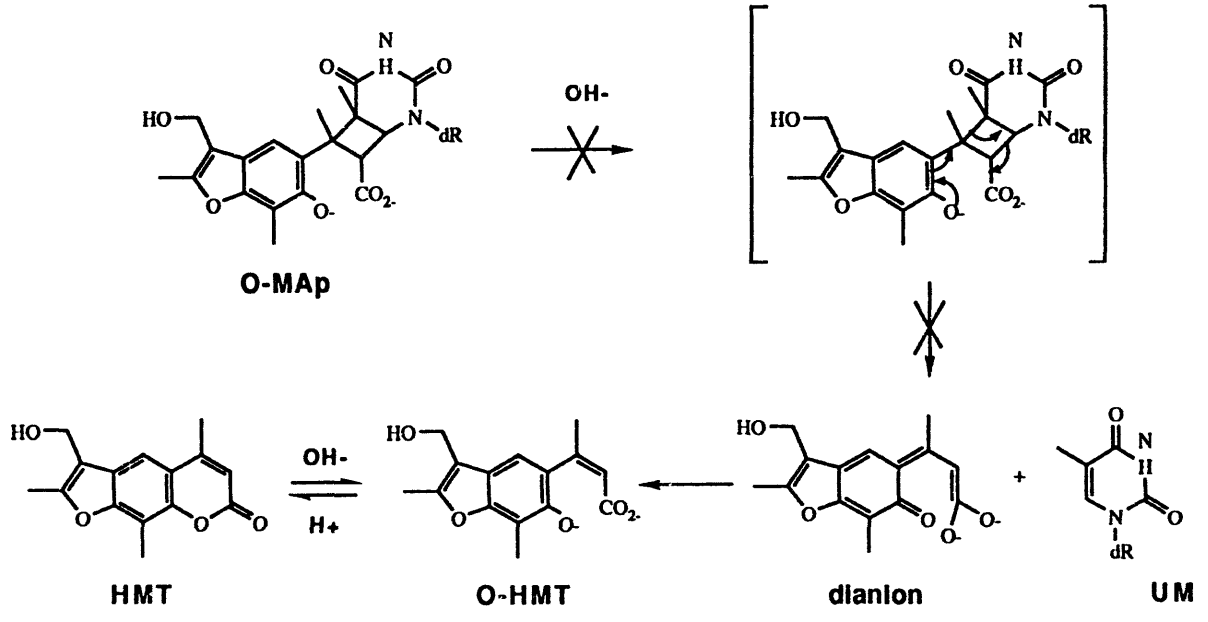

Figure 3.26 Scheme of why the pyrone-side monoadduct is resistant to Base-catalyzed reversal

strongly basic conditions of the reaction, base catalyzed decomposition of the deoxyribose ring could then occur, leading to strand scission, and the appearance of smaller fragments of DNA. This reaction would not necessarily need to occur on the furan-side of the adduct. To a first approximation, the cyclobutane rings on either end of a cross-link have the same stability. A test of this mechanism would be to take a pyrone-side adducted DNA oligomer and treat it under strongly basic conditions, and monitor the resultant products (if any). If this argument is true, then this is a possible method for the introduction of single and double stranded breaks into DNA at sites where psoralens are adducted. The reaction could be tuned by the use of other psoralen derivatives (probably not yet invented) that would promote deglycosylation in preference to BCR, and the use of a base that gave better elimination reactions and less lactone hydrolysis (such as N,N-dimethylaniline, or piperidine). The proposed mechanism also accounts for the resistance of the pyrone-side adduct to cleavage under these conditions. In figure 3.26 the pyrone-side adduct is shown in the ring-open form. If the electrons from the phenolate anion were to assist the cleavage of the cyclobutane ring by forming an ortho-quinone type intermediate, the carboxylate would be required to form a dianion. Dianions of carboxylic acids are known, but they only exist in aprotic media. Such an intermediate is of too high an energy to be accessible under the conditions that the BCR is carried out at. Use of the high power laser to synthesize micromole quantities of HMT cross-linked molecules greatly facilitates the synthesis of pyrone-side monoadduct by the BCR reaction. Before the twin innovations of laser irradiation and HPLC purification, preparation of even 20 μg of these adducts was a massive undertaking. Psoralen monoadducted oligonucleotides have been used as probes to detect specific nucleic acid sequences and as tools to study hybridization kinetics and thermodynamics (Gamper *et al.*, 1987; Gamper *et al.*, 1986). The results described here indicate that a faulty result may be produced if psoralen-adducted DNAs are treated under denaturing alkaline conditions such as alkaline agarose gel electrophoresis. A failure to detect psoralen cross-linkage when a sample is assayed under these conditions may be

simply due to the base-catalyzed reversal of the psoralen-DNA adducts formed. Similarly, results obtained from processes involving alkaline treatment of cross-linked DNA samples could be underestimates of the actual number of psoralen adducts formed. While base-catalyzed reversal of a psoralen-DNA cross-link prevents it from being handled under denaturing alkaline conditions, it provides for an efficient way to make psoralen pyrone-side monoadducted DNA.

Part IV: Applications of site-specifically psoralen modified DNA

The construction of a site specifically psoralen modified plasmid is one use for these site specifically psoralen adducted oligomers. Easy access to these modified oligomers allows for many different approaches to the construction of site specifically modified plasmids. To investigate the mechanism of excision repair in the human system, a site specifically psoralen modified DNA substrate needs to be constructed. From the UVR ABC system, it is known that in psoralen cross-link repair, the sites of excision around the lesion are different for the furan-side and the pyrone-side. In order to accurately determine the size of the repair patch in a human system, the DNA sequence around the lesion must be known. It should be possible to determine the size of the repair patch because we propose to introduce the modified oligomer into a specific site of a plasmid whose sequence is known, and which is flanked by many restriction sites. We have tried three separate methods for producing large quantities of site specifically modified plasmids.

The first is to take a single stranded plasmid and anneal a primer to it that has been modified and synthesize the double stranded molecule using a polymerase and NTP's. The nick in the newly synthesized strand is then sealed by employing DNA ligase. This approach is similar to site-directed mutagenesis commonly used by molecular biologists. A site specifically psoralen adducted replicative form M13 viral DNA has been made using this method and the T4 DNA polymerase system (Hansson and Wood, 1989; Kodadek

and Gamper, 1987). Incomplete synthesis of the double stranded molecule, nick translation by the polymerase through or into the adduct, strand displacement synthesis and the inability of ligase to efficiently close the nick are some problems associated with this method. In spite of these pitfalls, this approach is currently being pursued in our laboratory. The system that we are investigating is to anneal the furan-side monoadducted 19 mer prepared in part I of this chapter to the single stranded circular phage DNA M13mp18, and extend the oligonucleotide using Sequenase. Sequenase is a modified phage T7 DNA polymerase that has a very low 5' to 3' exonuclease activity. Preliminary experiments indicate that this approach will be successful.

The second method is to insert a double stranded fragment into a plasmid using restriction enzymes ala' standard genetic engineering cloning practices, followed by recircularization of the new construct (Sladek *et al.*, 1989). The primary difference between cloning and the construction of a site specifically damaged substrate, is that in cloning a plasmid there is a selection and amplification step performed on the plasmid by a living organism in between the construction of the new plasmid from the old. Obviously, only competent molecules are amplified, and a site-specific psoralen adduct will not be placed by the cell into the resulting plasmid. In these systems, nicks in the plasmid do not adversely affect the outcome of the transformation reaction. In fact, some cloning methods call for the dephosphorylation of the vector prior to ligation of the insert into it to force the plasmid to accept only one copy of the insert. Our assay for excision repair uses the incorporation of radioactive nucleotides with DNA polymerase into the gap created by the action of the repair complex at the damaged site and therefore cannot have any single stranded nicks because these site act as primers for the polymerase (see chapter 2).

Our first attempt at creating a site specifically psoralen modified plasmid was to insert a site specifically HMT cross-linked 13/20mer into pBR322 using standard double stranded cloning techniques (figure 3.27). The plasmid pBR322 has two Pfl M1 sites which are separated by 49 base pairs and a unique Ava 1 site. Pfl M1 is a restriction

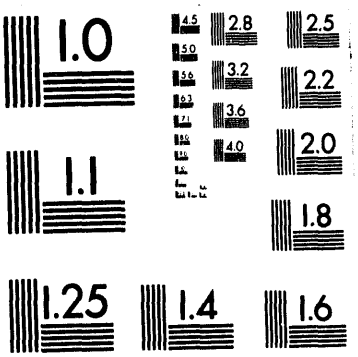
1.0
1.1
1.25
1.4
1.6
1.8
2.0
2.2
2.5
2.8
3.2
3.6
4.0
4.5
5.0
5.6
6.3
7.1
8.0
9.0
10.0
11.2
12.5
14.0
16.0
18.0
20.0
22.4

3 of 3

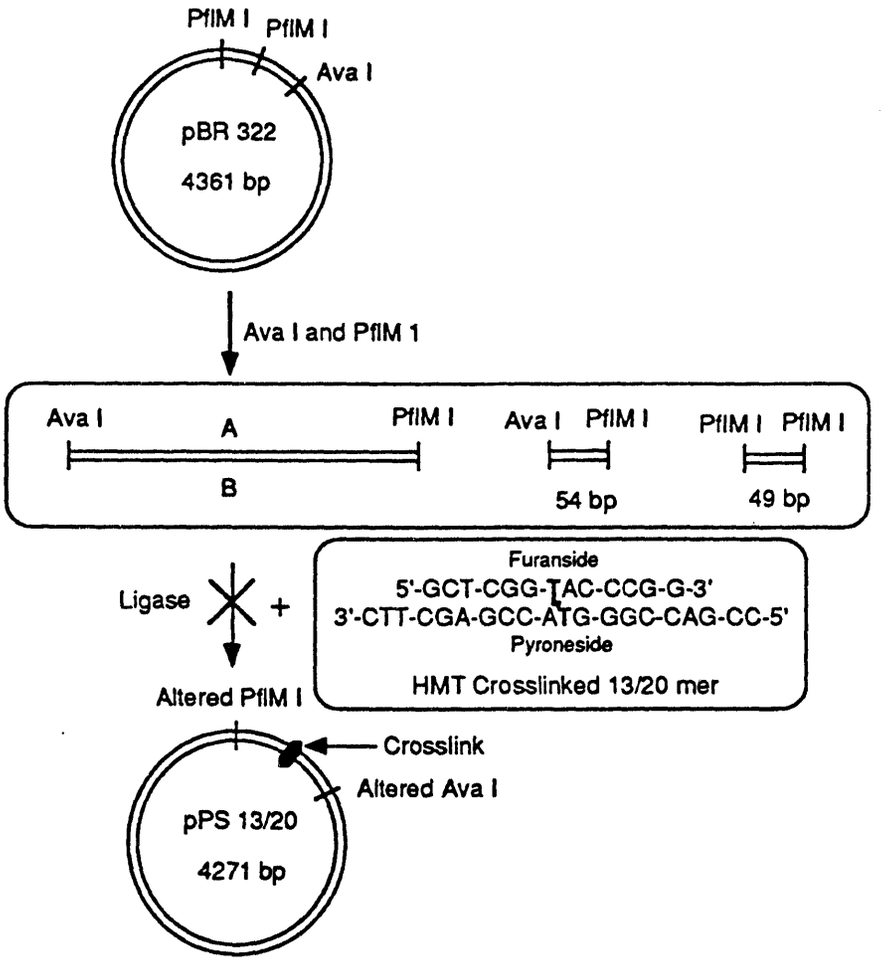

HMT crosslink site specifically placed in the plasmid

Figure 3.27 Flow chart for the failed attempt at the site specific placement of a HMT crosslink into the plasmid pBR 322

enzyme that recognizes the sequence 5'-CCANNNNNTGG-3' cutting to give a three base, 3'-overhang of a sequence determined by the substrate, not the restriction enzyme. The first step in the synthesis of the site specifically modified plasmid was to double restrict with PflM 1 and Ava 1. This gives a plasmid with two unique ends and a 49 base paired duplex from the cut between the two Pfl M1 sites and a 61 base pair fragment from the cut between PflM 1 and Ava 1. Ava 1 leaves a 5' overhang of four bases and PflM 1 leaves a 3' overhang of three bases. The next step was he ligation of a 13mer cross-linked to a 20mer that had ends complementary to the ends of the doubly restricted plasmid. If this strategy had worked, only one modified 13/20mer could have been inserted into a covalently closed circular plasmid. The has two different ends. When a ligation reaction is performed with the cross-linked oligomer and the restricted plasmid, four products can result: The first is no reaction between the inset and the plasmid, the second is to ligate an insert to each end of the plasmid, both of these classes of molecules are dead to any further ligation reaction that could close the molecule into a circle, and the other two possibilities are ligation of one insert to either end of the plasmid. This class of molecules could go on to form circles, but, double stranded ligation is an inherently inefficient process. Following numerous attempts to form covalently closed circular molecules, this approach was abandoned.

Our second approach was to make a modified pUC 19 plasmid (figure 3.28). The first step was to restrict the plasmid with Sal I and BamH I. This removes 12 base pairs to give two 5' overhanging ends that are not complementary. The 12 mer was identified by kinasing an aliquot of the reaction mixture and running it out on a denaturing polyacrylamide gel. We then ligated in a synthetic DNA fragment formed from a 39 mer and a 35 mer which on one end is complementary to the BamH I end of the plasmid, and

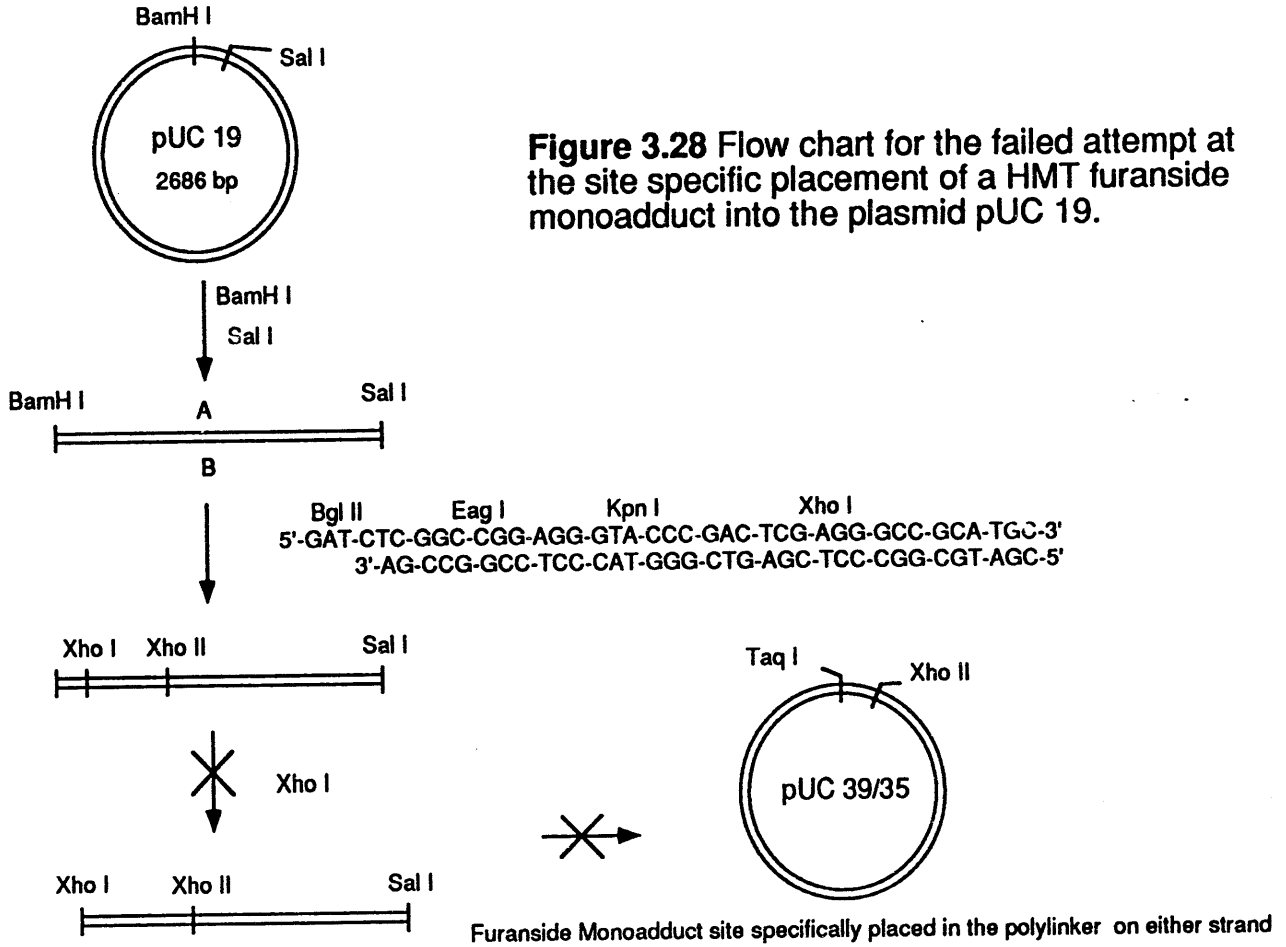

Figure 3.28 Flow chart for the failed attempt at the site specific placement of a HMT furanside monoadduct into the plasmid pUC 19.

Furanside Monoadduct site specifically placed in the polylinker on either strand

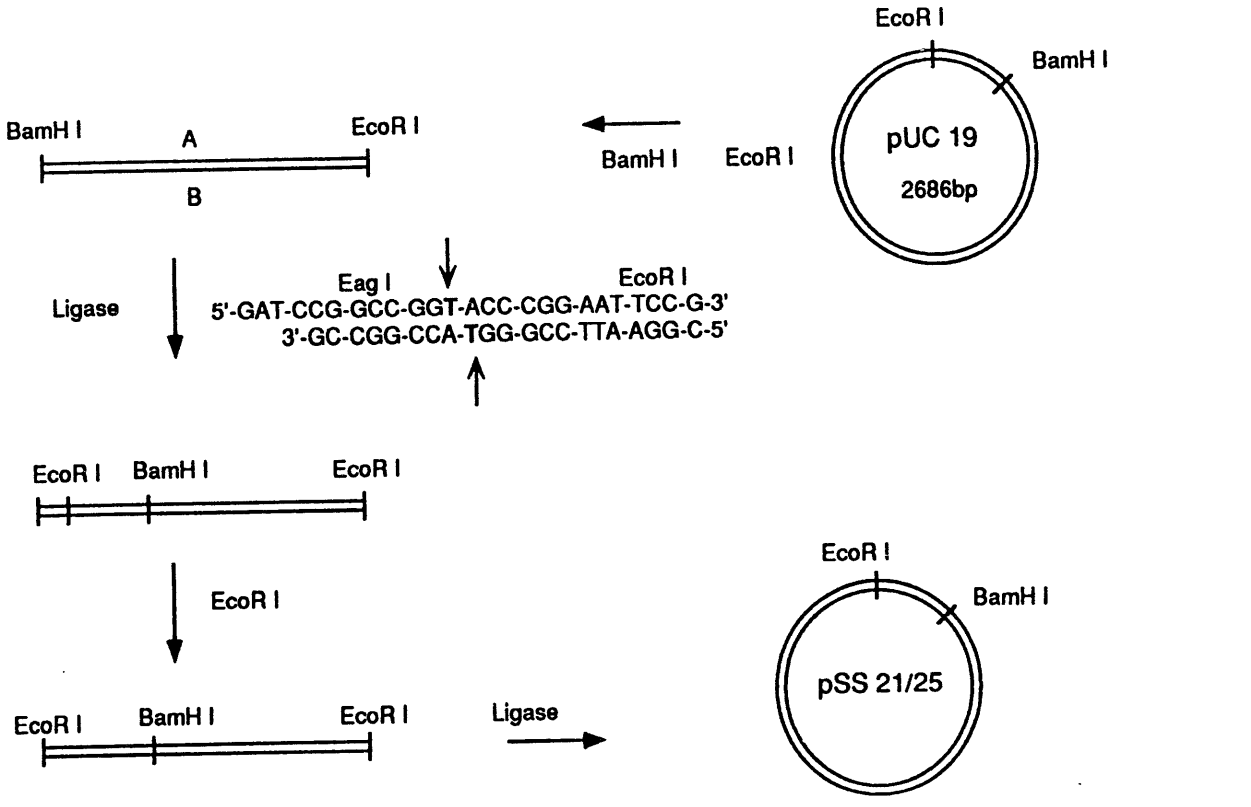

Figure 3.29 Scheme for the site specific placement of a HMT furanside monoadduct into the plasmid pUC 19 by double stranded ligation of an insert containing the adduct into the plasmid. The arrows pointing at the insert indicate the position of the monoadduct.

blunt on the other end. This synthetic fragment would contains the lesion. The two oligos were:

```
            Eag I       Kpn I       Xho I
5'-GAT-CTC-GGC-CGG-AGG-GTA-CCC-GAC-TCG-AGG-GCC-GCA-TGC-3'
     3'-AG-CCG-GCC-TCC-CAT-GGG-CTG-AGC-TCC-CGG-CGT-AGC-5'
```

The 5' overhang of this double strand is a Bgl II site that is complementary to the BamH I site on the restricted plasmid. Both of these restriction sites are destroyed upon ligation of these complementary, with formation of a Xho II site. The Eag I site is introduced with the linker, and can be used to diagnose the plasmid product for the presence of the adducted DNA. The lesion was to be introduced at the Kpn I site. This is the only 5'-TpA-3' site on the oligo, and is the favored site for photoadduction of the psoralen. We labeled the 5' end of the 35 mer with ^{32}P so that we could determine the efficiency of the first ligation reaction. Ligation with a 100 fold excess of unmodified 35 / 39 mer went with good efficiency as determined by autoradiography of the ligated linear plasmid. There were some multimerization products of the plasmid under the ligation conditions. Restriction with Xho I should have given us a 5' sticky end complementary to the Sal I end of the pUC 19. Both of these restriction sites are destroyed upon ligation of these two ends, with the formation of a Taq I site. Because the Xho I restriction lops off the 5' end of the 35 mer, there would be no radioactive label present in the final product. However, Xho I was very inefficient at restricting the ligated plasmid. It worked quite well to restrict the unligated 35 / 39 mer oligomers. Recent data from New England Biolabs indicates that Xho I activity is very dependent upon the length of the oligomer being cut and the flanking sequences around the oligomer. Because we were unable to efficiently cut our synthetic plasmid, even over digesting with a 100 fold excess of the enzyme, we were unable to get enough substrate to attempt cyclization reactions.

Another approach being currently being attempted is to make a modified pUC 19 plasmid by a similar method to method 2 (figure 3.29). The first step was to restrict the

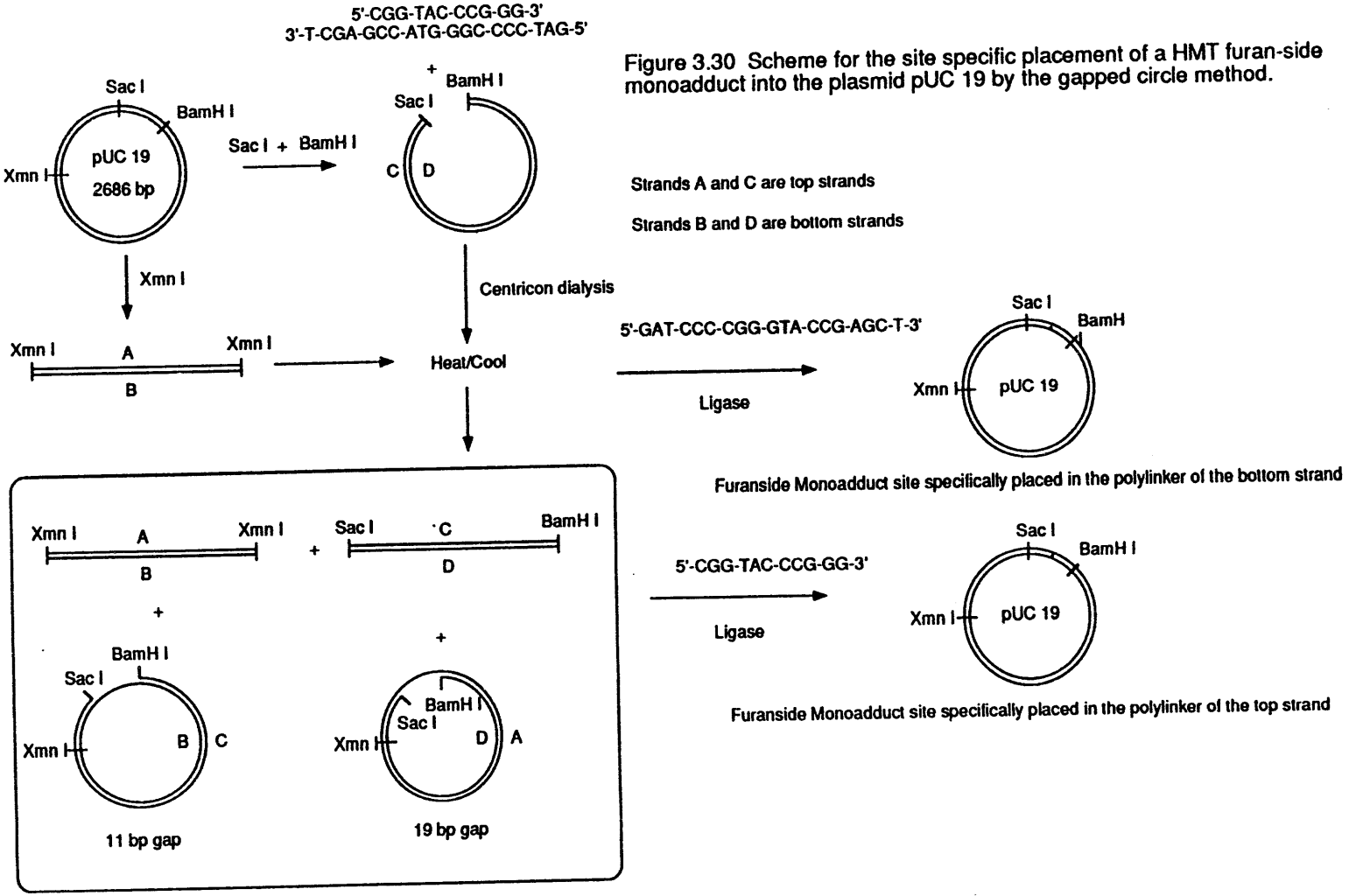

Figure 3.30 Scheme for the site specific placement of a HMT furan-side monoadduct into the plasmid pUC 19 by the gapped circle method.

plasmid with EcoR I and BamH I. This removes 21 base pairs to give two 5' overhanging ends that are not complementary. The 21 mers was identified by kinasing them with ^{32}P and running the products of that reaction out on a denaturing polyacrylamide gel. We then ligated in a synthetic DNA fragment formed from a 25 mer and a 21 mer which on one end is complementary to the BamH I end of the plasmid, and blunt on the other end. This fragment contains the lesion at the thymidine on the 25 mer indicated by the arrow. The synthesis of the 25mer furan-side monoadduct is described above. The two oligos are:

```
                    ↓
5'-GAT-CCG-GCC-GGT-ACC-CGG-AAT-TCC-G-3'
     3'-GC-CGG-CCA-TGG-GCC-TTA-AGG-C-5'
        Eag I          EcoR I
              Kpn I
```

Our third approach was to make a gapped circular molecule using pUC 19 (figure 3.30)(Basu *et al.*, 1987) (Johnson *et al.*, 1986; Lasko *et al.*, 1987; Michaels *et al.*, 1987) (Pinto *et al.*, 1986; Taylor and O'Day, 1989). In one reaction, pUC 19 is double restricted with BamH I and Sac I which removes a 19 nucleotide fragment from one strand and an 11 nucleotide fragment from the other. In a second reaction, a different aliquot of pUC 19 is restricted with Xmn I to linearize it. The Xmn I site is 500 bp from the BamH I and Sac I site. The short oligo from the double restriction is removed at the same time that the buffer is changed by employing a centricon 30 micro concentrator. The two restricted plasmids are then mixed together and annealed in the presence of a 100 fold excess of either a psoralen modified 19 mer or a modified 11 mer of the same sequence that was removed by the initial double restriction. This generates a gapped circle where the modified oligomer is hybridized into the gap formed by the hetero duplex. After the plasmids have annealed, they are subjected to a 100 fold excess of polynucleotide ligase to seal the nicks in the plasmid. To remove any nicked circles, the products are subjected to a cesium chloride/ethidium bromide density gradient centrifugation. This separates nicked circle from covalently closed circular molecules.

References

Anderson, J. E., Ptashne, M., and Harrison, S. C. (1987) *Nature 326,*

Ashikawa, I., Kinosita, K., and Ikegami, A. (1984) *Biochim. Biophys. Acta 782,* 87-93.

Averbeck, D. (1988b) *Arch. Toxicol. Suppl. 12,* 35-46.

Averbeck, D., Papadopoulo, D., and Moustacchi, E. (1988a) *Cancer Res. 48,* 2015-2020.

Basu, A., Niedernhofer, L., and Essigmann, J. (1987) *Biochemistry 26,* 5626-5635.

Bobst, A. M. (1979) *Spin Labeling, Vol II. Theory and Applications,* ed., Academic Press, New York.

Bobst, A. M., Kao, S.-C., Toppin, R. C., Ireland, J. C., and Thomas, I. E. (1984) *J. Mol. Biol. 173,* 63-72.

Boorstein, R. J., Hilbert, T. P., Cadet, J., Cunningham, R. P., and Teebor, G. W. (1989) *Biochemistry 28,* 6164-6170.

Boyer, V., Moustacchi, E., and Sage, E. (1988) *Biochemistry 27,* 3011-3018.

Cantor, C. R. and Schimmel, P. R. (1980) *Biophysical Chemistry,* ed., W.H. Freeman, San Francisco.

Cheng, S., Sancar, A., and Hearst, J. E. (1991) *Nucleic Acids Research 19,* 657-663.

Cheng, S., Van Houten, B., Gamper, H., Sancar, A., and Hearst, J. E. (1988a) in *Mechanisms and Consequences of DNA Damage Processing* (Friedberg, E. and Hanawalt, P., Ed.) pp. 105-113, Alan R. Liss, New York.

Cheng, S., Van Houten, B., Gamper, H., Sancar, A., and Hearst, J. E. (1988b) *Journal of Biological Chemistry 263,* 15110-15117.

Cimino, G. D., Gamper, H., Isaacs, S., and Hearst, J. E. (1985) *Ann. Rev. Biochem. 54,* 1151.

Cimino, G. D., Shi, Y., and Hearst, J. E. (1986) *Biochemistry 25,* 3013-3020.

Demaret, J.-P., Brunie, S., Ballini, J. P., and Vigny, P. (1989) *Photochem. Photobiol. 50,* 7-21.

Doetsch, P. W., Henner, W. D., Cunningham, R. P., Toney, J. H., and Helland, D. E. (1987) *Mol. Cell. Biol. 7,* 26-32.

Dugas, H. (1977) *Acc. Chem. Res. 10,* 47.

Friedberg, E. C. (1985) *DNA Repair,* ed., W.H. Freeman and Co., New York.

Friedberg, E. C. (1987) in *Molecular Biology of DNA Repair* (Collins, A., Johnson, R. T., and Boyle, J. M., Ed.) pp. 1-23, The Company of Biologists, Ltd., Cambridge.

Friedberg, E. C. (1988) *Microbiol. Rev. 52,* 70-102.

Gaffney, B. J. (1976) *Spin Labeling. Theory and Applications,* ed., Academic Press, New York.

Gamper, H., Piette, J., and Hearst, J. E. (1984) *Photochemistry and Photobiology 40,* 29-34.

Gamper, H. B., Cimino, G. D., and Hearst, J. E. (1987) *J. Mol. Biol. 197,* 349-362.

Gamper, H. B., Cimino, G. D., Isaacs, S. T., Ferguson, M., and Hearst, J. E. (1986) *Nucleic Acids Res. 14,* 9943-9954.

Gossett, J., Lee, K., Cunningham, R. P., and Doetsch, P. W. (1988) *Biochemistry 27,* 2629-2634.

Hansson, J. and Wood, R. D. (1989) *Nucleic Acids Res. 17,* 8073-8091.

Hearst, J. E. (1981) *Ann. Rev. Biophys. Bioeng. 10,* 69.

Hearst, J. E., Isaacs, S. T., Kanne, D., Rapoport, H., and Staub, K. (1984) *Q. Rev. Biophys. 17,* 1-44.

Heiger-Bernays, W., Essigmann, J., and Lippard, S. (1990) *Biochemistry 29,* 8461-8466.

Hemmings and De Jager (1989) in *Biological Magnetic Resonance* (Berliner, L. J. and Reuben, J., Ed.) pp. Plenum, New York.

Hyde and Feix (1989) in *Biological Magnetic Resonance* (Berliner, L. J. and Reuben, J., Ed.) pp. Plenum, New York.

Issacs, S., Rapoport, H., and Hearst, J. E. (1982) *J. Labelled Compd. Radiopharm. 19,* 345.

Johnson, D. L., Reid, T. M., Lee, M. S., King, C. M., and Romano, L. J. (1986) *Biochemistry 25,* 449-456.

Jones, B. K. and Yeung, A. T. (1988) *Proc. Natl. Acad. Sci. U.S.A. 85,* 8410-8414.

Kamzolova, S. G. and Postnikova, G. B. (1981) *Q. Rev. Biophys. 14,* 223.

Kanne, D., Straub, K., Hearst, J. E., and Rapoport, H. (1982a) *J. Am. Chem. Soc. 104,* 6754-6764.

Kao, S. C. and Bobst, A. M. (1985) *Biochemistry 22,* 5563-5568.

Keana, J. F. W. (1978) *Chem. Rev. 78,* 37.

Kim, S. H., Peckler, S., Grave, B., Kanne, D., Rapoport, H., and Hearst, J. E. (1983) *Cold Spring Harbor Symp. Quant. Biol. 47,* 361.

Kirchner, J. J., Hustedt, E. J., Robinson, B., and Hopkins, P. (1990) *Tetrahedron Letters 31,* 593-596.

Kodadek, T. and Gamper, H. (1987) *Submitted*

Kornberg, A. (1980) *DNA Replication,* ed., W.H. Freeman and Co., San Francisco.

Koudelka, G. G., Harrison, S. B., and Ptashne, M. (1987) *Nature 326,* 846-852.

Lasko, D. D., Basu, A. K., Kadlubar, F. F., Evans, F. E., Lay, J. O., and Essigmann, J. M. (1987) *Biochemistry 26,*

Likhtenshtein, G. I. (1974) *Spin Labeling Methods in Molecular Biology,* ed., Nauka, Moscow.

Lin, J. J. and Sancar, A. (1989) *Biochemistry 28,* 7979-7984.

Maniatis, T., Fritsch, E. F., and Sambrook, J. (1982) *Molecular Cloning,* ed., Cold Spring Harbor Laboratory, Cold Spring Harbor, NY.

Manley, J. L., Fire, A., Cano, A., Sharp, P. A., and Gefter, M. L. (1980) *Proc. Natl. Acad. Sci. (USA) 77,* 3855-3859.

Michaels, M. L., Johnson, D. L., Reid, T. M., King, C. M., and Romano, L. J. (1987) *J. Biol. Chem. 262,* 14648-14654.

Modrich, P. (1989) *J. Biol. Chem 264,* 6597-6600.

Moustacchi, E. (1988) *Arch. Toxicol. Suppl. 12,* 26-34.

Moustacchi, E., Papadopoulo, D., Averbeck, D., Diatloff-Zito, C., Rousset, S., and Nocentini, S. (1988) in *Mechanisms and Consequences of DNA Damage Processing* (Friedberg, E. C. and Hanawalt, P. C., Ed.) pp. 371-380, Alan R. Liss, Inc., New York.

Myles, G. M. and Sancar, A. (1989) *Chem. Res. Toxicol. 2,* 197-226.

Ohnishi, S. I. and McConnell, H. M. (1965) *J. Am. Chem. Soc. 97,* 2293.

Opella, S. J., Wise, W. B., and DiVerdi, J. A. (1981) *Biochemistry 20,* 284-290.

Papdopoulo, D., Averbeck, D., and Moustacchi, E. (1988) *Photochem. Photobiol. 47,* 321-326.

Peterson, K. R., Ossanna, N., Thliveris, A. T., Ennis, D. G., and Mount, D. W. (1988) *J. Bacteriol. 170,* 1-4.

Piette, J. and Hearst, J. E. (1983) *Proc. Natl. Acad. Sci. U.S.A. 80,* 5540.

Pinto, A. L., Naser, L. J., Essigmann, J. M., and Lippard, S. J. (1986) *J. Am. Chem. Soc. 108,* 7405-7407.

Pu, W. T., Kahn, R., Munn, M. M., and Rupp, W. D. (1989) *J. Biol. Chem. 264,* 20697-20704.

Rauben, J. and Gabbay, E. J. (1975) *Biochem. 14,* 1230.

Rauckman, E. J. and Rosen, G. M. (1976a) *Synth. Commun. 6,* 325.

Rauckman, E. J., Rosen, G. M., and Abou-Donia, M. B. (1976b) *Org. Prep. Proce. Int. 8,* 159.

Robinson, B. H., Lerman, L. S., Beth, A. H., Frisch, H. L., Dalton, L. R., and Auer, L. (1980) *J. Mol. Biol. 139,* 19-44.

Sage, E. and Moustacchi, E. (1987) *Biochemistry 26,* 3307-3314.

Sancar, A. and Sancar, G. B. (1988) *Annu. Rev. Biochem. 57,* 29-67.

Schneider and Freed (1989) *Spin-Labeling Theory and Applications,* ed., Plenum, New York.

Selby, C. P. and Sancar, A. (1988) *Biochemistry 27,* 7184-7188.

Shi, Y. and Hearst, J. E. (1986) *Biochemistry 25,* 5895-5902.

Shi, Y. and Hearst, J. E. (1987a) *Biochemistry 26,* 3786-3792.

Shi, Y. and Hearst, J. E. (1987b) *Biochemistry 26,* 3792-3798.

Shi, Y., Lipson, S., Chi, D. Y., Spielmann, H. P., Monforte, J., and Hearst, J. E. (1990) in *Bioorganic Photochemistry: Photochemistry and the Nucleic Acids* (Morrison, H., Ed.) pp. 341-378, John Wiley and Sons, New York.

Shi, Y., Spielmann, H. P., and Hearst, J. E. (1988) *Biochemistry 27,* 5174-5178.

Sibghat-Ullah, H., Carlton, W., and Sancar, A. (1989) *Nucleic Acids Res. 17,* 4471-4484.

Sladek, F. M., Munn, M. M., Rupp, w. D., and Howard-Flanders, P. (1989) *J. Biol. Chem. 264,* 6755-6765.

Smith, C. A. (1988) in *Psoralen DNA Photobiology* (Gasparro, F. P., Ed.) pp. 87-116, CRC Press, Inc., Boca Raton.

Smith, K. C., Want, T.-c. V., and Sharma, R. C. (1989) *BioEssays 10,* 12-16.

Spaltenstein, A., Robinson, B., and Hopkins, P. B. (1989) *Biochemistry 28,* 9484-9495.

Straub, K., Kanne, D., Hearst, J. E., and Rapoport, H. (1981) *J. Am. Chem. Soc. 103,* 2347-2355.

Taylor, J. S. and O'Day, C. L. (1989) *J. Am. Chem. Soc. 111,* 401-402.

Tessman, J. W., Isaacs, S. T., and Hearst, J. E. (1985) *Biochemistry 24,* 1669-1676.

Thomas, D. C., Levy, M., and Sancar, A. (1985) *J. Biol. Chem. 260,* 9875-9883.

Thompson, L. H., Weber, C. A., and Carrano, A. V. (1988) in *Mechanisms and Consequences of DNA Damage Processing* (Friedberg, E. C. and Hanawalt, P. C., Ed.) pp. 289-293, Alan R. Liss, Inc., New York.

Tomic, M., Wemmer, D., and Kim, S. H. (1987) *Science 238,* 1722-1725.

Van Houten, B., Gamper, H., Holbrook, S., Sancar, A., and Hearst, J. E. (1986a) *Proc. Nat. Acad. Sci. U.S.A 83,* 8077-8081.

Van Houten, B., Gamper, H., Sancar, A., and Hearst, J. E. (1986b) *Journal of Biological Chemistry 261,* 14135-14141.

Van Houten, B., Gamper, H., Sancar, A., and Hearst, J. E. (1988) *Journal of Biological Chemistry 263,* 16553-16560.

Voigt, J. M., Van Houten, B., Sancar, A., and Topal, M. D. (1989) *J. Biol. Chem. 264,* 5172-5176.

Vos, J. M. H. and Hanawalt, P. C. (1987) *Cell 50,* 789-799.

Walter, R. B., Pierce, J., Case, R., and Tang, M.-s. (1988) *J. Mol. Biol. 203,* 939-947.

Weiss, R. B., Gallagher, P. E., Brent, T. P., and Duker, N. J. (1989) *Biochemistry 28,* 1488-1492.

Wood, R. D. (1989) *Biochemistry 28,* 8287-8292.

Wood, R. D., Robins, P., and Lindahl, T. (1988) *Cell 53,* 97-106.

Yeung, A. T., Jones, B., and Chu, C. T. (1988) *Biochemistry 27,* 3204-3210.

Yeung, A. T., Jones, B. K., Capraro, M., and Chu, T. (1987) *Nucl. Acids Res. 15,* 4957-4971.

DATE FILMED

2/22/94

END